



<https://theses.gla.ac.uk/>

Theses Digitisation:

<https://www.gla.ac.uk/myglasgow/research/enlighten/theses/digitisation/>

This is a digitised version of the original print thesis.

Copyright and moral rights for this work are retained by the author

A copy can be downloaded for personal non-commercial research or study, without prior permission or charge

This work cannot be reproduced or quoted extensively from without first obtaining permission in writing from the author

The content must not be changed in any way or sold commercially in any format or medium without the formal permission of the author

When referring to this work, full bibliographic details including the author, title, awarding institution and date of the thesis must be given

Enlighten: Theses

<https://theses.gla.ac.uk/>
research-enlighten@glasgow.ac.uk

Comparative Studies in Experimental Hypertension and Cardiac Failure.

By

© Craig Alexander Lygate B.Sc. Hons. (University of Strathclyde),
M.Res. (University of Manchester), M.R.Pharm.S.

This being a thesis submitted for the degree of Doctor of Philosophy in the Faculty of
Medicine of the University of Glasgow.

Institute of Biomedical & Life Sciences,
West Medical Building,
University of Glasgow,
Glasgow,
UK.

January 2000

ProQuest Number: 10390787

All rights reserved

INFORMATION TO ALL USERS

The quality of this reproduction is dependent upon the quality of the copy submitted.

In the unlikely event that the author did not send a complete manuscript and there are missing pages, these will be noted. Also, if material had to be removed, a note will indicate the deletion.



ProQuest 10390787

Published by ProQuest LLC (2017). Copyright of the Dissertation is held by the Author.

All rights reserved.

This work is protected against unauthorized copying under Title 17, United States Code
Microform Edition © ProQuest LLC.

ProQuest LLC.
789 East Eisenhower Parkway
P.O. Box 1346
Ann Arbor, MI 48106 – 1346

GLASGOW
UNIVERSITY
LIBRARY

Declaration

I declare that this thesis has been composed entirely by myself and it has not been accepted in any previous application for a degree. The work, of which it is a record, has been done by myself, except as indicated in the acknowledgements, and all sources of information have been specifically referenced.

.....
CRAIG A. LYGATE

Acknowledgements

I gratefully acknowledge the support of my supervisors Prof. Anna Dominiczak and Dr. John Gordon. I also thank Dr. Julia Brosnan for advice and training in Northern blot analysis and Dr. N. Anderson for statistical advice. Dr. Martin Hicks taught me the rat surgery and assisted in all the surgical procedures. Mr. Simon McGrory instructed me in confocal microscopy and assisted in imaging the vessels in Chapters 4 & 5. Dr. Ian Montgomery assisted with infarct size histology, while Dr. J. Morton measured plasma neuroendocrine concentrations. Finally, Mr. Bill Brown measured blood pressure by tail-cuff plethysmography.

Dedication

This thesis is dedicated with love to Katherine, Jamie (age 5) and Morven (3 months).

Contents

	Page
1. Introduction	1
1.1 Epidemiology of cardiovascular disease	1
1.1.1 Epidemiology of hypertension	1
1.1.2 Epidemiology of cardiac hypertrophy	2
1.1.3 Epidemiology of heart failure	4
1.2 Hypertension	7
1.2.1 Animal models of hypertension	7
1.2.2 Spontaneously Hypertensive Rat	9
1.2.3 SHRSP	11
1.2.4 Genetics	12
1.2.5 Sympathetic nervous system	13
1.2.6 Atrial natriuretic peptide (ANP)	14
1.2.7 Brain natriuretic peptide (BNP)	16
1.2.8 Vascular function	16
1.2.9 Vascular structure	20
1.3 Cardiac hypertrophy	29
1.3.1 The hypertrophic response	29
1.3.2 Apoptosis in hypertrophy	30
1.3.3 LV function in hypertrophied hearts	31
1.3.4 Influence of blood pressure	32
1.3.5 Influence of genetics	33
1.3.6 Role of the renin-angiotensin system	33
1.3.7 Adrenergic stimulation	36
1.3.8 Role of nitric oxide	36
1.3.9 Cytokines in LVH	38
1.3.10 The cytoskeleton in LVH	39
1.3.11 Intracellular Ca^{2+} and LVH	39
1.3.12 Intracellular signalling	40
1.3.13 Coronary reserve	41
1.4 Heart failure	42
1.4.1 Models of heart failure	42

1.4.2	Haemodynamics in heart failure.	45
1.4.3	Neuroendocrine response in heart failure	48
1.4.4	Renin-Angiotensin-Aldosterone System	50
1.4.5	Arginine-vasopressin (antidiuretic hormone)	53
1.4.6	Atrial natriuretic peptide	53
1.4.7	Brain natriuretic peptide	55
1.4.8	Prostacyclin and prostaglandin E	55
1.4.9	Nitric oxide	57
1.4.10	Cytokines in heart failure	57
1.4.11	Endothelin	59
1.4.12	LVH after MI	61
1.4.13	Extracellular changes in the LV	62
1.4.14	Apoptosis in the failing heart	63
1.4.15	Myocyte function	65
1.4.16	Heart rate & arrhythmias	66
1.4.17	Skeletal muscle abnormalities	66
1.4.18	Vascular function in heart failure	67
1.4.19	Vascular structure in heart failure	72
2.	Methods	74
2.1	General laboratory Practice	74
2.2	Preservation of tissues & RNA extraction	76
2.3	Northern blot analysis	79
2.4	Confocal microscopy	84
3.	Assessment of Left Ventricular Structure and Function by Echocardiography in the Rat	90
3.1	Introduction	90
3.2	Methods	105
3.3	Results	109
3.4	Discussion	123
3.5	Conclusions	135
4.	Prevention of Cardiac and Vascular Hypertrophy in a Model of Genetic Hypertension	136
4.1	Introduction	136
4.2	Methods	141

4.3	Results	144
4.4	Discussion	162
4.5	Conclusions	172
5.	Cardiac and vascular remodelling after coronary artery ligation in the rat.	173
5.1	Introduction	173
5.2	Methods	175
5.3	Results	179
5.4	Discussion	200
5.5	Conclusions	210
6.	Coronary artery ligation in SHRSP: feasibility study	211
6.1	introduction	211
6.2	Results & discussion	213
7.	Venous function in the rabbit after coronary artery ligation	216
7.1	Introduction	216
7.2	Methods	217
7.3	Results	218
7.4	Discussion	224
7.5	Conclusions	225
8.	General discussion	226
	Appendix I	229
	Appendix II	233
	References	240

List of Figures

	Page
Figure 1.1 Schematic representation of the progression from normal myocardium to heart failure.	7
Figure 1.2 The role of natriuretic peptides in blood pressure control.	15
Figure 1.3 Mulvany nomenclature for describing re-modelling of blood vessels.	21
Figure 1.4 Relationship between peripheral vasoconstriction and impaired cardiac performance in heart failure.	68
Figure 2.1 Example of 1% agarose gel incorporating ethidium bromide for checking integrity of total RNA.	78
Figure 2.2 BNP PCR products run on a 1.5% agarose gel.	83
Figure 2.3 Anatomical selection of 3 rd order mesenteric resistance arteries.	85
Figure 2.4 Schematic representation of a resistance artery in cross-section indicating the relationship between imaging plane and vessel wall.	87
Figure 2.5 Extended focus view through the vessel wall of a mesenteric resistance artery by LSCM.	89
Figure 3.1 M-mode echocardiogram showing the heart of a SIIRSP rat	94
Figure 3.2 Two-dimensional echocardiogram of a SHRSP rat heart.	95
Figure 3.3 Positions of the four echocardiographic imaging windows shown in relation to the rib cage.	96
Figure 3.4 Orientation of the two imaging planes referred to in this thesis.	97
Figure 3.5 M-mode echocardiogram showing methods for measurement of cardiac dimensions.	98
Figure 3.6 Growth curves for LV mass against body weight constructed from autopsy data.	110
Figure 3.7 Parasternal long-axis view in a SHRSP rat.	111
Figure 3.8 Correlation between LV mass estimated by echocardiography and actual LV mass measured at autopsy.	112
Figure 3.9 Systolic blood pressure measured by tail-cuff plethysmography	114

in SHRSP and WKY rats.

Figure 3.10	Lack of relationship between LV mass normalised to body weight and systolic blood pressure.	115
Figure 3.11	Sample 2-D echocardiograms from the parasternal short-axis view.	117
Figure 3.12	Ejection fractions for WKY and SHRSP rats.	118
Figure 3.13	Effect of length of halothane exposure on cardiac contractility as measured by ejection fraction.	119
Figure 3.14	Assessment of repeatability between echocardiographic measurement of myocardial cross-sectional area measured on two separate occasions within 48 hours.	121
Figure 4.1	Systolic blood pressure measured by tail-cuff plethysmography in control and treated SHRSP.	144
Figure 4.2	Left ventricular mass measured by echocardiography and normalised to body weight.	145
Figure 4.3	Sample M-mode echocardiograms of the left ventricle	149
Figure 4.4	Correlation between LV mass and systolic blood pressure.	151
Figure 4.5	Northern blot indicating relative gene expression of GAP and ANP in the left ventricle of the SHRSP.	152
Figure 4.6	Northern blot indicating relative gene expression of GAP and BNP in the left ventricle of the SHRSP.	153
Figure 4.7	Correlation between mRNA expression of ANP in the left ventricle with (a) left ventricular mass (b) blood pressure in control animals measured at 8 weeks.	154
Figure 4.8	Correlation between mRNA expression of BNP in the left ventricle with (a) left ventricular mass (b) systolic blood pressure in control animals measured at 8 weeks.	155
Figure 4.9	Change in heart rate during treatment from baseline values.	156
Figure 4.10	Relative thickness of the component parts of the arterial wall as measured by LSCM.	158
Figure 4.11	Representative cross-sections through a section of the mesenteric resistance artery wall.	160
Figure 4.12	Lack of relationship between media thickness in mesenteric	161

	resistance arteries and mean systolic blood pressure in SHRSP.	
Figure 5.1	Examples of infarct size histology using the Azan dye technique.	181
Figure 5.2	Organ weights normalised to body weight in sham and ligated animals 8-weeks after surgery.	182
Figure 5.3	Ejection fraction measured by echocardiography in rats before and after sham or CAL surgery.	183
Figure 5.4	Cross-sectional area (CSA) of the left ventricular cavity measured at diastole by echocardiography in rats before and after sham or CAL surgery.	184
Figure 5.5	Representative 2-D echocardiograms from the parasternal short-axis view.	185
Figure 5.6	Thickness of the non-infarcted posterior LV wall measured at diastole by echocardiography.	186
Figure 5.7	Sample M-mode echocardiograms of the left ventricle in a WKY rat before and eight weeks after coronary artery ligation.	187
Figure 5.8	Northern blot analysis of ANP gene expression in the atria of sham and ligated WKY rats.	189
Figure 5.9	Northern blot analysis of BNP gene expression in the atria of sham and ligated WKY rats.	190
Figure 5.10	Northern blot analysis of ANP gene expression in the left ventricle of sham and ligated WKY rats.	191
Figure 5.11	Northern blot analysis of BNP gene expression in the left ventricle of sham and ligated WKY rats.	192
Figure 5.12	Noradrenaline concentration response curves in isolated aortic rings from sham and coronary artery ligated rats.	193
Figure 5.13	Acetylcholine concentration response curves in isolated aortic rings pre-contracted with noradrenaline.	194
Figure 5.14	Sodium nitroprusside (SNP) concentration response curves in isolated aortic rings pre-contracted with noradrenaline.	195
Figure 5.15	Relative thickness of the component parts of the arterial wall as measured by LSCM.	196
Figure 5.16	Measurement of lumen diameter in mesenteric resistance arteries of sham and ligated rats by LSCM.	196

Figure 5.17	Smooth muscle cell density (number of cells per mm ³ of media) from mesenteric resistance arteries of sham and ligated rats.	197
Figure 5.18	Representative 3-D reconstructions through the arterial wall of mesenteric resistance arteries.	198
Figure 6.1	Parasternal short-axis view of the left ventricle in a SHRSP rat before and two weeks after surgical ligation of a coronary artery.	215
Figure 7.1	Left ventricular ejection fraction in rabbits 32-weeks after coronary artery ligation.	219
Figure 7.2	Relaxation responses to 1µM ACh in rabbit saphenous vein from sham and ligated animals.	219
Figure 7.3	ACh concentration response curves in rabbit saphenous vein 32-weeks after CAL.	220
Figure 7.4	Frequency response curves in rabbit saphenous vein from sham and ligated animals.	221
Figure 7.5	Frequency response curves in rabbit saphenous vein in the presence of cocaine (10 ⁻⁶ M) from sham and ligated animals.	222
Figure 7.6	Frequency response curves in rabbit saphenous vein in the presence of L-NAME (10 ⁻⁴ M) from sham and ligated animals.	223

List of Tables

	Page
Table 1.1 Risk factors for developing LVH.	3
Table 1.2 Genetic models of hypertension.	8
Table 1.3 Possible mechanisms for endothelial control of vascular growth	23
Table 1.4 Animal models of heart failure.	43
Table 1.5 Cardiac haemodynamic parameters after coronary artery ligation in the rat.	47
Table 3.1 Echocardiographic derived parameters in WKY and SHRSP rats.	116
Table 3.2 Variability between two sequential echocardiographic studies 48 hours apart performed in 18 rats.	122
Table 3.3 Validation studies for echocardiographic determination of LV mass	125
Table 3.4 Co-efficient of repeatability for echocardiographic parameters measured 48 hours apart.	131
Table 4.1 Echo-derived LV measurements obtained at baseline.	146
Table 4.2 Echo-derived LV measurements obtained at 4 weeks of treatment.	147
Table 4.3 Echo-derived LV measurements obtained at 8 weeks of treatment and LV and RV mass at autopsy.	148
Table 4.4 Plasma concentrations of renin and aldosterone at sacrifice.	157
Table 4.5 Measurements of vessel dimensions and cell numbers using LSCM.	159
Table 5.1 Body and organ weights 8 weeks after sham or CAL surgery	180
Table 5.2 Densitometric analysis of ANP & BNP mRNA expression in the heart.	188
Table 5.3 Plasma concentrations of renin, ANP & BNP eight weeks post-infarct.	193
Table 5.4 Measurements of vessel dimensions and cell numbers using LSCM.	199
Table 6.1 Outcome in SHRSP after coronary artery ligation.	213

Abbreviations

ACE	Angiotensin converting enzyme
ACh	Acetylcholine
Ang II	Angiotensin II
ANP	Atrial natriuretic peptide
ASE	American Society of Echocardiography
AT	Angiotensin receptor
AWT	Anterior wall thickness
BNP	Brain natriuretic peptide
BP	Blood pressure
CAD	Coronary artery disease
CAL	Coronary artery ligation
CHF	Congestive heart failure
CO	Cardiac output
CSA	Cross-sectional area
ECE	Endothelin converting enzyme
ECG	Electrocardiogram
EDCF	Endothelium-derived contracting factor
EDD	End diastolic diameter
EDHF	Endothelium-derived hyperpolarising factor
EDV	End diastolic volume
EF	Ejection fraction
EFS	Electrical field stimulation
eNOS	Endothelial nitric oxide synthase
ESD	End systolic diameter
ET	Endothelin
FS	Fractional shortening
GAPDH	Glyceraldehyde-3-phosphate dehydrogenase
H+H	Hydralazine + hydrochlorothiazide
HR	Heart rate
IM	Intramuscular
iNOS	Inducible nitric oxide synthase
IP	Intraperitoneal

LAD	Left anterior descending
LSCM	Laser-scanning confocal microscopy
LV	Left ventricle/left ventricular
LVEDP	Left ventricular end diastolic pressure
L.VH	Left ventricular hypertrophy
MAP	Mean arterial pressure
MHC	Myosin heavy chain
MI	Myocardial Infarction
NA	Noradrenaline
NGF	Nerve growth factor
NO	Nitric oxide
NYHA	New York heart association
OD	Optical density or absorbance
PCR	Polymerase chain reaction
PE	Phenylephrine
PSS	Physiological salt solution
PWT	Posterior wall thickness
RAS	Renin-angiotensin system
RV	Right ventricle
SERCA	Sarcoplasmic-endoplasmic reticulum Ca ²⁺ -ATPase
SHHF	Spontaneously hypertensive – heart failure prone rat
SHR	Spontaneously hypertensive rat
SHRSP	Stroke-prone spontaneously hypertensive rat
SMC	Smooth muscle cell
SNS	Sympathetic nervous system
SOD	Superoxide dismutase
TNF	Tumour necrosis factor
TPR	Total peripheral resistance
WKY	Wistar-Kyoto

Summary

The common theme of this thesis is the characterisation of cardiac and vascular hypertrophy in animal models of cardiovascular disease. The pathophysiology of hypertension, left ventricular hypertrophy and heart failure are discussed, with particular emphasis on cardiac and vascular alterations in animal models. Echocardiography was validated for use in rats, and applied to a genetic model of hypertension, the stroke-prone spontaneously hypertensive rat (SHRSP), and to the rat coronary artery ligation (CAL) model of heart failure. Likewise, laser scanning confocal microscopy (LSCM) was utilised to examine vascular remodelling in both these models.

The utility of trans-thoracic echocardiography for estimating left ventricular (LV) mass was validated in lightly sedated SHRSP and WKY rats. Two-dimensional and M-mode parasternal short-axis views were readily obtainable and used to calculate LV mass using the cubed formula, which was then compared to blotted LV weight at autopsy. A significant correlation between estimated and autopsy LV mass was obtained, $r = 0.86$, $n = 75$, equation of line $y = 0.92x + 0.08$. Left ventricular hypertrophy (LVH) was defined for this colony of rats as a LV mass-to-body weight ratio of greater than 2.86g/Kg. The accuracy of echocardiography in detecting LV hypertrophy was determined: sensitivity 92%, specificity 64%, false-positive rate 22%, and false negative rate 14%. LVH in the SHRSP was apparent as a 28% higher LV mass compared to WKY rats. The anterior wall was 23% thicker, and the posterior wall 17% thicker. Differences in systolic function were measured by ejection fraction and fractional shortening, and were found to be anaesthetic dependent, with the SHRSP being more prone to halothane-induced cardiac depression. Intra-observer variability was quantified using repeat examinations in a sub-group of 18 rats. Co-efficient of repeatability was calculated for a range of echocardiographic parameters. The most reliable measurements were myocardial cross-sectional area (15%), LV wall thickness (16%), and end diastolic dimension (18%). LV mass had a co-efficient of repeatability of 21%.

The ability of antihypertensives to prevent the rise in blood pressure and associated complications of cardiac and vascular hypertrophy were examined in the SHRSP. At

weeks 6-7 of age, 24 SHRSP (M:F=12:12) were assigned to three groups and given in their food either irbesartan (Irb, 16mg/kg/Day), hydrochlorothiazide + hydralazine (H+H, 4mg/kg/day of each), or control (C). Systolic blood pressure was measured twice weekly by tail cuff plethysmography, and cardiac hypertrophy quantified using echocardiography at 0, 4 and 8 weeks of treatment. LV gene expression of natriuretic peptides was assessed by Northern blot analysis. To examine the effects on vascular hypertrophy, 3rd order mesenteric resistance arteries were fixed in formalin at half systolic blood pressure, stained with propidium iodide, and imaged using LSCM. One-way ANOVA was used to compare between groups, correcting for multiple comparisons using the Newman-Keuls test. There was no initial difference in blood pressure between groups, but from week 4 onwards, blood pressure in the control group was significantly higher e.g. by week 8 Irb 127±5, H+H 131±7 versus control 166±6mmHg ($P<0.001$). By 4 weeks, ventricular wall thickness and left ventricular mass were significantly increased in the control group when compared to either drug group: wall thickness Irb 1.75±0.05, H+H 1.80±0.47 vs. C 2.14±0.05mm ($P<0.01$), LV mass Irb 322±19, H+H 347±15 vs. C 428±19mg ($P<0.01$). LV myocardial expression of mRNA for atrial natriuretic peptide (ANP) was significantly higher in control animals compared to either treatment group ($P<0.001$), and gave a good positive correlation with systolic blood pressure. Myocardial gene expression of brain natriuretic peptide (BNP) was similar in control and H+H groups and correlated with LV mass, but was significantly lower in irbesartan treated animals ($P<0.01$). Vascular hypertrophy was also evident in control rats. Arterial wall thickness was 53±7, compared to Irb 43±8 and H+H 44±7µm ($P<0.05$). This difference was mainly due to a significantly thicker media layer in controls, without an increase in cell number. In conclusion, both regimens were equally effective in preventing the rise in blood pressure, and associated cardiac and vascular hypertrophy.

Cardiac and vascular remodelling were examined in a rat model of heart failure. Male WKY rats (300-400g) were subjected to coronary artery ligation (CAL; n=10) or sham operation (n=9) and cardiac function and structure were determined by echocardiography at two-week intervals. After 8 weeks, animals were euthanased by anaesthetic overdose and plasma ANP and BNP concentrations were determined, along with mRNA expression in atria and surviving LV. Rings of thoracic aorta were mounted in an organ bath for testing of endothelial function. Third order mesenteric

resistance arteries were pressure-fixed in formalin at 50mmHg, stained with propidium iodide, and imaged using LSCM. Ligated animals had significantly reduced ejection fraction at all time points after surgery (8 weeks: $46\pm 7\%$ versus $77\pm 5\%$ for sham), and showed progressive LV dilatation ($P<0.001$) and LVH ($P<0.001$) by echocardiography. Atrial levels of natriuretic peptide were unaffected by CAL, but ANP mRNA expression in the ligated LV was double sham values ($P<0.05$), this was reflected in higher plasma concentrations ($P<0.01$). There was a non-significant trend for increased BNP mRNA in the LV and for plasma concentrations in the ligated animals. Functional responses of the thoracic aorta to noradrenaline, acetylcholine, L-NAME and sodium nitroprusside were identical for both groups. Only minor, non-significant, changes were observed in lumen diameter and wall thickness of mesenteric resistance arteries. However, ligated animals had 24% fewer smooth muscle cells in the media layer ($P<0.01$), suggesting extensive eutrophic remodelling. Conclusion – Heart failure was mild and well compensated in these animals. Despite this, a novel type of remodelling was observed in mesenteric resistance arteries, which could have implications for small artery function.

A small study was undertaken to examine the feasibility of performing CAL in the SHRSP. Of eleven animals, six survived to 2-weeks, while only three of these, with the smallest infarcts, survived the full 8 weeks. Peri-surgical death was similar to WKY, but arrhythmic death more common. Future approaches to bring mortality within acceptable limits could include the use of anti-arrhythmic drugs or blood pressure lowering immediately after surgery.

1. Introduction

1.1 Epidemiology of cardiovascular disease

1.1.1 Epidemiology of hypertension

Hypertension is often defined clinically as a resting blood pressure greater than 140/90 mmHg measured on multiple occasions. It has a very high prevalence, affecting almost 1 in 4 adults in the USA and is the most common risk factor for cardiovascular and renal disease (Kannel, 1996).

Much of our knowledge of cardiovascular epidemiology is derived from the Framingham Heart Study, which will be referred to frequently in this section. This was a cohort study set up in 1948 to determine the incidence of heart failure, and has included 36 years of follow up over two-generations in 9405 subjects (Covic, 1999). In the Framingham Heart Study, two-thirds of the originally normotensive population developed hypertension over a 30-year follow up. This is because prevalence of hypertension increases with age, with an average 20mmHg rise in systolic blood pressure occurring between the ages of 30 and 65 years. Before middle age, women have lower blood pressure than men, however, the increase with age is more pronounced, probably due to the menopause. Hypertension is also more common in African-American blacks than in whites. Prevalence has not changed despite health education aimed at primary prevention of hypertension e.g. advice on diet, smoking, exercise and alcohol, probably because of an increasingly elderly population (Kannel, 1996).

Hypertension is a risk factor for all types of cardiovascular disease. Compared to age-controlled normotensives, middle-aged hypertensive men have a 4-fold risk of developing heart failure and stroke, and a 2-fold increased risk of coronary disease such as myocardial infarction (MI), angina and sudden death. Relative risks are even higher when other risk factors are present such as old age, diabetes, smoking or elevated cholesterol. In addition, hypertensives have an increased prevalence of metabolic disorders that add to the atherogenic risk e.g. dyslipidemia, obesity and diabetes. (Kannel, 1996).

Effect of treatment

Treatment of hypertension has a significant impact on cardiovascular risk. For each 5-6 mmHg drop in diastolic blood pressure, the incidence of stroke falls by 38% and coronary heart disease by 16% (Hedner, 1998). However, a couple of recent studies have shown that the risk is not normalised. In a prospective study by Andersson *et al.* (1998), 686 middle-age hypertensive men being treated for hypertension were compared with 6810 non-hypertensive men over a 22-year follow-up period. Cardiovascular and all cause mortality between groups did not differ in the first 10 years, but increased steadily over the next 12-years in the treated hypertensives to become highly significant. Therefore, despite good blood pressure control, treated hypertensives still had twice the death rate from stroke and ischaemic heart disease.

Similarly, Alderman (1998) followed morbidity and mortality over an 18-year period in 8690 mild to moderate hypertensive patients. The most common morbid events were MI and stroke, which occurred at a stable rate throughout the years. However the rate of heart failure increased 10-fold after 10 years of treatment to become the second most common outcome after MI. Together these studies indicate a failure of antihypertensive medication to normalise cardiovascular risk in the long-term. There may be a number of reasons for this. It may be necessary to treat hypertension more aggressively by aiming for below 140/90mmHg (Hedner, 1998). Control of blood pressure may not result in regression of cardiac and vascular hypertrophy, that are themselves independent risk factors. Further, treatment requires optimising as out-with the clinical trial situation only 21% of treated hypertensives have good blood pressure control. This may be due to sub-optimal dosing and/or poor compliance (Kannel, 1996). It is also worth noting that in the general population, around one-third of hypertensives may be unaware of their condition. Vascular damage or LV hypertrophy may well be present before treatment begins, or the first indication of hypertension may present as end-organ damage (Kannel, 1996).

1.1.2 Epidemiology of cardiac hypertrophy

When discussing the incidence of LVH, older studies using electrocardiograms (ECG) for diagnosis of hypertrophy probably grossly underestimated the scale of the problem. In the Framingham Heart Study, ECG diagnosed LVH occurred in 5-7% of the elderly population. In similar cohorts diagnosed by echocardiography, the incidence ranges from 25-30% of elderly men and 30-50% of elderly women. However, despite the

unreliable nature of the ECG for diagnosis, clear ECG evidence of LVH was associated with a very poor prognosis (Levy, 1991).

The Framingham Heart Study used echocardiography to identify the major independent risk factors for LVH in 3220 subjects over 40 years old, free from cardiovascular disease on entry. LVH is relatively rare in young subjects, but increases with age. The age dependency is particularly strong in females, where the risk increases by 67% per decade after the menopause. The incidence of LVH increases with increasing blood pressure for all age groups and with obesity. The single biggest risk factor was having had a previous myocardial infarction. Table 1.1 shows the risk associated with a given factor expressed as an odds ratio using multivariate analysis.

Table 1.1 Risk factors for developing LVH established in the Framingham Heart Study (Levy, 1991; Levy *et al.*, 1990)

Risk factor	Males odds ratio	Females odds ratio
Age (per 10 years)	1.15	1.67
Systolic BP (per \uparrow 20mmHg)	1.43	1.25
Body mass index (per 2Kg/m ²)	1.47	1.51
Previous myocardial infarction	3.45	3.52
Valvular heart disease	3.42	2.35

The presence of LV hypertrophy is in itself a major risk factor for other cardiovascular disease. For each 50g rise in LV mass there is a 60% increase in the incidence of coronary artery disease in men and 45% in women. Likewise, all cause mortality increases from 4.0% in men without, to 9.1% for men with LVH. The risk appears to be continuous with no obvious threshold apparent (Levy, 1991).

The prevalence of LVH in hypertensive subjects has been more difficult to quantify satisfactorily, as the figures obtained depend heavily not only on the criteria for defining hypertrophy, but on the severity of hypertension and treatments given. In one study, 42% of hypertensive patients with mild to moderately severe hypertension had LVH on echo examination. In another, 17% of borderline hypertensives and 21% of established hypertensives were affected (Devereux *et al.*, 1987). In genetic models of hypertension such as the SHRSP, the incidence of LVH is 100% in the adult rat (Yamori *et al.*, 1979).

For obvious ethical reasons, it has not been established whether all hypertensives, if left for long enough without treatment, would also develop LVH.

In man, LVH predisposes to ventricular arrhythmias. McLenachan *et al.* (1987) compared the incidence of ventricular arrhythmias in a group of hypertensive patients with patients exhibiting hypertension and LVH. Of the patients with LVH, 28% had episodes of ventricular tachycardia, compared to 8% of non-LVH hypertensives and 2% of normal controls. These results may explain why LVH patients are at higher risk of sudden death.

1.1.3 Epidemiology of heart failure

Estimates of the burden heart failure exerts on society vary according to methodology, age of the population and the definition of heart failure applied. What they all agree on is that heart failure is increasing in prevalence in the elderly, prognosis remains poor despite optimising treatment and the economic costs are huge.

Prevalence

Around 15 million people world-wide are thought to suffer from heart failure. In the USA, the annual incidence is 400 000, with an estimated prevalence of 2.3 - 3 million. At any given time the Germans estimate that 3% of their population are affected (Eriksson, 1995). There is no clear consensus for diagnosing heart failure and this is reflected in the variation in prevalence between studies. For example, the Framingham Heart Study may have underestimated prevalence, as the criteria used identified only patients with severe heart failure. In the Swedish "study of men born in 1913" the prevalence of heart failure increased with age affecting 2% at 50 years of age and 13% by the age of 67 (Eriksson, 1995). It is a consistent finding in all studies that age is a major risk factor. The Helsinki ageing study followed 501 subjects aged 47-86 years over a 4-year period. Prevalence of heart failure in this elderly population was approximately 8% (Kupari *et al.*, 1997). Closer to home, the number of discharges from Scottish hospitals where CHF was the principal diagnosis rose steadily in the years 1980-1990 (Dargie *et al.*, 1996).

Epidemiological studies have consistently found that heart failure is becoming more prevalent and a number of reasons have been postulated. Firstly, the population is ageing. Secondly, survival after MI has much improved due to specialised coronary care units and the widespread use of aspirin and thrombolytics. Patients who may otherwise

have died after MI are surviving only to develop heart failure later (Dargie *et al.*, 1996). And thirdly, there are improved diagnostic tests for heart failure (Eriksson, 1995).

Mortality & morbidity

Mortality and morbidity of untreated heart failure is unknown, even the earliest studies had access to diuretics. Mortality depends on severity of the disease. In severe CHF requiring hospitalisation, mortality in the CONSENSUS 1 study was as high as 52% after 1 year in the placebo group, and was still 36% with ACE inhibitors (Dargie *et al.*, 1996). As a consequence of the diagnostic criteria, mortality rate may have been over-reported in the Framingham Heart Study. Six years after diagnosis of heart failure, 82% of men and 67% of women were dead. In the "study of men born in 1913" five year mortality was not as severe, mainly because most subjects had mild to moderate heart failure (Eriksson, 1995). For the Helsinki ageing study, mortality in the CHF population was 46% over 4 years, representing a 4.2-fold increase in mortality (Kupari *et al.*, 1997).

Approximately half of all deaths from heart failure are sudden. Anti-arrhythmics have little influence on this type of death, and the occurrence of ventricular arrhythmias does not appear to correlate with sudden death in CHF. Meta-analysis of trials for ACE inhibitors show a 23% decrease in mortality by slowing progression, however the gain in life expectancy is measured in months not years (Cowie *et al.*, 1997).

Aetiology

In the Framingham Heart Study, hypertension was the primary underlying cause of heart failure (Eriksson, 1995). With more effective anti-hypertensive therapy the balance has shifted towards ischaemic heart disease as the most common primary aetiology. In the SOLVD trial (Studies of LV Dysfunction), ischaemic heart disease accounted for 53% of cases in men and 42% in woman, while hypertension was responsible for 15% in men and 22% in women. Aortic or valvular disease accounted for most of the remainder (Eriksson, 1995). The assignation of a primary underlying cause may be misleading, as in reality many patients have several co-morbid conditions which may all contribute to the onset of heart failure. In the Helsinki ageing study, ischaemic heart disease was the most common cause, however, 54% had co-existing hypertension, 54% had coronary artery disease (CAD), 51% had heart valve disease and 62% LVH at echocardiography (Kupari *et al.*, 1997). Hypertension as a primary

underlying cause may also be underestimated since patients with heart failure may no longer exhibit high blood pressure, therefore hypertension may be missed if it has not been observed prior to heart failure (Cowie *et al.*, 1997).

After myocardial infarction, 35% of patients develop either established or transient heart failure. When heart failure is transient LV function may be compromised but patients are asymptomatic. Some may go on to have recurrent MIs, but with time many will progress to heart failure in the absence of other major morbid events (Dargie *et al.*, 1996). The process governing disease progression is poorly understood, but is likely to include neuroendocrine, vascular and renal responses.

The presence of heart failure increases the risk of other cardiovascular events. Heart failure patients in the Framingham Heart Study had a 4-fold increased risk of stroke and a 2.5 – 5 fold increased risk of myocardial infarction (Eriksson, 1995).

Economic burden of heart failure

Heart failure represents a major financial strain on national health budgets. In Europe this amounts to approximately 1% of the health budget, with inpatient treatment the major contributor to this cost (Cowie *et al.*, 1997). In the USA, the estimate is even higher at almost 5% of the health budget, which in 1991 was \$38 billion. It is estimated that 35% of those diagnosed with heart failure are admitted to hospital per year (Eriksson, 1995). In the UK, there are between 100 000 and 200 000 hospital admissions per annum due to heart failure (Eriksson, 1995).

Risk factors for heart failure

The risk factors for developing heart failure are similar to those for coronary artery disease (CAD), and so it is unsurprising that CAD is also a risk factor for heart failure. The major risk factors of hypertension and LV hypertrophy are mentioned earlier. In the Framingham Heart Study, 20% of those who had a MI developed heart failure within 5-6 years. Dilatation of the LV greatly increased the risk, and LVH was the single biggest risk factor for developing heart failure (15-fold increase) (Cowie *et al.*, 1997). Others include smoking, obesity (especially abdominal fat), excess alcohol consumption, stress and metabolic disorders such as diabetes (Eriksson, 1995).

In clinical trials, treatment with antihypertensives may decrease incidence of heart failure by up to 50% (Cowie *et al.*, 1997). However, this figure is unlikely to remain true in the general population where poor compliance is often a problem, and changes in

medication are common. The continuation rate for all classes of antihypertensive agents after 6 months treatment is only 40-50% (Jones *et al.*, 1995).

The progressive deterioration from normal non-hypertrophied myocardium to overt failure is summarised in figure 1.1. LVH is central to this process and progression may be driven by a number of interacting factors such as hypertension, trophic hormones and increased afterload.

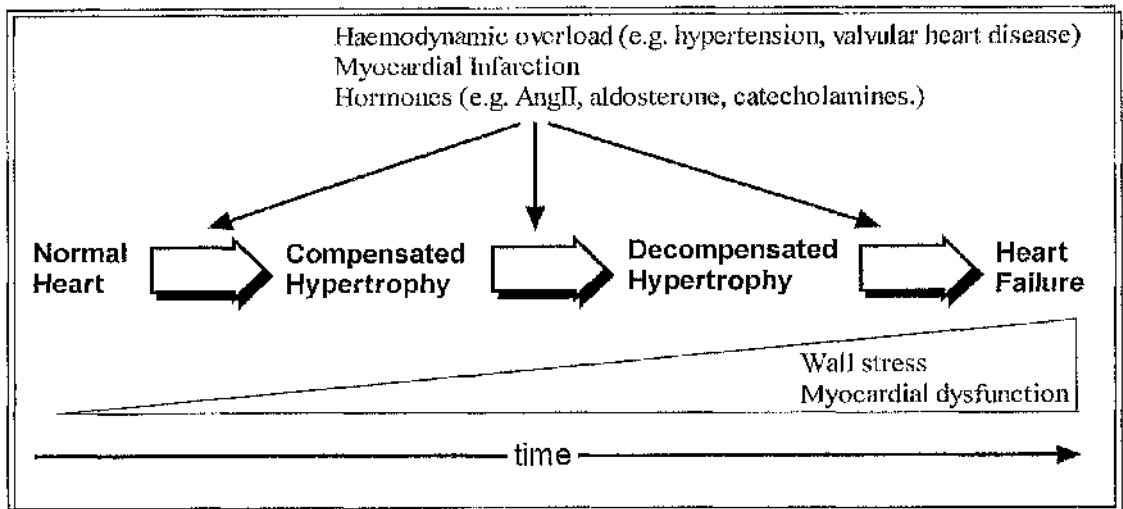


Figure 1.1 Schematic representation of the progression from normal myocardium to heart failure. Adapted from Izumo & Aoki (1998).

1.2 Hypertension

1.2.1 Animal models of hypertension

Animal models are required for studying the basic mechanisms of blood pressure control that are not possible in humans. Rats are by far the most common species used in hypertension research (mouse, dog and cat trail far behind). Hypertension in the rat may either be surgically induced e.g. aortic stenosis, Goldblatt rats, or more commonly, selectively bred for genetic hypertension (Pinto *et al.*, 1998). There are at least eight genetically hypertensive rat strains currently available, and their salient characteristics are outlined in table 1.2. For the purposes of this introduction only the spontaneously hypertensive rat (SHR) and its stroke-prone relative (SHRSP) will be discussed fully, as the SHR is the most commonly used in hypertensive research and the SHRSP is used in chapters 3 and 4 of this thesis.

Table 1.2 Genetically hypertensive rat strains.

Strain	Systolic BP	Major defects	Life-span	Complications
Spontaneously hypertensive rat	SHR WKY	↑ sympathetic tone Ion transport abnormalities	18-20 months (24 months WKY)	H.F. at 18 months Stroke MI
Wistar-Kyoto rat	SHRSP	↑ sympathetic tone	6-13 months	80% die of stroke by 9-13 months
Stroke-prone SHR WKY	GH	↑ peripheral resistance Ca ²⁺ mis-metabolism Prostaglandins	Not formally assessed > 12 months	L.V.H. 40-60%
New Zealand genetically Hypertensive strain	LII LN	Altered CNS function to ↑ sympathetic tone	Not assessed But ↓ life-span	↓ renal function at 13 weeks Stroke, MI
Random-bred albinos	SBH SBN	Sodium retention Baroreceptor defect	Not assessed > 12 months	NaCl or DOCA – renal arterial defects. LV hypertrophy.
Lyon hypertensive	MHS	Abnormal kidney function	22 months	L.V.H.
Lyon normotensive	MNS	↑ sympathetic tone Baroreceptor defect	MNS 21 months	Low kidney weight
Sabra Hypertensive	SS/Jr	Defect in adrenal steroid pathways.	All dead by 8 weeks on 8%NaCl	Renal lesions Vascular inflammatory response Heart failure 4-5 months
Sabra normotensive	FH	Abnormal kidney function	Mortality starts at 32 weeks	Death due to renal lesions & heart failure, MI

Data provided for male animals only. All models exhibit left ventricular hypertrophy and impaired endothelium-dependent relaxations (Pinto *et al.*, 1998). References: Yamori & Lovenburg (1987); Vincent & Sassard (1987); Ben-Ishay *et al.* (1987); Iwai (1987); Rapp (1987); Kuipers *et al.* (1987).

Rat models offer a number of advantages for hypertension research. They are relatively low cost, with a short life span and accelerated disease progression, which allows breeding/genetic studies, and the opportunity for prevention studies. Rats are suitable for invasive techniques eg. nephrectomy, coronary artery ligation, sympathectomy, LV catheterisation, and there are fewer problems with variability i.e. uniform age, severity of disease, compliance (Ganten, 1987). Primary essential hypertension accounts for 95% of human hypertension, therefore genetically transmitted models are of particular interest. Inbred rats are often used to fix genetic traits and offer an advantage as symptoms and complications occur at a predictable age (Ganten, 1987).

1.2.2 Spontaneously Hypertensive Rat

The SHR is over 10-fold more popular than that of the next nearest model of hypertension, the closely related SHRSP (Pinto *et al.*, 1998). In 1959 Okamoto and Aoki started selective breeding for high blood pressure in a colony of Wistar rats. The normal blood pressure in these animals ranged from 120-140mmHg. However, their starting point was identifying a male animal which consistently had a systolic blood pressure of 145-175mmHg, which they mated with a female at 130-140mmHg. After 6 generations of selecting for blood pressure and brother-sister mating, a population of rats had been produced where blood pressure was consistently >180mmHg by 20 weeks of age. Subsequent brother-sister mating was used to fix this strain, culminating in October 1969 with the SHR as we now know it (Yamori & Lovenberg, 1987).

The SHR has since been distributed world-wide, with many institutions and commercial breeders maintaining colonies 20 years or more distant from their progenitors. It can therefore be expected that significant genetic drift due to chance mutations will have occurred over this time frame, which may lead to variability in data generated from different laboratories (Yamori & Lovenberg, 1987).

The SHR has many similarities with man in the pathophysiology of hypertension. For example:

1. Blood pressure increases with age (however, onset during development in the rat).
2. Haemodynamic pattern is similar. In established hypertension both have normal cardiac output and increased total peripheral resistance.
3. Both exhibit LVH with poor correlation to blood pressure and involvement of non-haemodynamic factors.
4. Heart failure develops in a sub-set of animals at 18-24 months of age.

5. Both show increased vascular resistance across most vascular beds.
6. Impaired endothelium-dependant relaxation (as with all rat models of hypertension).
7. Increased proteinuria, decreased creatinine clearance, although renal failure has not been described in the SHR
8. Resetting of the baroreceptors (increased heart rate)
9. Salt-sensitive: further increase in blood pressure with dietary NaCl.
10. Genetic susceptibility (polygenic).
11. No known primary aetiology (95% of human hypertensives are essential)
12. Treatment that is effective in rats is usually effective in man.
13. Early neuronal involvement i.e. sympathetic nervous system.

However, unlike humans, the SHR, in common with all other rat models, does not exhibit thrombotic or atherosclerotic lesions, and has a low incidence of stroke. It also has a lower body weight than age-matched controls, whereas, there is a tendency for human hypertensives to be overweight (Frohlich, 1986; Pinto *et al.*, 1998).

The underlying defects contributing to hypertension in the SHR are poorly understood. The initiating event is thought to be an increase in peripheral resistance due to increased neurogenic vasoconstriction, which is maintained due to structural alterations in the vessel walls (Yamori & Lovenberg, 1987). Evidence for this will be discussed below. The Wistar Kyoto rat (WKY) is commonly used as a normotensive control strain for both SHR and SHRSP, but may not be ideal for the job. In the original selection by Okamoto and Aoki, 26% of WKY males and 16% of WKY females exhibited spontaneous systolic blood pressure greater than 150mmHg (Yamori & Lovenberg, 1987). This contrasts with the Sprague-Dawley strain where no rats were in this range when selecting for Lyon hypertensive animals (Vincent & Sassard, 1987). This suggests that WKY may not always be a true normotensive control. When other genetically hypertensive strains such as the Sabra rat and Milan hypertensive rat were developed, the normotensive reference strain was developed simultaneously with selection for low blood pressure (Ben-Ishay *et al.*, 1987; Ilorie *et al.*, 1986). This type of bi-directional selection was not employed for the WKY and may explain why the WKY has the highest blood pressure of any of the normotensive reference strains (Horie *et al.*, 1986). However, the WKY is the only option with the appropriate genetic background for the SHR.

The genetic homogeneity of SHRs and WKY was tested in five different breeding colonies using DNA fingerprinting with mini-satellite markers to identify areas of genetic variability, by Samani *et al.* (1989). The authors found the SHR from all sources to be identical, but WKY rats showed genetic heterogeneity. The most likely explanation is that the founding animals of the WKY colonies were distributed before they were fully inbred. The genetic heterogeneity of WKY colonies may explain, along with environmental interactions, why discrepancies occur in results comparing SHR with WKY in different laboratories. (Samani *et al.*, 1989)

1.2.3 SHRSP

Working with the SHR in 1971, Okamoto and colleagues had three main substrains. They noticed that the incidence of cerebral lesions (or stroke) was high in substrain A, but low in substrains B and C. They used this as a basis for selectively breeding the stroke-prone phenotype, using the offspring of couples in which one or both parents had developed spontaneous stroke. This was no mean feat requiring thousands of cross matings and over 10 000 offspring. Before selective breeding, the incidence of stroke in males from substrain A was 39% and was increased by the mating programme to 77%. In contrast, B and C substrains had an incidence of only 5%.

The SHRSP exhibited a more rapid increase in blood pressure compared to the SHR, and peaked at 240-250mmHg systolic compared with a maximum of 200mmHg in the SHR. In those developing strokes, the lifespan of the male was 33-41 weeks, and in the females 68 weeks (Okamoto *et al.*, 1974).

Most animals dying of stroke had macroscopically visible lesions. The most common lesion site was in the left occipital area, affecting 38%, and in the right occipital area (26%). The remainder tended to occur in the left or right frontal and medial regions. The area affected corresponded with the boundary between the main cerebral arteries, the middle cerebral and anterior or posterior cerebral artery. The authors noted a poor collateral supply in this area. Lesions included both intracerebral haemorrhage and infarction. The incidence of stroke was intricately linked with blood pressure, with large increases in blood pressure at an early age being associated with an increased incidence of stroke. However, blood pressure is not the only factor controlling stroke incidence. When fed 1% NaCl in drinking water, SHRs had a blood pressure similar to SHRSP, but still had fewer cerebral lesions (50% versus 80% in SHRSP) (Okamoto *et al.*, 1974).

Hypertensive rat models have seldom been compared directly, with most of the data coming from independent studies. However, Horie *et al.* (1986) compared seven genetically hypertensive rat strains in the same laboratory under identical conditions at 12 weeks of age. Rank blood pressure order was SHRSP>SHR>Lyon>NZ genetically hypertensive>SS/Jr>Milan>Sabra. Two populations of SHRSP were tested, one colony from Japan, another from the USA. These had systolic blood pressures of 227mmHg and 193mmHg respectively, which may suggest genetic drift in this strain. The SHRSP also had the most severe left ventricular hypertrophy when normalised to body weight and was the only strain to show a significant increase in aortic weight compared to its control at 12 weeks (Horie *et al.*, 1986). Since the SHRSP clearly has the most severe hypertension and cardiac and vascular hypertrophy, it is often used as a model of hypertension, but is obviously limited by a short life-span due to stroke.

Pathogenesis of hypertension

1.2.4 Genetics

The genetic basis of hypertension is apparent in the observation that offspring of hypertensive parents are themselves much more likely to develop hypertension. In addition, correlations between blood pressure in related individuals improves in proportion to the genetic similarity of the subjects studied. For example, blood pressure correlates are better between identical twins, than between non-identical twins (Feinleib *et al.*, 1977). In families with both adopted and biological children, parental blood pressure significantly correlates with the blood pressure of biological, but not adopted, offspring (Biron *et al.*, 1976; Mongeau *et al.*, 1986).

Several unknown genes are thought to contribute to hypertension, each with a small but additive effect. These interact with environmental factors such as stress and a high salt diet. Sensitivity to NaCl may itself be genetically controlled, and not all hypertensives are sensitive to salt. Thus, the combination of genes contributing to hypertension may differ in different ethnic populations (Burke & Motulsky, 1992).

The candidate gene approach has been utilised to link alterations in a specified gene with hypertensive phenotypes. Candidates have been selected for their known involvement in the pathophysiology of the disease e.g. RAS components, ion transport systems, and ANP. However, results have been inconsistent and no consensus has been formed on the involvement of any single gene, with the possible exception of

angiotensinogen. Total genome scans are now being used by linking traits with a large number of polymorphic markers spread throughout the genome. This approach is more powerful due to its ability to identify novel genes (Hoike & Jacob, 1998).

In genetically hypertensive rats, several putative gene loci on at least ten chromosomes have been described as cosegregating with hypertension. For SHR crosses, the loci have been described in or around genes for ACE, neuropeptide Y, nerve growth factor, renin, and substance P receptor. However, this does not prove the direct involvement of these genes as they may simply be cosegregating with other nearby genes (Dominiczak *et al.*, 1998; Hoike & Jacob, 1998). In the SHRSP, three quantitative trait loci for blood pressure have been described by this laboratory, with two found on chromosome 2 and one on chromosome 3 (Clark *et al.*, 1996).

Further work in this laboratory has demonstrated that a proportion of the genetic influence of hypertension resides in the Y chromosome. SHRSP and WKY crosses were created with the male progenitor being either SHRSP or WKY. Blood pressure in the resulting F₂ generations were measured by radiotelemetry. Those animals with an SHRSP Y chromosome had significantly higher systolic and diastolic pressures at baseline and after salt loading (Davidson *et al.*, 1995).

1.2.5 Sympathetic nervous system

An overactive sympathetic nervous system has been implicated in the pathogenesis of hypertension. There is evidence of perivascular sympathetic hyperinnervation in the pre-hypertensive SHRSP. At 30 days of age, SHRSP had significantly higher densities of adrenergic nerve fibres in the middle cerebral artery compared to WKY. This difference gradually decreased in the fully hypertensive stage. Such hyperinnervation may play a role in the development and maintenance of hypertension by increasing peripheral resistance, and similar differences have been observed in the SIIR (Kondo *et al.*, 1991).

The association of sympathetic hyperinnervation with hypertension was confirmed in a study by Brock *et al.* (1996). They injected a single dose of anti-serum to nerve growth factor (NGF) in 3-week-old SHR and WKY. They found that when blood pressure was measured at 3-4 months, mean blood pressure was significantly reduced in the SHR, while it remained normal in the WKY. This indicates that hyperinnervation is necessary to initiate hypertension in this model. More wholesale destruction of the sympathetic nervous system using sympathectomy by anti-NGF, guanethidine injections

and removal of the adrenal medulla at an early age, prevents not only hypertension, but cardiac and vascular hypertrophy too (Lee *et al.*, 1991a).

Nerve growth factor itself has been reported to be elevated in mesenteric artery, spleen and sciatic nerves, in 3 week old SHR (Ueyama *et al.*, 1992). The renin angiotensin system may participate in regulating tissue concentrations of NGF in the SHR. Infusion of exogenous angiotensin II to young WKY rats increases nerve growth factor to SHR levels. In addition, treating young SHR with Losartan completely prevents the nerve growth factor elevation (Jefferson *et al.*, 1995). It has been suggested that a decrease in sympathetic innervation could explain why ACE inhibitors can maintain lower blood pressure for some time after cessation of treatment (Charchar *et al.*, 1998).

There is also increased density of neuropeptide Y-containing nerve fibres in the mesenteric and caudal arteries of the SHR at one month and ten months old. Neuropeptide Y is vasoconstricting and is trophic for vascular smooth muscle cells, so an increase in the prehypertensive stage may have a role in the pathogenesis of hypertension (Fan *et al.*, 1995; Michel & Rascher, 1995).

In summary, there is strong evidence for activation of the sympathetic nervous system in the pre-hypertensive SHR and SHRSP, which may be an important early factor in the development of hypertension.

1.2.6 Atrial natriuretic peptide (ANP)

ANP is expressed in the normal heart with the atria being the major site of production. In normotensive WKY rats, expression of ANP mRNA in the left ventricle is only around 7% of atrial levels, with peptide concentrations at about 1%, such that 95% of secreted ANP originates from the atria (Ogawa *et al.*, 1991). Similar patterns for relative abundance have been demonstrated in normotensive human subjects (Mukoyama *et al.*, 1991; Saito *et al.*, 1989). In the SHRSP, ANP secretion from the whole heart increases by approximately 50%, particularly in the LV, which experiences a 30-fold elevation in ANP secretion, so much so in fact, that in the hypertensive heart, the LV becomes the primary source of ANP secretion (Ogawa *et al.*, 1991). The role of the natriuretic peptides in blood pressure control is outlined in figure 1.2.

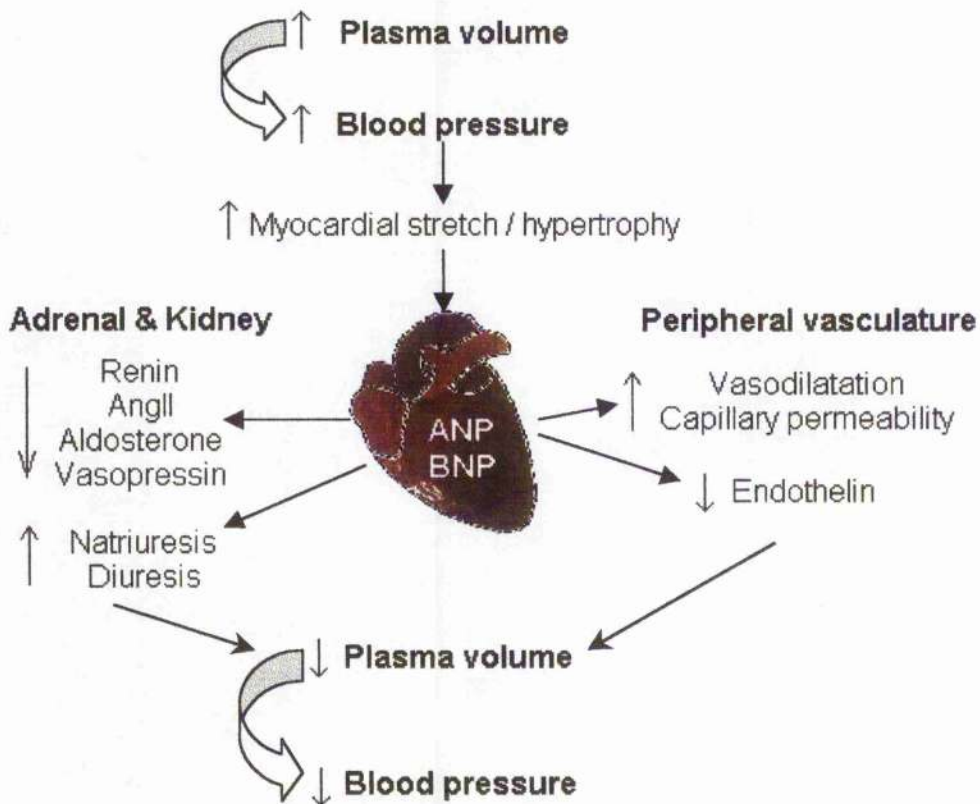


Figure 1.2 The role of natriuretic peptides in blood pressure control. Adapted from Levin *et al.* (1998).

ANP is released from the atria in response to stretch, but also from the LV when it hypertrophies. In models of renal hypertension with volume expansion (1Kidney,1Clip), there is a positive correlation between plasma ANP and blood pressure. Interestingly, within 6 hours of reversing hypertension, plasma ANP concentrations are close to normal, despite continued presence of LVH. This suggests that control of ANP secretion responds in a sensitive and dynamic way to increased atrial stretch (Garcia *et al.*, 1987). The left ventricle can also respond to stretch with secretion of ANP. In isolated perfused rat hearts, increased LV pressure elicits a stretch-dependent increase in active ANP secretion. Both hypertensive and normotensive animals can react in this way, however, there is also a significant correlation between ANP secretion and LVH in the SHR (Kinnunen *et al.*, 1992). In patients with mild untreated hypertension, ANP plasma levels may be normal, although there is a positive relationship with atrial size and LV septal thickness. In long-term treated hypertensives, ANP is generally increased and probably reflects chronic exposure to increased blood pressure or cardiac involvement (Testaert *et al.*, 1989).

Infusion of ANP is known to have acute vasodilator effects, which result in a reduced mean arterial pressure and LV filling pressure, with no change in cardiac output. By comparing the haemodynamic effects of ANP and sodium nitroprusside infusion in hypertensive subjects, Semigran *et al.* (1994) demonstrated that the haemodynamic profile of ANP is due to reduced pre- and after-load, with no direct effects on the heart to alter systolic or diastolic performance (Semigran *et al.*, 1994). However, ANP is not without effect in the heart. In normotensive rats, ANP may enhance reflex bradycardia in response to rapid blood pressure elevation via an influence on afferent cardiac vagal nerves. In the SHR, this effect is lost, and appears to be related to the presence of LVH (Thomas C.J. *et al.*, 1998). The consequences for patients with LVH is a loss of a potentially cardioprotective action of ANP to protect from rapid rises in afterload.

1.2.7 Brain natriuretic peptide (BNP)

BNP is also expressed in the normal heart, but with a different pattern of distribution. In the normotensive WKY, BNP mRNA is expressed in all four chambers. Expression in the LV is around 40% of atrial levels, but when corrected for tissue weight, it becomes clear that the LV is the dominant source of BNP in the heart, accounting for around 60% of total heart secretion (Ogawa *et al.*, 1991). This does not appear to be the case in the dog, where BNP levels in the LV are virtually undetectable, and atrial sources are dominant (Luchner *et al.*, 1998). However, the rat pattern of distribution more closely mirrors the situation in normotensive human subjects (Mukoyama *et al.*, 1991).

In the hypertensive heart from SHRSP there is a 2-fold increase in BNP mRNA expression and BNP secretory rate (Ogawa *et al.*, 1991). Brosnan *et al.* (1999b) describe significantly higher plasma concentrations of BNP in SHRSP compared to WKY. BNP gene expression is switched on in the process of myocyte cellular hypertrophy, discussed later (Molkentin *et al.*, 1998). The haemodynamic and natriuretic properties of BNP are similar to ANP.

1.2.8 Vascular function

Endothelium-dependent relaxations are impaired in the SHR and in a wide variety of other hypertensive models. This parallels the blunted response to acetylcholine found in the forearm of hypertensive patients, while responses to NO-donating vasodilators are

normal, confirming that the defect is at the endothelial level and not the smooth muscle cells. Further to this, NOS blockade (eg with L-NAME) causes less vasoconstriction in hypertensive patients than in normal controls suggesting that basal as well as stimulated release of NO is impaired (Vanhoutte, 1996). Such defects in the nitric oxide pathway have been implicated in the pathogenesis of hypertension and may contribute to the increase in peripheral resistance.

Classical organ bath studies using aortic rings have shown that endothelium-dependent relaxation in response to ACh is impaired in both SHR and SHRSP versus WKY. This dysfunction may be secondary to elevated blood pressure since it was not present in 12-week-old rats despite already being fully hypertensive (Shimamura *et al.*, 1991). Impaired endothelium-dependent relaxation and reduced basal activity of NOS have also been described for the SHRSP compared to WKY in this laboratory (McIntyre *et al.*, 1997).

Other studies suggest that impaired NO production is not the primary underlying factor in the pathogenesis of hypertension in the SHR. Indeed, Vaziri *et al.* (1998) demonstrated that NO production was actually increased in the plasma and aorta in both 3-week-old prehypertensive and 12-week-old SHR, perhaps to compensate for increased tone. At the protein level, SHRs had more eNOS and iNOS in the aorta and kidney (Vaziri *et al.*, 1998). Basal nitric oxide release is normal in the small coronary arteries (200µm in diameter) of the 20-week-old SHR, (Garcia & Bund, 1998) as measured in isolated vessels using a pressure myograph (Bund, 1998). However, conflicting results are obtained in the coronary circulation in rats of the same age when using a whole-heart Langendorff preparation. Basal and maximal coronary flow is reduced in the SHR, as is the L-NAME sensitive flow suggesting a reduced production of NO (Crabos *et al.*, 1997). It seems likely that different vascular beds and vessel sizes will produce dissimilar results, depending on their exposure to elevated pressure and shear stress (Qiu *et al.*, 1998).

Human resistance arteries from hypertensive subjects have been studied using perfusion myography of subcutaneous vessels obtained from buttock biopsies. The results obtained are in broad agreement with results from animal models. In such a study by Falloon and Heagerty (1994) endothelium-dependent relaxation to ACh was significantly impaired in hypertensive patients compared to normotensive controls, while relaxation to nitrovasodilators was unaffected. Contractions to noradrenaline were identical, but on removal of the endothelium, the increased response to

noradrenaline was significantly greater in the normotensive subjects. This suggests that endothelium-dependent relaxation is defective in hypertensive patients at the level of the endothelium, and that basal release of endothelium-derived relaxing factors (EDRFs) is lower in hypertensives (Falloon & Heagerty, 1994).

Role of superoxide

Impaired endothelium-dependent relaxation and increased basal tone may be explained by differences in nitric oxide production or availability i.e. how much nitric oxide actually reaches the smooth muscle cells. In vivo, nitric oxide may be inactivated by superoxide before it has time to diffuse to the site of action. Tschudi *et al.* (1996) used a porphyrinic microsensor to directly measure nitric oxide released from isolated third order mesenteric resistance arteries in SHRSP and WKY. On maximal stimulation of nitric oxide by calcium ionophore, the concentration of nitric oxide was significantly lower in the 15-week-old SHRSP compared to WKY. This difference was abolished in the presence of superoxide dismutase (SOD), which scavenges superoxide. This suggests that NO production is similar between SHRSP and WKY, but that NO availability is lower due to inactivation by superoxide (Tschudi *et al.*, 1996).

Grunfeld *et al.* (1995) used endothelial cells cultured from the aortas of SHRSP and WKY rats to directly measure nitric oxide production using a porphyrinic microsensor. Stimulated release of NO in response to bradykinin was much lower in the SHRSP cells at approximately one-third of WKY values. Pre-treatment with superoxide dismutase (SOD) increased NO production in both groups. However the relative increase in released NO was significantly greater from SHRSP cells suggesting the SHRSP produces more superoxide to reduce NO availability. This was confirmed by direct measurement of superoxide using a chemiluminescent technique, where SHRSP cells produced almost double the concentration of superoxide (O_2^-) than WKY cells.

These results were mirrored in organ bath studies of aortic rings. As expected, endothelium-dependent relaxation to carbachol was impaired in the SHRSP. They then added diethyldithiocarbamic acid (DECTA), an inhibitor of endogenous SOD, to quantify the accumulation of O_2^- by measuring its effect on reducing carbachol relaxations. The percentage decrease in relaxation to carbachol was greater in SHRSP aortic rings, indicating enhanced O_2^- accumulation in hypertensive animals (Grunfeld *et al.*, 1995).

An increase in O_2^- production in the SHRSP was confirmed in a further study by this group using lucigenin chemiluminescence (Kerr *et al.*, 1999). If this were the case, we would expect some benefit of antioxidant treatment in removing excess superoxide. Indeed, infusion of Vitamin C into the forearm of humans increases the response to acetylcholine presumably due to an antioxidant effect (Taddei *et al.*, 1998).

Other defects are suggested by rat models. Acetylcholine can cause contraction in quiescent aortic rings of the SHR due to release of endothelium-derived contracting factors (EDCFs), which are not observed in the WKY. These contractions can be abolished with indomethacin, indicating that EDCF's are cyclooxygenase products (Vanhoutte, 1996). A similar effect is observed in the mesenteric arteries of the SHRSP (Sunano *et al.*, 1999), and in hypertensive subjects where indomethacin can restore normal responses to infused acetylcholine (Vanhoutte, 1996). It has been increasingly realised in recent years that the endothelium releases hyperpolarising factors (EDHF) which may participate in normal relaxation of some arteries, and may be reduced in hypertensive animals (Taddei *et al.*, 1998). Using electrophysiological techniques, Sunano *et al.* (1999), observed that the hyperpolarisation in response to acetylcholine was smaller in the SHRSP compared to WKY, implicating that a reduced release of EDHF contributes to vascular dysfunction in the SHRSP.

Significance of endothelial dysfunction

Endothelial dysfunction is associated with increased cardiovascular risk and further deteriorates if associated with other risk factors such as ageing, diabetes mellitus, smoking and post-menopause. This close association with risk is probably related to the loss of the inhibitory effects of NO on platelet aggregation, smooth muscle cell proliferation and expression of adhesion molecules. Thus loss of NO availability promotes thrombosis and atherosclerosis. This suggests that correcting endothelial dysfunction should be a major goal of antihypertensive treatment in order to reduce long-term cardiovascular risk. Successful treatment must specifically correct NO availability and not simply improve endothelium-dependent relaxations (Taddei *et al.*, 1998). ACE inhibitors may improve vascular function in two ways by preventing the local production of the potent vasoconstrictor AngII, and preventing the breakdown of vascular bradykinin. (Vanhoutte, 1996). However, even after two to three years of ACE inhibition, relaxation to acetylcholine was improved, but not normalised in patients with

essential hypertension. This may be explained by a genetic component to endothelial dysfunction. Impaired acetylcholine relaxations have been observed in young normotensive offspring of patients with essential hypertension (Taddei *et al.*, 1998).

To summarise, impaired endothelium-dependent relaxation probably occurs secondary to hypertension. NO production may be normal or even elevated in the young SHR, but deteriorates with age until marked defects in the L-Arginine/NO axis may become apparent. Both a decrease in NO production and decreased availability may be involved in the advanced stages.

1.2.9 Vascular structure

Hypertension is characterised by an increased total peripheral resistance (Struyker Boudier *et al.*, 1990). Elevated neurohormonal output is thought to increase blood pressure, which results in structural adaptations in the vasculature such that blood pressure is maintained or deteriorates (Mulvany, 1991). The structural alterations governing this consist of:

- 1) Reduction in lumen diameter of arterioles and resistance arteries
- 2) An increase in arterial wall mass
- 3) Rarefaction of arterioles and capillaries (fewer parallel vessels and/or , reduction in vessel number)

The relative importance of structural versus functional abnormalities is poorly understood (Struyker Boudier *et al.*, 1990; Mulvany, 1991). However, structural changes need not be great to have a powerful effect, as vascular resistance is determined by Poiseuille's law:

$$\underline{1.8nL}$$

$$R = N \pi r^4$$

Where N = number of blood vessels

L = length of vessels

n = viscosity of blood

r = radius of the vessel

R = total resistance

Therefore, a small change in lumen diameter can have large effects on resistance, as the relationship is to the power of four.

Vascular remodelling

The term “remodelling” was originally coined to describe a change in wall/lumen ratio with no change in media cross sectional area, i.e. rearrangement of material around a smaller or larger lumen. Since then “remodelling” has been used to describe any structural alteration in blood vessels. In order to restore descriptive power to the term, Mulvany *et al.* (1996) suggested a new terminology with recent modifications (Mulvany, 1999). This is shown below in figure 1.3.

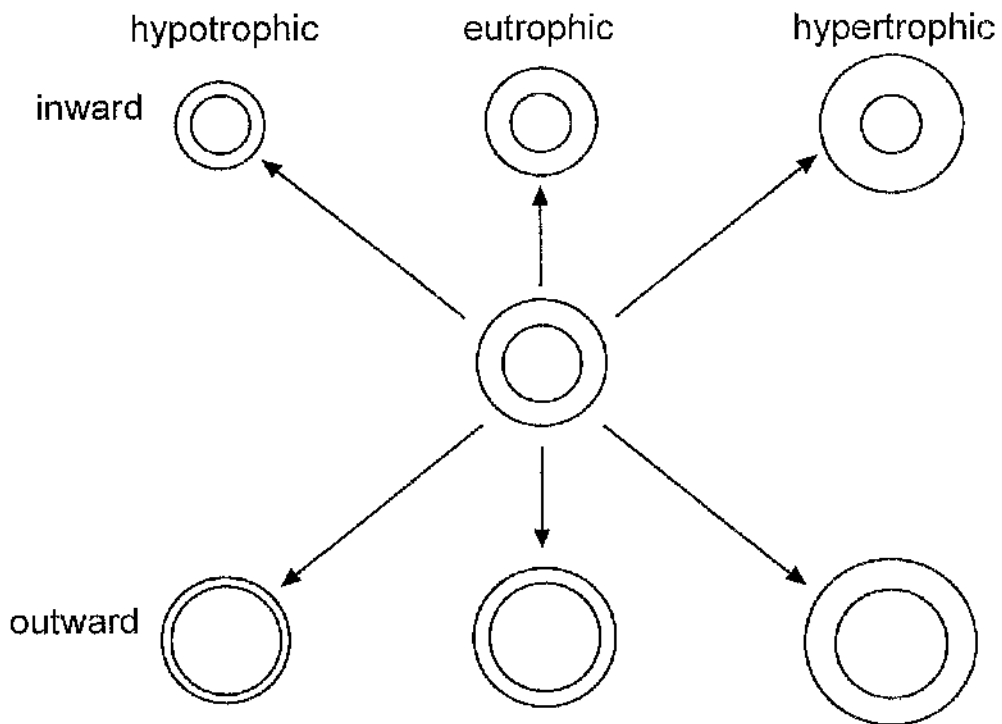


Figure 1.3 The Mulvany nomenclature for describing re-modelling of blood vessels in cross-section from the central starting point (reproduced from Mulvany, 1999).

In brief, they proposed that remodelling could result in inward or outward remodelling of the lumen diameter and be subclassified as hypotrophic (decrease in cross sectional area), eutrophic (no change in cross sectional area) or hypertrophic (increase in cross sectional area) (Mulvany, 1999).

They also included some important clarifications:

- 1) That the term remodelling only truly applies to changes that occur in one vessel e.g. before and after an intervention, or pathology, and not between. For example age-

matched normotensive and hypertensive. When used in this context, remodelling describes a "difference in development" as the hypertensive artery may never have been identical to the normotensive and so it is wrong to say that it has remodelled from it.

- 2) Remodelling of an artery is not necessarily towards a pathogenic state. It may for instance describe an element of normal growth.
- 3) Eutrophic remodelling describes a situation of no net change in cross sectional area. This does not preclude considerable structural alterations which balance each other out e.g. smooth muscle cell hypertrophy and apoptosis resulting in no net change (Mulvany, 1999).

However, a consensus view has yet to be established on the proposed terminology, which provoked considerable debate when first published. In the ensuing correspondence, a number of pertinent points were raised which are worth mentioning here. In the SHR (and SHRSP) hypertensive remodelling occurs at a young age and so is superimposed upon a growing and developing vasculature and is therefore not simply a rearrangement of materials (Korner & Angus, 1997). The remodelling process is therefore likely to be different from human arteries, where alterations in response to hypertension develop within a mature vasculature, and may be a product of many years of elevated blood pressure.

With regard to the nomenclature, Lee *et al.* (1997) make several important points. Firstly, there is no agreement on standard methods for measuring structural changes. Thus, results may be method dependent. Wire-myography requires stretching the vessel on wires, which is distinctly non-physiological. Pressure-myography may cause vessel elongation thereby affecting lumen size, and there is no agreement on intravascular pressure at which to take measurements. Lee *et al.* conclude that *in situ* methods such as intravital microscopy or confocal microscopy of pressure-fixed vessels represent the best techniques for quantifying structure in the relaxed state. Secondly, Lee and colleagues highlight that the Mulvany terminology fails to include scenarios where no change in lumen diameter occurs.

In a commentary by Folkow (1997) he questions the pre-occupation with wall thickness and stresses the importance of inner radius (r_i), as it is r_i that determines vascular resistance and therefore flow. Folkow makes the reasonable suggestion that remodelling can be adequately described by simply stating percentage changes in r_i and

wall/ t_1 ratio, which is far more descriptive, and provides quantitative information on haemodynamics.

Differences of structural adaptations often occur between different vascular beds. Given the number of factors that may control vascular growth, this should not be surprising e.g. growth factors, neurotransmitters, hormones, cytokines, extracellular matrix components, mechanical stimuli, and local autocrine factors (Daemen & de Mey, 1995). It would be remarkable if all these factors maintained similar profiles regardless of the organs they serve. This point is illustrated in table 1.3, which lists some of the ways in which the vascular endothelium can effect vascular growth.

Table 1.3 Possible mechanism for endothelial control of vascular growth

Effect of endothelium	Example
Shields smooth muscle cells from circulating growth factors	Insulin, IGF, growth hormone
Shields smooth muscle cells from platelet-derived growth factors	PDGF, TGF- β
Controls monocyte and T lymphocyte infiltration, therefore controls exposure to cytokines	IL-1, IL-2, IL-6
Local ACE monoamine oxidase activity	Ang II, 5-HT
Production of growth promoters	EGF, FGF, IL-1, IL-6, PDGF, endothelin
Production of growth inhibitors	TGF- β , interferon- γ , PGI $_2$
Respond to haemodynamic changes, therefore affects wall/lumen ratio	Blood flow, shear stress → Control lumen diameter by release of PGI $_2$, NO etc.

Compiled from Struyker Boudier *et al.*, 1990; Owens, 1989.

Resistance arteries

Resistance arteries have been defined as pre-capillary arterics with internal diameter no greater than 500 μ m. They are so called, as it is in these small arteries where the increased peripheral resistance of essential hypertension is thought to reside (Heagerty *et al.*, 1993). Pressure measurements in the SHR from aorta to capillaries suggests that

the greatest resistance to blood flow resides in the small arteries and more distal arterioles (Mulvany, 1991).

In a study by Aalkjaer *et al.*, (1987), resistance arteries were obtained by subcutaneous biopsy from subjects with essential hypertension, and mounted on a myograph. Vessels from hypertensives had an increased media/lumen ratio and gave an increased maximal response to all contractile agonists tested, with no change in sensitivity. This increase was directly related to greater media thickness as active media stress (force per CSA of smooth muscle) was normal (Mulvany, 1991a). Likewise in the SHR, as a consequence of increases in media-to-lumen ratio, the maximum force generated in response to contractile agonists is higher (Mulvany, 1991b). This increase in wall/lumen ratio is most prominent in vessels larger than 100 μ m lumenal diameter (Mulvany, 1991a).

Structural alterations may be a result of growth or loss of material, or as rearrangement of existing material (remodelling). Vascular smooth muscle cells in the SHR are not thought to exhibit hypertrophy, i.e. individual cell volume does not change. Likewise in human subcutaneous resistance arteries re-organisation of existing material probably accounts for medial changes (Mulvany, 1991b). In human essential hypertension, most evidence suggests that resistance vessels exhibit inward eutrophic remodelling. That is, a rearrangement of existing material around a smaller lumen (Mulvany, 1999).

However, data from this laboratory using confocal microscopy, has demonstrated hypertrophic inward remodelling in the mesenteric resistance arteries of the SHRSP. Compared to WKY, lumen diameter was decreased, while wall CSA and thickness increased, indicating an increase in material. This was not due to smooth muscle cell hyperplasia as there was no change in cell number (Arribas *et al.*, 1997). The same group, (Arribas *et al.* (1996) used the same technique in basilar arteries of SHRSP versus WKY. The pattern of remodelling was similar. Uniquely, they also discovered smooth muscle cell disorientation in the SHRSP, (normal smooth muscle cells lie perpendicular to the longitudinal axis of the vessel), which they speculated may represent a weakness in the vessel and therefore could contribute to the pathogenesis of stroke in the SHRSP.

There is a wealth of evidence implicating AngII in vascular remodelling. Infusion of AngII results in hypertrophy of rat mesenteric resistance arteries (Daemen & de Mey, 1995), and resistance artery hypertrophy is regressed by ACE inhibitors, but not hydralazine (Struyker Boudier *et al.*, 1990). Treatment, with ACE inhibitors, results in outward hypotrophic remodelling (Mulvany, 1999).

Conduit arteries

During hypertension, flow-rate in large arteries is unchanged, and therefore so is lumen diameter. The media exhibits hypertrophy and hyperplasia to compensate for the elevated pressure i.e. to normalise wall-stress (Mulvany, 1999).

In the aorta of SHRSP, vascular smooth muscle cells exhibit polyploidy (multiple DNA copies in the absence of cell division) suggesting an increased cell mass. This can be prevented by treatment with perindopril or losartan (Dominiczak *et al.*, 1996). Since a hypotensive dose of hydrochlorothiazide + hydralazine is ineffective in this regard, this indicates a role for AngII in smooth muscle cell hypertrophy independent of elevated blood pressure (Devlin *et al.*, 1995).

AngII could regulate vascular growth in several ways; 1) a direct trophic action on smooth muscle cells, 2) by releasing neuropeptides and/or growth factors, 3) via mechanical forces produced during AngII vasoconstriction (Owens, 1989). AngII does not produce proliferation in rat aortic smooth muscle cells cultured in serum-free medium, but does result in cellular hypertrophy with associated protein synthesis. In the presence of serum, there have been conflicting reports stating that growth rates are either normal or greater with AngII present (Owens, 1989). In organoid culture of rat aortic segments, AngII stimulates protein synthesis but not DNA synthesis i.e. hypertrophy not hyperplasia, even under conditions of passive stretch (Holycross *et al.*, 1993).

There is good evidence for a local renin angiotensin system in the vascular wall. On a molecular level, all the necessary components have been described e.g. angiotensinogen, ACE and AT-receptors (Min *et al.*, 1993). On a functional level, ACE inhibitors can relax vessels *in vitro*. Also, the local tissue RAS can alter tone in vessels downstream. In an elegant study using carotid (donor vessel) and mesenteric resistance artery (recipient) perfused in series, AngII was released from the carotid to cause constriction in the recipient. Blocking this with ACE inhibitors increased the diameter of the recipient artery (Henrion *et al.*, 1997).

The carotid artery of hypertensive rats exhibits reduced compliance (dv/dP) i.e. a stiffer vessel wall. Vasomotor tone is one component of this, as compliance increases when smooth muscle cells are poisoned with potassium cyanide. However, compliance remains lower than normotensive animals, indicating an influence of underlying structural changes. Alterations in the elastin-to-collagen ratio are thought to be

intimately involved in this process, as these components contribute considerably to the mechanical properties of the vessel. For example, collagen content has been found to increase with both age and hypertension thereby stiffening the vessel wall. In man concomitant atherosclerosis may play a contributory role (Safar *et al.*, 1992).

The consequences of reduced large artery compliance are an increase in pulse pressure, which in the older patient is an independent risk factor for LVH and coronary heart disease (Safar *et al.*, 1992). Likewise, elevated pulse pressure was found to be a major predictor of LVH in a F₂ cohort of a SHRSP x WKY cross (Dominiczak *et al.*, 1996).

Microcirculation

The structure of the microcirculation may also be altered in the hypertensive state via a variety of mechanisms e.g. increased tone, temporary shut-down of microvascular networks or rarefaction of capillaries and terminal arterioles. The microcirculation consists of arterioles and capillaries distal to the resistance arteries with a diameter of less than 120µm. It functions to maintain optimal hydrostatic pressure to allow efficient capillary transfer. The blood pressure entering the microcirculation is a matter of continuing debate, and may range anywhere from 35-90mmHg depending on tissue and species studied. There is however, consensus that by the level of the capillaries, no difference in blood pressure is observed between hypertensives and normotensives. Therefore, the microcirculation must be responsible for a considerable proportion of the pressure gradient (Vicaut, 1992). As with the resistance arteries, the microcirculation of hypertensive rats demonstrates an impaired endothelium-dependent relaxation. For example, the very small pre-capillary arterioles in skeletal muscle have increased vascular tone in the SHR versus WKY, as measured by dilatation to locally applied vasodilators using intravital microscopy (Schmid-Schönbein, 1987). Changes in media-to-lumen ratio or medial CSA may also occur but are highly variable between and even within, vascular beds. The mechanisms involved are likely to be similar to those discussed above for resistance arteries (Vicaut, 1992).

A potentially important additional mechanism is arteriolar rarefaction. This has been described in the skeletal muscles of genetic and renal hypertensive models, whereby constriction of terminal arterioles occludes the vessel to such an extent, that erythrocytes can no longer pass (Vicaut, 1992). This has also been described in the fingers of patients with moderate hypertension, where both temporary closure and anatomical absence of capillaries were noted (Antonios *et al.*, 1999). Such closure of

whole vessels may have consequences for end-organ damage. For example, reduction in capillary density due to rarefaction may significantly increase oxygen diffusion pathways, affecting the ability of the circulation to meet tissue oxygen demands at times of increased metabolic need. This may sensitise tissue to hypoxic damage (Vicaut, 1992).

Coronary arteries

Vascular changes in the left anterior descending (LAD) coronary artery occur early in the development of hypertension in the SHR, mirroring the early rise in LVH. At 45-days-old, Anversa *et al.* (1984) demonstrated marked fibrotic changes within the arterial wall with a 119% increase in collagen and ground substance. In addition, elastin increased 77% and smooth muscle mass by 34% compared to age-matched WKY. These changes were not observed at 28 days when blood pressure was already higher in the SHR. This suggests that such alterations occur secondary to hypertension, but early enough (at 6 weeks) to influence blood pressure development, which does not peak until 12 weeks. Changes in structural proteins such as collagen and elastin may reduce vascular compliance, while smooth muscle cell mass may alter media-to-lumen ratio. The role of these changes in end-organ damage e.g. MI and heart failure, needs to be assessed. These findings have been confirmed in twenty-week-old SHR (Crabos *et al.*, 1997). Coronary flow-pressure curves in isolated perfused hearts indicate that in coronary resistance vessels the media encroaches into the lumen even when maximally dilated and at normal vascular tone (Hallback-Nordlander *et al.*, 1979).

Cause or effect?

Whether structural changes have a primary role in the pathogenesis of blood pressure or represent a secondary adaptation is open to debate. Increased media thickness of small arteries has been described prior to blood pressure elevation in the SHR. However, some commentators deny the existence of a prehypertensive stage in the SHR, stating that blood pressure is always higher than WKY (Mulvany, 1991). The rate of blood pressure rise after antihypertensive treatment may provide an indirect method of assessing importance of structural changes. In the SHR, hydralazine has minimal effect on mesenteric resistance artery wall/lumen ratio and blood pressure rises rapidly after discontinuing treatment. In contrast, captopril is much more effective in normalising wall/lumen ratio and elevated blood pressure returns slowly when treatment is stopped.

(Mulvany, 1991) However, given the multivarious mechanisms of ACE inhibition caution must be applied in interpreting such data in this way.

Early treatment of SHR with ACE inhibitors or AT₁ receptor antagonists for 10 weeks from weaning prevents the elevation in blood pressure that normally occurs in the first 12 weeks of life. Upon cessation of treatment, a small residual antihypertensive effect is observed for up to 30 weeks, which does not occur when treatment is with β -blockers, vasodilators, or calcium-channel antagonists (Mulvany, 1991). This indicates a role for AngII in the developmental stage of hypertension that has long-term implications for maintenance of elevated blood pressure. Mesenteric resistance arteries from these treated animals had a reduced media-to-lumen ratio as measured by wire myography. However, animals treated for four weeks post-weaning exhibited a similar long-term antihypertensive benefit with no reduction in media-to-lumen ratio, suggesting that small artery structural changes do not account for the long-term effects on blood pressure control (Mulvany, 1991).

To examine the question of whether structural changes are a cause or consequence of raised blood pressure, a partial ligation of the iliac artery has been used in the 5-week-old SHR, such that distal to the ligation intravascular pressure was normal. Small femoral arteries from this distal portion were comparable to WKY vessels, while small arteries from the control hypertensive leg had a reduced internal diameter and increased media thickness. Thus, vessels from the same genetically hypertensive animal exhibit remodelling only when exposed to elevated blood pressure, suggesting structural changes are a secondary adaptation (Heagerty *et al.*, 1993).

Regardless of structural changes, it appears that certain factors can override any effect they may have. For example, blood pressure in renal hypertensive rats (1K1C) returns to normal within hours of removing the clip, despite structural wall changes in the vasculature. A renal vasodilating factor has been implicated. Similarly, AngII infusion causes gradual rise in blood pressure over ten days accompanied with structural alterations in small arteries. However, blood pressure falls rapidly on stopping the infusion (Mulvany, 1991) This is evidence against a primary fundamental importance of vascular structural remodelling in the hypertensive state.

1.3 Cardiac hypertrophy

As discussed earlier, cardiac hypertrophy is a common consequence of hypertension in response to pressure overload. In hypertensive patients, cardiac hypertrophy is an independent risk factor for increased cardiovascular mortality (Levy *et al.*, 1990). The same process of hypertrophy is also observed in the surviving myocardium after myocardial infarction to compensate for loss of function. It seems likely, therefore, that maladaptive cardiac hypertrophy is one of the most important factors in the progressive deterioration in left ventricular function observed in hypertensive heart disease.

In discussing the pathophysiology of cardiac hypertrophy it is important to recognise a number of interacting factors. The hypertrophic response involves cardiomyocytes and non-myocytes and is linked to perivascular and interstitial fibrosis. The process of hypertrophy is not confined simply to enlargement of existing cells, but includes a shift to foetal isoforms of proteins that may be important in contraction. The relative roles of hypertrophic stimuli need to be examined. For example, the importance of pressure-overload or wall-stress compared to the pro-mitogenic effects of neurohumoral factors such as noradrenaline, angiotensin II or endothelin. Other systems may be in place to counteract these effects, and so keep hypertrophy in check e.g. nitric oxide and bradykinin. Hypertrophy may require the presence of permissive factors such as growth hormones or genetic susceptibility. In recent years progress has been made on elucidating intracellular signalling pathways that link the hypertrophic stimuli on the cell surface with changes in myocyte gene expression. All these factors will be discussed below with particular emphasis on disease progression.

1.3.1 The hypertrophic response

Hypertrophy may be defined at the organ level as an increase in LV internal diameter and/or wall thickness (Levy, 1991), or at a cellular level as an increase in cell size without cell division (Izumo & Aoki, 1998). Most commentators hold to the belief that cell division does not occur in myocytes after 3 weeks of age. Hypertrophy of myocytes and non-myocytes and hyperplasia of non-myocytes accounts for increased LV mass after this point (Tanase *et al.* (1982b). It is possible to distinguish between hypertrophy and hyperplasia as the latter involves an increase in DNA content per milligram tissue.

Not only do myocytes hypertrophy by increasing cross-sectional area they also change cellular composition, with a shift from adult to foetal phenotypes of several contractile and structural proteins. In the untreated SHRSP, gene expressions of the foetal contractile proteins skeletal α -actin and β -myosin heavy chain (β -MHC) are increased, while mRNA for the adult isogene, α -MHC, is decreased (Kim *et al.*, 1996). There is a strong positive relationship between LV α -MHC protein content and maximum rate of pressure development in rat hearts *in vitro* (Boluyt *et al.*, 1991). Such changes may result in significant alterations in contractile performance, and represent a mechanism for the progressive deterioration of cardiac function leading to heart failure. Concomitant changes occur in molecules involved in interstitial fibrosis. For example, there is an increase in collagen type IV gene expression and in transforming growth factor- β 1 (TGF- β 1) mRNA, which are known to stimulate collagen production. Interstitial fibrosis may lead to diastolic dysfunction by altering myocardial stiffness, thereby impairing left ventricular relaxation. There is also a 7.5 fold increase in ANP gene expression in the left ventricle of SHRSP compared to WKY (Kim *et al.*, 1996). Similar results are obtained with LVH due to aortic banding in the mouse, with upregulation of gene expression of ANP, BNP, β -MHC, and a down-regulation of SERCA (sarcoplasmic-endoplasmic reticulum calcium ATPase) (Harada *et al.*, 1998), and after myocardial infarction in the rat (Reiss *et al.*, 1993), indicating that such changes occur across species and aetiologies.

1.3.2 Apoptosis in hypertrophy

The apoptotic index is higher in the heart of the SHR at 8- 16- and 30-weeks-old versus WKY controls (Hamet *et al.*, 1995). This has been confirmed in the LV at 30-weeks, when the majority of affected cells were identified as myocytes. This could be prevented by treatment with losartan, even in animals where blood pressure was not normalised, suggesting blockade of AT₁-receptors prevents apoptosis in the heart independent of haemodynamic effects (Fortuno *et al.*, 1998). This does not necessarily directly implicate AngII, as AT₁-receptor blockade will effect other parameters such as ANP. Similarly, induction of apoptosis is more pronounced in cultures of vascular smooth muscle cells from the SHR (Hamet *et al.*, 1995). Therefore, at a time of active LV hypertrophy in the SHR, this is counterbalanced by an increase in apoptosis, suggesting a role in cardiac remodelling.

1.3.3 LV function in hypertrophied hearts

When we talk about the hypertrophied heart being compensated, it means that despite the structural changes and increased afterload, systolic function is uncompromised. Indeed, the process of myocyte hypertrophy is a compensatory response to maintain function when faced with a prolonged increase in afterload. For instance, in isolated perfused hearts, maximal cardiac performance at high afterloads is better in hypertrophied SHR hearts than in hearts from normotensive animals. At any given pressure, the average tension per unit layer of cardiac muscle is actually lower than in non-hypertrophied myocardium. The structural adaptation of wall thickening allows normal stroke volume to be produced despite pumping against an increased arterial pressure. However, hypertrophy does result in a rightward shift in the Frank-Starling mechanism i.e. the SHR has a lower stroke volume at diastolic filling pressures under 10mmHg. This is compensated for by doubling the left atrial pressure to 10mmHg, at which stroke volume is almost normalised (Hallback-Nordlander *et al.*, 1979). A similar picture of well compensated LV hypertrophy was described by Pfeffer *et al.* (1979) for the 6 month old SHR *in vivo*. They found no difference between SHR and normotensive controls for rate of developed pressure, stroke volume, end-diastolic volume, ejection fraction or maximum acceleration of aortic blood flow, indicating normal systolic function. Only peak developed pressure was higher in the SHR, which of course is necessary to pump normal stroke volumes against the increased afterload. More recently, echocardiography has been used in animal models to assess systolic function *in vivo*, and the results are consistent. Four to five weeks after aortic banding of the abdominal aorta in rats, LV mass is increased by 35%, but the heart remains well compensated. There are no changes in systolic or diastolic cavity dimensions, fractional shortening, ejection fraction or cardiac index and Doppler flow velocities through the aortic root and pulmonary valve are normal (Pawlush *et al.*, 1993).

With time, for reasons that are poorly understood, the hypertrophied heart is no longer able to maintain normal function, and this is termed decompensation. Systolic function may get progressively worse and when the heart can no longer meet the energy demands of the body, the heart is said to be in failure. By 18 months of age, SHRs exhibit signs of cardiac decompensation. In males, left ventricular end diastolic pressure (LVEDP) is elevated, maximum stroke volume is decreased, as is ejection fraction from 73% in 6 month old animals to 44%. There is also marked LV dilatation as end-diastolic volume

increases, while $-dP/dt$, an indicator of ventricular relaxation, is normal. In short, systolic function is impaired while diastolic function is normal (Pfeffer *et al.*, 1979). Factors influencing decompensation and the consequences for the failing heart will be discussed later in this section.

Age is a major risk factor for cardiac hypertrophy (Levy, 1991), and the functional outcome of hypertrophy may also be less favourable. After aortic constriction in adult Fischer 344 rats, mild cardiac hypertrophy was associated with an increase in pressure-generating capacity, representing a beneficial adaptive response. However, the same procedure in aged rats (25-28 months) resulted in a decrease in pressure-generating capacity. The reasons for this age-related difference in adaptation are unknown, although aged-rats already have a lower proportion of α -MHC in the left ventricle (Boluyt *et al.*, 1989).

1.3.4 Influence of blood pressure

In both animal studies and man it is a common finding that blood pressure exhibits a poor correlation with LV mass. Although measuring ambulatory or maximum blood pressure during exercise achieves some improvement, the correlation coefficient typically remains around 0.50-0.65 (Devereux *et al.*, 1991), and the correlation with diastolic pressure is even weaker (Devereux *et al.*, 1987). This suggests that although elevated blood pressure may be a trigger, it is not the sole determinant of hypertrophy.

Blood pressure may not even be the initiating trigger in animal models of hypertension. In both the SHRSP and SHR, cardiac hypertrophy compared to WKY rats has been reported as young as 30 days when there is still no difference in blood pressure (Yamori *et al.*, 1979). Although this result depends on the accuracy of measuring blood pressure in such young animals, it suggests greater importance for genetic or other trophic factors in determining LVH.

It is perhaps unsurprising that LV mass correlates poorly in established hypertension. Pfeffer *et al.* (1979a) found that 6 month old female SHRs exhibited an increased LV mass of 25% compared to normotensive controls, and that 18 month old SHRs showed 64% more hypertrophy, despite no further increase in blood pressure. Other factors must be involved in the continued increase in LV mass. A lack of dependence on blood pressure is also indicated in the SHR after peripheral sympathectomy. In that model, the elevation in blood pressure is prevented, and yet LV mass continues to rise

(Cuttilletta *et al.*, 1977). In a similar fashion, hydralazine may control blood pressure in the SHR but does not prevent LVH (Jespersen *et al.*, 1985). Therefore, an increase in systolic blood pressure is not a requirement for LVH in the SHR.

In man, a clear relationship is also elusive. In one study examining normal and mildly hypertensive patients, combining measures of stroke volume and LV contractility with arterial pressure, gave a good correlation co-efficient with LV mass of 0.82. Neither parameter alone had a correlation co-efficient above 0.60, and this demonstrates that cardiac performance may also influence the hypertrophic response (Devereux *et al.*, 1991). This makes sense as a decrease in function after myocardial infarction is a trigger for hypertrophy (discussed later).

1.3.5 Influence of genetics

Tanase *et al.* (1982a) attempted to quantify the extent to which LV mass is determined by genetics. In a large study of 23 inbred rat strains (including SHR & SHRSP), segregation analysis estimated that between 65-75% of the variability in LV mass was attributable to genetic causes. This suggests that genetic factors are more influential than blood pressure in determining heart weight. Analysis of normotensive strains alone showed a similarly large influence of genetic factors. It is not clear, therefore, from this study whether genetic influence plays a greater role in the development of hypertrophy compared to determination of normal heart weight. The authors conclude that LV mass is a highly heritable trait.

Since then, a number of studies have used the candidate gene approach to identify genetic loci that co-segregate with LV hypertrophy, independent of blood pressure. These include loci in or around the ACE gene on chromosome 10, the ET-3 gene on chromosome 3 and the renin gene on chromosome 13. Genome wide scans have identified a QTL on chromosome 17 that is protective for LVH, and a QTL on chromosome 14 in the SHRSP, which is a susceptibility gene (reviewed in Dominiczak *et al.*, 1997).

1.3.6 Role of the renin-angiotensin system

Neurohumoral activation during hypertension or after myocardial infarction is thought to have an important role in determining cardiac hypertrophy. A great deal of evidence exists to implicate activation of the RAS and in particular angiotensin II in this process. This has been strengthened by the discovery of a local cardiac RAS. Protein and

mRNA expression of renin, angiotensinogen, ACE, and AT₁ receptors have all been identified in the heart (Yamazaki & Yazaki, 1997). Stretching cardiomyocytes in culture has been shown to stimulate secretion of AngII directly from secretory granules in the ventricular myocytes, the concentration of which is high enough to trigger the hypertrophic response. There is concomitant increase in angiotensinogen and ANP gene expression and of proto-oncogenes associated with hypertrophy. An AT₁ receptor antagonist, but not an AT₂ receptor antagonist, nor antagonists of α - or β -adrenoceptors could prevent these responses (Sadoshima *et al.*, 1993).

This autocrine action of AngII in the heart may explain why ACE inhibitors are so effective at regressing LVH in low renin-dependent models of hypertension such as the SHRSP (Kim *et al.*, 1996), and in patients with essential hypertension despite a normal or decreased plasma renin activity (Trippodo & Frohlich, 1981). Indeed, experimental hypertrophy in the rat correlates with myocardial AngII levels (Johnston, 1994), and the cardiac RAS is activated with increased mRNA for angiotensinogen, ACE and the AT₁ receptor (Yamazaki & Yazaki, 1997). This mechanism is not unique to pressure-overload hypertrophy. Activation of the cardiac RAS also occurs within three days of myocardial infarction in the rat, when there is an increase in AngII receptor mRNA, and a 44% increase in AngII receptors measured by radioligand binding (Reiss *et al.*, 1993). However, over the time period that SHR and SHRSP develop LVH, plasma AngII concentration is not elevated (Campbell *et al.*, 1995; Devlin *et al.*, 1995).

Conflicting results for the role of tissue RAS have been obtained in the SHR, when compared to normotensive Donryu rats at 6, 10 and 20 weeks of age. The authors found the SHR to have lower plasma renin and ACE activity, and importantly lower AngII tissue levels in the adrenal, aorta, brown adipose tissue, lung and similar levels in kidney and heart (Campbell *et al.*, 1995). Therefore, hypertrophy in SHR does not appear to be due to increased plasma or tissue AngII. However, this does not exclude AngII acting as a permissive factor for LV hypertrophy.

The property of ACE inhibitors and AT₁ receptor antagonists to regress cardiac hypertrophy over and above their effect on blood pressure is one of the most convincing arguments for the intimate involvement of AngII in the hypertrophic response. These drugs can lower LV mass at subpressor doses (Yamazaki & Yazaki, 1997). After aortic banding in rats, a low dose of enalapril totally prevented LVH despite having no effect on blood pressure. After surgery, plasma levels of angiotensin I and renin were elevated

only transiently, suggesting that any hypertrophic effect of AngII was due to local tissue conversion. This was reinforced by finding increased angiotensinogen mRNA in the hypertrophied LV (Baker *et al.*, 1990). In a similar fashion, again in aortic-banded rats, low dose ramipril prevented LVH despite an increased blood pressure (Linz & Schölkens, 1992). Chronic administration of the same non-hypotensive dose of ramipril was studied in SHRSP. After 15 weeks of treatment these animals exhibited myocyte hypertrophy and interstitial fibrosis and changes to foetal gene expression characteristic of LVH. However, these changes were prevented in rats given an antihypertensive dose of ramipril (Zimmerman *et al.*, 1999). Therefore low dose ACE inhibition may be sufficient to prevent LVH despite elevated blood pressure in the short term, but ultimately loses efficacy with time. Possible explanations for this may be 1) influence of blood pressure on LVH increases with length of exposure, 2) difference in models, genetic hypertension versus acute surgical, 3) other trophic mechanisms gain in influence.

In the SHRSP, the AT₁-receptor antagonist, losartan, caused a significantly greater reduction in LV mass compared to a calcium channel blocker, despite an identical effect in lowering blood pressure (Kim *et al.*, 1996). This effect is also observed in man. A recent meta-analysis of published randomised double blind clinical trials examined the effectiveness of anti-hypertensive medication to regress cardiac hypertrophy. ACE inhibitors were found to be the most effective in this regard with an average 13% decrease in LV mass, compared with 9% for calcium channel blockers, and only 7% and 6% for diuretics and β -blockers respectively (Schneider *et al.*, 1996).

Another important finding is that administration of exogenous AngII mimics the hypertrophic responses to pressure overload. Kim *et al.* (1995) infused low dose AngII in rats. After 24 hours, gene expression of skeletal α -actin, β -MHC, ANP and fibronectin were all increased, and by three days TGF- β 1 and collagen types I and III were also increased, as was LV mass. An AT₁ receptor antagonist prevented these changes in LV mass and gene expression, while hydralazine did not, despite normalisation of blood pressure (Kim *et al.*, 1995). This strengthens the assertion that Ang II contributes to hypertrophic remodelling *in vivo* independent of blood pressure. The transgenic rat TGR(mRen2)27 has been used in this laboratory to examine the effect of over expression of the renin gene. As expected, these animals have elevated

systolic blood pressure, LVH and increased plasma concentrations of AngII and renin. Further, the extent of cardiac hypertrophy was positively related to the number of copies of the renin gene (Brosnan *et al.*, 1999a).

Despite the wealth of evidence implicating a central role for AngII in the development of all kinds of cardiac hypertrophy, it appears that its role is not obligatory, and that the heart can hypertrophy perfectly well without it. Knockout mice lacking the AT_{1A} receptor which were subjected to aortic banding developed LVH, with associated switch to foetal gene expression, identical to the wild type controls. This result was not due to an ineffective knockout, as infusion of AngII resulted in LVH in wild type but not knockout mice (Harada *et al.*, 1998).

1.3.7 Adrenergic stimulation

An increase in noradrenaline turnover has been observed in the SHR at 30 to 60 days old, before blood pressure increases. This has led to speculation that the adrenergic system may be involved in LVH in this model (Yamori *et al.*, 1979). This is apparently contradicted since LVH is not prevented in the SHR by peripheral sympathectomy using nerve growth factor antiserum, despite preventing the increase in blood pressure (Cuttilletta *et al.*, 1977). However, this procedure causes compensatory catecholamine release from the adrenal medulla, which may be responsible for LVH (Yamori *et al.*, 1979).

Further evidence for adrenergic involvement has been obtained from experiments on cultured cardiomyocytes. Cardiomyocytes in serum-free medium exposed to noradrenaline exhibit a 1.5 to 2-fold increase in cell size with no change in cell number i.e. hypertrophy without hyperplasia. This was accompanied by hallmark changes towards foetal gene expression (Bishopric *et al.*, 1987). Molkenin *et al.* (1998) also showed the α_1 -adrenoceptor agonist phenylephrine (PE) to stimulate hypertrophy in cultured myocytes, and that this was via a calcineurin-dependent pathway. This is discussed further in the section "intracellular signalling".

1.3.8 Role of nitric oxide

Nitric oxide (NO) appears to have an antihypertrophic effect on the myocardium analogous to its antiproliferative action on vascular smooth muscle cells (Garg & Hassid, 1989). In cultured rat cardiomyocytes stimulated to hypertrophy with

phenylephrine, addition of a NO donor inhibited the increase in protein to DNA that is indicative of cellular hypertrophy. Bradykinin gave an identical response by stimulating production of NO, which was measured as an increase in its stable nitrite and nitrate metabolites. In addition, nitrite and nitrate concentrations gave a good negative correlation with protein/DNA ratio (Ishigai *et al.*, 1997). This suggests a further mechanism for ACE inhibitors to elicit regression of cardiac hypertrophy. Since bradykinin is also a substrate for angiotensin converting enzyme, then ACE inhibition results in an increase in bradykinin levels and hence nitric oxide. This was tested in the same study, where addition of an ACE inhibitor prevented an increase in protein/DNA ratio. In turn, this effect could be abolished by a kinin B₂-receptor antagonist, a NO synthase inhibitor, or methylene blue which inhibits guanylate cyclase (Ishigai *et al.*, 1997). The NO system has also been implicated in mediating the beneficial effects of ACE inhibition *in vivo*. A B₂-bradykinin receptor antagonist abolished the prevention of LVH by ramipril after aortic banding in rats (Linz & Schölkens, 1992).

Therefore, ACE inhibitors may regress hypertrophy even when the hypertrophic stimulus is not AngII dependent by activation of the bradykinin/NO pathway. In theory, this suggests a benefit of ACE inhibitors over AT₁ antagonists, which do not elevate bradykinin levels. However, in practice, there appears to be no evidence for this distinction, perhaps because Ang II associated hypertrophy is most dominant.

Basal release of nitric oxide may keep hypertrophy in check in the normal rat heart. In WKY rats, inhibition of nitric oxide *in vivo* using L-NAME resulted in elevated systolic blood pressure and cardiac hypertrophy. Hypertrophy was accompanied by an increase in skeletal α -actin gene expression with no change in collagen type 1, indicating myocyte hypertrophy in the absence of interstitial fibrosis (Devlin *et al.*, 1998). Plasma concentrations of both renin and AngII were significantly increased in this model which reinforces the importance of the RAS in hypertrophic remodelling. It was not possible from this study to distinguish whether hypertrophy was due to elevated AngII or loss of nitric oxide.

Similarly, in eNOS knockout mice, blood pressure is elevated and there is concentric LV hypertrophy, while LV function and chamber dimensions are normal. This suggests that endothelium-derived NO has a role in blood pressure homeostasis, and is not detrimental to function (Yang *et al.*, 1999).

NO on the heart and vessels of the SHRSP has an important role in preventing a runaway effect of hypertension as administration of L-NAME in these animals causes death within 24-48 hours (Dominiczak *et al.*, 1997). This can be prevented by concomitant treatment with perindopril, suggesting the importance of NO in keeping the RAS in check (Dominiczak *et al.*, 1996).

Conflicting evidence exists concerning alterations in NO activity in the SHR heart. In one study, treatment with large doses of L-arginine in the drinking water for 12 weeks did not alter blood pressure, but did decrease LV mass in the SHR but not WKY. Also cGMP and nitrite/nitrate content were lower in the hearts of the SHR indicating impaired NO production in the heart of the SHR that could be corrected for by L-arginine, independent of blood pressure (Matsuoka *et al.*, 1996). However, a proposed NO defect may be species dependent. It has been reported that L-arginine does not decrease LVH in the SHRSP (Stier *et al.*, 1991). Neither is it a consistent finding in the SHR. In a separate study, NOS enzyme activity was determined in heart homogenates from SHR and WKY rats. eNOS activity was found to be 2-3x higher in the adult SHR heart, with most of the activity residing in endocardial or coronary endothelial cells. Since young SHR had normal eNOS activity, and the right ventricle had lower activity than the LV, this suggests the increase in eNOS activity is compensatory to the increase in blood pressure. No iNOS activity was detected in any of the hearts (Nava *et al.*, 1995).

1.3.9 Cytokines in LVH

Tumour necrosis factor- α (TNF- α) may have a role in ventricular remodelling in chronic pressure-overload. In the 6-month-old SHR, Bergman *et al.* (1999) found an increased secretion of bioactive TNF- α from LV tissue homogenates when compared to Sprague-Dawley controls. In addition, TNF- α secretion gave a good positive correlation with LV mass ($r = 0.76$) and blood pressure ($r = 0.68$). However, at 12 months and 18 months these differences were no longer apparent and circulating levels of TNF- α were undetectable in serum at all ages. In the same study, spontaneously hypertensive-heart failure prone rats (SHHF) followed the same pattern, but exhibited increased TNF- α again when overt failure had developed (there is a wealth of evidence for the involvement of cytokines in heart failure, and this will be discussed in a later section). This study suggests that TNF- α is elevated in the early stages of genetic hypertension, where it may participate in LV hypertrophy. However, any putative role

is lost once hypertension/hypertrophy is established. The effect of TNF- α antagonism on LVH development has yet to be studied.

1.3.10 *The cytoskeleton in LVH*

In feline right ventricular hypertrophy caused by surgical constriction of the pulmonary artery, there is an increase in microtubule density within the hypertrophied cardiomyocyte. This has been shown to exert a viscous load on the contractile apparatus, which could explain the increased energy expenditure of the hypertrophied myocardium (Tagawa *et al.*, 1997). However, this phenomenon appears to be dependent on species, hypertrophic stimuli, and in the right ventricle only. Similar defects have not been observed after aortic banding in guinea pigs, or in feline right ventricular hypertrophy due to atrial septal defect (Walsh, 1997). Other types of cytoskeletal abnormalities may have importance in cardiac hypertrophy or failure, and the work by Tagawa *et al.* (1997) demonstrates how such changes could have a direct effect on function.

1.3.11 *Intracellular Ca²⁺ and LVH*

There is precious little data regarding molecular changes in human compensated LVH. This is due to the relatively few opportunities for obtaining tissue, as opposed to the failing heart that can be collected at transplantation. One study by Schotten *et al.* (1999) confirms the theory of altered Ca²⁺ regulation as being pertinent to LVH in man. They obtained LV tissue during surgery from patients with either hypertrophic obstructive cardiomyopathy or aortic valve stenosis who had a normal cardiac index, and compared it with tissue from heart donors free of cardiovascular disease. Western blot analysis revealed a 30% reduction in protein expression of SERCA in patients with LV hypertrophy. There was no compensatory change in the relative abundance of phospholamban, calsequestrin or the Na⁺/Ca²⁺-exchanger. Further, there was a significant negative correlation between SERCA expression and interventricular thickness i.e. patients with the greatest LVH also had the lowest SERCA expression. The SERCA pump is central to control of intracellular [Ca²⁺]. It is located on the membrane of intracellular calcium stores and functions to pump Ca²⁺ from the cytosol against its electrochemical gradient into the stores at the expense of ATP. The activity of this pump is largely responsible for the very low resting Ca²⁺ concentration in the

cytosol (Simpson *et al.*, 1995). The Schotten study indicates a decrease in the SERCA pump protein in hypertrophied hearts. If this translates into a functional abnormality, then it may explain impaired relaxation in LVH, due to impaired Ca^{2+} sequestration into the intracellular stores. Unfortunately, the authors failed to examine diastolic function in these patients (Schotten *et al.*, 1999).

1.3.12 Intracellular signalling

It is not proposed to provide a detailed description of intracellular signalling involved in LV hypertrophy, as it does not have direct impact on the results in this thesis. However, one study is of particular interest as it unites the theories of increased foetal gene expression and intracellular Ca^{2+} mismanagement as the trigger for cardiac decompensation and ultimately the transition to heart failure.

Molkentin *et al.* (1998) developed transgenic mice that express activated forms of the Ca^{2+} regulatory protein calcineurin in heart tissue. These mice exhibited marked hypertrophy of the left and right ventricles, and progressed to develop left ventricular dilatation and pulmonary oedema characteristic of heart failure. They were also highly susceptible to sudden death. Other hallmarks of hypertrophy were present such as a change to foetal gene expression, with up-regulation of mRNA for β -MHC, α -skeletal actin, BNP and down-regulation of α -MHC, SERCA and phospholamban. This suggests that calcineurin has a pivotal role in hypertrophic signalling, which was further supported by the complete prevention of hypertrophy by treatment with the immunosuppressant drugs cyclosporin A (CsA) and FK506, both of which are known to inhibit calcineurin signalling. In cultured cardiomyocytes exposure to AngII or phenylephrine (PE) could induce hypertrophy. Since this could be abolished by CsA or FK506, this indicates that calcineurin signalling is a mechanism common to both hypertrophic stimuli (Molkentin *et al.*, 1998).

All hypertrophic stimuli increase intracellular Ca^{2+} (including the binding of AngII and PE to their receptors), and the role of calcineurin may be to integrate this signal into the hypertrophic response of foetal gene expression. Elevated intracellular $[\text{Ca}^{2+}]$ has been implicated in the pathophysiology of hypertrophy and heart failure, but the mechanism was missing by which the myocyte might interpret this signal from the background of calcium oscillations occurring within each cycle of contraction and relaxation (Izumo & Aoki, 1998). Calcineurin fulfils this role. It is a ubiquitously expressed phosphatase

with calmodulin and Ca^{2+} binding domains, which is only activated by prolonged exposure to elevated intracellular Ca^{2+} , being insensitive to transient fluctuations (Molkentin *et al.*, 1998). This raises the possibility of using the immunosuppressant drugs CsA or FK506 to treat cardiac hypertrophy if the serious immunological side-effects of these drugs could be overcome.

1.3.13 Coronary reserve

The consequences of endothelial dysfunction and vascular remodelling in hypertension are a reduced coronary reserve, which may contribute to the pathogenesis of coronary artery disease, myocardial ischaemia and congestive heart failure, through an inability to increase myocardial perfusion upon demands of exercise or stress. Coronary reserve represents coronary resistance at rest, as a ratio of coronary resistance when the arteries are maximally dilated (Harrison *et al.*, 1991). In hypertensive patients free of coronary artery disease, coronary flow is normal under resting conditions, however when coronary vessels are maximally dilated, coronary vascular resistance is 20% higher than in control subjects, i.e. coronary reserve is decreased. As a result, blood flow is reduced by 40%. In addition, around half of such patients with reduced coronary reserve exhibit ST-segment depressions during electrocardiography consistent with transient myocardial ischaemia similar to patients with established coronary artery disease (Motz *et al.*, 1991). With treatment that normalises blood pressure, but not coronary reserve, patients may be unable to dilate coronary vessels to maintain perfusion pressure (Harrison *et al.*, 1991).

Left ventricular hypertrophy may play a role to exacerbate the decrease in coronary reserve. As left ventricular mass increases, coronary vessels fail to increase in diameter to accommodate the perfusion demands of the greater tissue mass. The result is a 50% decrease in the ratio of vessel diameter to left ventricular mass (Harrison *et al.*, 1991). In human hypertension this may contribute to the large reduction in coronary reserve observed after prolonged hypertension. The relative importance of this mechanism probably depends on the ability to compensate by producing new coronary resistance arteries, suggesting that the control of angiogenic factors may be important. Angiogenesis is thought to account for the gradual normalisation of coronary reserve that occurs in the SHR when maximal left ventricular hypertrophy has been attained. However, this species difference may be related to the duration of hypertension, as coronary reserve is reduced in the SHR during left ventricular development (Harrison *et*

al., 1991). It is worth noting that left ventricular hypertrophy is not an overriding influence on coronary reserve and diminished coronary reserve can occur independently of left ventricular hypertrophy (Motz *et al.*, 1991).

1.4 Heart failure

Heart failure can be defined as an inability of the heart to maintain an adequate supply of oxygen to the major organs (Katz, 1992). The aetiology of the condition may be acute such as myocardial ischaemia after infarction of a coronary artery, or may be insidious such as the long-term structural changes that occur in cardiac hypertrophy. What both have in common as triggers for heart failure is a convergence on a series of complex haemodynamic and neurohumoral changes, that are initiated to protect against the insult, but which in the longer term are detrimental, feeding back to worsen the failing heart. This section on the pathophysiology of heart failure will discuss the “syndrome” of heart failure and how this may lead to decompensation of the failing heart with subsequent morbidity and mortality. Particular emphasis will be placed on findings from animal models of heart failure secondary to MI as they pertain to the work presented in this thesis.

1.4.1 Models of heart failure

At least 30 different models of heart failure have been developed in 11 species. Induction of heart failure may be genetic, surgical or due to administration of cytotoxic agents as summarised in table 1.4. It is a commonly held view that no single model mimics the full range of alterations with heart failure in man, but that all involve certain pertinent features. It would not be appropriate to review all the models here, for reviews see (Dogrell & Brown, 1998; Verdouw *et al.*, 1998; Hasenfuss, 1998). This introduction will concentrate on the most popular model of coronary artery ligation (CAL) in the rat, which is utilised in chapter five of this thesis.

Table 1.4

Animal models of heart failure.

Method	Species	Comments
Surgical		
Coronary artery ligation	Rat, dog, rabbit, pig, mouse	Model of human ischaemic h.f. 2° to MI Variable infarct size as in man. Partial occlusion or reperfusion studies.
Aortic banding	Rat, sheep, guinea-pig	LVH then high output failure in some animals at 20 weeks. No human equivalent.
Pacing tachycardia	Dog Rabbit	200bpm for 3-6 weeks 400bpm for several weeks, reversible, Neurohumoral activation without LVH
Pulmonary artery banding	Cat	Pulmonary hypertension, RV hypertrophy leading to failure at 14-90 days.
Micro-embolism	Dog	Weekly microspheres IV. H.f. after 3 months.
Mitral valve damage	Dog	Mitral regurgitation, LVH, failure by 3 months
Aortic valve perforation	Rabbit	Severe aortic regurgitation, LVH, failure.
Renal artery occlusion	Rat	Hypertensive, LVH then failure at 2 weeks
Genetic		
Systemic hypertension Ageing SHR, SHHF	Rat	SHR: transition LVH to h.f. at 18-24 months SHHF: transition LVH to h.f. before 18 months
Salt-sensitive hypertension	Dahl rat	LVH at 8 weeks, h.f. at 15-20 weeks.
Spontaneous cardiomyopathy	Syrian hamster, Dog, Cow	LVH and overt h.f. at 7-10 months Doberman Pinschers Hereditary dilated cardiomyopathy
Toxicity		
Chronic ethanol	Rat	
Catecholamine infusion	Rat	Isoprenaline or NA infusion
Doxorubicin	Rabbit	H.f. after bi-weekly injection for 6-9 weeks.
Transgenics (examples)		
Myogenic factor 5	Mouse	Overexpression – cardiomyopathy and h.f.
G _{sa}	Mouse	Overexpression – cardiomyopathy and h.f.
TGF- β	Mouse	Knockout – myocarditis & h.f.
Muscle LIM protein	Mouse	Knockout – dilated cardiomyopathy & h.f.

Adapted from Hasenfuss (1998), Dogrell & Brown (1998), Iannini & Spinale (1996). LVH:left ventricular hypertrophy; h.f.: heart failure; MI: myocardial infarction; RV: right ventricle.

As a heart failure model the rat is more popular than all the other species combined. It has obvious advantages over larger mammals in terms of cost, gestation period and life span. Studies involving large numbers of animals can be performed relatively easily with follow-up from birth to death. The sheer number of studies in the rat means that cardiovascular physiology and pharmacology are better characterised than in any other

species. The disadvantages of rat models for heart failure research are mainly centred around differences in cardiac physiology when compared to man.

- 1) The action potential in rat hearts is shorter, without a sustained plateau phase.
- 2) The SERCA pump has an enhanced role over the Na^+ - Ca^{2+} exchanger in removing Ca^{2+} from the cytosol.
- 3) α -MHC is the dominant isoform in the rat heart.
- 4) Heart-rate at rest is five times higher than humans and there is an altered force-frequency relationship.
- 5) Cholesterol levels are half that of humans.

(Hasenfuss, 1998; Iamini & Spinale, 1996)

Coronary artery ligation in the rat

In 1960, Selye *et al.* described a simplified method for coronary artery occlusion in the rat. This superseded previous attempts, which produced highly variable infarcts limiting the usefulness of the technique. They described a thoracotomy similar to the technique described in appendix II, but in unventilated rats. For this reason, emphasis was on speed, with a window of only 2-3 minutes to tie the ligature around the left anterior descending (LAD) coronary artery and close the chest wall. The authors claimed a surgical mortality of only 10% and could produce up to 60 ligated rats in a single afternoon. This early study also provides an excellent description of the rat coronary vasculature, with a detailed guide to placing the ligature. Since 1960, the technique has been refined considerably, and virtually all laboratories now use mechanical ventilation. Even with the thorax open for less than one-minute animals experience severe hypoxia in the absence of ventilation, a possible experimental confounder (Horstick *et al.*, 1999).

CAL in the rat results in a wide range of infarct sizes. Pfeffer *et al.* (1979b) saw this as an advantage that provided the opportunity to mimic the full range of cardiac failure found in man. They stratified animals depending on infarct size on an arbitrary basis that many labs still use today. Since then there has been interest in trying to standardise infarct size with a recent report that CAI in Lewis inbred rats results in a uniformly large infarct with paradoxically reduced mortality (Liu *et al.*, 1997).

The study by Pfeffer *et al.* (1979b) examined the effect of infarct size on haemodynamic and cardiac performance after the scar was healed at 3-weeks post-ligation. They

observed a wide range of function that was directly proportional to infarct size. Animals with small infarcts were well compensated, with no alterations in cardiac haemodynamics, whereas those with large infarcts had congestive heart failure evidenced by a reduced rate of developed pressure (+dP/dt) and impaired pressure development in response to aortic occlusion.

Studies on the pathophysiology of MI-induced heart failure are hampered by the difficulty in comparing results from different laboratories. The genetic homogeneity of the SHR provides a good reproducible hypertrophy associated with hypertension, but no equivalent model for myocardial infarction exists. Most studies of MI-induced heart failure use outbred Sprague-Dawleys or Wistars, providing a genetically heterogeneous population. In addition, the measurements obtained are heavily dependent on infarct size. There is not even universal agreement on how infarct size should be measured e.g. as percentage of whole left ventricle, % of free ventricular wall, or % of area at risk. Add to this the variable time course of starting medication i.e. early or late after MI, the dose or route of administration of drugs, and whether animals are in failure or not, and it is easy to understand how conflicting results may arise.

1.4.2 Haemodynamics in heart failure.

In the absence of symptoms, heart failure in animal models is often described in terms of cardiac haemodynamics (see table 1.5). After myocardial infarction the damaged left ventricle must continue to meet the oxygen demands of the body despite a reduced myocardial mass. Loss of working muscle causes a fall in stroke volume such that less blood is pumped with each beat (Hu *et al.*, 1998a). Sensing the decreased arterial volume, the sympathetic nervous system and RAS are activated to maintain perfusion pressure by increasing afterload and preload. With a reduced power-generating capacity with which to push against an increased total peripheral resistance (TPR) (Hu *et al.*, 1998a), there is an increase in left ventricular end diastolic pressure (LVEDP) (Nasa *et al.*, 1996), which together with the neurohormonal activation, provide a signal for hypertrophy of the surviving myocardium. This serves to compensate for lost tissue and so normalise wall stress (Hu *et al.*, 1998a). LV mass gets progressively lower in the first three weeks as the infarcted myocardium is replaced by the much thinner scar tissue, but over the next few months, returns to normal or higher values as hypertrophy takes hold (Pfeffer *et al.*, 1991).

Elevated LVEDP represents a resistance to blood returning from the pulmonary circulation, and if sufficiently high, right ventricular pressure will increase to maintain the pressure gradient across the pulmonary bed. The result is pulmonary congestion and right ventricular hypertrophy (Pfeffer *et al.*, 1984; Pfeffer *et al.*, 1979b). This may be exacerbated by increased preload due to elevated central venous pressure (Mulder *et al.*, 1996).

In the early stages post-MI, LV volume increases due to ballooning of the infarct zone. This is particularly evident at low filling pressures ($<2.5\text{mmHg}$) when the pressure-volume relationship shifts to the right. A progressive thinning and dilatation of the infarct zone occurs over the first week before scar tissue forms. This is termed infarct expansion and is thought to be due to myocyte slippage as more cells are lost from around the infarct region (Pfeffer *et al.*, 1991).

After one week, LV volume at high filling pressures (20mmHg) also becomes enlarged (Pfeffer *et al.*, 1991). In order to maintain stroke volume in the face of a lower ejection fraction, the LV evokes the Frank-Starling mechanism by dilating. This provides a mechanical advantage, as the same stroke volume can be attained with a decrease in myocyte circumferential shortening (Pfeffer *et al.*, 1984).

This type of change in LV structure and geometry allows the heart to compensate in the short-term. For example, for small and moderate sized infarcts, the maximum developed pressure during aortic occlusion is close to normal (Pfeffer *et al.*, 1979b), indicating an ability of the heart to compensate via the mechanisms outlined above. However, structural and geometrical alterations to the LV become more pronounced with increasing infarct size and time since insult, and are ultimately detrimental (Pfeffer *et al.*, 1991).

Table 1.5 Cardiac haemodynamic signature and structural alterations after coronary artery ligation in the rat.

Measured parameter	Δ	Example references
Haemodynamics		
Mean blood pressure	↓	Drexler & Wenyuan (1992); Feng <i>et al.</i> (1996), Baggia <i>et al.</i> (1997)
Heart rate	↔	Hu <i>et al.</i> (1998a); Oie <i>et al.</i> (1998); Mulder <i>et al.</i> (1997b)
LV systolic pressure	↓	Nasa <i>et al.</i> (1996); Toyoshima <i>et al.</i> (1998); Mulder <i>et al.</i> (1996)
LV end diastolic pressure	↑	Gaudron <i>et al.</i> (1994); Sakai <i>et al.</i> (1996); Mulder <i>et al.</i> (1997a)
Right atrial pressure	↑	Hu <i>et al.</i> (1998b); Gaudron <i>et al.</i> (1994)
Central venous pressure	↑	Mulder <i>et al.</i> (1996); Mulder <i>et al.</i> (1997a); Mulder <i>et al.</i> (1997b)
Peak developed pressure	↓	Pfeffer <i>et al.</i> (1979b); Pfeffer <i>et al.</i> (1984); Hu <i>et al.</i> (1998)
LV dP/dt	↓	Baggia <i>et al.</i> (1997); Teerlink <i>et al.</i> (1994); Latini <i>et al.</i> (1998)
Aortic flow	↓	Toyoshima <i>et al.</i> (1998); Yamaguchi <i>et al.</i> (1998)
Cardiac output	↓	Nekooeian & Pang (1998); Xu <i>et al.</i> (1997)
Stroke volume	↓	Hu <i>et al.</i> (1998b); Hu <i>et al.</i> (1998a)
Ejection fraction	↓	Liu <i>et al.</i> (1997)
Fractional shortening	↓	Mulder <i>et al.</i> (1997b); Oie <i>et al.</i> (1998)
Cardiac structure		
LV mass	↑	Thomas D. <i>et al.</i> (1998); Feng <i>et al.</i> (1996); Oie <i>et al.</i> (1998)
RV mass	↑	Lindsay <i>et al.</i> (1992); Drexler & Wenyuan (1992); Pfeffer <i>et al.</i> (1979b)
Atrial weight	↑	Drexler & Wenyuan (1992); Fabris <i>et al.</i> (1990); Gu <i>et al.</i> (1998)
Wall thickness (surviving)	↑	Mulder <i>et al.</i> (1997b); Gaudron <i>et al.</i> (1994)
LV end diastolic volume	↑	Mulder <i>et al.</i> (1997b); Oie <i>et al.</i> (1998); Liu <i>et al.</i> (1997)
LV circumference	↑	Mulder <i>et al.</i> (1997b); Orenstein <i>et al.</i> (1995); Mulder <i>et al.</i> (1997a)
LV % collagen density	↑	Taylor <i>et al.</i> (1998); Latini <i>et al.</i> (1998); Mulder <i>et al.</i> (1997b)

With time, too much LV dilatation becomes unfavourable and is no longer sufficient to maintain stroke volume. Indeed LV dilatation is a marker for poor prognosis in man (Pfeffer *et al.*, 1984; Sutton *et al.*, 1997). The mechanism by which LV dilatation becomes deleterious leading to decompensated failure has yet to be elucidated. Contributing factors are likely to include insufficient hypertrophy, reduced contractility at a cellular level or increasing afterload due to peripheral vascular dysfunction (Pfeffer *et al.*, 1991).

In rats after CAL, structural changes in the LV allowed normalisation of wall stress within 3 weeks in animals with small infarcts. However, even after 106 days, rats with large infarcts had significantly higher wall stress. The authors concluded, that in those animals there is a continued drive towards LV hypertrophy and dilatation in an effort to

normalise wall stress, for which they are unable to compensate (Pfeffer *et al.*, 1991). In man, continued progressive LV dilatation has been described two years after MI despite treatment with ACE inhibitors. Again this indicates a long-term drive towards altered LV geometry (Sutton *et al.*, 1997).

Early dilatation and thinning of the infarct zone predicts later deterioration in ventricular function. Subjects with the greatest infarct expansion are much more likely to develop dilatation affecting the whole myocardium, and significantly more of these patients die (Eaton *et al.*, 1979). Preventing early dilatation of the infarct area may provide significant advantages. In sheep after CAL, surgically applying a mesh to give mechanical support to the infarct zone allowed cardiac haemodynamics to return to normal within one week. Animals without the mesh showed progressive deterioration in LV function (Kelley *et al.*, 1999).

1.4.3 Neuroendocrine response in heart failure

This syndrome of heart failure takes a similar course independent of aetiology, and leads to the overt clinical symptoms of heart failure of shortness of breath, exercise intolerance, and pulmonary & peripheral oedema. At this stage the heart is said to be decompensated when the neurohumoral changes no longer compensate adequately for the failing heart.

The heart failure syndrome involves the activation of a whole host of neurohumoral systems involved in homeostasis of blood pressure and cardiac performance. These include the sympathetic nervous system, renin-angiotensin system, vasopressin, natriuretic peptides, nitric oxide, endothelin, prostaglandins and cytokines. The interactions are complex, with counter-regulatory systems feeding back on themselves and each other (Schrier & Abraham, 1999). This makes the relative importance of these systems difficult to ascertain.

Sympathetic nervous system

The chain of events probably starts with activation of the sympathetic nervous system (SNS). For example, an ischaemic insult to the myocardium reduces cardiac output, and results in underfilling of the arteries. This is sensed by the carotid baroreceptors, which signal to the nucleus tractus solitarius to activate the sympathetic nervous system and so start a reflex of sodium and water retention to aid the troubled heart (Schrier & Abraham, 1999). Activation of the SNS is essential for survival immediately after MI.

In rats given a sympathectomy, coronary artery ligation causes death within five minutes due to a drastic fall in cardiac output (Botting *et al.*, 1983).

There is a wealth of evidence for sympathetic nervous system activation in heart failure. Plasma noradrenaline (NA) concentration is significantly elevated (3-fold) three weeks after MI in the rat and remains elevated at three months (Deck *et al.*, 1992; Latini *et al.*, 1998). In patients with congestive heart failure there is an increase in sympathetic nerve firing, and more NA is released from nerve endings, resulting in an increased noradrenaline spillover from the heart (Meredith *et al.*, 1993), with a concomitant reduction in plasma clearance of up to 30%. The combined effect is to double the plasma noradrenaline concentration (Kaye & Esler, 1995). The increase in sympathetic tone together with the release of adrenaline and noradrenaline from the adrenal medulla act directly to increase force and rate of cardiac contraction via β_1 -adrenoceptors. Stimulation of α -adrenoceptors causes a generalised arterial and venous constriction, thereby increasing both afterload and preload, and so increasing cardiac workload (Schrier & Abraham, 1999). Sodium and water retention is promoted in three ways

- i) Activation of RAS by direct stimulation of renin release from the cells of the juxtaglomerular apparatus via β -adrenoceptors.
- ii) Renal vasoconstriction causing a decreased glomerular capillary filtration pressure and hence lower glomerular filtration rate, resulting in less sodium and water excretion
- iii) A direct α -adrenoceptor effect to increase sodium transport in the proximal convoluted tubule. This results in a decreased concentration of sodium reaching the distal portion of the nephron and collecting duct, which stimulates release of renin and aldosterone (Schrier & Abraham, 1999).

These effects may be beneficial in the short-term to maintain perfusion pressure and bolster left ventricular dysfunction, however, there are consequences of prolonged exposure to an activated sympathetic nervous system. Noradrenaline is cytotoxic to cardiac myocytes, and may trigger cell death due to calcium overload or apoptosis. Noradrenaline may also increase cardiac hypertrophy, directly, via α_1 - or β -adrenoceptors, or indirectly by activating the RAS by the mechanisms just outlined (Schrier & Abraham, 1999).

In addition, β -adrenoceptor function is impaired, probably as a direct consequence of prolonged exposure to elevated noradrenaline concentrations. The chronotropic and

inotropic response to β -agonists is attenuated via a number of mechanisms; 1) catecholamine depletion from vesicle stores (Krum, 1997), 2) reduced receptor density (Gu *et al.*, 1998), and 3) uncoupling of adenylyl cyclase from β_1 -adrenoceptors (Jaber *et al.*, 1996). A 50% decrease in β_1 -adrenoceptor mRNA has been observed in human heart failure coupled with an increase in mRNA and enzyme activity of β -adrenergic receptor kinase, which deactivates the receptor (Kaye & Esler, 1995).

The baroreceptor reflex is also blunted in heart failure. The increase in NA spillover that occurs in response to systemic vasodilatation is reduced in heart failure patients i.e. subnormal change in heart rate for any given change in blood pressure (Newton & Parker, 1996).

Parasympathetic nervous system

Activity of the parasympathetic nervous system is depressed in human heart failure. In subjects where adrenoceptors have been blocked by propranolol, parasympathetic blockade with atropine elevates heart rate to a greater extent in normal subjects than in those with heart disease (Eckberg *et al.*, 1971). There is some evidence to link high initial plasma renin activity with this process (Osterziel *et al.*, 1994), and AngII is thought to directly inhibit central parasympathetic outflow (Du *et al.*, 1998). This may in part explain how ACE inhibitors improve baroreflex control and have an anti-arrhythmic action in the ischaemic heart (Deck *et al.*, 1992).

1.4.4 Renin-Angiotensin-Aldosterone System

The RAS is stimulated both directly and indirectly by the sympathetic nervous system via the mechanisms above. It is also sensitive to a drop in cardiac output, as the resultant decrease in glomerular filtration rate, lowers sodium concentration in the distal tubule, which stimulates the release of renin. In mild heart failure there is little or no increase in plasma renin or aldosterone concentrations, however, levels can be considered to be inappropriate due to the high blood volume of these patients. In severe heart failure both renin and aldosterone concentrations are elevated (Schrier & Abraham, 1999).

Angiotensin II has numerous effects on the cardiovascular system,

- i.) It increases afterload by a generalised vasoconstriction.

- ii.) Vasoconstriction of afferent and efferent renal arterioles helps to maintain glomerular capillary pressure and hence filtration rate. This is why ACE inhibitors may cause a decrease in renal function in some patients with severe heart failure.
- iii.) Angiotensin II is mitogenic for myocytes and is thought to have an important role in hypertrophic cardiac remodelling.
- iv.) Angiotensin II increases thirst by stimulation of the central thirst centre and thereby increasing water retention.
- v.) Increases synthesis and release of aldosterone from the zona glomerulosa of the adrenal medulla.

(Schrier & Abraham, 1999; Molkentin *et al.*, 1998)

Aldosterone increases sodium reabsorption in the distal tubules via a poorly understood mechanism. It may also be released in direct response to low plasma sodium or high potassium concentrations. The importance of aldosterone in this cycle of sodium and water retention has been emphasised recently by the success in adding spironolactone, an aldosterone receptor antagonist, to existing therapy in the treatment of severe human heart failure. The trial was stopped early due to an overwhelming benefit of spironolactone to decrease both mortality and non-fatal hospitalisation by 30% (Pitt *et al.*, 1999).

Renin acts to split angiotensinogen into angiotensin I, which is then converted to the active angiotensin II form by angiotensin converting enzyme (ACE). The formation of AngII from AngI may also take place via the serine protease, chymase. This appears to be a source of local tissue AngII, and is not thought to contribute to plasma levels (Wolny *et al.*, 1997). The relative importance of chymase over ACE is a matter of considerable debate, but there is some evidence to suggest that AngII production by chymase increases in importance to compensate for long-term inhibition of ACE, and in the failing human heart where it is the major source of AngII generation in the myocardium and coronary vessels (Wolny *et al.*, 1997). Indeed, in one study, captopril only reduced AngII forming activity by 11% in the LV of patients with ischaemic cardiomyopathy, whereas a serine proteinase inhibitor blocked 80% of AngII activity (Urata *et al.*, 1990). This suggests that the RAS is incompletely blocked by ACE inhibitor therapy in heart failure, and may explain why ultimately these drugs fail to halt progression of the disease. Since AT₁ antagonists will block all AngII regardless of source, this argues for an additional benefit for AT₁ antagonists over ACE inhibition.

There is strong evidence from numerous studies that the local RAS is activated after CAL in the rat. Plasma AngI and AngII concentrations are significantly elevated within six hours of MI and local AngII is increased for three days in the non-infarcted myocardium and for seven days in the infarct zone. These changes can be attenuated by ACE inhibition but not nephrectomy confirming that local production is of primary importance (Leenen *et al.*, 1999). AT-receptor mRNA, receptor density and ACE activity are also all up-regulated within days in the surviving myocardium (Reiss *et al.*, 1993). The findings are not universal, and may be related to the severity of insult. One group reports mRNA for ACE and renin is only increased in the border zone of the infarct area, with no increase in the rest of the left ventricle, arguing against a major role in LV hypertrophy (Passier *et al.*, 1996; Passier *et al.*, 1995). Since the highest ACE content appears in the infarct zone (5-fold increase), it has been suggested that AngII may be involved in the wound healing process (Fabris *et al.*, 1990).

Other studies have indicated that in the longer-term (after one month) when animals are often regarded to be in failure, plasma ACE and renin activity are normal (Hirsch *et al.*, 1991; Yoshida *et al.*, 1998). However, again, evidence is strong for a local production in the surviving LV. There is also an increase in the right ventricle where ACE activity positively correlates with infarct size (Hirsch *et al.*, 1991). In humans with idiopathic cardiomyopathy, ACE protein is elevated in both the left and right ventricles (Zisman *et al.*, 1998). At this stage, renal involvement may gain in importance. At 4-6 weeks post-MI, there is a doubling of glomerular AT₁ receptors despite an increase in plasma AngII that would normally result in down-regulation of the receptor. Renin and angiotensinogen mRNA are also increased in the renal cortex. These results may explain the strong intra-renal vasoconstriction observed with heart failure (Mento *et al.*, 1998).

Numerous studies using CAL in the rat have demonstrated beneficial effects of both ACE inhibitors and AT₁ receptor antagonists. A reduction in LVH is almost universal, with corresponding decrease in myocyte CSA (Liu *et al.*, 1997), ANP gene expression (Ambrose *et al.*, 1999), and subsequent improvements in capillary density and oxygen diffusion distance (Liu *et al.*, 1997). Fibrosis of the surviving myocardium is reduced, with a decrease in collagen deposition (Richer *et al.*, 1992; Liu *et al.*, 1997; Smits *et al.*, 1992) and a reduction in non-myocyte proliferation (Faylor *et al.*, 1998). LV dilatation is improved with normalisation of LVEDP, LV wall stress and an increase in maximal

stroke volume (Liu *et al.*, 1997; Hu *et al.*, 1998b). These are fairly consistent findings for a wide range of compounds from both classes. Where a study has failed to show major benefits, this is usually due to sub-optimal dosing e.g. losartan (Hu *et al.*, 1998b). The benefits obtained in blocking the RAS underlines its major role in the pathophysiology of heart failure.

1.4.5 Arginine-vasopressin (antidiuretic hormone)

Arginine vasopressin has also been reported as elevated after CAL in the rat (Stassen *et al.*, 1997a). The important effects of vasopressin in the cardiovascular system are,

- i.) Vasopressin activates V₂ receptors in the collecting duct to promote synthesis and translocation of aquaporin-2 water channels from cytoplasmic vesicles to the cell surface thereby promoting increased water retention. This occurs even at very low concentrations.
- ii.) At higher concentrations, vasopressin activates vasoconstriction via V₁ receptors on vascular smooth muscle cells. Vasoconstriction is generalised, equally affecting all vascular beds, including the coronary circulation (Schrier & Abraham, 1999).

1.4.6 Atrial natriuretic peptide

In human subjects with healed MI, ANP protein and mRNA levels are markedly increased in the LV adjacent to the infarct scar, and also in both atria. Both atrial and LV secretion correlate well with severity of heart failure as measured by LVEDP, suggesting LV stretch as the initiating factor in increasing gene expression (Saito *et al.*, 1989). Plasma ANP also correlates with systolic and diastolic dysfunction in heart failure patients, and is related to increased filling pressures (Wijbenga *et al.*, 1999). Impaired renal clearance may also contribute as ANP levels correlate with creatinine clearance (Missouris *et al.*, 1998).

In the rat after CAL, ANP mRNA expression is consistently elevated in all parts of both ventricles from day one onwards (Passier *et al.*, 1996; Oie *et al.*, 1998; Gidh-Jain *et al.*, 1998), and plasma levels are also increased (Yoshida *et al.*, 1998; Stassen *et al.*, 1997a). In rats with heart failure secondary to aortocaval fistula, ANP gene expression increases in the LV but not the atria. In these animals, urinary ANP concentration remains normal; suggesting increased ANP secretion not reduced clearance elevates plasma levels. ANP mRNA was also elevated in the stomachs of these animals. This extra-

cardiac source of ANP may explain why BNP is a better marker of prognosis in heart failure (Poulos *et al.*, 1996).

Atrial natriuretic peptide (ANP) can be thought of as an endogenous antagonist of the renin-angiotensin system. Infusion of ANP in dogs with heart failure prevents sodium retention, renal vasoconstriction and activation of aldosterone and renin (Lee *et al.*, 1989). Likewise in post-MI rats, when ANP is markedly raised, then salt retention, renin and aldosterone activity are normal, again suggesting an inhibitory role on the RAS (Hodsman *et al.*, 1988; Stassen *et al.*, 1997a).

Usually, increased blood volume due to sodium and water retention increases atrial pressure, causing the atria to stretch. This is sensed by atrial myocytes, which respond by releasing ANP. The stimulus for ANP production in heart failure may be raised LV pressure (stretch) and/or cardiac hypertrophy. Plasma ANP correlates with LVH in rats post-MI, but not with body sodium, and so is probably released independent of salt and water retention in this scenario (Hodsman *et al.*, 1988).

The effects of ANP and BNP are similar,

- i.) Afferent arteriolar dilatation results in an increased glomerular filtration rate and therefore enhanced sodium excretion (Schrier & Abraham, 1999).
- ii.) In the collecting duct, sodium reabsorption is decreased, thereby increasing sodium excretion (Schrier & Abraham, 1999).
- iii.) Inhibition of renin and aldosterone secretion which may prevent overt activation of the RAS in heart failure patients (Missouris *et al.*, 1998)
- iv.) Stimulation of cGMP in smooth muscle cells giving rise to vasorelaxation (Nakamura *et al.*, 1998).

These are all beneficial effects that counteract the over-stimulation of the sympathetic nervous system and RAS observed in heart failure. However, heart failure patients derive little benefit from exogenous natriuretic peptides, and appear to be resistant to their effects. Vasodilatory responses to infused ANP and BNP are impaired in heart failure patients (Nakamura *et al.*, 1998). In rats with chronic heart failure, infusion of ANP results in less natriuresis and blood pressure lowering than in sham animals (Kohzuki *et al.*, 1989). A number of reasons have been suggested for this. For example, down-regulation of renal receptors, or increased degradation by neutral endopeptidase. In addition, the activated RAS means that less sodium is delivered to the collecting duct resulting in less sodium available for excretion (Schrier & Abraham, 1999).

1.4.7 Brain natriuretic peptide

BNP elevation associated with heart failure occurs across models and species. Even in the dog, where initial BNP levels are low in the LV, there is an increased BNP secretion from the LV after rapid ventricular pacing (Luchner *et al.*, 1998).

In human congestive heart failure secretion of BNP from the LV increases in direct proportion to the severity of the disease, correlating with NYHA classification. In normal subjects, plasma ANP concentration is higher than BNP, but with development of heart failure BNP levels dominate (Mukoyama *et al.*, 1991).

Yamamoto *et al.* (1996) report a prospective study to examine plasma natriuretic peptide concentrations as markers of LV dysfunction in patients with heart failure. Plasma BNP concentration was found to be superior to ANP in detecting LV hypertrophy, elevated LVEDP or ejection fraction below 45%, providing good correlations with depressed systolic and diastolic function (Yamamoto *et al.*, 1996). This has been confirmed in further studies in chronic heart failure patients, where plasma BNP is superior to ANP or noradrenaline as a prognostic marker. Survival in patients with high plasma BNP is significantly reduced, which may indicate that the beneficial effects of BNP to compensate for RAS activity may be blunted in patients with severe heart failure (Tsutamoto *et al.*, 1997; Yu & Sanderson, 1999). Indeed, in patients with CHF, infusion of BNP results in an impaired natriuretic response compared to normal controls. The distal portion of the nephron is thought to have reduced responsiveness to BNP (Jensen *et al.*, 1999).

Immediately after MI in humans, plasma BNP is elevated. In those patients who develop LV dilatation, BNP levels are much higher than in those without, and BNP remains higher over the next six months. Both the acute and sustained elevation of BNP has prognostic significance in accurately detecting patients with LV dilatation (Nagaya *et al.*, 1999). It seems likely that BNP concentration reflects levels of wall stress around the infarct zone, giving rise to the correlation with LV geometry.

1.4.8 Prostacyclin and prostaglandin E

Elevated levels of angiotensin II, noradrenaline and renal nerve stimulation all act to increase synthesis of prostacyclin and prostaglandin E from arachidonic acid. Both these prostanoids are potent vasodilators that attenuate the vasoconstrictor effects of angiotensin II and noradrenaline. They may be particularly important as a counter

balance to neurohormonal induced renal vasoconstriction, as blocking their production with non-steroidal anti-inflammatory drugs can precipitate acute renal failure in patients with severe heart failure (Schrier & Abraham, 1999).

1.4.9 Nitric oxide

Nitrates and nitrites are the stable degradation products of nitric oxide (NO). Patients with heart failure have elevated plasma nitrate levels regardless of aetiology (dilated cardiomyopathy, rheumatic valvular disease or ischaemic heart disease) suggesting an overall increase in NO production (Winlaw *et al.*, 1994; Ramesh *et al.*, 1999). In addition, there is a positive correlation between plasma nitrate concentration and NYHA functional class (Winlaw *et al.*, 1995). This difference could be explained by increased release of basal nitric oxide via eNOS or by induction of the calcium independent isoform iNOS.

However, most evidence suggests that endothelial nitric oxide synthase (eNOS) is down-regulated in heart failure resulting in lower production of NO. This means that there is less basal NO to counteract the actions of angiotensin II, noradrenaline and vasopressin, resulting in augmented vasoconstriction by these agents (Schrier & Abraham, 1999). This will be discussed below under "vascular function". Attention has therefore focused on iNOS activity in heart failure.

The normal rat heart contains only eNOS activity (Nava *et al.*, 1995; Schulz *et al.*, 1992). However, Schulz *et al.* (1992) demonstrated that myocytes, and not just inflammatory cells, were capable of iNOS activation with resultant increase in cGMP when exposed to lipopolysaccharide or cytokines such as TNF- α and IL-1 β . After CAL in the rabbit iNOS activity is increased in the infarct zone, associated with macrophage infiltration, but remains normal in non-infarcted myocytes. Maximal activity occurs at 3-5 days, returning to normal within three weeks, which coincides with scar maturation (Wildhirt *et al.*, 1995). Plasma nitrate/nitrite (NO_x) concentration shows excellent positive correlation with iNOS activity in the infarcted region. Also, administration of a specific iNOS inhibitor prevented the increase in plasma NO_x. Taken together, these results suggest that increased iNOS activity accounts for most of the elevated NO_x post-MI (Akiyama *et al.*, 1997).

Similar results have been obtained from human failing hearts, where iNOS activity was greatest in the infarcted regions, and correlated strongly with density of macrophage infiltration. However, in this study, eNOS activity was also elevated, principally in subendocardial layers of the LV (Fukuchi *et al.*, 1998). In human heart failure, iNOS activity is not only increased in the acute healing phase, but is elevated in patients with old infarcts and in other aetiologies such as dilated cardiomyopathy and valvular heart disease (Haywood *et al.*, 1996). However, the expression of iNOS is variable and not universal to all failing hearts. Haywood *et al.* (1996) found iNOS mRNA expression in 71% of biopsies from human hearts with various aetiologies. In these patients, iNOS protein was detected in all four chambers in the cytoplasm of cardiomyocytes.

The mechanism for iNOS activation is likely to be driven by cytokines, which are discussed below. Both TNF- α and IL-1 β can induce iNOS in the rat heart *in vivo* (Schulz *et al.*, 1992). Activation of α -adrenoceptors may be synergistic in this regard enhancing cytokine-induced NO activity via a protein kinase C dependent pathway (Ikeda *et al.*, 1996).

The functional significance of elevated NO production in the myocardium is a deleterious effect on myocyte contractility. *In vitro*, contractility of cultured rat cardiomyocytes decreases when exposed to NO from LPS-activated macrophages (Joe *et al.*, 1998; reviewed in Balligand *et al.*, 1996). Nitric oxide may also have direct cytotoxic effects, and trigger apoptosis, thereby contributing to loss of myocyte mass (Wildhirt *et al.*, 1995).

1.4.10 Cytokines in heart failure

TNF- α is released from immune cells such as macrophages and monocytes. Cardiac myocytes are also capable of synthesising TNF- α in response to ischaemia and are probably as active as LV macrophages in this regard (Meldrum, 1998). There are two receptor subtypes TNFR1 and TNFR2, both of which are expressed in adult human cardiomyocytes. After exposure to TNF- α these receptors can be cleaved from the membrane and circulate as soluble receptors, which may bind and inactivate TNF- α . However, they may also act as a slow-release mechanism for bound TNF- α (Bozkurt *et al.*, 1996).

TNF- α functions to increase synthesis of inflammatory mediators such as eicosanoids, oxidative free radicals, NO and other cytokines e.g. IL-1 (Meldrum, 1998). While activating iNOS, TNF- α , has the opposing effect on eNOS (Yoshizumi, 1993).

Levine *et al.* (1990) observed that plasma TNF- α was significantly elevated in around 40% of patients with heart failure. High TNF- α levels were linked to activation of the RAS, as these patients also had significantly higher plasma renin activity (Levine *et al.*, 1990). Elevated TNF- α has since been confirmed in a number of studies reviewed by Bozkurt *et al.* (1996).

After CAL in the rat, mRNA expression for several cytokines (TNF- α , IL-1 β , IL-6) are increased transiently in the infarct zone. Of greater interest is the continued elevation in the non-infarcted myocardium at twenty weeks. Further, all three cytokines provided good positive correlations with LV dilatation, and IL-1 β also correlated with collagen density (Ono *et al.*, 1998). The implication is a possible role for pro-inflammatory cytokines in the pathophysiology of LV remodelling post-MI. Bioactive TNF- α secretion from the LV is also increased as SHHF rats make the transition into failure (Bergman *et al.*, 1999), implicating cytokines in the process of decompensation.

Artificially raising TNF- α activity can mimic many of the hallmarks of failure. Infusion of TNF- α at levels found in heart failure patients resulted in LV remodelling and dysfunction in normal rats. Cardiac contractility was depressed within five days of starting the infusion and recovered on cessation, suggesting a causal relationship (Bozkurt *et al.*, 1998). TNF- α also promoted LV dilatation and a thinning of the posterior wall. Wall thinning was not reversible, as it involved loss of myocytes by apoptosis and reduced deposition of fibrillar collagen. Corroborating these findings, transgenic mice that overexpress TNF- α in cardiac myocytes developed severe LV dilatation with markedly depressed ejection fraction, pulmonary oedema and premature death (Bryant *et al.*, 1998). The severity of LV dysfunction is related to the level of transgene expression (Franco *et al.*, 1999).

TNF- α may directly impair contractility by two mechanisms. Elevating NO causes myofilament desensitisation to calcium resulting in sustained dysfunction, while sphingosine-mediated interruption of calcium-induced calcium release may be involved in immediate dysfunction (Meldrum, 1998).

1.4.11 Endothelin

Endothelin (ET-1) is a 21 amino acid peptide with three isoforms cleaved from its precursor pro-ET-1 by the activity of endothelin converting enzyme (ECE). ET gene expression has been reported in numerous tissues e.g. cardiomyocytes, kidney, vascular smooth muscle cells and vascular endothelial cells. Rat neonatal cardiomyocytes can synthesise and secrete ET-1 suggesting the existence of local ET systems. Two receptor subtypes have been identified, ET_A and ET_B. The ET_A receptors on smooth muscle cells mediate the potent vasoconstricting effects of endothelin, with involvement of ET_B receptors in some vascular beds. ET_B receptors in the vascular endothelium can stimulate the release of NO to cause vasorelaxation (Love & McMurray, 1996; extensively reviewed in Rubanyi & Polokoff, 1994).

In the heart, ET has positive inotropic and chronotropic effects and is a potent vasoconstrictor of coronary arteries (Rubanyi & Polokoff, 1994). Both ET_A and ET_B receptors are found in the human heart, although only ET_A are thought to be functionally significant (Sakai *et al.*, 1996). In the atria, ET_A are linked via G_{q/11} to the phosphoinositide system and to inhibition of adenylyl cyclase via G_i. In the LV, ET_A are only coupled to phosphoinositide (Ponicke *et al.*, 1998). In subjects with severe heart failure these systems remain at normal levels, with no change in receptor density, G-proteins or inositol phosphate levels. This is despite elevated plasma ET-1, which would be expected to down-regulate the system, suggesting that in the failing heart ET-1 signalling is inappropriately normal (Ponicke *et al.*, 1998).

In the infarcted rat heart ET has been implicated in wound healing. The gene expression of ET precursor preproendothelin-1 (ppET-1) was upregulated 25-fold in the infarct zone over the first three weeks, and the presence of ET-1 in the infarct was confirmed by immunostaining. In the same study, ppET-1 mRNA was also expressed at high levels in the non-infarcted LV. Since ET-1 has been demonstrated to stimulate LV hypertrophy, fibroblast proliferation and collagen deposition, it has been postulated that ET-1 may have a role in LV remodelling post-MI (Oie *et al.*, 1997).

ET may have a role in pulmonary hypertension secondary to congestive heart failure by causing excessive pulmonary vascular constriction. It is noteworthy that tissue ET-1 and mRNA concentrations are elevated in the lung and right ventricle in rats with heart failure (Sirvio *et al.*, 1997). Infusion of the non-specific ET receptor antagonist, bosentan, into patients with heart failure reduces pulmonary vascular resistance to a greater degree than systemic vascular resistance. In addition, the elevated plasma levels

of ET-1 in heart failure have been found to correlate with severity of pulmonary hypertension, filling pressures and pulmonary vascular resistance (Kiowski *et al.*, 1995).

The local (autocrine) actions contribute to systemic and renal vasoconstriction (Schrier & Abraham, 1999). Release of ET from the vascular endothelium contributes to basal vascular tone in both normal and heart failure subjects. Even non-constricting levels of ET-1 sensitise vessels to the contractile responses of catecholamines or AngII. There are numerous interactions between ET-1 and other vasoconstrictors. For example, ET-1 can increase synthesis of NO and AngII in vascular endothelial cells. The effect is a synergistic action to promote vasoconstriction and sodium retention. However, to counteract this, the vasodilators NO, prostacyclin and ANP may all inhibit ET-1 synthesis in the endothelium (Love & McMurray, 1996).

Further evidence for the role of ET arises from the beneficial effects of endothelin antagonism in animal models of heart failure. Using an ET_A receptor blocker in rats post-MI, Sakai *et al.* (1996) demonstrated a dramatic improvement in survival. Treatment normalised central venous pressure, RV systolic pressure and improved LV contractile function (Sakai *et al.*, 1996). Long-term treatment with bosentan significantly reduced mortality nine months after MI in rats (Mulder *et al.*, 1997b; Fraccarollo *et al.*, 1997). Similar beneficial effects have also been obtained in short-term (16 days) treatment with bosentan. However, ET-receptor antagonism did not alter changes towards a foetal gene expression characteristic of LVH, arguing against a direct regulatory role for ET in MI induced hypertrophy (Oic *et al.*, 1998). Bosentan has been tested in human heart failure with similar beneficial results (Sutsch *et al.*, 1998).

There remains controversy concerning whether to use selective ET_A receptor antagonists over non-selective antagonists. In rats eight weeks after CAL, ET_A blockade resulted in increased LV dilatation, and there was no effect on mortality or cardiac haemodynamics (Hu *et al.*, 1998b). Similarly, a different ET_A antagonist caused scar thinning and LV dilatation in the same model (Nguyen *et al.*, 1998). That bosentan is clearly better, implicates ET_B receptors as unfavourable after MI. Although mediating vasodilatation via endothelial cells, ET_B on smooth muscle cells cause vasoconstriction. One hypothesis is that ET_B vasoconstriction in the kidney may promote water and sodium retention, resulting in the increased LV volume (Hu *et al.*, 1998b). However, in healthy volunteers, administration of a selective ET_B receptor antagonist resulted in peripheral vasoconstriction, which suggests endogenous ET_B

receptors have a predominately vasodilatory role, at least in the non-diseased state (Strachan *et al.*, 1999).

Finally, ET-1 is a powerful prognostic indicator of mortality in heart failure patients and is elevated in proportion to NYHA functional class. As an independent indicator, it is more powerful than NYHA, ANP, NA or ejection fraction in predicting outcome (Pousset *et al.*, 1997).

1.4.12 LVH after MI

Hypertrophy of the surviving myocardium occurs in response to MI. As with pressure-overload hypertrophy, LVH is associated with a change to foetal gene expression. In the first few weeks after CAL in the rat, mRNA expression is elevated for β -MHC, α -skeletal actin, collagen types I & III, ANP, BNP and there is a decrease in α -MHC (Gidh-Jain *et al.*, 1998; Nakayama *et al.*, 1997). As with pressure-overload hypertrophy, transition to foetal gene expression can be prevented by either ACE inhibition or AT₁-receptor antagonists, suggesting a role for AngII in the response (Yoshiyama *et al.*, 1999). Therefore, control of hypertrophy after MI is likely to involve all of the mechanisms discussed earlier for hypertrophy in the hypertensive heart.

Cellular morphometry has indicated that within three days of a large MI in rats, individual myocytes have an increased cell volume per nucleus of 28%, due to increases in both cell length and diameter (Anversa *et al.*, 1985a). Depending on the size of the infarct, such changes may take four weeks to become significant. At 4-6 weeks, myocyte length has increased by 38% and may be an important factor in the development of LV dilatation (Anand *et al.*, 1997). As with pressure-overload hypertrophy, elevated wall stress is thought to be a major stimulus. In the case of MI, wall stress is high due to asymmetric ventricular geometry (Anversa *et al.*, 1985a). Cellular growth is mirrored by tissue growth of 29% in the viable myocardium (Anversa *et al.*, 1985b). However, while the surviving myocardium hypertrophies, there is a failure of the capillary network to compensate with equivalent growth. There is no change in capillary length or luminal or endothelial volumes. The consequence is that the same blood supply must supply more tissue, with a subsequent increase in the path length of O₂ transport. This may predispose the post-infarct heart to further ischaemic damage (Anversa *et al.*, 1985b; Liu *et al.*, 1997).

The contractile function of myocytes from surviving myocardium may be normal despite hypertrophy and the confirmation of global systolic dysfunction. This is not a consistent finding, and may vary depending on how distal the myocyte is from the infarct area, and on time since infarction. However, it does suggest that factors such as wall stress, extracellular changes and LV geometry are sufficient to explain LV dysfunction, in the absence of a decrease in myocyte contractility (Anand *et al.*, 1997).

As with pressure-overload hypertrophy, there has been interest in further dissecting the role of AngII in the hypertrophic response. In one study, a reduction in LVH was achieved using a dose of perindopril that had no effect on LV systolic or filling pressures, indicating that this effect was not due to simply lowering blood pressure (Chiba *et al.*, 1994). A similar result has been obtained for the AT₁ antagonist irbesartan (Ambrose *et al.*, 1999). Conflicting results have been observed for perindopril. When the hypotensive effect was prevented by salt-loading, the ACE inhibitor no longer prevented cardiac hypertrophy, suggesting that it is blood pressure and not local ACE inhibition that is important for LVH after MI in the rat (Yoshida *et al.*, 1998).

Hu *et al.* (1998b) found that reduced LV mass with quinapril was abolished by co-administration of a B₂-kinin receptor antagonist, suggesting a bradykinin mediated effect. Similarly, Liu *et al.* (1997) showed that reductions in myocyte CSA and collagen deposition by ramipril were also kinin-dependent. In the same study, the authors found an AT₁ antagonist could decrease LVH, myocyte CSA and LV dilatation. Interestingly, these benefits could be mostly prevented by co-administration of an AT₂ antagonist. The authors speculate that blocking AT₁ receptors increases renin and angiotensin levels resulting in increased activation of AT₂ receptors that mediate the benefits on LVH (Liu *et al.*, 1997).

1.4.13 Extracellular changes in the LV

After MI, there is a 70% increase in myocardial fibrosis i.e. a deposition of myofibrillar collagen. Such changes alter the stiffness of the myocardium and result in impaired relaxation i.e. diastolic dysfunction (Thai *et al.*, 1999). AT₁-receptor antagonism inhibits collagen deposition in the rat heart after MI (Smits *et al.*, 1992), and decreases mRNA expression of collagen I and III (Yoshiyama *et al.*, 1999). This decreased

fibrosis has functional significance as it normalises passive myocardial stiffness and provides a partial improvement in relaxation (Thai *et al.*, 1999).

In one study comparing enalapril and losartan, the ACE inhibitor was more effective in reducing non-myocyte proliferation in the surviving myocardium and reduced collagen deposition. The authors concluded that fibrotic changes in the LV were not a result of a direct AngII effect on AT₁-receptors (Taylor *et al.*, 1998). This is in contrast to the aforementioned studies. In support of this is a beneficial effect of the β -blocker, metoprolol, to reduce interstitial fibrosis and collagen deposition (Latini *et al.*, 1998).

Although myofibrillar collagen is increased in heart failure, this belies the fact that there is also significant breakdown of the collagen matrix, and a wholesale restructuring of the extracellular components. This may be vitally important as alignment of the collagen matrix is thought to be seminal in translating myocyte contractions into global LV performance (Mann & Spinale, 1998). Recently, attention has focused on matrix metalloproteinases (MMPs), which can be secreted from fibroblasts and cardiac myocytes and act to degrade the extracellular matrix. The balance between MMPs and their endogenous inhibitors, tissue inhibitors of metalloproteinases (TIMPs), are thought to be important in remodelling of the extracellular matrix (Mann & Spinale, 1998). For example, in the failing human heart MMP activity is also elevated and there is a corresponding down-regulation of TIMPs (Li *et al.*, 1998). Many neurohumoral factors have been implicated in MMP activation in the failing heart. These include all the usual suspects i.e. noradrenaline, AngII, endothelin, and TNF- α (Mann & Spinale, 1998).

1.4.14 Apoptosis in the failing heart

DNA laddering, indicative of apoptosis has been identified in the myocardium in response to a variety of insults in animal models, for example after, myocardial infarction, pressure-overload hypertrophy, hypertensive left ventricular hypertrophy and mechanical stretch (Davies, 1997).

In culture systems, NO has been shown to induce apoptosis in adult rat ventricular myocytes in a dose dependent manner. ANP can also induce apoptosis in both cultured vascular smooth muscle cells and in neonatal rat cardiomyocytes in a dose-dependent manner. In the heart, this has been shown to be mediated by cGMP. Noradrenaline, endothelin and AngII all promote smooth muscle cell growth and increase survival.

The net effect in the heart or vasculature will depend on the balance of all these factors (Wu *et al.*, 1997).

Apoptosis has also been described in the myocardium of patients with symptomatic end-stage heart failure, which has led to the hypothesis that loss of viable myocytes due to apoptosis may contribute to left ventricular remodelling and dysfunction in the terminal stages of heart failure. (Narula *et al.*, 1997)

A huge range of apoptotic indices have been reported from 0.2% of total cardiomyocytes (Ruffalo & Feuerstein, 1998) to 35% (Davies, 1997). There is a problem in interpreting what this might mean, i.e. are enough myocytes lost via apoptosis to have a significant effect on ventricular function and progression of heart failure? At present, no-one is able to answer this question. Quantification of apoptosis represents a snapshot of cell death at that particular time. To extrapolate such results by estimating an apoptotic rate requires too many assumptions that are probably not valid. For example, 1) the time course of apoptosis is often quoted as within 24 hours (Ruffalo & Feuerstein, 1998), but this is based on cell culture data, and it is not actually known how long the process may last *in vivo*. 2) It is assumed that the number of cells undergoing apoptosis within that 24 hours is constant for any given 24-hour period. This is obviously flawed as apoptotic index may be high in response to acute stimuli (for example after myocardial infarction), examination of the same tissue one week later could find no apoptotic cells, but this does not mean that apoptosis has not been prominent. 3) Apoptosis is evenly distributed in the tissue. Not true, as apoptosis has been described as higher in the infarct border zone, and may occur in focal areas in patients with idiopathic cardiomyopathy (Davies, 1997). 4) Apoptosis represents irreplaceable loss of myocytes as these cells are terminally differentiated. Recent evidence has cast doubt on this assumption. For the first time, true myocyte mitosis has been described in the human heart. Using confocal microscopy, myocardial sections were stained with a nuclear dye to visualise mitotic cells and counter-stained with a myocyte-specific antibody to confirm localisation of mitosis to the myocytes. Further to this, the authors found a ten-fold increase in mitotic index in hearts from patients with end-stage ischaemic heart disease and idiopathic dilated cardiomyopathy (Kajstura *et al.*, 1998). For similar reasons to those outlined, it would be wrong to extrapolate a mitotic rate from this data to determine the significance of this process. However, if confirmed, this groundbreaking study would suggest a dynamic interplay between cell death and cell birth in the failing heart.

1.4.15 Myocyte function

Depressed myocyte contractility has been described in animal models of LV hypertrophy and heart failure, with defective calcium handling a major culprit. Calcium transients are often reported as decreased in amplitude and prolonged, sometimes with high diastolic concentrations (de Tombe, 1998). Several key components of Ca^{2+} homeostasis are thought to be involved, described in both human and animal models.

- 1) There is considerable evidence for reduced expression of the SERCA pump at the mRNA and protein level, leading to depressed Ca^{2+} uptake into the sarcoplasmic reticulum (SR) (de Tombe, 1998; Balke & Shorofsky, 1998; Yamaguchi *et al.*, 1998).
- 2) The ryanodine-sensitive receptor that releases Ca^{2+} from the intracellular stores may also be down-regulated, resulting in reduced function, although this finding has not been consistent (de Tombe, 1998; Yamaguchi *et al.*, 1998).
- 3) The L-type Ca^{2+} channel, which allows extracellular Ca^{2+} to enter the myocyte has variably been reported to decrease (de Tombe, 1998). Recently, an alteration in the juxtaposition between sarcolemmal Ca^{2+} channels and ryanodine-release channels in the sarcoplasmic reticulum, has been suggested to explain the reduced ability of the incoming Ca^{2+} current to trigger SR Ca^{2+} release in hypertrophied and failing rat hearts. This could explain defects in Ca^{2+} signalling in the face of normal levels of cellular components (Gómez *et al.*, 1997).
- 4) The $\text{Na}^+ / \text{Ca}^{2+}$ -exchanger in the plasma membrane extrudes Ca^{2+} and so contributes to relaxation. Expression and activity is often increased in the failing heart, probably to compensate for decreased SERCA pump performance. Indeed, increased $\text{Na}^+ / \text{Ca}^{2+}$ -exchanger is associated with preserved diastolic function, whereas, when there is no change despite reduced SERCA, this results in dysfunction (Hasenfuss *et al.*, 1999).

Since many of these changes are typically observed in both pressure-overload hypertrophy and in heart failure, it seems likely that depressed myocyte function is involved in the gradual decompensation to overt failure. Such defects have been described in rats after CAL (Yamaguchi *et al.*, 1998), however; it is not clear how large a contribution reduced myocyte contractility contributes to global dysfunction.

1.4.16 Heart rate & arrhythmias

Patients with congestive heart failure have a decreased variability in heart rate with depressed diurnal rhythm, which may reflect a decreased parasympathetic or increased sympathetic activity (Casolo *et al.*, 1989). Blunting of the circadian rhythms for both blood pressure and heart rate in such patients correlates with poor cardiac function (van de Borne *et al.*, 1992). Similar depression of circadian rhythms have been observed for blood pressure and heart rate after MI in the rat (Teerlink & Clozel, 1993). Low heart rate variability correlates with high plasma NA concentration and so may be a marker for neurohormonal activity. In addition, drugs which reduce neurohormonal activity also improve heart rate variability e.g. digoxin, β -blockers. This could explain why heart rate variability is a good predictor of mortality (Tuininga *et al.*, 1994).

Arrhythmias are a common complication of MI and are fatal in around 50% of patients in the first few hours after infarct. Rats have been used to study arrhythmias after MI using implantable radiotelemetry probes for continuous measurement of ECG. In common with humans, rats exhibit two distinct arrhythmogenic periods, for the rat, these are between 0-33mins and 1.5-9 hours post-infarct, with relatively few arrhythmias outwith these times. It is worth noting that ventricular tachycardia or ventricular fibrillation affected over 95% of rats, with a mortality of 65% only occurring during the arrhythmogenic windows. The incidence of arrhythmias correlates positively with size of ischaemic area (Opitz *et al.*, 1995). In patients with congestive heart failure, the incidence of ventricular tachycardia is strongly associated with sudden death (Dovak *et al.*, 1996).

1.4.17 Skeletal muscle abnormalities

Heart failure is associated with exercise intolerance manifesting as breathlessness and fatigue. Indeed, poor performance in a walk test is a useful diagnostic indicator (Harrington & Coats, 1997). Measurements of systolic or diastolic dysfunction (e.g. cardiac output and ejection fraction) fail to provide good correlations with markers of exercise capacity such as peak oxygen consumption. For this reason, abnormalities in skeletal muscle have been examined as contributing factors. A number of abnormalities have been described and are outlined below (see also reviews by Harrington & Coats, 1997; and Coats, 1996).

Muscle atrophy affects up to 70% of heart failure patients and is associated with a shift in fibre types, reduced fibre size, decreased mitochondrial density, and metabolic abnormalities resulting in increased early lactate build-up (Harrington & Coats, 1997; Coats, 1996). Vascular defects may be causative, as they occur prior to skeletal abnormalities (Thomas D. *et al.*, 1998). For example, hindlimb blood-flow in response to exercise is significantly decreased in rats after MI (Musch & Terrell, 1992), and the microcirculation exhibits enhanced responses to a range of vasoconstrictors (Didion *et al.*, 1997).

It has been hypothesised that these defects may contribute to the pathophysiology of heart failure by over-sensitising the skeletal muscle ergoreflex system and so promoting sustained SNS activation (Coats, 1996).

1.4.18 Vascular function in heart failure

The elevated total peripheral resistance in chronic heart failure has stimulated interest in alterations to vascular function that may contribute to this effect. As described earlier, increased afterload maintains perfusion pressure in the face of a reduced stroke volume. However, in the long-term it is detrimental and could form part of a “vicious cycle”, whereby increased afterload places more strain on the heart (figure 1.4). The injured myocardium must pump against the increased resistance thereby increasing LVEDP, wall stress and the subsequent compensatory responses of LV hypertrophy and dilatation. If as a result, cardiac output falls further, the drive to increase afterload becomes greater and so on.

Many of the neurohormonal mechanisms outlined above will have a role in determining vascular tone in the heart failure patient. There is increased activity of vasoconstricting agents NA, adrenalinc, AngII, endothelin, vasopressin, sympathetic nervous system, but also of vasodilatory agents such as ANP, BNP, nitric oxide. Obviously, the degree of tone will depend on the balance of all these factors. However, there is also evidence for altered vascular function at a local level.

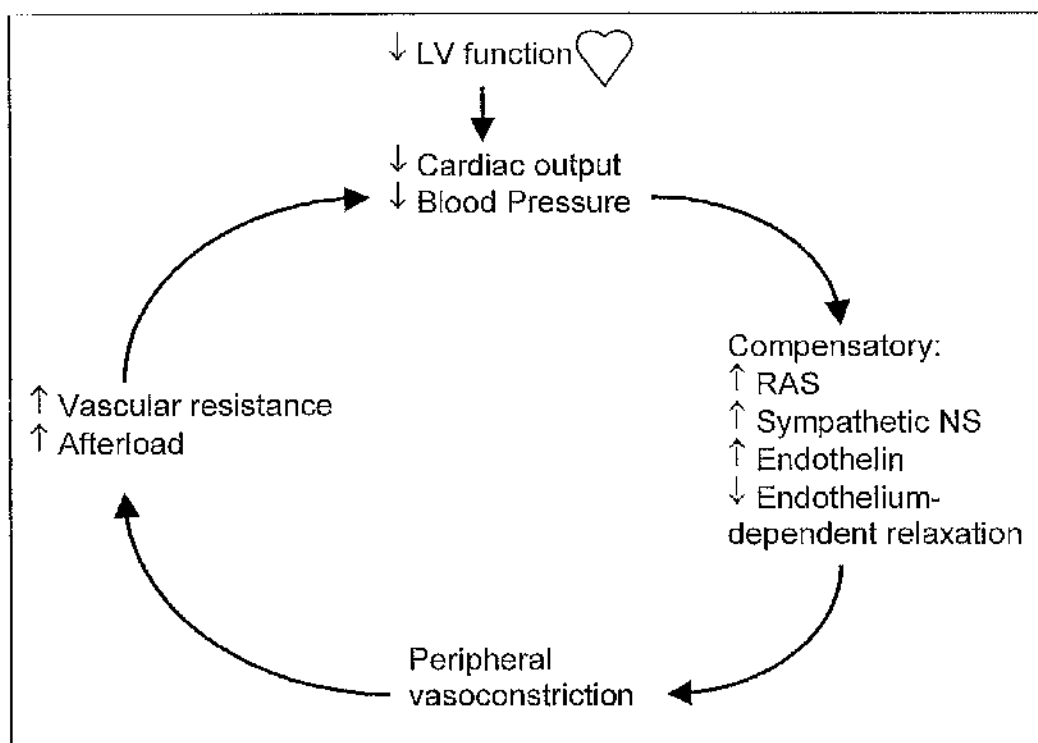


Figure 1.4 Relationship between peripheral vasoconstriction and impaired cardiac performance in heart failure. Modified from Hornig *et al.*, (1998a).

The best evidence for vascular dysfunction in heart failure is in the release of NO by the endothelium. One of the earliest reports was in rats with confirmed heart failure after CAL. In organ bath studies sensitivity to acetylcholine (ACh) was reduced in both the thoracic and pulmonary artery. Endothelium-dependent release of NO was implicated, as relaxation to nitro-glycerine (endothelium-independent) was normal or slightly increased. Basal release was measured by the increase in tension in response to excess haemoglobin, but was diminished only in the pulmonary artery. This vessel difference may reflect the presence of pulmonary hypertension, as RV weight was increased in these heart failure rats (Ontkian *et al.*, 1991). Reduced endothelium-dependent relaxation has since been confirmed in the thoracic aorta of the rat heart failure model by Lindsay *et al.* (1992), Nasa *et al.* (1996), de Vries *et al.* (1997), and Toyoshima *et al.* (1998). In the study by Nasa and colleagues, the impaired relaxation to ACh could be partially restored by addition of a cyclooxygenase inhibitor, suggesting that release of prostaglandin constricting factors may account for some of the dysfunction. In addition, release of basal NO was reduced in these animals (Nasa *et al.*, 1996).

The above studies were performed in rats with heart failure and healed infarcts. Vascular function in thoracic aorta at one week post-MI exhibits different derangements. In these animals, stimulated NO release was found to be normal. However, an enhanced contractility to NA was observed, which could be explained by an impaired basal release of NO from the endothelium. In the absence of endothelium, maximal NA contractility was actually depressed, which was due in part to a reduced α_1 -adrenoceptor sensitivity and a general decrease in smooth muscle cell contractility (Teerlink *et al.*, 1994). One could speculate that the additional defects observed in this study may be related to the early stage after infarction when neurohormonal activation is at its highest (Stassen *et al.*, 1997a) e.g. high plasma NA which could down-regulate receptors.

Resistance arteries

As discussed earlier, vascular resistance resides in the small arteries and dilator dysfunction has also been described in these vessels. In heart failure rats, where the hindlimb is perfused to allow study of an entire vascular bed, the maximal relaxation to ACh is diminished in rats with large infarcts, while response to nitro-glycerine and NOS-inhibition are normal (Drexler & Wenyuan, 1992). Again, this suggests that endothelium-dependent release of NO is normal under basal conditions but that stimulated release is impaired. This result has been confirmed in isolated resistance arteries from the femoral and mesenteric beds. The femoral arteries exhibited significantly greater impairment than the mesenteries (37 versus 63% maximal dilation respectively), suggesting endothelial dysfunction is heterogeneous between vascular beds (Mulder *et al.*, 1996). More evidence for this is the impaired stimulated and basal release of NO reported by Baggia *et al.* (1997) in the pulmonary arteries, but not in abdominal aorta or 3rd order mesenteric resistance arteries (Baggia *et al.*, 1997). Stassen *et al.* (1997b) also report heterogeneity in contractile dysfunction between vessels in the ligated rat. In mesenteric resistance arteries they describe a generalised reduction in maximal response to a range of contractile agents, which could not be explained by a reduction in muscle mass. In contrast, the same agents demonstrated hyperreactivity in vessels from the non-infarcted myocardium, which they hypothesise may be due to exposure to locally high levels of contractile / pro-mitogenic factors in the myocardium.

Meanwhile, there was no evidence of contractile dysfunction in the thoracic aorta (Stassen *et al.*, 1997b).

In contrast with many of the above studies, Buus *et al.* (1999) recently reported that maximal relaxation to ACh was normal in third order mesenteric resistance arteries from CAL rats at both 8 and 26 weeks post-MI. This time, a reduced basal release of NO was noted. However, the authors note that NOS inhibition induced contractions are very small in the mesenteric resistance arteries, and so basal NO may not be a major determinant of tone in these vessels (Buus *et al.*, 1999). The between study discrepancies in ACh-induced relaxations may be due to differences in experimental protocol, in particular, whether endothelium-derived contractile prostanoids have been inhibited or by not controlling for EDHFs.

Since EDRF has been implicated in endothelial dysfunction, the most obvious approach is to measure the expression of eNOS mRNA and eNOS protein, by Northern and Western blots respectively, to determine if the decrease in EDRF-mediated relaxation is due to a reduced expression of the eNOS enzyme. Smith *et al.* (1996) performed these experiments in dogs with pacing-induced heart failure, measuring eNOS expression in endothelial cells scraped from the thoracic aorta. Comparing heart failure animals with sham operated, they found a 56% reduction in eNOS mRNA expression with a corresponding decrease of ~70% in actual eNOS protein, and reduced enzyme activity.

In a similar fashion, Comini *et al.* (1996) measured eNOS protein levels in the thoracic aorta of Sprague-Dawley rats given monocrotaline, which induces congestive heart failure secondary to pulmonary hypertension. They measured eNOS in both endothelium and smooth muscle and found it to be differentially regulated. In heart failure, endothelial eNOS decreased to 5% of sham levels, whereas smooth muscle eNOS increases by over 200% compared to the sham animals. This supports the assertion that vascular changes during CHF are complex and local, occurring in both endothelium and smooth muscle layers. In this experiment the total aortic eNOS fell to 60% of control levels, and this is consistent with the physiological changes showing depressed relaxation in CHF. iNOS was not detected in this preparation (Comini *et al.*, 1996).

By measuring blood flow and noradrenaline gradient across an organ there is evidence to suggest that the degree of sympathetic activity displays regional differences. Cardiac sympathetic activity may increase between three- and fivefold, while renal activity threefold, and splanchnic sympathetic tone increases only twofold (Kaye & Esler,

1995). This may help explain the regional differences in vascular function observed in human and experimental heart failure. For example, the popular use of mesenteric arteries for examining vascular function in the rat may not represent the best opportunity for observing alterations in noradrenergic transmission. Further evidence for this is that while β -adrenoceptor function is blunted in the heart, there appears to be no evidence for similar down-regulation in the peripheral circulation, and this may be due to the higher sympathetic activity in the heart (Kaye & Esler, 1995).

Human vessels

Studies of vascular function in humans may be confounded by concomitant therapy and by underlying pathologies such as hypertension, atherosclerosis and by smoking. However, similar defects to the rat have been described. In gluteal subcutaneous resistance arteries from patients with heart failure of ischaemic origin, Angus *et al.* (1993) described a generalised hyperreactivity to contractile agonists such as KCl, NA and AngII, and an impaired stimulated release of EDRF. In contrast, Stephens *et al.* (1998) examining the same vessels found no alterations in contractile function, or relaxation. However, heart failure was mild in these patients.

Due to the difficulty in obtaining vessels from humans, many studies have examined blood flow of the whole forearm using plethysmography. This has the advantage of measuring responses from a whole vascular bed, and because vessels are *in situ*, they remain under the influence of the SNS and circulating vasoactive factors. Using this technique, heart failure patients were found to have impaired stimulated endothelium-dependent relaxation (Kubo *et al.*, 1991). This result has been confirmed by Hirooka *et al.* (1992) and Katz *et al.* (1993). In the latter study, several layers of dysfunction were apparent. As well as reduced EDRF release, cGMP-mediated relaxation was impaired at the smooth muscle level. Indomethacin did not affect basal blood flow, but did increase blood flow in response to ACh in heart failure, but not normal patients. Therefore endothelium-derived contracting factors of prostanoid origin may also contribute to the diminished ACh response in human heart failure (Katz *et al.*, 1993).

The extent of vascular dysfunction is directly related to the severity of heart failure. Carville *et al.* (1998) found impaired relaxation to ACh in subjects with moderate heart failure, which was significantly worse in those with severe disease. In addition, only those with severe heart failure exhibited impaired relaxation to sodium nitroprusside.

As with hypertension, abnormalities in the NO-system with heart failure have been linked to reduced availability of NO, probably via destructive interaction with oxygen free radicals. Acute intravenous and chronic oral treatment with the antioxidant vitamin C improved NO-dependent flow in the radial artery of heart failure patients compared with controls. (Hornig *et al.*, 1998b)

Coronary vessels

In the coronary vessels a reduction in maximal dilatory response (as discussed above), represents a loss of cardiac reserve. In the healed rat heart post-myocardial infarction, reduction in vasodilator response has been observed in the surviving hypertrophied myocardium, manifesting as a decreased maximal tissue perfusion. The authors speculate that resistance arteries feeding this part of the myocardium may already be vasodilated to supply the increased needs of an hypertrophied left ventricle. The inability of these vessels to further vasodilate in response to increased demand would make the hypertrophied part of the left ventricle most at risk from further ischaemic attacks. (Kalkman *et al.*, 1997)

Vascular function – summary:

- 1) Impairment of either (or both) stimulated and basal release of EDRFs are common observations in blood vessels of all sizes from animals and humans with heart failure irrespective of aetiology.
- 2) Extent of dysfunction is proportional to severity of heart failure. Generalised hyporeactivity to vasoconstricting factors and impaired smooth muscle cell relaxation pathways, are probably more common in severe heart failure.
- 3) Vascular dysfunction is highly heterogeneous between vascular beds, dysfunction occurs in isolated vessels and so is related to local defects, not just to elevation in systemic neurohormonal mechanisms.

1.4.19 *Vascular structure in heart failure*

Vascular structural alterations in heart failure are mild and not always apparent. This is surprising considering the well-defined vascular remodelling observed in hypertension, and the higher levels of neurohumoral factors present in heart failure. For example, noradrenaline, AngII, endothelin, ANP and NO can all affect vascular growth and apoptosis.

In data obtained after CAL in the rat, large conduit vessels have been reported to have a reduced medial CSA and decreased media-to-lumen ratio i.e. inward hypertrophic remodelling. This has been described in the thoracic aorta, abdominal aorta, renal artery, superior mesenteric artery and carotid artery (Heeneman *et al.*, 1995). However, studies are just as likely to show no change in these vessels, at least in the thoracic aorta, which has been most extensively studied (Stassen *et al.*, 1997b; Richer *et al.*, 1992; Ceiler *et al.*, 1998).

In the resistance arteries the picture is not any clearer. For the mesenteric resistance arteries, a number of studies have found no change in media CSA or media-to-lumen ratio for a wide range of time points from one day to one year post-infarct (Mulder *et al.*, 1996; Stassen *et al.*, 1997b). Negative results have also been obtained in femoral resistance arteries (Mulder *et al.*, 1996), myocardial resistance arteries (Kalkman *et al.*, 1996) and in human subcutaneous resistance arteries (Stephens *et al.*, 1998). Only two studies report structural alterations in the mesenteric resistance arteries. In both, medial CSA remains close to normal while lumen diameter increases, resulting in a lower media-to-lumen ratio (Heeneman *et al.*, 1995; Buus *et al.*, 1999). Therefore, there is no change in quantity of material, but remodelling of existing material around a slightly enlarged lumen.

In summary, vascular structural alterations in heart failure are borderline and may only be observed dependent on severity and time course of failure. A fine balance of vasoactive factors may contribute to maintaining the status quo. For example, in normal rats, infusion of AngII increases blood pressure and results in vascular hypertrophy. An identical infusion in rats after CAL has neither of these effects. However, co-infusion of AngII + NOS inhibitor in CAL rats, still does not increase blood pressure, but vascular hypertrophy is observed. This suggests that during heart failure NO counters the mitogenic effects of AngII (Heeneman *et al.*, 1997).

2. Methods

This chapter describes general laboratory practice and details techniques that are common to more than one chapter. The experimental protocols for each group of experiments are described in the relevant chapters, along with techniques applicable only to that chapter.

2.1 General laboratory Practice

All experiments were performed using the highest quality reagents available and using the appropriate level of safety as prescribed in the Control of Substances Hazardous to Health regulations i.e. lab coat, safety goggles, mask or fume cupboard where appropriate.

Animal strains

All rat work was undertaken in accordance with the Animals (Scientific Procedures) Act 1986 under the project licence "Spontaneously Hypertensive Studies" 60/1982, held by Prof. Dominiczak.

Animals were provided by an in-house breeding programme of SHRSP and WKY rats. Inbred colonies of these strains have been maintained in Glasgow by brother-sister mating since 1991, when 6 males and 7 females of each were gifted by Dr. D.F. Bohr from the Department of Anatomy and Cell Biology at the University of Michigan, USA. The original breeding stock was obtained over 15 years previous from the National Institutes of Health, Bethesda, USA. In order to preserve the hypertensive versus normotensive phenotype, only adult animals with the following characteristics are selected as breeders. Male SHRSP with systolic blood pressure 200-230mmHg, and females with 170-190mmHg and WKY males 130-150mmHg, females 100-130mmHg. All rats were kept in a controlled environment for temperature (21°C) and humidity, with a 12-hour light/dark cycle. Normal rat chow (rat and mouse No.1 maintenance diet, Special Diet Services) and water was available *ad libitum*. Individuals were housed with siblings in same sex groups until on procedure, when they were housed one per cage.

Body weight and tibial length measurements

Body weights of animals were taken immediately prior to all manipulations and procedures using a Ohaus Lume-O-Gram balance. Animals undergoing surgery also had external tibial length measured with Mitutoyo digital calipers (Jencons Scientific Ltd.).

Blood pressure measurement

Systolic blood pressure was measured by tail-cuff plethysmography (Evans *et al.*, 1994). In order to fully dilate the vessels in the tail, rats were pre-warmed to 36°C in a well-ventilated polystyrene box containing familiar bedding to minimise stress. The animals were then wrapped in a cloth to keep them placid while an inflation cuff was placed around the tail. The cuff was controlled by a Hartman & Braun type 2 current/pressure transducer, capable of delivering 1mmHg steps over a range of 0-300mmHg. A piezoceramic transducer was incorporated for pulse detection over this range of pressures, and interfaced to an IBM-compatible personal computer. The pulsation signal was displayed as a function of pressure to enable automated estimation of the systolic blood pressure. A minimum of three such readings were made for each rat, and the average taken as the blood pressure for that sitting.

Tissue harvest & blood sampling

Where blood samples were required, these were collected by cardiac puncture. Animals were deeply anaesthetised using halothane 5% in O₂, and the chest wall quickly opened. A 10ml syringe with green 21G needle was rinsed with heparin sodium (1000 units/ml) and used to withdraw blood directly from the still beating left ventricle. A quantity of between 4 and 10ml of blood could be extracted per animal. This was transferred to heparinised tubes and stored on ice. The blood was fractionated by centrifugation at 2500 revolutions per minute, 4°C for 10 minutes (Centra-7R, International Equipment Company). The plasma supernatant was collected and stored at -20°C until required.

Neuroendocrine measurements

Plasma renin activity was measured using an antibody-trapping method adopted for use with rat plasma (Morton & Wallace, 1983). Plasma aldosterone were analysed using a commercial radioimmunoassay (Peninsula Laboratories, California, USA).

Rat ANP was measured in plasma by radioimmunoassay, after prior extraction on C18 Sep-Pak columns, with a modification of the method of Richards *et al.* (1987). The antibody cross-reacted 100% with rat ANP. Rat BNP was measured with a radioimmunoassay kit (RIK 9103, Peninsula Laboratories) again after prior extraction.

2.2 Preservation of tissues & RNA extraction

Tissue harvest and general laboratory practice

Where rat hearts were collected for Northern blot analysis, both atria were removed and approximately 25% of the left ventricular free wall proximal to the mitral valve. Tissue was immediately snap frozen in liquid N₂, and stored at -70°C until required. Dissection was rapid to minimise degradation of RNA by endogenous RNAases.

To protect the samples from RNAases present in the environment, all work was performed using RNAase-free technique. This involved wearing gloves at all times, and changing them frequently to prevent self-contamination. All work surfaces and equipment were cleaned with a 3% solution of hydrogen peroxide, and all solutions were made using a 0.1% solution of the RNAase inhibitor diethyl pyrocarbonate (DEPC) in distilled water followed by autoclaving. At all times during processing, samples were kept on ice to slow down any degradation. By strict adherence to these principles, no problems due to RNA degradation were experienced.

RNA extraction

To isolate RNA, each tissue sample was removed from the freezer and dropped into a test-tube containing 4ml of chilled RNazol B (Biogenesis), then homogenised using a Kinematica polytron homogeniser (Philip Harris Scientific, Aberdeen, UK). To each sample was added 400µl chloroform followed by vortexing for 15 seconds, and left on ice for 5 minutes. Tubes were then spun at 4°C in a centrifuge at 2500 revolutions per minute for 10 minutes (Centra-7R, International Equipment Company). The

supernatant containing RNA was transferred by sterile Pasteur pipette into 15ml glass test-tubes. Care was taken not to disturb the interface between layers to prevent contamination with DNA. An equal volume of isopropanol was added and the tube mixed by inversion before being allowed to precipitate on ice for at least 30 minutes.

After RNA precipitation, tubes were spun in a centrifuge at 4°C and 10000 revolutions per minute for 15 minutes (Model J2-21, Beckman). After discarding the supernatant, the resulting pellet was washed with 2ml of 70% ethanol to dissolve salts, followed by vortexing, and a further 15 minutes of centrifugation at the same settings. Ethanol was then removed using a sterile Pasteur pipette, and the pellet left on ice to dry. The pellet was re-suspended with 100-200µl of DEPC H₂O, and stored in a sterile Eppendorf tube at -70°C.

Agarose gel electrophoresis

Integrity of the RNA solution was then checked using agarose gel electrophoresis. A 1% agarose gel was made with tris-acetate (TAE) buffer and incorporating 1µl ethidium bromide. This was placed in an electrophoresis tank and immersed in TAE buffer. To each well was added 2µl of the RNA solution to be tested, 3µl DEPC H₂O, and 1µl of agarose gel blue loading dye (6x strength). One well was reserved for running molecular weight markers created by the restriction enzyme λ Hind III (Promega). The gel was then run by applying a potential difference of 5 volts per cm until the loading dye had migrated two thirds of the way down the gel. RNA was then visualised under an ultraviolet (UV) transilluminator (UVP). Good quality RNA samples showed clear strong bands of 28S, 18S and 5S ribosomal RNA and a light smear representing the full range of mRNAs which are present only at low concentrations. An example is shown in Figure 2.1.

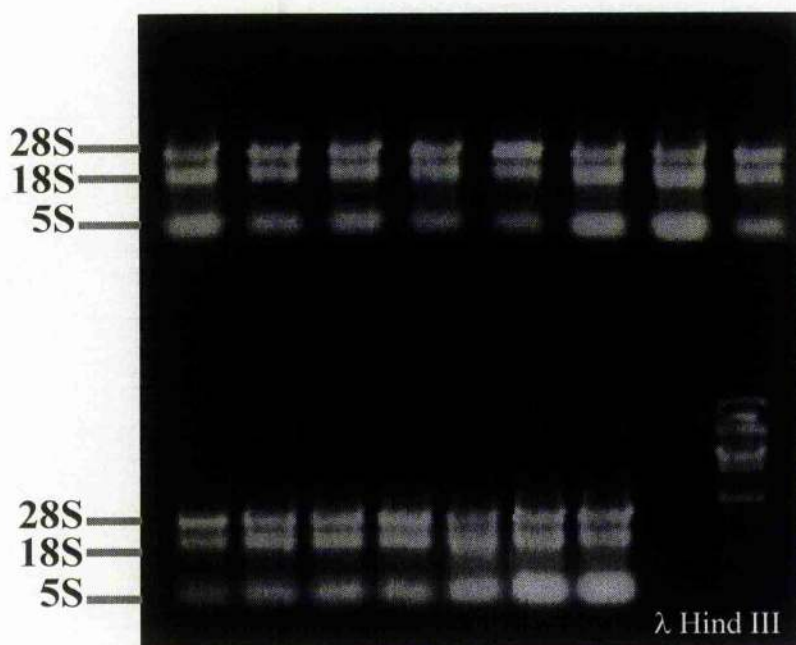


Figure 2.1 Example of 1% agarose gel incorporating ethidium bromide for checking integrity of total RNA. Each lane contains sample RNA from the left ventricle of either WKY or SHRSP animals. The three distinct bands in each lane represent the high abundance 28S, 18S and 5S ribosomal RNAs which are approximately 5000, 2000 and 160 nucleotides long respectively. The final lane has been loaded with the digest product of the restriction enzyme λ Hind III.

RNA quantification

RNA concentration and purity was measured by spectrophotometry. A quartz UV transparent cuvette was filled with 1ml of DEPC H₂O and the absorbance zeroed on spectrophotometer (Ultrospec 2000, Pharmacia Biotech, St. Albans) at a wavelength of 260nm. RNA solution was then added to the cuvette in 2 μ l and 4 μ l volumes to give dilutions of 1 in 500 and 1 in 250 respectively. The use of two different dilutions provided an internal check that the measured absorbance was in a linear relationship with the concentration of RNA. Measurements were repeated at a wavelength of 280nm.

The optical density (OD) or absorbance was used to determine the purity of the RNA sample. The optical density at 260nm (OD_{260}) is a measure of RNA concentration, whereas the OD_{280} reading corresponds to the protein concentration. A ratio of these values, $OD_{260}:OD_{280}$, in the range 1.8 to 2.3 was taken to be indicative of a satisfactory level of purity.

The OD_{260} value was further used to calculate the concentration of single strand RNA (ssRNA) in the sample solution. Since an OD_{260} of 1.0 is equivalent to 40 μ g of ssRNA in a 1000 μ l sample, it was calculated that,

$$\text{ssRNA concentration of sample } (\mu\text{g/ml}) = OD_{260} \times 40 \times \text{dilution factor}$$

(Sambrook *et al.*, 1989)

2.3 Northern blot analysis *(see Appendix for solution recipes)*

A quantity of sample containing 10 μ g total RNA was mixed in an Eppendorf with 3 volumes of 100% ethanol, and 1/10th volume of 3M Sodium Acetate, then stored overnight at -70°C.

The next day, samples were defrosted and pelleted by centrifugation at 14000 revolutions per minute for 30 minutes at 4°C (Eppendorf 5402). The supernatant was removed and pellet washed with 180 μ l of 70% ethanol before re-spinning for 15mins. Again the supernatant was removed and samples left on ice to dry.

A 1% (w/v) agarose gel was made incorporating 10% 10x denaturing gel buffer (Ambion), without ethidium bromide. Pelleted samples were re-suspended in 5 μ l DEPC H₂O and 15 μ l northern sample loading dye (Ambion) then incubated for 15 minutes at 65°C to denature secondary structure. The samples were loaded on the gel, with one lane containing 5 μ l DNA fragments from λ Hind III as size markers. The electrophoresis tank was filled with 1x denaturing gel buffer (Ambion) and run at a potential difference of 5 volts per cm until the loading dye had migrated two thirds of the way down the gel.

Capillary transfer

The size fractionated RNA was transferred from the gel to a positively charged nylon membrane (Boehringer 1417240) by capillary transfer. A perspex bridge was placed in a tray containing 20x SSC solution, and covered by 3 layers of Whatmann 3MM paper

which had been soaked in 20x SSC. Assemblage was such that both ends of the paper were in the 20x SSC solution, and so could act as a wick. The gel was placed on top of the bridge and then the nylon membrane cut to size and soaked in 2x SSC. A further 3 layers of Whatmann 3MM paper soaked in 2x SSC were cut to the same size as the gel and added, and finally a 2 inch thick bundle of tissue paper which was weighted down with a 500g weight. At all stages, care was taken to remove air bubbles between layers. Contact between upper and lower layers, except through the gel, was prevented by carefully sealing around the gel with Parafilm. The transfer assembly was left overnight.

The next day the transfer system was disassembled and the membrane rinsed in 6x SSC, air dried for 30 minute, then baked in an oven for 30 minutes at 80°C to deglyoxylate the RNA. Cross-linking to the membrane was achieved by irradiating with 2400 joules ultraviolet light (Stratalinker 2000, Stratagene Ltd., Cambridge). The lane containing DNA molecular size markers was cut off and visualised by staining for 5 minutes in 0.04% (w/v) methylene blue in 0.5M NaOAc (pH 5.5), followed by washing for 20 minutes in distilled H₂O.

Hybridisation

The membrane was placed into a hybridisation flask (Techne) containing 10ml per 100cm² pre-hybridisation solution (Ambion) and washed for 1 hour at 42°C in a hybridisation oven (Hybridiser HB-1, Techne).

In the meantime, the DNA probe was radiolabelled. In all experiments the blot was initially hybridised with a cDNA fragment of glyceraldehyde phosphate dehydrogenase (GAP). In an Eppendorf, 2µl GAP fragment (15ng/µl) and 43µl distilled H₂O were mixed then denatured at 95°C for 3 minutes (Griffin block heater) and placed on ice for 2 minutes. The contents of the Eppendorf were used to re-suspend Ready to Go DNA labelling beads (Pharmacia Biotech 27-9240-01), to which was added 5µl radioactive dCT³²P (Amersham Pharmacia Biotech.) followed by incubation at 30°C for 30 minutes. To purify the probe, a Nick column (Pharmacia Biotech) was washed through with 3ml TE solution, the probe was added followed by 400µl TE, which was collected in an Eppendorf and discarded. A second 400µl TE solution was added to the column and collected in a clean Eppendorf, this aliquot contained the purified radiolabelled probe,

demonstrated by high radioactive counts on a Geiger counter. Again, DNA was denatured at 95°C for 3 minutes followed by cooling on ice for 2 minutes. The radiolabelled probe was added to hybridisation solution (10ml per 100cm² of blot, Ambion) and replaced the pre-hybridisation solution in the hybridisation flask. The probe was incubated with the membrane overnight at 42°C with continuous turning. Subsequent hybridisation e.g. for ANP, BNP or iNOS, followed the same protocol for radiolabelling, but with a comparative quantity of appropriate cDNA substituted for GAP.

Blot washing & visualisation

The next day, the blot was washed to remove non-specific radioactivity using the wash protocols and solutions detailed in appendix I. The blot was then wrapped in cling film and placed in a cassette with two enhancement screens for autoradiography using high performance autoradiography film at -70°C (Hyperfilm, Amersham). Initial exposure time was for 24 hours, when film was developed using a Kodak X-OMAT automated developer. If necessary the blot was re-exposed for a length of time dependent on the signal intensity and signal-to-noise ratio.

Densitometry and analysis

Developed blots were scanned using a Fluor-S MultiImager (Bio-Rad) and analysed on a personal computer using Multi-Analyst Version 1.1 software (Bio-Rad, Hercules, USA). Measurements of optical density were made on-line by using the freehand drawing tool to draw round individual bands on the blot. Background readings of optical density were also taken, and the optical density (OD) of a given band calculated as -

$$\text{O.D.} = (\text{OD}_{\text{band}} - \text{OD}_{\text{background}}) \times \text{Area of band}$$

This allowed for comparison of relative abundance of RNA between lanes on a single blot. The molecular sized markers were used to check that the observed RNA band was at the expected size for that gene product e.g. 1.8 kb for GAP.

If blots were to be re-probed for visualising other gene products, then the blot was stripped by repeated washing in a solution of 0.1% SDS w/v at 100°C.

Preparation of cDNA for hybridisation

Complimentary DNA (cDNA) was used as the hybridisation probe. Probes for GAP and ANP Northern were available from previous work in this lab. The cDNA for BNP was prepared utilising the reverse transcriptase-polymerase chain reaction (RT-PCR) to produce multiple copies of the region of interest. Forward and reverse primers were designed based on the known sequence for rat BNP (Brosnan *et al.*, 1999), and were synthesised by Oswel DNA service (Southampton, UK). The nucleotide sequence was as follows,

Forward primer AGACAAGAGAGAGCAGGACAC

Reverse primer AGACTGTCGGTAAGGTAGAGG

The annealing temperature for these primers was estimated from the GC content as 59°C. It was calculated that the product would be approximately 750 base pairs long and so would require a longer than normal cycle time for elongation. Therefore, the conditions for PCR were set at 1 minute at 94°C, followed by 1.5 minutes at 59°C for annealing, then 2 minutes elongation time at 72°C. This cycle was repeated 30 times.

In a 96-well tray, the following components were added to give a final volume of 20µl in each of 12 wells.

5µl of 20ng/µl WKY genomic DNA

5µl of 1µM primers solution to give final concentration of 0.25µM

10µl Mastermix (Promega) containing dNTPs, 10x buffer, dH₂O, 10x Mg²⁺ (final Mg²⁺ concentration of 1.5 mM, and 0.375 units of Taq DNA polymerase (Promega).

This reaction mixture was covered by a drop of mineral oil to prevent evaporation. Before adding the Mastermix the DNA and primers were given a hot start of 4 minutes at 94°C to denature secondary structure. Water blanks were run in two of the wells in which WKY genomic DNA was replaced with dH₂O in order to check for contamination by foreign DNA.

After 30 cycles of PCR, the contents of the wells were combined, mixed with 6x loading dye, and run on a 1.5% agarose gel together with the water blanks and λHind III molecular weight markers. The agarose gel incorporated 1µl ethidium bromide to enable visualisation and so check that the product was the expected size (Figure 2.2).

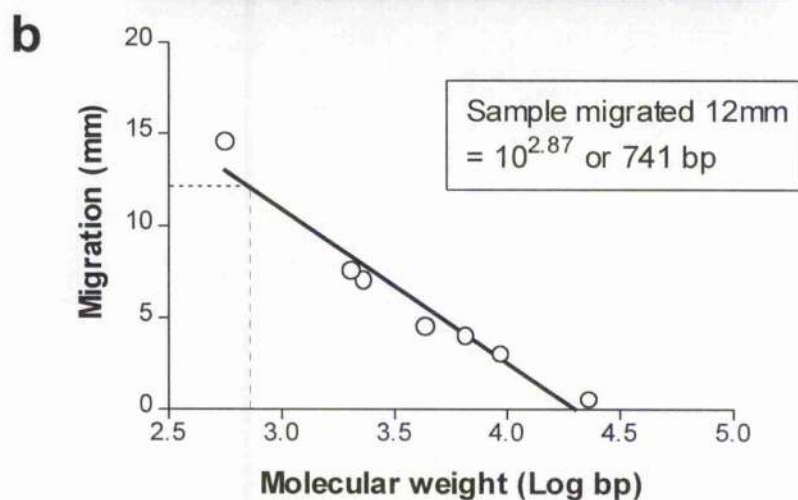
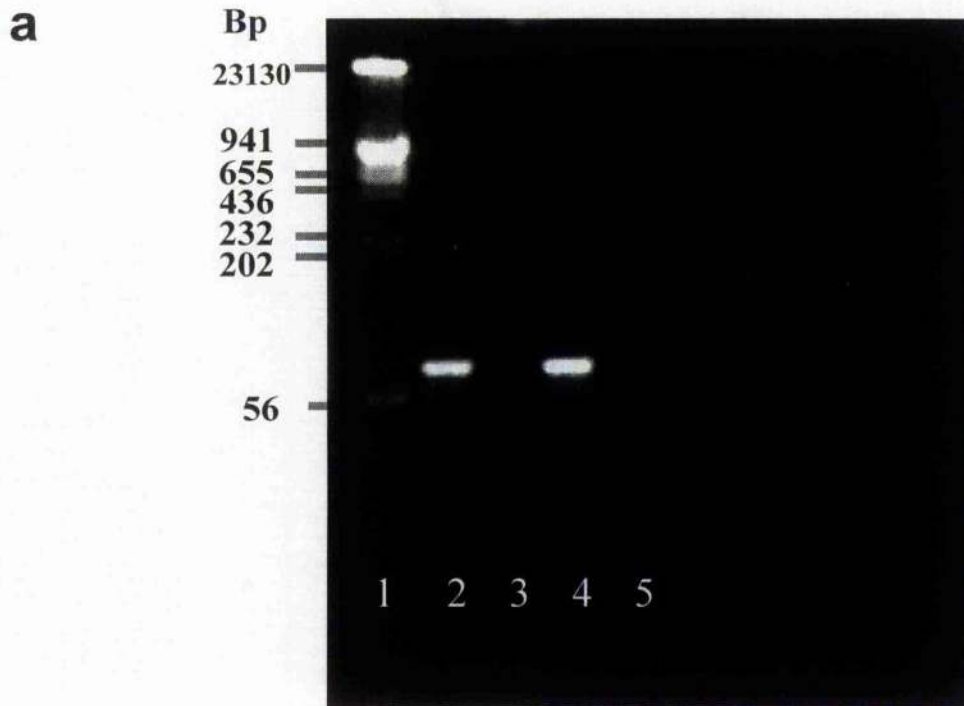


Figure 2.2 Panel (a) shows BNP PCR products run on a 1.5% agarose gel. Lane 1 was loaded with λ Hind III molecular weight markers with size of fragments in base pairs (bp) indicated on the left-hand side. Lanes 2 and 4 contain 1 μ l samples of PCR product, and lanes 3 & 5 contain water blank controls. Panel (b) is a standard curve of migration distance against molecule weight for the molecular weight markers. The PCR samples migrated 12mm, which corresponds to a molecular weight of 741 base pairs.

To prepare a solution of the cDNA, the band obtained from the agarose gel was cut-out and placed into a small section of dialysis tubing that had been pre-soaked in distilled water. The tube was filled with a few millimetres of 1x TAE and sealed, taking care to

remove air bubbles from the bag. The dialysis tubing was placed in an electrophoresis tank orientated such that the band of gel was orientated towards the negative electrode. A current of 80 volts was then applied for 30 minutes in order to electrophorese the DNA out of the gel and into solution. Purification of the cDNA was by standard phenol and chloroform extraction. The cDNA was then radiolabelled prior to hybridisation as described earlier in section 2.3.

2.4 Confocal microscopy

Confocal microscopy for imaging rat mesenteric resistance arteries is utilised in hypertensive rats (Chapter 4) and in rats after coronary artery ligation (Chapter 5). The methodology applied to each was identical, and was based on a technique developed in this laboratory (Arribas *et al.*, 1996; McGrath *et al.*, 1995; Arribas *et al.*, 1997).

A large section of the mesenteric arcade was dissected from an area supplying the jejunum, and bathed in PPS while fine dissection of 3rd order mesenteric resistance arteries was performed. The basis for artery selection is described in Figure 2.3. Arteries were mounted on a perfusion myograph and fixed with formal saline under pressure (Living Systems Instrumentation). Vessels for Chapter 4 were fixed at half the systolic blood pressure measured *in vivo* by tail-cuff plethysmography. Since blood pressure data was not available for heart failure rats, vessels from these animals were fixed at 50mmHg, which had been calculated from wire myography experiments to be 90% of *in vivo* lumen diameter.

Nuclei were stained by incubation with 10µmol/l. propidium iodide for 1 hour, then washed for 3 hours. Vessels were visualised following the method of Arribas *et al.* (1997) with an Odyssey Real Time Laser Scanning Confocal Microscope (Noran instruments), using excitation at 488nm from an argon ion laser, and emission at 515nm with a slit size of 15µm. The lumen was visualised with a 10x air objective through the widest section of the vessel. A 40x water immersion objective was used for wall thickness measurements, when the plane was focused in the middle of the artery and 1µm z-axis segments were taken through the vessel wall. Metamorph software (Universal Imaging Corporation) was used to make calibrated measurements from a minimum of three lumen images and two wall thickness stacks per vessel.

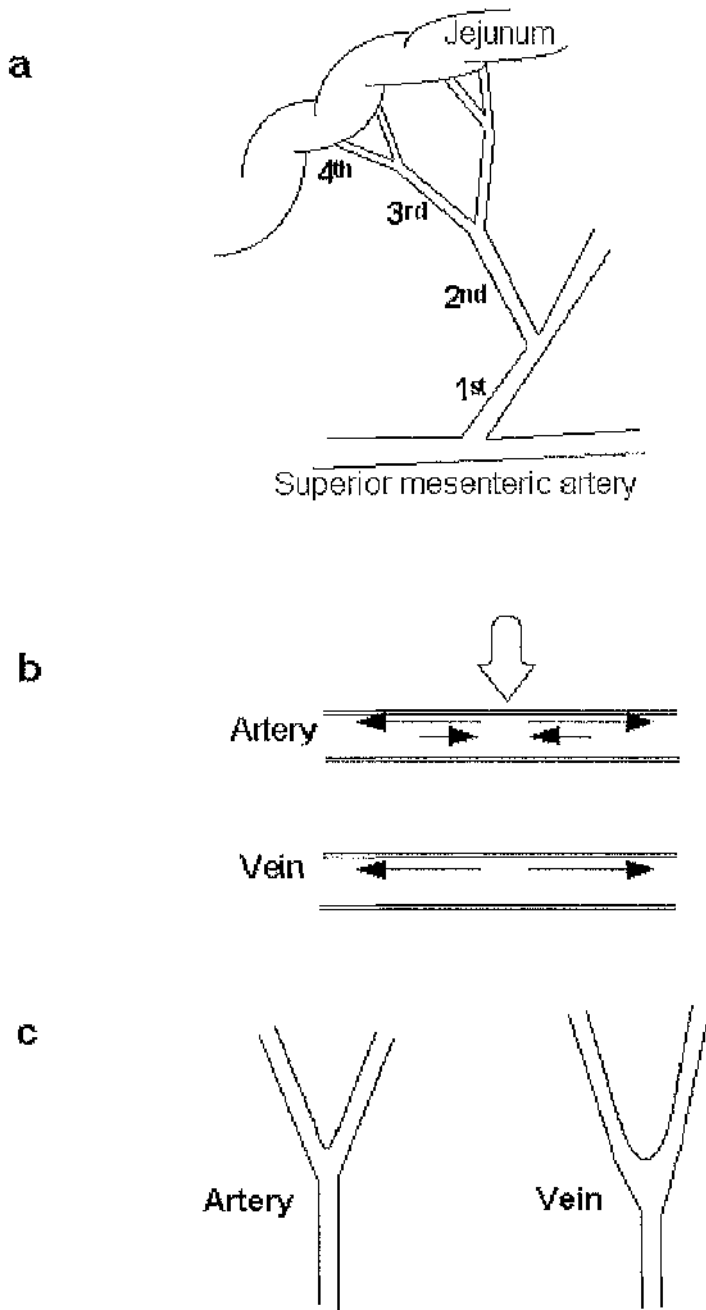


Figure 2.3 Anatomical selection of 3rd order mesenteric resistance arteries. Typical internal diameter ranges from 150-250 μ m. Panel A indicates the position of 3rd order vessels in the mesenteric arcade. Panels B & C illustrate methods employed for differentiating arteries from veins. When depressed with forceps, blood contained in arteries (but not veins) will return to the area of depression due to the muscular walls (panel b). The junctions in arteries also differ from veins (panel c).

The arrangement of the imaging plane perpendicular to the artery is demonstrated in Figure 2.4. Multiple imaging planes were taken along the z-axis, probing deeper into the vessel wall in 1µm increments. The scale diagram indicates that the width of the imaging plane at 102µm is wide enough that some curvature should be expected in these small vessels if the artery in cross-section remains perfectly round. It therefore becomes important to adopt a protocol to ensure that curvature does not result in an overestimation of the wall thickness when measuring between the most distant points of the inner and outer surfaces. Fortunately, the effects of curvature are easy to identify, for instance, when endothelial cells are visible in the centre of the image, with smooth muscle cells occurring in bands above and below. In these cases, only cells included within the central band were used to calculate dimensions, while all cells were counted for cell number data. A computerised counting system was utilised to ensure cells were not double counted in error.

The following data are measured directly, wall thickness, adventitial, medial and intimal thickness and cell numbers. The method for identification of cell types is shown in Figure 2.5. Other parameters such as cross-sectional area (CSA) or volumes are calculated as outlined below. The assumptions made in these calculations are that vessels are of uniform thickness and composition along their length and circumference, and that they form a perfect circle in cross-section.

We know from calibration of the microscope the area of each plane (image) in the stack, which remains constant throughout the experiments.

$$\text{Area of image} = 10404 \mu\text{m}^2 \quad \equiv \quad 0.010404 \text{ mm}^2$$

The number of endothelial cells (nEC) is counted from a set of 4 – 8 images and calculated as endothelial cell number per mm².

$$\text{nEC/mm}^2 = \text{Total nEC} / (\text{Area of image} \times \text{Number of images}) \quad \text{Equation 1}$$

The external diameter was not measured directly, but was simply calculated as,

$$\text{External diameter} = \text{lumen diameter} + (2 \times \text{wall thickness}) \quad \text{Equation 2}$$

Using this, the cross-sectional area (CSA) was calculated assuming the cross-section to form a circle, such that area = πr^2 , where r = radius of circle. The CSA using the internal dimensions could then be subtracted from CSA of external dimensions to obtain the area of each layer of interest.

$$\text{Vessel wall CSA} = [\pi(\text{External diameter}/2)^2] - [\pi(\text{lumen diameter}/2)^2] \quad \text{Equation 3}$$

Adventitial CSA was calculated using equation 3 by including medial and intimal thickness with lumen radius when calculating internal dimensions. Media and intima CSAs were calculated in a similar way.

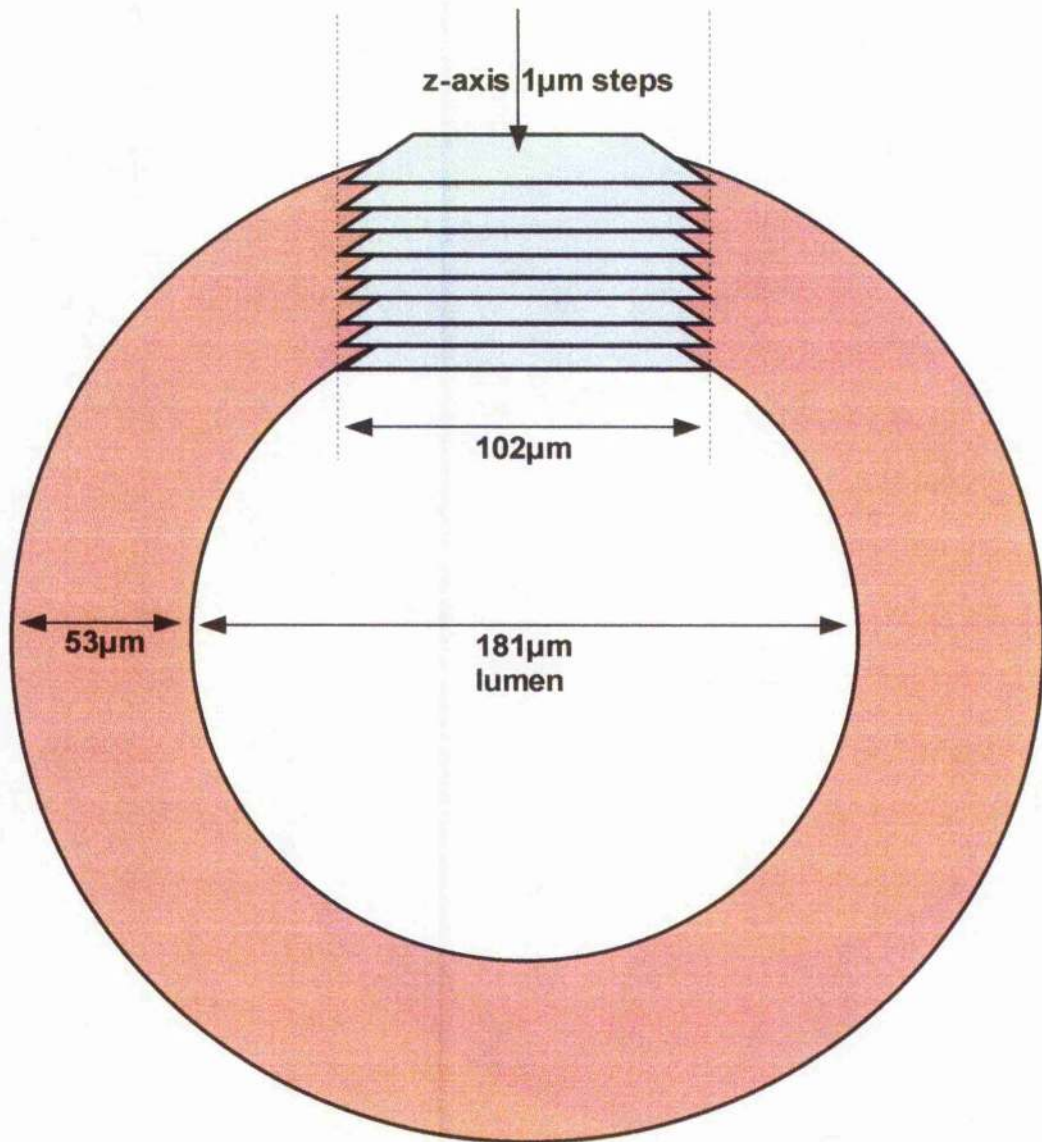


Figure 2.4 Schematic representation of a resistance artery in cross-section indicating the relationship between imaging plane and vessel wall. Diagram is drawn to scale based on data from hypertensive SHRSP using a x40 objective. Optical sections are taken along the z-axis in 1 μm steps, while each imaging plane occupies a 102x102 μm square.

A measurement of volume could then be obtained by multiplying CSA by length of vessel, assuming the vessel to have a cylindrical shape. For the purposes of simplicity, a standard segment length of 1mm was chosen, such that CSA in mm² was equal to volume of a 1mm segment in mm³.

The volume of a stack was calculated as,

$$\text{Volume of stack mm}^3 = \text{Area of image} \times \text{Wall thickness} \quad \text{Equation 4}$$

N.B. Conversion from μm^3 to mm^3 requires multiplication by 1×10^{-9} .

Since we know both the volume of the stack and the number of smooth muscle cells (SMC) contained within it, then it is possible to calculate the total number of SMC in a 1mm segment of artery by determining the number of stacks required to represent that artery.

$$\text{Number of stacks / 1mm}^3 = \text{Wall volume} / \text{Volume of stack} \quad \text{Equation 5}$$

$$\text{Total nSMC} = (\text{Number of stacks} / \text{1mm}^3) \times (\text{nSMC in stack}) \quad \text{Equation 6}$$

Finally, cell density was calculated by correcting total cell number for volume of the appropriate layer.

$$\text{SMC density (n/mm}^3) = \text{Total nSMC} / \text{Media volume} \quad \text{Equation 7}$$

The equivalent parameters for adventitial total cell number and density were calculated in an identical fashion.

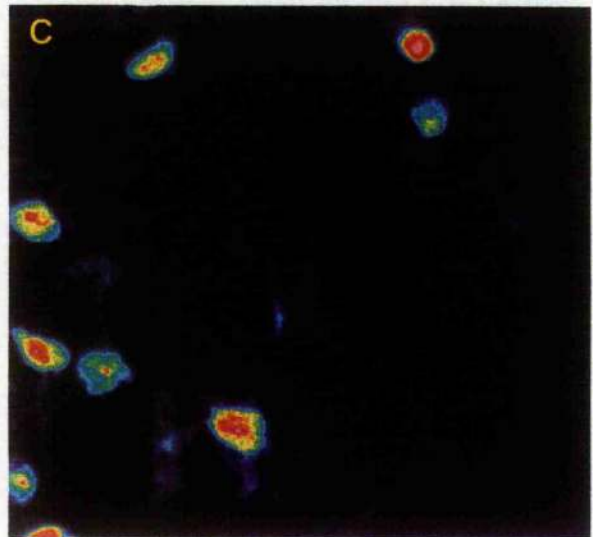
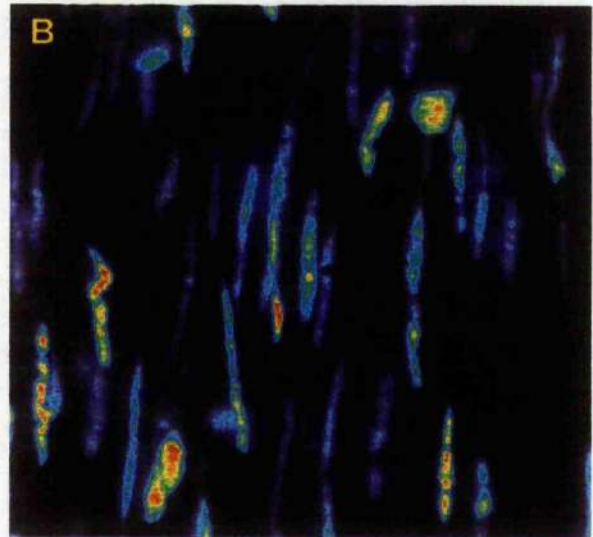
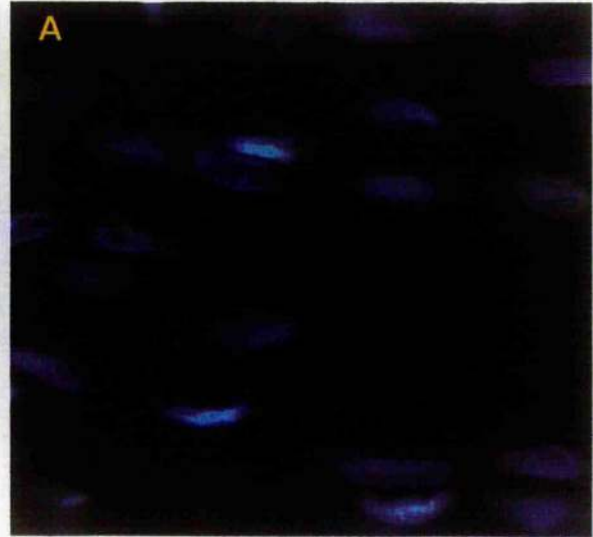
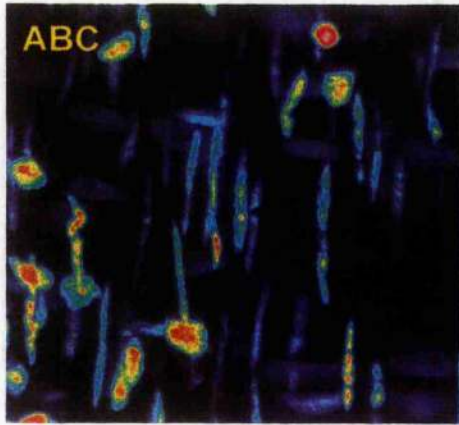


Figure 2.5 Extended focus views through the vessel wall of a mesenteric resistance artery using laser scanning confocal microscopy. Nuclei have been stained with propidium iodide. ABC is a 3-D reconstruction through the entire wall. It can be optically dissected according to cell type to give images A, B & C. Image A shows endothelial cells in the intimal layer. These lie oriented in the same plane as blood flow through the vessel. Image B shows the smooth muscle cell layers, which lie perpendicular to flow. Image C shows adventitial cells, which are typically rounded, and stain brightly. This type of optical dissection allows cellular quantification of arterial component parts.

3. Assessment of Left Ventricular Structure and Function by Echocardiography in the Rat

3.1 Introduction

Ultrasound as a body imaging technique has been used clinically for several decades, and has become increasingly important in the diagnosis and assessment of prognosis in hypertensive heart disease, cardiac hypertrophy and heart failure (Savage *et al.*, 1987). It is only in the last 10 years that technology has advanced sufficiently to allow imaging of small, fast moving objects such as the rat heart. Since the rat is the most common animal used to model cardiovascular disease, there are obvious benefits in studying left ventricular (LV) parameters in these animals using echocardiography. Previously, larger mammals such as dogs had to be used for non-invasive studies evaluating LV function and geometry.

The main problems in using ultrasound in the rat are the small size of cardiac structures, and the much higher heart rate. In addition, the formulae for calculating echocardiographic (echo) parameters such as ejection fraction and left ventricular mass, were derived in man. When applied to a different species and scale, the assumptions made in these calculations may no longer be true, especially since all estimations of LV mass make assumptions about cardiac geometry. Since there have only been a handful of studies validating the use echocardiography in the rat, it is necessary to determine whether the assumptions made in calculating these parameters are still valid for the WKY and SHRSP strains. It also represented an opportunity to establish baseline data for a variety of cardiac parameters in the Glasgow WKY and SHRSP strains.

The specific aims of this chapter are as follows,

1. To validate echocardiographic calculation of LV mass with LV mass measured at post-mortem in SHRSP and WKY.
2. To determine the accuracy of echo derived LV mass in detecting LVH in rats.
3. To determine baseline characteristics of dimensions, geometry and function and establish how these differ between WKY and SHRSP.

4. To determine the reproducibility of echo derived parameters for its application in future longitudinal studies.

To answer these questions requires some knowledge of the principles of ultrasound diagnostics, in particular, those that impose technical restraints on the use of echocardiography in the rat. To this end, this chapter will discuss ultrasound technology, techniques, methods of calculation and sources of variability, with particular emphasis to its adaptation in rats.

Principles of ultrasound

Ultrasound is high frequency sound above the 20kHz threshold of human hearing. The clinically useful range is found between 1.5 and 7.5MHz. The transducer both generates ultrasound and receives the echo reflected from the surface of objects. From this a grey scale image is produced on a monitor based on the strength of these reflections. The transducer consists of a piezoelectric crystal that oscillates at a determined frequency when a potential difference is applied across it. These oscillations produce the alternating compression and rarefaction of the sound wave. The thickness of the piezoelectric crystal determines the wavelength of the ultrasound, with crystals manufactured to be one half wavelength of the desired ultrasound frequency (Monaghan, 1990). Therefore to produce an ultrasound transducer that operates at a frequency of 7.5MHz, the piezoelectric crystal would have to be cut 0.1mm thick, since the wavelength would be 0.2mm. This is because wavelength is inversely proportional to frequency and vice versa, such that,

$$\lambda = V / f \quad \text{Equation 1}$$

Where λ = wavelength (m), V = velocity of sound (m/s) in soft tissues such as the heart this is 1540m/s, f = frequency (Hz : number of wavelengths per second).

It is an advantage to have a high frequency, low wavelength ultrasound, since the wavelength is an important determinant of resolution. Therefore, a high frequency transducer improves the ability to resolve small cardiac structures. However, the downside is that high frequency sound is more easily absorbed and diffracted by tissue interfaces, making penetration of the beam poorer (Monaghan, 1990). This makes the

highest ultrasound frequencies unsuitable for use in adult humans, but is not a problem in rats where the path length is only a few centimetres, and so the highest frequency transducer available is generally used.

The transducer generates ultrasound as pulses. As the pulse travels through tissue a proportion is reflected back towards the transducer as an echo each time it crosses a material interface e.g. as the sound wave travels between myocardium and blood. The remainder will be transmitted until the next interface, and so on. The amount of ultrasound reflected (the strength of echo), is dependent on the difference in densities between the two materials, known as the acoustic impedance. For example, the strong reflection at the tissue/air interface is responsible for the high level of noise produced by the lung. To prevent high levels of reflection from the contact between transducer and tissue ruining image quality, a water-based gel is applied to the surface to replace any trapped air, and so reduce acoustic impedance.

The reflected sound is detected by the piezoelectric crystal, which mechanically vibrates at the same frequency as the incoming ultrasound. This generates a potential difference across the crystal that is proportional to the energy of the returning ultrasound. This can be measured by the electrodes, and represented as a grey scale on the monitor. By measuring the time taken from transmission of the ultrasound pulse until receiving its echo, it is possible to determine the distance travelled, since,

$$D = V \times \frac{1}{2} t$$

Equation 2

Where D = distance from transducer to reflecting interface (m)

V = velocity of sound (m/s)

t = time from pulse transmission to return (s)

The velocity of sound is the same for the forward and return journeys, but the time taken is halved, to determine the distance for one direction only (Marshall *et al.*, 1992).

Since the same crystal is used to transmit and receive ultrasound, the sound is generated in pulses. The pulses are short, at only a few wavelengths, as this maintains good resolution (if the pulse is longer than the distance between two interfaces, then the echo from these will merge and be detected as one). This also allows a fast sampling rate of

around 1000 measurements/second allowing visualisation of moving structures (Monaghan, 1990).

Resolution

Echocardiography in rats requires the imaging of very small structures in the mm range. For this reason, particular attention should be paid to understanding the factors governing resolution of the system. When discussing resolution above, this referred to the axial resolution, that is, the ability to differentiate between two points lying along the same path of the sound beam. However, in 2-D echocardiography we also deal with lateral resolution, the ability to differentiate between two points lying side by side relative to the beam path. The lateral resolution is dependent on beam width, for if two objects lying side by side fall within the same beam path, they will appear as one. It is only when the distance between these objects straddles two or more beam paths that both objects will be resolved. In turn, the beam width is dependent on depth, power output, receiver gain and the focal point. The lateral resolution is never as good as the axial resolution, and may be several mm. It is for this reason that the M-mode is the preferred format for taking measurements from, as it relies purely on axial resolution (Marshall *et al.*, 1992).

M-mode echocardiography

M-Mode or time-motion echocardiography is a single beam path expressed as a function of time. An example of a rat M-mode echocardiogram is shown in Figure 3.1. The advantages of taking measurements in M-mode are the improved resolution and edge definition. It also has greater temporal resolution than 2-D images, due to the high sampling rate. This makes it particularly suited to following wall motion, the correct identification of end systole and end diastole or identifying cardiac arrhythmias. This gains importance in the fast beating rat heart (Litwin *et al.*, 1994).

Two-dimensional echocardiography

The second major viewing mode is 2-D echocardiography. The ultrasound beam is moved through a 30°- 90° arc to capture the heart in two dimensions. This is achieved by either 1) mechanical means, whereby the transducer is physically swept through an arc containing >100 scan lines, or 2) using a phased-array system where the

piezoelectric crystal has been divided into 64 or 128 individual elements, each with a separate electrical connection (Monaghan , 1990).

Two-dimensional echocardiography is the display of the full arc of beams as a cross-sectional moving image of the heart (example in Figure 3.2). Multiple beam paths are required to form one picture, and so the frequency at which a single point is revisited decreases in proportion with the number of beam paths. For this reason, the sampling rate is much lower in two-dimensional echocardiography, 30-126 frames per second compared to 1000 samples/sec for the M-mode format (Marshall *et al.*, 1992). Two-dimensional echocardiography is useful for checking the anatomical orientation of the M-mode, and most modern machines combine M-mode and 2-D on one screen for this purpose. It is considered superior for determination of ejection fraction as it takes into consideration asymmetries that may be present in the ventricle (Wallerson & Devereux, 1987). It is also easy to detect wall motion abnormalities and akinetic regions.

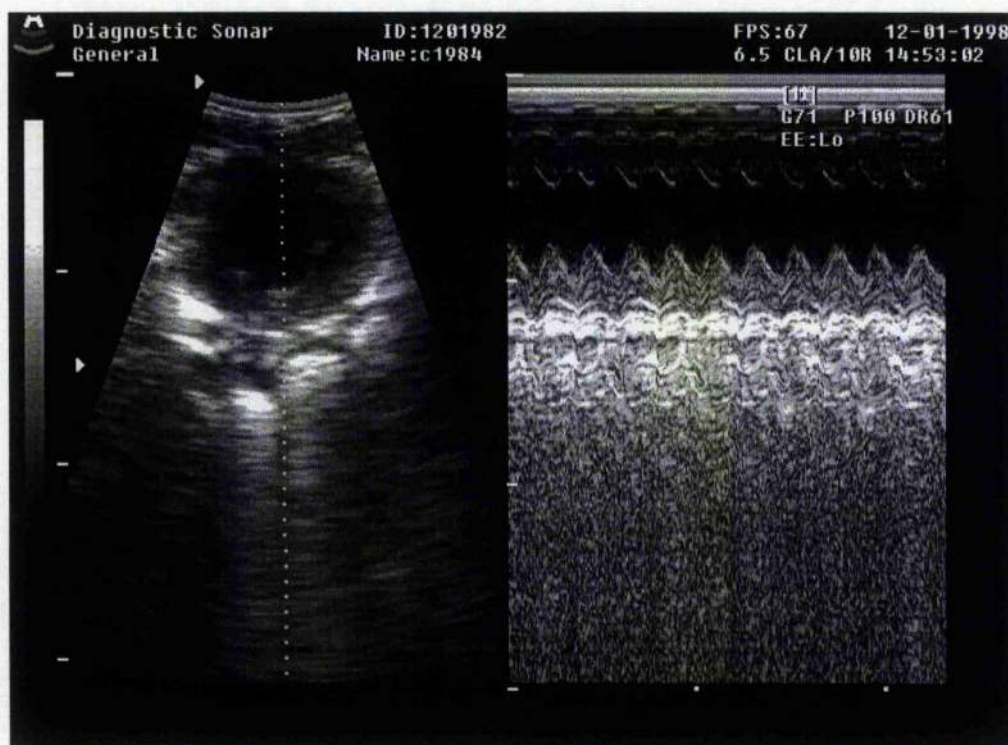


Figure 3.1 M-mode echocardiogram showing the heart of a SHRSP rat. Movement of the line cursor on the 2-D image (left-hand side) selects the beam path of interest. The wave motion on the M-mode represents the cardiac cycle, as points in the beam path move inwards and outwards during systole and diastole.

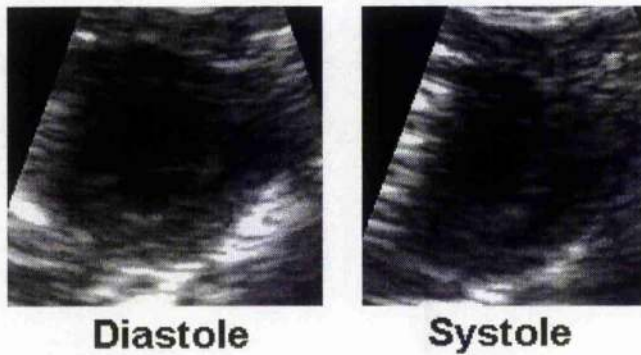


Figure 3.2 Two-dimensional echocardiogram of a SHRSP rat heart. The image is a short-axis view at the level of the papillary muscles, taken through the parasternal window. On the left side the heart is in diastole, and on the right in systole. The papillary muscles can be seen protruding into the LV cavity during diastole.

Imaging windows

Obtaining an echocardiographic image of the heart is hampered by the rib cage. Bone is a very poor transmitter of ultrasound, and when the lungs are filled with air, almost all the ultrasound is reflected. For this reason there are only 4 main imaging windows that afford unimpeded views of the heart. The positions of these relative to the heart are shown in Figure 3.3. The dominating position of the sternum necessitates imaging to occur either above it, in the suprasternal notch, or below it, termed subcostal. Two windows are available to the left of the sternum, imaging between the 3rd and 5th intercostal spaces. These are the parasternal view, and the apical view (Marshall *et al.*, 1992).

Any particular window can afford a multitude of imaging planes through the heart. For example, the parasternal view can obtain sections transversing anywhere from the mitral valve to the apex. In order for measurements to be reproducible and comparable between subjects, the same plane of enquiry should be imaged at every echocardiographic examination. To aid this the heart is described as having a long and a short axis. The long-axis of the heart runs down through the centre of the heart from mitral valve to apex, while the short-axis runs perpendicular to this from the anterior wall to the posterior wall (Figure 3.4). Images can then be obtained from a determined point along the selected axis e.g. the papillary muscles in a parasternal short-axis view. By using the papillary muscles as a landmark, it is hoped to avoid errors of oblique angulation of the beam.

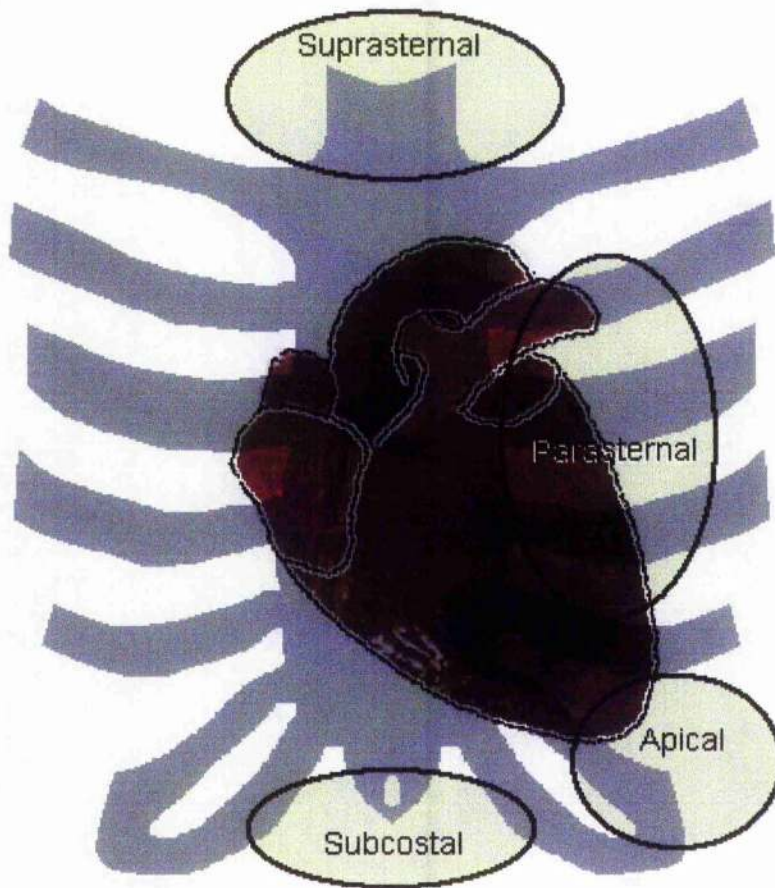


Figure 3.3 Positions of the four echocardiographic imaging windows shown in relation to the rib cage.

Since the M-mode only measures in one dimension, measurements taken from the short-axis view make the assumption that both short-axis dimensions are equal i.e. in Figure 4 that the dimensions from a to b (anterior-posterior) and from a to c (interventricular septum- posterior) are equal.

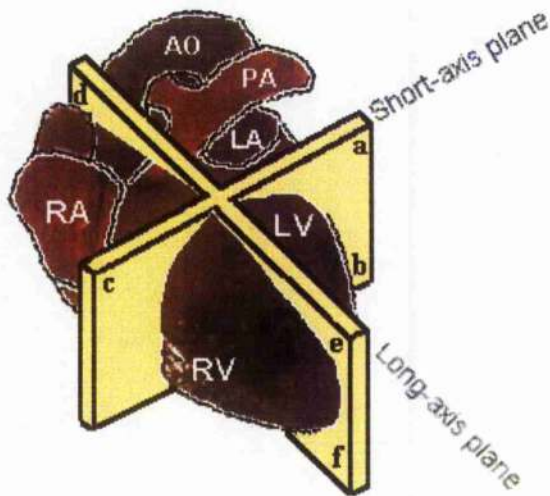


Figure 3.4 Orientation of the two imaging planes referred to in this thesis. In a parasternal view, the transducer would be imaging from above. The short-axis plane runs through the heart from a to b, while the long-axis images a plane from e to f. LV : left ventricle; RV: right ventricle; LA : left atrium; RA : right atrium; PA : pulmonary artery; AO : aorta.

Measurement of LV dimensions

Wall thickness and LV cavity dimensions are often measured from the M-mode. To standardise how measurements are made, various conventions have been advocated. All of these were derived for humans, and include the National Institutes of Health (NIH), American Society of Echocardiography (ASE), and the Penn conventions. The earliest of these was the 1973 NIH convention, which stated that measurements should be taken from the centre of the line that defines the interface. This has since been superseded by the other two conventions, as it fails to standardise at what point in the cardiac cycle parameters should be measured, and there is no supportive evidence from post-mortem validation studies (Wallerson & Devereux, 1987). The Penn convention was empirically derived from autopsy validation by Devereux & Reichek (1977). This method does not include the thickness of the endocardial interface when measuring wall thickness, instead including it in the measurement of end diastolic diameter. The Penn convention has never been validated in rats, and indeed there was shown to be no advantage over ASE when taking measurements in rabbits (Young *et al.*, 1986). The ASE or leading edge convention is the most commonly used, and defines measurements to be taken from the leading edge of one interface to the leading edge of another. This

removes error inherent in the echo system associated with display of thin lines (Sahn *et al.*, 1978). It was selected on the basis of reproducibility between sonographers, and has since been validated by autopsy in man and rat (de Simone *et al.*, 1990; Pawlusch *et al.*, 1993). It provides good correlation with post-mortem LV mass, but may systematically overestimate it, requiring use of a correction factor (Devereux *et al.* 1986). Examples of ASE and Penn methodologies are shown superimposed on a representative M-mode in Figure 3.5. Whichever convention is used, LV dimensions should be measured from at least three consecutive cycles on the M-mode tracings, to allow for beat-to-beat variation. In subjects where respiration has not been controlled, it has been suggested that measurements be made from six cardiac cycles, in order to include all phases in the respiratory cycle (Wallerson & Devereux, 1987).

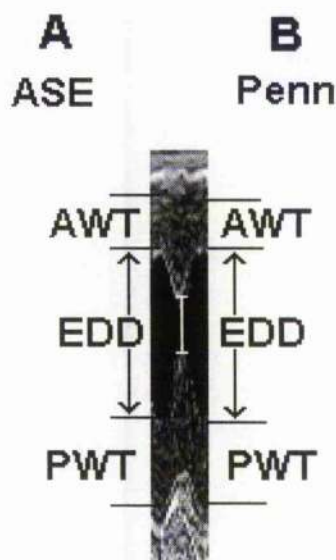


Figure 3.5 M-mode echocardiogram showing methods for measurement of cardiac dimensions; anterior wall thickness (AWT), posterior wall thickness (PWT), end diastolic diameter (EDD), and end systolic diameter (shown in white). The left hand side indicates defined interfaces of the American Society of Echocardiography (ASE), while the right side indicates the same measurements using the Penn convention. Adapted from Devereux and Reichek (1977).

LV mass determination

Echocardiographic estimation of LV mass provides important information concerning cardiac hypertrophy without the need for invasive or terminal studies, and with greater

accuracy than electrocardiography (Liebson *et al.*, 1987). There are numerous methods available, and these are outlined below. All of these techniques are concerned with calculating the volume of the LV myocardium, from which LV mass can be determined by multiplying by the specific gravity of myocardium, 1.04 g/ml (Troy *et al.*, 1972). Major assumptions are made in the calculation of LV mass, most notably on cardiac geometry. In general, three-dimensional events are being extrapolated from measurements made in one or two-dimensions.

1. **Cubed formula** – The simplest method assuming the heart during diastole forms a prolate ellipsoid, and the long-axis dimension is twice that of the short-axis. This may not be a fair assumption, especially in hearts exhibiting LV dilatation. Nevertheless, this method can produce good correlation with post-mortem LV mass in man and rats (Devereux & Reichek, 1979; Pawlusch *et al.*, 1993).

$$\text{LV mass} = 1.04[(\text{EDD} + \text{PWT} + \text{AWT})^3 - \text{EDD}^3] \quad \text{Equation 3}$$

Where, EDD = end diastolic dimension; PWT = posterior wall thickness; AWT = anterior wall thickness (de Simone *et al.*, 1990). Essentially, this calculation estimates the volume of the whole left ventricle from a single M-mode dimension, by cubing the short-axis external diameter. It then subtracts the volume of the LV cavity, to obtain LV myocardial volume. Great care is required when taking measurements using the cubed formula, since errors are greatly magnified by the cubed function, and it has a tendency to over-estimate.

2. *Modified cube formula* – gains in accuracy by incorporating long-axis length at diastole as a 2nd dimension. (e.g. Isgaard *et al.*, 1997). This depends on being able to obtain an accurate long-axis view, which is not always possible in the rat due to the thoracic anatomy and high heart rate (de Simone *et al.*, 1994). In the authors experience a clear long-axis view is available in only a few exceptional animals.
3. *Simpson's rule* – this also requires the long-axis dimension and multiple short-axis images, which are treated as a series of disks of known thickness along the long-axis. The summation of these disks is used to calculate myocardial

volume. The greater the number of disks, the higher the degree of accuracy in the determination. It is the only method that truly takes account of three-dimensional cardiac geometry, and as such, is the only method truly suited to estimates of LV mass after myocardial infarction (Pai & Shah, 1995). Simpson's rule forms the basis for the algorithms used in modern automated three-dimensional echocardiography, where the spatial positioning of the transducer (and hence the short-axis disks) is automatically described relative to the long-axis. This allows a 3-D computer-generated image of the heart to be constructed (Gopal *et al.*, 1997). Unfortunately, the accuracy of the transducer positioning system is not sufficient for imaging the rat heart. It is also very difficult to consistently obtain multiple short-axis images along the long-axis of the rat, which is around 12mm in length. A view shared by Litwin *et al.* (1994).

4. *Ellipsoidal method* – this was the method advocated by the first paper in rats to determine LV mass and compare it with necropsy validation (de Simone *et al.*, 1990). It assumes the heart at diastole to form a prolate ellipsoid. The authors recognised the difficulty of directly measuring long-axis length in the rat, and in a second paper suggested a modified method for the empirical estimation of long-axis from a learning series of rats, using body weight, fractional shortening, and posterior wall thickness in systole (de Simone *et al.*, 1994).

As with all these methods, accuracy is often improved by modelling the correlation line to a theoretical perfect of $y = x$, via a correction factor. This involves multiplying values by the reciprocal of the slope, and correcting for the y-axis intercept (Litwin *et al.*, 1994).

There are also numerous methods to estimate LV mass using 2-dimensional echocardiography. These include modifications of Simpson's rule, approximation to a cylinder, an ellipsoid, or a bullet shape (Wyatt *et al.*, 1979). The advantages are a potentially smaller standard error in the estimation, and the fact that some account is taken of changes in geometry in the short-axis view (Reichek, 1987; Schiller, 1987). However, 2-D imaging may over-estimate myocardial cross-sectional area, and has not proved itself to be superior to M-mode echocardiography (Reichek, 1987). Since some of these techniques require an apical view, and all require the long-axis dimension, they

have never been applied to LV mass evaluation in the rat, and will not be discussed further in this thesis.

For the purposes of this thesis, the cubed formula was selected for calculating LV mass as this requires only one imaging plane, and so is likely to work for all animals. Preliminary data using the modified ellipsoidal method showed that it was no more accurate at estimating LV mass than the much simpler cubed method.

To obtain an index of myocardial mass independent of assumptions concerning three-dimensional shape, some researchers calculate myocardial cross sectional area (CSA) (de Simone *et al.*, 1990).

$$\text{CSA (mm}^2\text{)} = \pi[(\text{EDD} + \text{PWT} + \text{AWT})/2]^2 - \pi(\text{EDD}/2)^2 \quad \text{Equation 4}$$

This, like all the M-mode methods above, still makes the assumption that the myocardial cross-sectional area is circular in shape.

Measurement of LV function

Ejection fraction is defined as the volume of blood leaving the LV with each heartbeat (stroke volume) expressed as a percentage of the total LV volume at diastole. The derivation is as follows:

$$\text{SV} = \text{EDV} - \text{ESV} \quad \text{Equation 5}$$

$$\text{EF} = \text{SV}/\text{EDV} \quad \text{Equation 6}$$

Where, SV = stroke volume (ml); EDV = end diastolic volume (ml); ESV = end systolic volume (ml); EF = ejection fraction (%). For the purposes of estimating ejection fraction using echocardiography, the equivalent calculation for two-dimensional cross-sectional area is often applied:

$$\text{EF} = (\text{EDA} - \text{ESA}) / \text{EDA} \quad \text{Equation 7}$$

Where, EDA (mm²) and ESA (mm²) are the cross-sectional areas of the LV cavity measured at diastole and systole respectively (Pai & Shah, 1995). This assumes that contractility is identical at all levels of the left ventricle. This is likely to be true for all normal and concentrically hypertrophied hearts, but is unlikely to hold for infarcted hearts.

Cardiac output (CO) may also be calculated if the heart rate (HR) is known, since:

$$\text{CO (ml/min)} = \text{SV (ml)} \times \text{HR (beats/min)} \quad \text{Equation 8}$$

The heart rate can be calculated from the number of cardiac cycles appearing on the M-mode. However, this Figure may be highly variable in the rat and should be treated with caution, due to the depressant effect of all anaesthetics and sedatives on heart rate. Cardiac output will therefore depend on depth of anaesthesia.

Doppler cardiac output

Some groups have been able to obtain an apical 5-chamber view in the rat to determine LV outflow velocity using Doppler flow measurements. This means that by measuring the diameter of the ascending aorta, and heart rate, it is possible to calculate cardiac output, as follows;

$$\text{C.O.} = \text{velocity time integral} \times [\pi (\text{LV outflow diameter} / 2)^2] \times \text{heart rate}$$

Equation 9 (Litwin *et al.*, 1994)

Echo Doppler may also be used to look for mitral regurgitation by placing the sample at the leaflets of the mitral valve, just inside the left atrium, and looking for back flow. Although one group have attempted this technique in the rat, they comment on the difficulty of imaging the aortic root which was often unobtainable due to difficulties with the imaging window (Pawlush *et al.*, 1993).

Sources of Error in Echocardiography

Sources of error in echocardiography were elucidated in a paper by Kuccherer *et al.* (1991), and are relevant to both 2-D and M-mode. They identified a variety of sources of variability contributing to the total variability of a given measurement.

Subject variability - is the variation that occurs within a subject echoed on two different occasions. It includes parameters such as difference in body position or autonomic tone. This is obviously important in protocols that demand serial evaluation, and can be quantified by measuring the same subject a few days apart.

Technical variability - describes variation arising from image acquisition and quantification. It includes inter- and intra- operator variability. Variability includes differences in selection of the correct imaging plane between two different operators, and between the same operator on different days.

Inter- and intra- reader variability - is a measure of variability in digitising and measuring recordings e.g. use of the leading edge method. It also includes beat-beat variability in measuring over a number of cardiac cycles. Intra-reader variability can be quantified by a blinded re-measuring of images

Kuccherer and colleagues showed determination of LV mass to have the greatest total variability of any echo parameter tested, and that technical variability was the largest contributor to this. Specifically, variability in measuring the short-axis dimensions was particularly high (understandably since using the cubed formula). There are obvious hazards in interpreting small changes in LV mass as significant, especially if based on single readings by only one operator. However in animal studies there is the option of increasing sample size to increase the power of the observation. The most reliable parameter measured was ejection fraction, where subject variability was the largest contributor to total variability. The conclusion is that ejection fraction is suitable for serial evaluation studies.

Problems specific to the rat

An important consideration for accuracy that occurs in the rat, but is not a problem in humans, is the very high heart rate in these animals. The heart rate of the anaesthetised rat is approx. 350-400 beats per minute. This means that ultrasound machines with a low sampling rate will only have a few images to represent the full cardiac cycle. It is therefore possible that end diastole and end systole can not be identified correctly, leading to errors in measurement. A sample rate of 25Hz (the minimum required to

depict moving images) would only deliver around 4 frames for every cardiac cycle. The Medison machine used in this study has a sampling rate of 126Hz i.e. a temporal resolution of ~8ms. It can therefore record ~20 frames per cardiac cycle, making it easy to accurately select end diastole and systole. However, even on this modern machine, the sample rate falls dramatically to as low as 18Hz if multiple functions are used simultaneously e.g. colour doppler with M-mode. Another approach is the use of simultaneous electrocardiography, such that representative images can be selected on the basis of synchrony with cardiac electrical activity. For example, diastolic measurements at the onset of the QRS complex in the ASE convention (Sahn *et al.*, 1978), or at the peak of the R wave in the Penn convention (Devereux & Reichek, 1977).

The other major difference between rat and human echocardiography is one of scale. Imaging a rat is technically very difficult as it requires measurement of structures as small as 1mm, close to the limit of spatial resolution. However, with due care, and the use of high frequency transducers, accurate results can be obtained. Indeed, echocardiography in mice has recently been described using the same techniques described here, but utilising a 15MHz transducer (Harada *et al.*, 1998; Yang *et al.*, 1999).

The final consideration when performing echocardiography in rats is the inability to control the respiration rate. The act of inspiration and expiration may cause problems due to lateral movement of the heart, or air-filled lungs reflecting ultrasound. A human subject can be requested to hold their breath, however, the rat has a resting respiration of 60-100 breaths per minute, making interference a common problem. Fortunately, these movements are easy to identify in an M-mode, and can be corrected for by always taking measurements at the same point in the respiration cycle. The problem can also be minimised by using only light sedation during the procedure, this ensures that the animals' breathing remains shallow.

3.2 Methods

Animal characteristics

Growth curves for LV mass against age and body weight were constructed from a total of 104 rats consisting of 54 SHRSP (24 males, 30 females) and 50 WKY (29 males, 21 females). A subset of these rats (n=75) were examined by echocardiography up to 24 hours before euthanasia, and these data are presented in the LV mass validation study. There were 42 SHRSP, 20 males and 22 females (M:F ratio 0.91), and 33 WKY, consisting of 16 males and 17 females (M:F ratio 0.94). Ages ranged from 52 days to 446 days old, and body weight between 102-494g. Since the male to female ratio was similar between groups, and the data normalised to body weight, echocardiographic parameters have been presented as combined data for males and females.

Echocardiographic examination

Equipment.

Two ultrasound machines were used in this study. The first 30 animals were imaged using an Acuson 128 ultrasound scanner and 7MHz paediatric probe, with images recorded on Super-VHS tape for analysis off-line. With the purchase of an ultrasound machine dedicated to animal work, the remaining animals were examined using a Medison Sonoace SA8800 (Diagnostic Sonar, Livingston, UK). This was interfaced to a JVC Super-VHS video recorder for continuous recording of moving images. In addition, this system had a scrolling memory that allowed review and selection of the best quality images, which were saved in digital format as bitmaps on a 650Mb PD drive (Panasonic). The transducer was a 7.5MHz, 128 line phased-array system, with an adjustable 60° imaging angle and a 2cm footprint. This provided a more than adequate image depth of 7.5cm, and 10% accuracy in measuring distances between 1 – 60mm. When measuring time in M-mode, at a sweep speed of 126MHz, accuracy was 5% for the range 0.01 – 8 seconds. All images were obtained at x2 magnification.

Imaging technique

Animals were lightly anaesthetised with Halothane 1-2% in oxygen (flow rate 2L/min) and the left side of the chest closely shaved. A copious quantity of ultrasound gel was used to dispel any pockets of air trapped in the fur. With the rat lying in the left lateral

position, short-axis 2-dimensional B-mode and corresponding M-mode images were taken through the left parasternal window at the level of the papillary muscles. All images were adjusted to obtain the optimal dynamic range of the displayed image. LV cavity was selected to appear black, and the myocardium a mid grey with special attention given to endocardial definition.

Each echo exam lasted between 5 and 15 minutes and consisted of 3 sets of 2-D images and a minimum of 3 independent M-mode images. In 2-D mode, end diastolic images were selected for good edge definition, a round cross-section, and the largest thinnest section of left ventricle. M-mode images were guided using information from simultaneous 2-D images, allowing the centre of the cross-section to be selected as the plane of interest. Care was taken to avoid measuring directly through the papillary muscles, as this would give the impression of a thicker wall. Similarly, the anterior wall may also appear thicker if imaged at the junction between septum and right ventricle. The M-mode was selected for good edge definition when both the epicardial and endocardial surfaces of the anterior and posterior walls were clearly visible, and when there was a regular cardiac cycle with little change in dimensions from beat to beat.

In 11 animals, a different anaesthetic was used to determine if there was a measurable effect of anaesthetic choice on echocardiographic parameters. These animals were lightly sedated using an intraperitoneal injection of 0.04-0.1ml Hypnorm. All other aspects of the examination were identical.

At the end of the echo exam (or within 24 hours) animals were euthanased by an overdose of halothane anaesthetic. The heart was immediately removed by thoracotomy, blotted and weighed. The right ventricle was carefully dissected from the left, the great vessels and atria removed, and the component parts blotted and weighed (Mettler Toledo PB302 balance). The left ventricle was defined as the combined left ventricular free wall and interventricular septum up to the level of the mitral annulus. The same operator weighed all hearts.

Data analysis.

Video recordings were digitised using a Ulead multimedia video card and software (Hauppauge Ltd.), and analysed on a PC running the Metamorph version 2.75 program (Universal Imaging Corporation). However, wherever possible, measurements were taken from the digital stills, due to the greatly improved clarity of image obtained by bypassing digital-analogue-digital conversions. For analysis of 2-D images, 3 measurements at systole and diastole were made for each of the 3 data sets, providing data on 9 cardiac cycles. The endocardial border was traced onto the screen aided by the use of a calibrated ellipsoid for automatic calculation of cross-sectional area (CSA). These were used to derive an estimation of ejection fraction (Equation 10), and the data averaged.

$$\text{Ejection Fraction (\%)} = \frac{\text{End diastolic CSA} - \text{End systolic CSA}}{\text{End diastolic CSA}} \quad (\text{Pye } et al., 1996)$$

Equation 10

A minimum of 3 independent M-mode images were acquired at each exam for measurements of wall thickness. LV dimensions were measured using the American Society of Echocardiography leading-edge method from six consecutive cardiac cycles on each of the M-mode tracings (Sahn *et al.*, 1978). This data was averaged and used to calculate left ventricular mass assuming a cubed model (Devereux & Reichek, 1979). Therefore a total of 24 measurements were taken and averaged for each dimension.

$$\text{LV mass} = 1.04[(\text{EDD} + \text{PWT} + \text{AWT})^3 - \text{EDD}^3]$$

Where PWT = Posterior wall thickness (mm)

AWT = Anterior wall thickness (mm)

EDD = End diastolic dimension (mm)

The following measurements were taken from the M-mode, AWT, PWT, EDD, ESD, PWT's. Where PWT's is posterior wall thickness measured at systole. The positioning of these in the echocardiogram are shown in Figure 3.5. The posterior wall was identified as having the steepest slope (Pawlush *et al.*, 1993).

End diastolic volume (EDV) and end systolic volume (ESV) were calculated from the M-mode using the technique of de Simone *et al.* (1990) which assumes the ventricle to have an ellipsoidal shape.

$$\text{EDV} = \pi/6 \text{ EDD}^2 [2(\text{EDD} + 2\text{PWT}) - 1.1\text{PWT}] \quad \text{Equation 11}$$

$$\text{ESV} = \pi/6 \text{ ESD}^2 [2(\text{ESD} + 2\text{PWTs}) - 1.1\text{PWTs}] \quad \text{Equation 12}$$

$$\text{Stroke volume (SV)} = \text{EDV} - \text{ESV} \quad \text{Equation 13}$$

Fractional shortening (FS) was also calculated as a measure of cardiac function calculated from the M-mode as follows,

$$\text{FS (\%)} = [(\text{EDD}-\text{ESD}) / \text{EDD}] \times 100 \quad \text{Equation 14}$$

(Pawlush *et al.*, 1993)

Repeatability study.

The intra-observer repeatability of echo derived parameters was quantified in 18 rats according to the methods of Bland & Altman (1986). These animals underwent an echo exam as above, with a second examination within two days. For any given measurement, the difference in values between study 1 and study 2 was calculated, together with the mean difference. A perfectly reproducible study will have a mean of differences equal to zero. Provided the mean of differences was not significantly different from zero, then the standard deviation of the differences was calculated. The co-efficient of repeatability is defined as twice this value (2SD) and represents the range within which 95% of differences occur. The co-efficient of repeatability can therefore be used to determine echo-derived parameters are accurate enough to be useful in serial studies.

All echocardiographic studies in this thesis were performed and measured by the same operator, and so no effort was made to ascertain the inter-operator or inter-reader variability.

Statistical analysis

All results are displayed as mean \pm standard deviation (SD) unless otherwise stated. Measurements between WKY and SHRSP animals were compared using an unpaired Student's *t* test. A P value < 0.05 was considered significant. LV mass by echocardiography was compared with actual LV mass by linear regression. The P value for this parameter tests the null hypothesis that the overall slope is zero.

3.3 Results

For the purposes of the validation study it was necessary to include a variety of animals, male and female, exhibiting a wide range of body weights and ages, in order to ensure a large range of LV mass for linear regression analysis. Therefore, when comparing echo-derived parameters of LV mass between WKY and SHRSP it is important to be comparing like with like. The standard method is to normalise to body weight, but other methods such as normalisation to tibial length, brain weight or body surface area may be applied. For any of these methods, it is assumed that rate of growth of the left ventricle is directly proportional to the rate of growth of the chosen denominator, throughout the range of values observed. This may not always be true, especially when the animal reaches full maturity and one factor continues to change. For example, normalisation to body weight would not be valid if the animals became obese, or lost weight due to surgical procedures. However, body weight is the preferred normalisation factor, due to ease of measurement and the ability to measure in live animals for use in serial studies. In addition, the SHRSP has a lower body weight at all ages, and so requires correction for this. To determine whether normalisation to body weight was a valid transformation in this population of rats, growth curves of LV mass against body weight were constructed from necropsy data, and are shown in Figure 3.6.

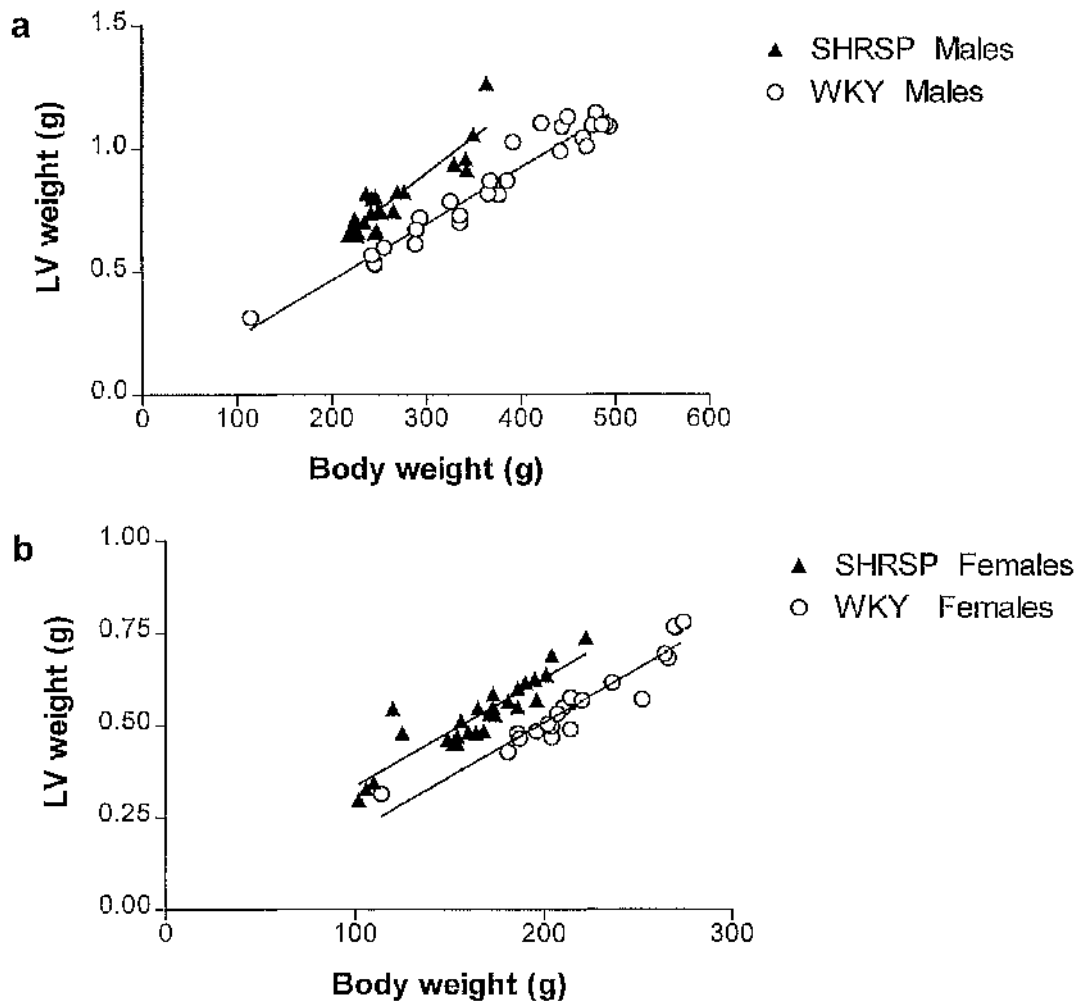


Figure 3.6 Growth curves for LV mass against body weight constructed from autopsy data. Panel (a) shows data with linear regression for male WKY and SHRSP, while panel (b) shows the same data for females. The linear relationships indicate that LV mass increases in direct proportion to body weight, throughout the range of body weights used in this study.

All four data sets shown in Figure 3.6 produced excellent correlation coefficients by linear regression analysis, ranging between $r = 0.90$ to 0.97 . These linear relationships indicate that LV mass increases in direct proportion to body weight throughout the range of body weights used in this study. Therefore, normalisation to body weight is an appropriate method in these animals. It is interesting to note that the rate of LV growth, as measured by the slope of the regression line, is almost identical within the four groups: SHRSP males $m=0.0030$, SHRSP females $m=0.0030$, WKY males $m=0.0023$,

WKY females $m=0.0030$. WKY males may be slightly lower due to the inclusion of one animal with very low body weight.

In light of this data, all echocardiographic parameters were normalised to body weight, with the obvious exception of ratio and percentage values. In the interests of simplicity, data has been analysed as males and females together. Normalising to body weight adequately accounts for any sex differences, as once data has been transformed, sex differences are indistinguishable (data not shown). In addition, there is no bias when comparing WKY and SHRSP in this way as the ratio of males : females are almost identical between the two groups.

In the validation experiments, LV mass was calculated using the cubed method (Equation 3). A modified cubed method using the long-axis as a second dimension was also considered. Figure 3.7 shows a parasternal long-axis view from a SHRSP rat, however, it was not possible to consistently obtain these views in all but a handful of animals, and this method was abandoned.



Figure 3.7 Parasternal long-axis view in a SHRSP rat. Long-axis measurements are taken from the mitral valve to the apex.

The correlation of calculated LV mass (from the echocardiogram) against actual LV weight measured at autopsy is shown in Figure 3.8. Linear regression of data from 75 animals measured, yields the equation of the line $y = 0.92x + 0.08$, $r = 0.86$, standard deviation of the residuals $(S_{y.x}) = 0.13$, $P < 0.0001$. This approximates well with the theoretical $y = x$, and to improve accuracy, was modelled to this line using the correction factor $x = (\text{Cubed method} - 0.08)/0.92$ (Figure 3.8, panel b).

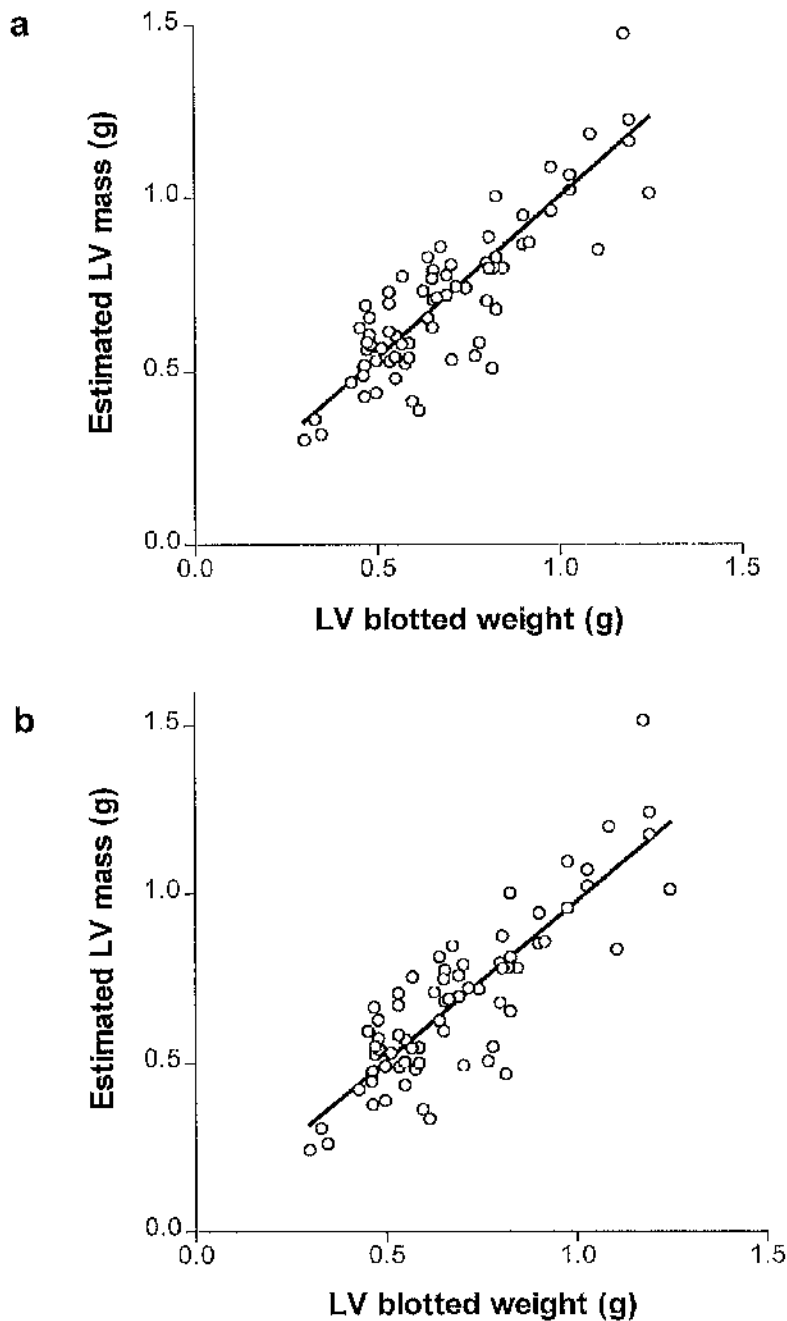


Figure 3.8 Correlation between LV mass estimated by echocardiography and actual LV mass measured at autopsy. Raw data shown in panel a, equation of the line $y = 0.92x + 0.08$, $n = 75$, $r = 0.86$. Panel b shows the same data with correction factor approximating to $y = x$. The co-efficient of repeatability for comparison between echo-derived and LV blotted weight is 0.26g.

The ability of echocardiography to accurately determine between animals with and without LV hypertrophy was examined by calculating sensitivity and specificity for this test. Since WKY rats do not exhibit LV hypertrophy, the highest value in this group was defined as the limit of normality. Therefore a LV mass to body weight ratio of greater than or equal to 2.86 g/Kg was adopted as the definition of “true” hypertrophy, and all animals below this as hypertrophy negative. Sensitivity was calculated to be 92%, and represents the probability of an animal with “true” hypertrophy giving a positive test. The specificity was 64%, which is the probability of an hypertrophy negative animal giving a negative test. The predictive (diagnostic) value was 78% i.e. 78% of rats giving a positive test actually have LV hypertrophy, or in other terms, a false-positive rate of 22%. The false-negative rate was only 14%. Thus, echocardiography could identify rats exhibiting LV hypertrophy with an acceptable degree of accuracy.

Of the animals used for the validation study, 54 had systolic blood pressure measured by tail-cuff plethysmography on at least two occasions. A comparison of mean systolic blood pressure is detailed in Figure 3.9, with 13-14 animals in each group. Blood pressure was compared by one-way ANOVA with Bonferroni’s correction for multiple comparisons. SHRSP males had a significantly higher blood pressure, 178 ± 20 mmHg when compared to any other group (all $P < 0.001$). In turn, SHRSP females at 147 ± 16 mmHg were significantly more hypertensive than either WKY males at 129 ± 9 mmHg ($P < 0.01$), or WKY females at 120 ± 5 mmHg ($P < 0.001$). There was no significant difference when comparing WKY males with females. There were no differences in heart rate measured at this time, with the mean heart rate being in the range of 440-460 beats per minute for all groups.

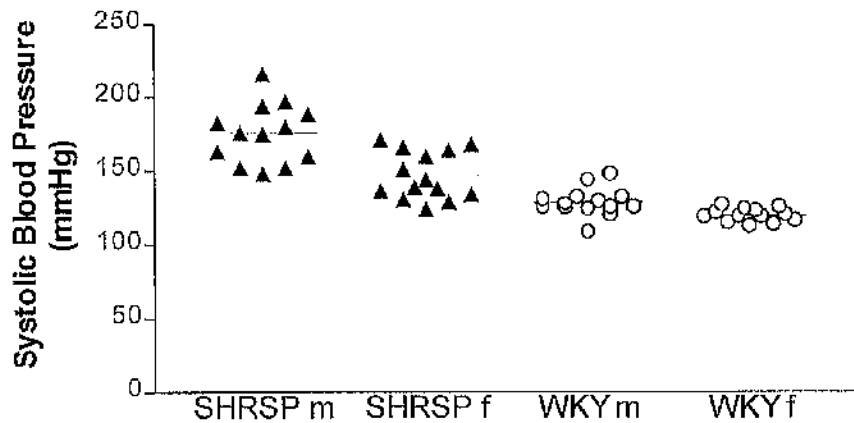


Figure 3.9 Systolic blood pressure measured by tail-cuff plethysmography in male (m) and female (f) SHRSP and WKY rats. The solid line represents the mean value in each group.

The relationship between cardiac hypertrophy and hypertension was examined by plotting autopsy LV mass (normalised to body weight) against systolic blood pressure, and performing linear regression analysis (Figure 3.10). No correlation was apparent for either WKY or SHRSP animals.

A large range of parameters were calculated from echocardiograms, describing LV dimensions, volume, cross-sectional area and mass (Table 1). All 75 animals used in the validation study were included, 33 WKY and 42 SHRSP. Data are presented as mean value \pm standard deviation, and comparison between WKY and SHRSP is by unpaired Student's *t*-test, with the *P* value reported. Where possible all values are represented as both raw data, and normalised to body weight.

The extent of LV hypertrophy was very pronounced in the SHRSP, and was significantly higher even before normalisation to body weight. At post-mortem there was on average 28% higher LV mass to body weight ratio in the SHRSP, and this was only slightly over-estimated at 31% using the cubed method. Right ventricular weight was also significantly higher in the SHRSP after normalisation to body weight ($P < 0.0001$). These differences were mirrored by myocardial cross-sectional area, which was again highly significant between groups. Thicker left ventricular walls appear to be the culprit. Both anterior and posterior aspects exhibited hypertrophy in the SHRSP. The difference in anterior wall thickness was greatest at 23% higher than the WKY,

compared to 17% for the posterior wall. This was reflected in the AWT: PWT ratio, suggesting that the SHRSP anterior wall is slightly more prone to hypertrophy than the posterior wall.

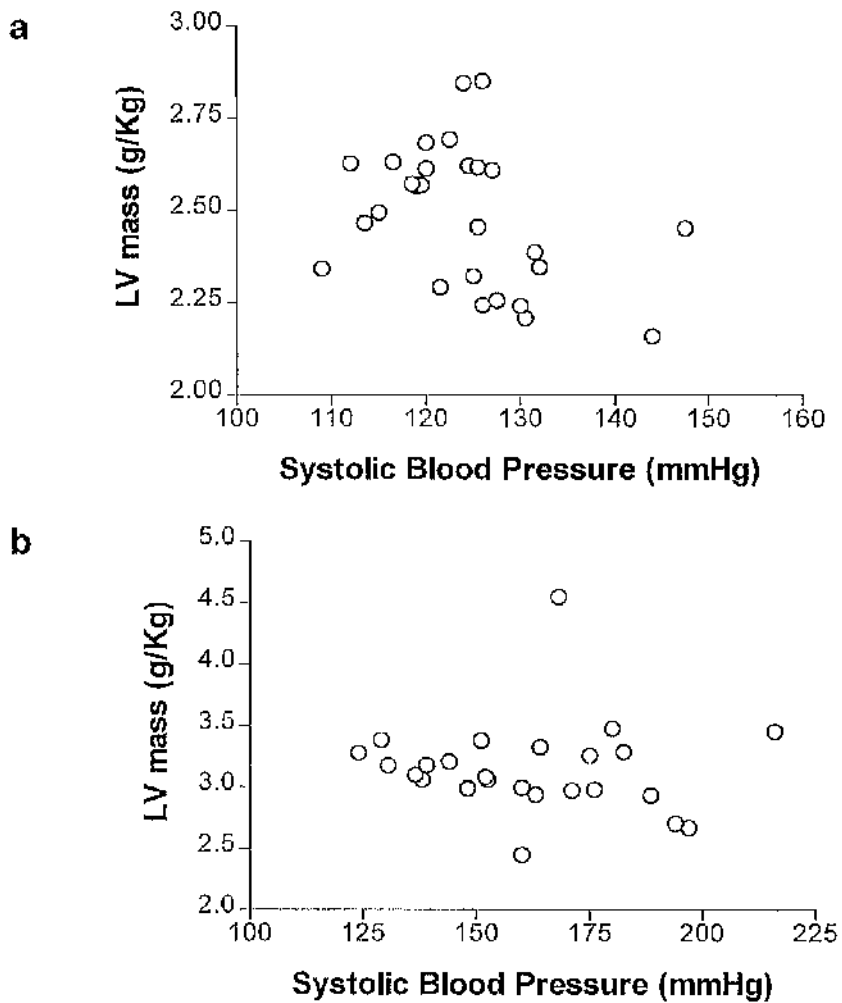


Figure 3.10 Lack of relationship between LV mass normalised to body weight and systolic blood pressure measured by tail-cuff plethysmography in (a) WKY and (b) SHRSP. Data from 13-14 each of male and female SHRSP and WKY.

Table 3.1 Echocardiographic derived parameters in WKY and SHRSP rats.

		WKY n=33		SHRSP n=42		P value
		Mean	± SD	Mean	± SD	
Body weight	Kg	0.245	0.073	0.230	0.066	0.40
LV mass post-mortem	g	0.621	0.198	0.730	0.219	0.046
	g/Kg	2.513	0.177	3.228	0.498	< 0.0001
LV mass cubed method	g	0.612	0.254	0.750	0.264	0.04
	g/Kg	2.507	0.684	3.296	0.585	<0.0001
RV mass post-mortem	g	0.170	0.05	0.138	0.03	<0.0001
	g/Kg	0.577	0.105	0.668	0.117	<0.0001
Myocardial CSA	mm ²	42.5	10.2	49.4	9.7	0.006
	mm ² /Kg	180.1	38.5	222.5	37.3	<0.0001
<i>Dimensions</i>						
AWT	mm	1.64	0.32	1.89	0.25	0.0006
	mm/Kg	7.06	1.74	8.67	1.98	0.001
PWT	mm	2.05	0.29	2.24	0.26	0.007
	mm/Kg	8.84	1.95	10.30	2.43	0.011
AWT : PWT ratio		0.803	0.090	0.840	0.055	0.02
PWTs	mm	2.63	0.37	2.86	0.43	0.02
	mm/Kg	11.22	2.61	12.93	2.70	0.01
EDD	mm	5.37	0.68	5.51	0.82	0.42
	mm/Kg	23.42	5.15	25.43	5.69	0.14
ESD	mm	3.31	0.56	3.51	0.76	0.21
	mm/Kg	14.39	3.43	16.18	4.26	0.07
Fractional Shortening	%	38.57	4.38	36.71	6.5	0.18
<i>LV lumen characteristics</i>						
Cavity CSA diastole	mm ²	20.86	5.55	22.48	8.64	0.39
	mm ² /Kg	87.9	19.7	96.8	24.8	0.13
Cavity CSA systole	mm ²	7.36	2.66	11.82	5.2	0.0001
	mm ² /Kg	30.9	10.9	52.9	21.4	< 0.0001
EDV	ml	0.263	0.093	0.277	0.095	0.52
	ml/Kg	1.118	0.304	1.253	0.325	0.09
ESV	ml	0.086	0.039	0.108	0.062	0.09
	ml/Kg	0.365	0.139	0.469	0.204	0.02
Stroke Volume	ml	0.177	0.057	0.186	0.068	0.55
	ml/Kg	0.753	0.191	0.825	0.214	0.16
Ejection Fraction	%	66.1	5.6	47.8	7.6	< 0.0001

All values are mean ± standard deviation. AWT represents anterior wall thickness; PWT, posterior wall thickness; EDD, end-diastolic diameter; ESD, end-systolic diameter; CSA, cross-sectional area; EDV, end-diastolic volume; ESV, end-systolic volume.

There was no significant difference in LV cavity geometry when measuring one-dimensional end-diastolic diameter (EDD) by M-mode, or in two-dimensions by cavity cross-sectional area from a 2-D image. It is not possible however; to say whether there was any difference in long-axis dimension, as long-axis views were not obtained in most animals. End diastolic volume (EDV) was calculated assuming there was no change in relationship between long-axis and short-axis dimensions, and although showing a tendency to be larger in the SHRSP, failed to reach statistical significance.

LV function

Large differences were observed in LV function as measured by ejection fraction. Representative 2-D images are shown in Figure 3.11.

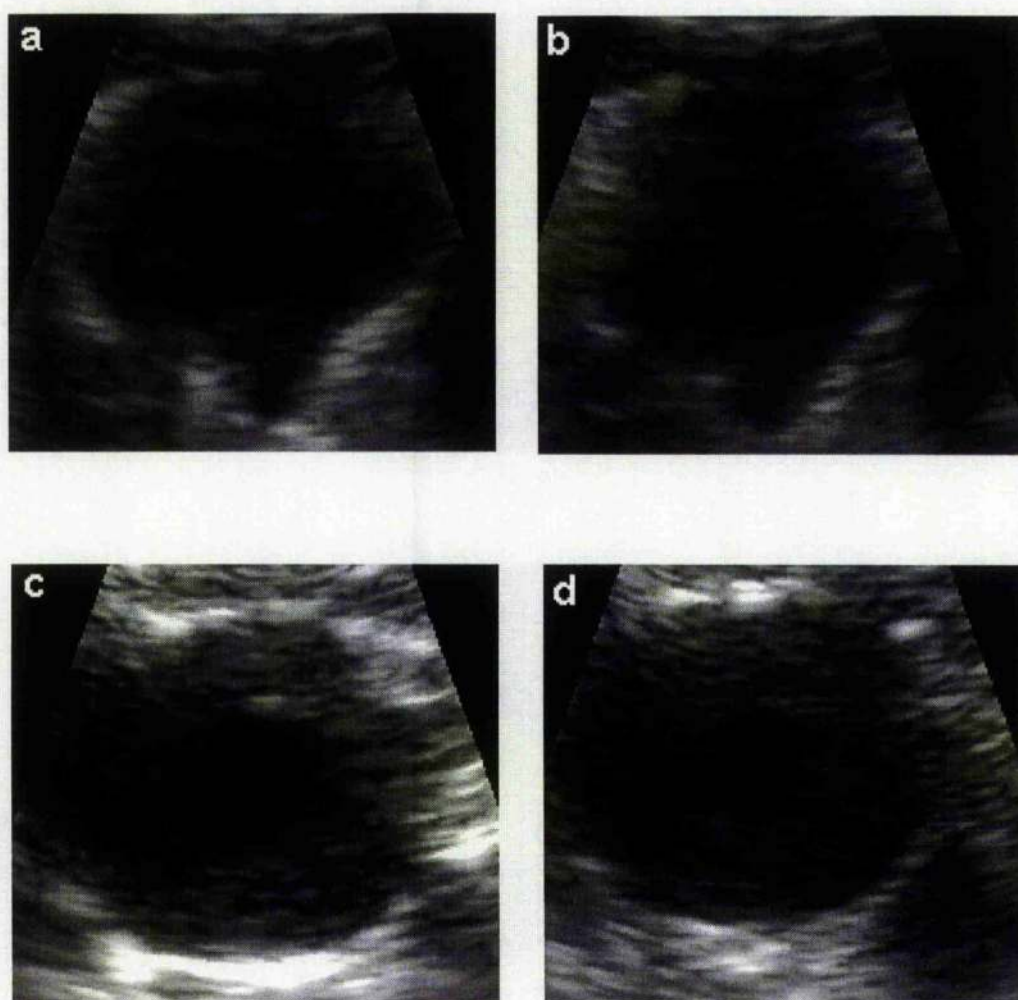


Figure 3.11 Sample 2-D echocardiograms from the parasternal short-axis view. Top panels are from a WKY rat at diastole (a) and systole (b); lower panels are from SHRSP diastole (c) and systole (d). Note thicker walls in the SHRSP.

In WKY rats, ejection fraction was $66.1 \pm 5.6\%$, but only $47.8 \pm 7.6\%$ in SHRSP rats ($P < 0.0001$). When graphed on a scatter plot to examine the spread of this data, there was a very clear difference between groups, with a few SHRSP exhibiting very low ejection fractions (Figure 3.12). This large difference is surprising, and is reminiscent of the mild LV dysfunction observed in coronary artery ligated rabbits (see Chapter 7).

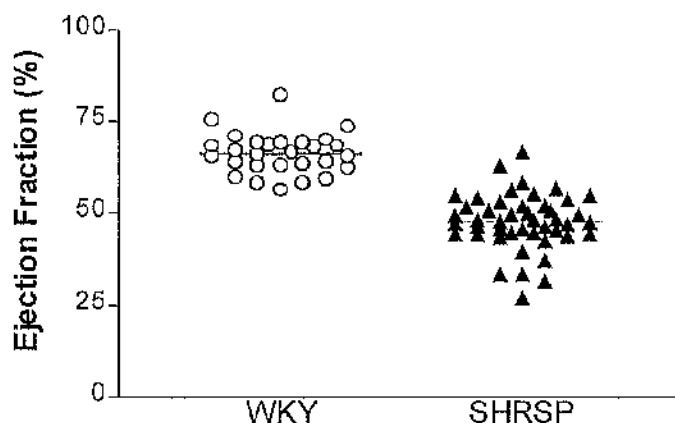


Figure 3.12 Ejection fractions for WKY and SHRSP rats. The solid line represents the mean value in each group. Comparison of means by Student's *t*-test, $P < 0.0001$.

In addition, although there was no significant difference in fractional shortening, it was very low in both groups at around 38%, compared to published data in the rat of 56% in normal animals (Pawlush *et al.*, 1993). Taken together, these results suggest that measurement of LV function in the present study may be grossly under-estimating contractility. No attempt was made to validate ejection fraction by comparing measurements with other techniques, so the question could not be addressed directly. However, it was decided to examine the effects of the anaesthetic on contractility, as the cardiac depressant effect of halothane was a prime suspect.

To perform an echocardiographic examination on rats without an anaesthetic would require months of animal training, and it is difficult to objectively assess depth of anaesthesia in the rat. Therefore, the effect of halothane exposure time on contractility was examined as a marker of its cardio-depressant effect. Ejection fractions from 24 animals (12 SHRSP, 12 WKY) were calculated at 3-4 different time points after

induction of anaesthesia. With each time point representing the mean of three cardiac cycles. No baseline was available (i.e. without halothane) and so the first ejection fraction for each animal was obtained within 5 minutes of induction of anaesthesia. This value was defined as unity and all subsequent measurements were expressed as a ratio of this value, to provide an index of contractility change with time of exposure to halothane (Figure 3.13). Where animals share a time point, data has been meaned.

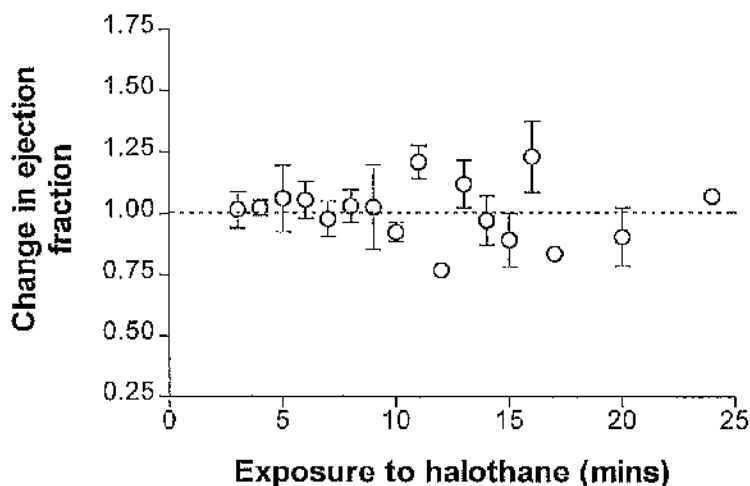


Figure 3.13 Effect of length of halothane exposure on cardiac contractility as measured by ejection fraction. All values are expressed as a ratio of the first measurement, and meaned with data from other animals sharing that time point. The number of animals at each time point therefore ranges from 1 to 8. All values are mean \pm standard error of the mean.

It is clear that from 3 minutes up to 24 minutes after induction of anaesthesia, halothane had no effect to systematically decrease contractility. However variability in the measurement does seem to increase after 10 minutes exposure, although this is partly due to fewer animals composing the time points in this range (most echo exams took less than 15 mins). Unfortunately, it was not possible to rule out an immediate (< 3 minutes) effect of halothane on contractility. The only way to determine this was by comparison with another anaesthetic. For these purposes a small number of animals were lightly sedated with 0.1ml Hypnorm® I.P., and ejection fraction measured. Ejection fraction was higher in both groups, at 77.9 ± 2.5 for WKY and 76.7 ± 2.4 for SHRSP, such that an inter-group difference was no longer discernible. This suggests

that halothane depresses contractility in both strains, but by an unknown mechanism affects the hypertrophic SHRSP heart to a greater degree.

Halothane anaesthesia, did not appear to affect measurements of LV dimensions, volume, or mass, as the values for these in Hypnorm sedated animals mirror the values obtained with halothane. Hypnorm was used for all subsequent echocardiographic examinations in this thesis.

Reproducibility

The stated aim of adapting echocardiography to the rat was to allow serial studies examining changes in echo parameters with time or treatment. In order to ascertain if real changes are being observed with time, it is necessary to determine the repeatability of measurements made a few days apart. The co-efficient of repeatability was calculated for 18 rats that had a repeat echocardiogram within 48 hours of the first. The data was analysed as the difference between 1st and 2nd studies expressed in terms of the mean for both values. A graphical representation of this is given in Figure 15 as an example. The mean value between measurements is shown as the line of identity, with $\pm 2SD$ (co-efficient of repeatability) on either side of this line. Values in future studies exceeding 2SD are likely ($P < 0.05$) to belong to a different population, and cannot be explained simply due to variability in the measurement process (Bland & Altman, 1986). Data was analysed in this way for a range of parameters, and the mean value \pm standard deviation are given in Table 3.2. Data normalised to body weight has been calculated in the same way to allow comparison of co-efficient of repeatability on this scale.

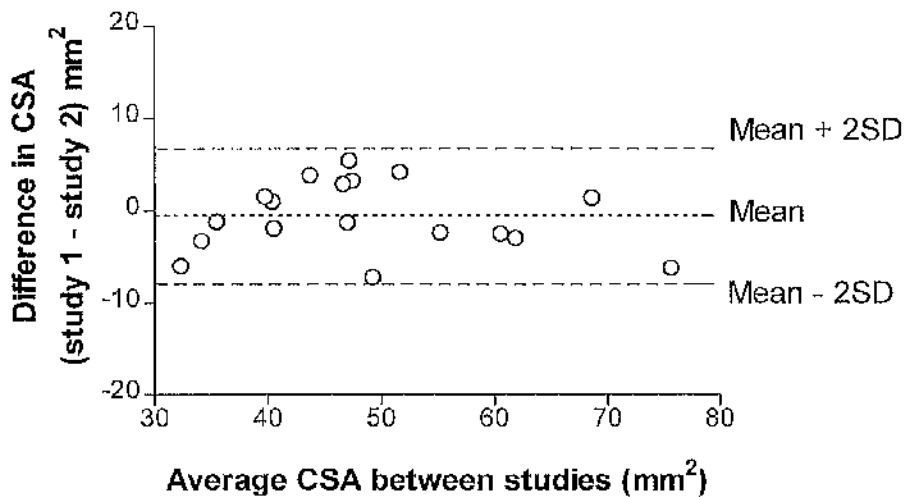


Figure 3.15 Assessment of repeatability between echocardiographic measurement of myocardial cross-sectional area measured on two separate occasions within 48 hours. This indicates the relationship between difference in measurements and the mean measurement for individual rats (n=18). The mean of differences and co-efficient of repeatability (2SD) are indicated by dashed lines.

The co-efficient of repeatability gives some indication of the reliability of measurements comparing WKY and SHRSP made earlier in this chapter (Table 3.1). Where the co-efficient of repeatability is smaller than the difference between WKY and SHRSP, we can confidently say that the difference is real and not due to variability in measurement. Therefore, the most reliable measurements when dealing with differences between WKY and SHRSP are, I.V mass (g/Kg), myocardial CSA (g/Kg), AWT (g/Kg), and ejection fraction. Of course, other parameters can be useful if the n number is sufficiently high. The usefulness of any given parameter will depend on the difference you would expect to observe between groups, and whether this is biologically significant.

Table 3.2 Variability between two sequential echocardiographic studies 48 hours apart performed in 18 rats.

		Study 1	Study 2	Mean of Differences	Co-efficient of Repeatability
LV mass "cubed" mg		0.769±0.267	0.790±0.29	-0.021	0.165
	g/Kg	3.15±0.50	3.20±0.38	-0.051	0.72
Myocardial CSA mm ²		48.5±11.8	49.1±12.2	-0.60	7.4
	mm ² /Kg	209±34	210±32	-1.46	32.8
AWT	mm	1.82±0.37	1.80±0.27	0.01	0.31
	mm/Kg	7.9±1.7	7.8±1.6	0.03	1.3
PWT	mm	2.17±0.33	2.19±0.32	-0.01	0.36
	mm/Kg	9.48±1.89	9.54±2.05	-0.05	1.69
EDD	mm	5.63±0.61	5.64±0.41	0.01	1.01
	mm/Kg	25.7±6.1	25.6±5.3	0.20	4.5
ESD	mm	3.49±0.49	3.53±0.44	-0.02	0.92
	mm/Kg	15.6±4.4	15.6±3.5	0.10	4.49
Cavity CSA	mm ²	22.5±4.7	21.7±5.2	0.76	10.1
Diastole	mm ² /Kg	97.9±24.7	93.4±20.4	4.47	48.0
Cavity CSA	mm ²	10.3±4.2	10.4±4.6	-0.13	7.4
Systole	mm ² /Kg	44.7±19.0	43.8±13.7	0.91	30.9
Stroke volume	ml	0.19±0.05	0.19±0.04	0.007	0.07
	ml/Kg	0.87±0.20	0.84±0.12	0.035	0.30
Ejection fraction	%	56.2±11.0	54.8±9.7	1.34	12.6

All values are mean ± standard deviation. AWT represents anterior wall thickness; PWT, posterior wall thickness; EDD, end-diastolic diameter; ESD, end-systolic diameter; CSA, cross-sectional area.

3.4 Discussion

All images were obtained using standard clinical ultrasound machines with paediatric probes. No modifications were required. The technique was well tolerated with zero mortality or morbidity regardless of the anaesthetic regime used. This was true of all of the 300+ echocardiographic examinations reported in this thesis. The best quality images were obtained with the rats lying in the left lateral position, with the chest fur closely shaved and using copious amounts of ultrasound gel. Care should be taken not to press too hard with the transducer against the thorax, as this was found to limit respiration and deform cardiac geometry.

The groups used in this study were fairly comparable with regards age range, body weight and sex ratio. However, the exception was SHRSP males, which tended to be younger and clustered around one age, with the oldest being 226 days old, compared to the 440 days in the other groups. This is because after 6 months of age male SHRSPs become much more likely to die of stroke, making it unusual to encounter an animal more than one-year-old (Okamoto *et al.*, 1974). There was a cluster of rats at around 100 days old, as this is the age that animals are most commonly used in this lab. Animals have reached maturity by this age, and the blood pressure of the SHRSP has attained its maximum (Davidson *et al.*, 1995). To avoid killing animals unnecessarily this study mostly used untreated rats that were being euthanased for other studies, or that were being culled as excess to requirements. Normalisation to body weight corrected for differences in body mass and sex (Figure 3.6).

Post-mortem validation of LV mass calculation

In human studies, there is still some debate concerning the relative benefits of M-mode and two-dimensional methodologies, and in choice of formulae for calculation of left ventricular mass (Liebson *et al.*, 1987). However, in the rat the situation is much clearer as technical considerations often dictate which methods can be used. One major constraint is the difficulty of reliably obtaining any views other than the parasternal short-axis. Although a parasternal long-axis view is shown in Figure 3.7, this was very much an exception rather than the rule. Indeed a number of groups have commented on the technical problems of obtaining an accurate long-axis view in the rat (Nakamura *et al.*, 1992; de Simone *et al.*, 1990). This severely limits choice of formulae, with the

cubed method being the most widely supported, and hence the method used in this study.

Table 3.3 summarises LV mass validation data from all published studies in the rat. From the correlation co-efficient comparing echo LV mass with autopsy LV mass, this study is in good agreement with the published data. As mentioned above, most groups have used the cubed method for calculating LV mass, due to the difficulty of obtaining a reliable long-axis view in the rat. The one exception to this has been de Simone *et al.* (1990 & 1994), who used the long-axis view as a second dimension in the ellipsoidal method, and in doing so gained in accuracy. However, in that study the long-axis view was not obtainable in all animals. The standard error of estimate in the present study is very low, and this simply reflects the large number of animals used (n=75) for the correlation. The accuracy of this study was calculated as sensitivity 92% and specificity 64%, which is again comparable to published data in the rat, and indeed to echo detection of LV hypertrophy in man (sensitivity 88% and specificity 84% using M-mode, Kucherer & Kuebler, 1992). The Penn convention has not been validated in the rat, with all groups choosing to follow the American Society for Echocardiography methodology. It is possible that the application of the Penn convention to echo measurements, may be beneficial in rats as it tends to result in lower estimations of LV mass than those obtained by ASE methods (Devereux & Reichek, 1977). For example, in studies using ASE convention and the cubed formula in man, the over-estimation of LV mass has been as large as 20% (Devereux, 1987). However, the present study had an echo/necropsy mass ratio of 1.05, indicating a relatively modest 5% over-estimation of LV mass, and by employing a simple correction factor this ratio was reduced to 1.00, such that systematic over-estimation was no longer a problem.

Study	Disease model	Method of LV mass calculation	Correlation co-efficient, r =	Standard error of estimate	P value	Sensitivity (%)	Specificity (%)	Predictive value (%)	False-positive (%)
Present study	SJRSP vs. WKY	Cubed ASE	0.86	0.01	<0.0001	92	64	78	22
de Simone <i>et al.</i> , 1990	41 Wistar, 3 SHRSP, 9 1K1C, 5 2K1C.	Ellipsoidal ASE	0.93	0.11	<0.00001	89	100		
Pawlush <i>et al.</i> , 1993	Surgical stenosis of aorta in Sprague-Dawley	Cubed ASE	0.87	0.14	<0.00001	44	100		
de Simone <i>et al.</i> , 1994	Hypertensive Wistar	Simplified ellipsoidal model ASE Cubed ASE	0.91	0.1	<0.00001	78	100		
Litwin <i>et al.</i> , 1994	Sprague-Dawley	Cubed ASE	0.87	0.1	<0.00001	56	100		
Nakamura <i>et al.</i> , 1991	Wistar SHR	Spherical ASE	0.87 0.94	0.12 0.09	<0.001 <0.001				

Table 3.3 Comparison of all published data comparing echo derived LV mass with LV mass at autopsy in the rat. Correlation co-efficient is given for linear regression between echo derived LV mass and actual LV mass at autopsy. Blank boxes indicate data unavailable. ASE = American Society of Echocardiography measuring convention.

Accuracy in detecting cardiac hypertrophy

The decision of where to set the upper limit of normality when describing LV hypertrophy will obviously have a pronounced effect on the calculations of accuracy, and it would be desirable to have an agreed value of what represented hypertrophy in the rat. It is not possible to compare this limit in the work of Pawlusch *et al.* (1993) as they normalise LV mass to tibial length. The only directly comparable studies, are those of de Simone *et al.* (1990 & 1994). In their 1994 paper, the critical value for LV hypertrophy was set at 1.62g/Kg. This is much lower than even the lowest measurement for WKY in this study, which can be explained by the fact that they normalised to body weight when using rats up to 763g in weight. In the 1990 paper, de Simone *et al.* set limits depending on body weight range. The critical value is 3.2g/Kg for animals between 100-299g body weights, dropping to 2.2g/Kg in animals with body weight between 300-499g. These are in rough agreement with the 2.86g/kg value in this study, and demonstrate that such limits can only be compared within a well-defined population. The limit is only likely to apply as long as the heart weight is increasing in direct proportion to the body weight, as observed in the growth curves (Figure 3.6). In humans, the Framingham heart study noted different limits for cardiac hypertrophy in men and women, even when normalised to body weight (Devereux, 1987). However, in a smaller study of normal subjects no sex difference was noted (Gardin *et al.*, 1987). As with the present study in rats, correction for body weight apparently accounted for any sex difference.

When assessing echocardiography as a diagnostic test in this way we are looking for a "yes" or "no" answer to the presence of hypertrophy. However, the population of rats in the current study does not lend itself well to this question, as it includes young SHRSPs that represent a continuous range of LV mass from normal to hypertrophied. Indeed, this is the same situation that occurs clinically in man, where, although it is possible to set a value for LV mass over which we define "hypertrophy", there is some concern that patients in the upper range of "normality" may have an increased clinical risk, despite a negative test (Liebson *et al.*, 1987). One reason why other groups appear to have a superior accuracy compared to this study is that they have greater polarity between normal and hypertrophied groups. If there is not a continuous range of values, but a clear difference between normal and hypertrophied (e.g. by age and sex matching),

then improved levels of accuracy are only to be expected. Another important consideration is that only one group reported the predictive value of the test, i.e. the number of true cases among all positive results, and the false-negative rate. These parameters give a better indication than sensitivity and specificity of the usefulness of a test where prevalence of the condition is known (Daly *et al.*, 1991).

Comparison of WKY with SHRSP

The blood pressure data for this study gives lower values for SHRSP animals than has been reported previously in this laboratory (Davidson *et al.*, 1995). The reason for this is the inclusion of a wide variation of ages, including young animals that may not yet have attained full hypertensive status. These were not excluded from this study as they provide the range of hypertensive / hypertrophic states important for the validation exercise. In contrast, Davidson *et al.* (1995) made standardised measurements at a constant age confirmed by telemetry. However, in this study, clear statistical differences were still observed between male and female SHRSP, and between both sexes of SHRSP and WKY.

There was no positive correlation between cardiac hypertrophy and systolic blood pressure in either WKY or SHRSP animals (Figure 3.10). This is a common finding in human and animal studies. In man, single measurements of systolic blood pressure are only weakly related to echo LV mass, with correlation co-efficients ranging from 0.24 to 0.45 (Devereux *et al.*, 1987). In the SHR, LV weight continues to rise for months after blood pressure has reached its maximum level (Pfeffer *et al.*, 1979), and may even be elevated before blood pressure begins to rise (Yamori *et al.*, 1979). Therefore, elevated blood pressure is only one of many factors that probably influence LV hypertrophy, such as, environmental, endocrine, or genetic differences. For example, in a genetic analysis that including SHR and SHRSP, Tanase *et al.* (1982a) estimated that 65-75% of variability in LV mass was attributable to genetic causes.

Table 3.1 indicates differences observed between WKY and SHRSP in echo-derived parameters. When normalised to body weight, the SHRSP heart had a significantly greater LV mass and myocardial cross-sectional area. This was due to a thickening of both aspects of the ventricular wall. There was no significant evidence for remodelling of the LV cavity, as only small increases were observed in end-diastolic dimension and

end-diastolic volume. This suggests that the increased wall thickness of the SHRSP models outwardly, as there is no encroachment into the LV luminal space. The hypertrophic response is not perfectly concentric as there was a small but significant difference between AWT:PWT ratio in WKY and SHRSP, indicating the anterior wall to exhibit a greater degree of hypertrophy.

In man, left ventricular wall thickness can show considerable regional variation. Wall thickness gets progressively less the closer measurements are made to the apex, and the anterior wall tends to be thicker than the posterior wall (Reichek, 1987). In this study the AWT:PWT ratio was less than 1, indicating a relatively thicker posterior wall, unlike in man. Why this should be so, is not entirely clear. It may in part be due to poor differentiation between inter-ventricular septum and anterior wall. In the rat it is difficult to define exactly which section of the wall is being measured, as the right ventricle is not usually visualised. Another confounding factor is the difficulty in obtaining good epicardial definition in the anterior wall, which in the rat, lies very close to the transducer and therefore not in the zone of optimal focus.

A further study in rats not included in Table 3.3 is concerned with the determination of stroke volume in male Wistar rats (Nakamura *et al.*, 1992). In this study, the ability to estimate stroke volume from short-axis measurements using a cubed formula was compared with simultaneous measurement using a pulsed Doppler flow meter placed around the aorta. The authors report very good correlations between measurements when a range of values were created either by atrial pacing ($r = 0.84$) or saline infusion ($r = 0.91$). The method of calculating stroke volume is very similar to that employed in the present study, and suggests that at least in the non-hypertrophied heart, the value obtained may be fairly accurate.

As a word of caution, care should be taken when comparing data from WKY and SHRSP, as any differences observed do not represent remodelling of the heart, since there is no evidence to suggest that SHRSP hearts were ever identical to WKY rats at any stage of development. The differences indicated are between a normotensive and hypertensive strain, and remodelling can only be said to occur when following longitudinal changes in the same animals.

It would have been useful to calculate LV wall stress in these animals, as pressure overload is thought to cause concentric LV hypertrophy by elevation of systolic wall stress (Kucherer & Kuebler, 1992). To measure this non-invasively requires the simultaneous measurement of blood pressure and LV dimensions by echocardiography (Fouad-Tarazi & Liebson, 1987). This could be achieved by continuous blood pressure monitoring after surgical implantation of a radiotelemetry probe. There is considerable experience of telemetric recording in this laboratory, and the combination with echocardiography may be investigated in the future.

Measurement of LV function

When using halothane anaesthetic, ejection fraction was consistently and significantly attenuated in the SHRSP (Figure 3.12). The decrease in function observed in this study was clearly contributable to the use of halothane, as although length of exposure was not an important determinant of function (Figure 3.13), changing anaesthetic to hypnorm greatly improved LV function in both WKY and SHRSP (78% versus 77% respectively), when the difference between groups was no longer apparent. However, the results from the halothane studies are interesting because it shows that in rats with severe cardiac hypertrophy, large differences in LV function may become unmasked under situations where the heart is suitably stressed.

Halothane was originally chosen as the anaesthetic in these studies due to practical considerations. A suitable vaporiser was available in the animal unit, and because induction and recovery are very rapid at between 1-3 minutes, the total anaesthetic time for each animal could be kept to an absolute minimum. However, halothane does have known depressant effects on the cardiovascular system, with a reduction in cardiac output and peripheral vasodilatation, resulting in a degree of hypotension. It also has a dose-dependent effect to depress respiration (Flecknell, 1996). Since almost all anaesthetics have some cardiac depressant effects it was hoped that WKY and SHRSP would be affected to a similar extent. In humans, the depressant effects of halothane may be more pronounced in infants, where it has been shown to decrease heart rate, fractional shortening, velocity of circumferential fibre shortening and cardiac index (Wodcy *et al.*, 1997). The interaction between cardiac hypertrophy and halothane has been examined in rabbits after aortic coarctation to induce LV hypertrophy (Rooke & Su, 1992). Using an *in vitro* set-up of skinned myocardial fibre bundles, both normal

and hypertrophied samples showed a dose-dependent effect of halothane to decrease contractility in response to maximal calcium concentration. Also, no difference was detected in the ability of halothane to inhibit calcium storage by the sarcoplasmic reticulum. The authors concluded that calcium sensitivity and storage are not the cause of the interaction between the cardiac depressant effects of halothane and hypertrophy. The mechanism remains to be elucidated.

When choosing a replacement anaesthetic, hypnorm was selected, as small doses are sufficient to produce sedation in the rat for echocardiographic examination. Thus, a much lighter depth of anaesthesia could be used, resulting in cardiac depressant effects that were much less pronounced. This worked well with an intraperitoneal dose of 0.04 – 0.1ml producing light sedation while major reflexes remained intact e.g. response to painful stimuli, righting reflex.

Even when using hypnorm, ejection fraction was around 75-80%, which although high in human terms is lower than 91-94% obtained in the study by Pawlusch *et al.* (1993). This may represent differences due to anaesthetic or strain, they used pentobarbital in Sprague-Dawley rats, or it may be inherent in the variability in measurements. However, it is important to remember that we are not trying to obtain absolute values for ejection fraction, rather to achieve reproducible measurements that can be compared to baseline data in longitudinal studies.

Use of echocardiography for serial evaluations.

The co-efficient of repeatability was determined for a range of echo-derived parameters using the method of Bland & Altman (1986). It would be wrong simply to use correlation co-efficient as a measurement of strength of relationship in this case, as we do not know the true value, and want to compare the agreement of two measurements. The correlation co-efficient will be high if the values lie on any straight line, but may not reflect actual agreement between values e.g. if one set of measurements incorporates a systematic error.

When using the co-efficient of repeatability to measure agreement between studies, it is first necessary to determine if any systematic error has affected either of the measurements. Calculating the mean of differences is used for this purpose. Normally

distributed data should be spread evenly above and below the mean, such that the mean of differences approximates to zero. If the mean of differences is significantly not zero, then this technique is not appropriate unless some consideration is given to correcting for the systematic error. As can be seen from Table 3.2, the mean of differences is close to zero for all parameters when compared to the mean values.

The co-efficient of repeatability can also be described as a percentage of the mean value obtained in the measurements, i.e. the percentage change in that parameter representing two standard deviations. This is similar to the method for deriving the co-efficient of variability described by Clark *et al.* (1980), and used in some studies. However, it should be noted that the co-efficient of repeatability incorporates two standard deviations, while the co-efficient of variability reports just one. Either method allows comparison between measurements to determine the most reproducible parameters, and hence the most useful for serial evaluations. Values for these are shown in Table 3.4, calculated from data in Table 3.2.

Table 3.4 Co-efficient of repeatability for echocardiographic parameters measured 48 hours apart, expressed as percentage change from the mean.

Echo-derived measurement.	Co-efficient of repeatability, Percentage of mean.
LV mass	21%
Myocardial CSA	15%
Anterior wall thickness	17%
Posterior wall thickness	16%
End diastolic dimension	18%
End systolic dimension	26%
Cavity CSA diastole	44%
Cavity CSA systole	71%
Stroke volume	37%
Ejection fraction	23%

This means that an observed change in LV mass of >21% would represent a shift of more than two standard deviations from the mean, such that there is a 95% chance that the change is real and not due to variability in measurement. This compares favourably

with the only other study in rats which used this methodology, which obtained a co-efficient of repeatability for LV mass of 32% (Jones *et al.*, 1992). The data in Table 3.2 indicates that the M-mode in rats is superior to two-dimensional imaging, as the repeatability of cavity cross-sectional areas, which are measured from 2-D, are very poor. In contrast, one-dimensional measurements from the M-mode such as anterior and posterior wall thickness and end diastolic dimension are much more reproducible. However, it is interesting to note that ejection fraction, as the ratio of these measurements, has a much improved co-efficient of repeatability. It is evident that for any given measurement the changes in CSA during diastole and systole retain the same relationship. The poor repeatability may be due to large subject variability, potentially exacerbated by use of halothane anaesthetic. Alternatively, problems in obtaining the identical short-axis imaging plane in both studies may be to blame. Angulation of the transducer beam away from the true short-axis may result in over-estimation of LV dimensions, or imaging too low down the heart may result in measurement of smaller dimensions. In human studies of serial echocardiography, positioning of the transducer was the most important technical consideration affecting reproducibility of the measurement (Wallerson & Devereux, 1987). However, since the plane for M-mode is selected from two-dimensional images, we would expect the same variability to be present in LV dimensions using this technique, which clearly there is not. The high variability in two-dimensional measurements is therefore most likely due to a combination of high intra-subject variability and less reliable measurements in 2-D mode, for example, due to poor edge definition.

The most reproducible, and therefore the most useful, measurement is myocardial cross-sectional area. Why this should be less variable than its individual component parts is probably due to the averaging out of errors incurred in measuring very small distances. In a study by Nakamura *et al.* (1991) post-mortem validation of myocardial CSA with echo-derived CSA gave very good correlations in Wistar ($r = 0.91$) and SHR ($r = 0.84$) rats, confirming the suitability of myocardial CSA as a marker of hypertrophy in its own right. As soon as we attempt to extrapolate into three dimensions we lose a good deal of repeatability, as can be seen by the higher co-efficient of repeatability for LV mass and stroke volume.

The repeatability of ejection fraction is not as good as expected. In the chapter on heart failure in rats, repeatability of ejection fraction in sham animals seems to be much improved. This may simply represent a learning curve for making echo-derived measurements. The heart failure data was collected at a time when the sonographer had a much greater experience (>200 examinations in rats).

For the use of echocardiography in serial studies it is concluded that where clear differences are expected, for example of the magnitude observed between WKY and SHRSP, most of the parameters studied will be useful. Appropriate power calculations can be performed to determine the number of animals required to show significant changes. However, for smaller incremental changes, more reliance should be placed on measurements from the M-mode, in particular individual wall thickness, myocardial cross-sectional area, and end-diastolic dimensions.

Sources of variability

The use of simultaneous two-dimensional imaging is probably of some considerable benefit in selecting the appropriate M-mode, but appears to be highly variable when taking measurements. The superior edge definition and temporal resolution of the M-mode makes it the most reliable in the fast moving rat heart, and this is borne out by the much lower co-efficient of repeatability for M-mode measurements in this study.

One major advantage of the M-mode that has already been mentioned is its high temporal resolution, which is vitally important with the high heart rate in the rat. Increasing heart rate may have an influence on accuracy of LV dimensions in serial measurements. One study in normal humans has shown a linear decrease in end-diastolic dimension when the heart rate was raised in 10 beats/min increments (Wallerson & Devereux, 1987). This decrease was small at 2.7%, and it is not known how this may relate to measurements in the rat. However, it follows that the effect of particular anaesthetics in lowering heart rate may have implications for accuracy of LV dimension in the rat.

Quality control

Although this study included criteria for choosing the best echocardiograms from which to take measurements, no criteria were adopted for rejecting unsatisfactory images. In human studies, it is common for patients to be excluded due to poor quality echocardiograms. For example, in the Framingham heart study, out of 6148 patients examined, only 80% had acceptable quality images when assessed against strict exclusion criteria. In addition, the authors describe a significant learning curve, with the acceptance rate as low as 28% in the first 5 months, rising to a high of 96% after 2 years (Savage *et al.*, 1987). Again, in the present study, as with all other studies in rats, no consideration was given to inclusion criteria or to the learning curve. This does not mean that it is easier to obtain acceptable images in the rat, rather that measurements are attempted regardless of the quality of the echocardiogram. Error introduced due to this will be accounted for within the calculations of accuracy, and it may be that these would be improved by adopting criteria for the rejection of images, as occurs in clinical studies.

A further problem relating to variability is that of systematic observer bias. This may occur when any clue is available as to the identity of the subject being measured. In this study, despite the reader being blinded as to whether rats were WKY or SHRSP, it was often easy to identify at a glance those animals exhibiting cardiac hypertrophy (see Figure 3.11 for example). Thus, a certain amount of bias may be unavoidable, depending on how easily groups can be differentiated. This is also true in data from the heart failure rats reported in Chapter 5, where it was often possible to visualise the infarct area or wall motion abnormalities, that would give away the operational status of the animal.

3.5 Conclusions

Despite the technical limitations in imaging small objects such as the rat heart, echocardiography has been shown to have sufficient accuracy and repeatability to be useful in serial studies in determining LV structure and function (where function is comparative not absolute). In particular,

- The SHRSP has been confirmed as a good model of severe cardiac hypertrophy with on average 28% greater LV mass to body weight ratio when compared to WKY.
- The extent of differences in cardiac mass and dimensions are such that it is suitable for detection by echocardiography using an unmodified machine.
- Cardiac hypertrophy does not correlate well with single point measurement of blood pressure.
- The SHRSP is much more susceptible to the cardiac depressant effects of halothane when compared to WKY (halothane unmasks LV dysfunction in the SHRSP). However, when using hypnorm sedation, LV function in the SHRSP is not compromised when compared to WKY.
- The use of echocardiography to determine LV mass in rats provides a good correlation with LV mass at post-mortem.
- The presence of cardiac hypertrophy in this strain of rats can be defined as a LV mass / body weight ratio of $>2.86\text{g/Kg}$.
- The accuracy for determining cardiac hypertrophy by echocardiography is comparable to that for the same technique in man, with sensitivity 92% and specificity 64%.
- The most reliable measurements for longitudinal studies are LV mass, myocardial cross-sectional area, and wall thickness.

4. Prevention of Cardiac and Vascular Hypertrophy in a Model of Genetic Hypertension

4.1 Introduction

As discussed in Chapter 1, the ability of antihypertensives to control complications of prolonged blood pressure elevation such as cardiac and vascular hypertrophy are thought to be important in preventing decline of cardiac function in the long-term. In this chapter, the ability of irbesartan, an angiotensin II type 1 receptor (AT₁) antagonist, was tested in preventing these complications in the stroke-prone spontaneously hypertensive rat (SHRSP), a severe model of genetic hypertension. Irbesartan treatment from 6 weeks of age was compared to untreated control SHRSP, as well as rats given an equihypotensive dose of hydralazine + hydrochlorothiazide (H+H). The hypothesis was that blockade of AT₁ receptors provides additional benefits over and above the blood pressure lowering effect.

Prevention of left ventricular (LV) hypertrophy was quantified by trans-thoracic echocardiography before and during treatment. In addition, natriuretic peptide gene expression in the LV was assessed, since ANP and BNP have been suggested as molecular markers of LV hypertrophy (Kawakami *et al.*, 1996). The influence of irbesartan on medial hypertrophy of resistance arteries was studied, for the first time, using laser scanning confocal microscopy (LSCM). This allowed the quantification of vascular wall thickness and of cell number, in order to evaluate the relative importance of hypertrophy and hyperplasia.

Hydralazine + hydrochlorothiazide was chosen for this study as previous work in this laboratory has shown a dose of 4mg/Kg/day of each to be as effective as the ACE inhibitor perindopril in lowering blood pressure in the SHRSP (Devlin *et al.*, 1995). Hydrochlorothiazide is a thiazide diuretic and therefore inhibits sodium reabsorption in the early distal convoluted tubule, its antihypertensive action also involves direct vasodilatory effects. Hydralazine is classed as a vasodilator and probably acts directly on the smooth muscle, but its mechanism of action is poorly understood, and may

involve modulation of intracellular calcium handling or a direct interaction with the contractile apparatus (Jacobs, 1984).

Irbesartan pharmacology

Irbesartan (BMS-186295 or SR 47436) is an angiotensin II type 1 receptor antagonist (AT₁RA). It is one of four AT₁RAs currently licensed in the UK to treat hypertension, the class leader being losartan (BNF No.38 September 1999). AT₁RAs interact with the renin-angiotensin system, which has a central role in regulating blood pressure and electrolyte balance (discussed in Chapter 1). In this respect they are similar to ACE inhibitors which inhibit angiotensin-converting enzyme, preventing the conversion of angiotensin I to angiotensin II (AngII). ACE inhibitors represent the gold standard in this area and have been used clinically to treat hypertension and heart failure with considerable success for many years. Theoretically, AngII receptor antagonism may offer several advantages over ACE inhibition by providing a more complete blockade of the RAS. This is because inhibiting the angiotensin-converting enzyme does not prevent the production of AngII by non-ACE pathways, whereas antagonism of the AngII receptor will block the effects of all AngII, whatever the source. In addition, inhibition of ACE can result in accumulation of bradykinin since ACE also masquerades as kininase II, which inactivates bradykinin. Excess bradykinin in the bronchial mucosa may be responsible for the persistent cough, which is a common side effect of ACE inhibitors. This is not a problem with AT₁RAs (Powell *et al.*, 1998).

It is the angiotensin type 1 receptor (AT₁) which mediates the deleterious effects of AngII such as vasoconstriction, cellular hypertrophy, sodium retention and increased aldosterone release. Blockade of the AT₁ receptor in the juxtaglomerular apparatus leads to an increase in plasma renin activity and therefore a rise in circulating AngII. This rise in AngII (1.5 – 2 fold for irbesartan) does not interfere with the inhibition of AT₁ receptors, as antagonism by irbesartan is insurmountable. Furthermore, the increased activity of AngII at AT₂ receptors may contribute to the beneficial effect of AT₁RAs since the AT₂ receptor is thought to mediate an antiproliferative effect on coronary endothelium and to inhibit growth in vascular smooth muscle. (Powell *et al.*, 1998). However, the clinical importance of these AT₂-mediated effects have not been firmly established.

Irbesartan is highly potent, in radioligand binding studies it has ten times the affinity over losartan for AT₁ receptors in rat liver membranes and vascular smooth muscle cells (IC₅₀ = 1.7nM). It is selective for AT₁ with a greater than 10000 times lower affinity for AT₂ receptors, and no affinity for α -adrenergic, serotonin, bradykinin, or vasopressin receptors or calcium channels at concentrations up to 30 μ M (Powell *et al.*, 1998). It has the advantage over losartan of not requiring transformation to an active metabolite to attain its full effect.

The pharmacokinetics of irbesartan are favourable. After oral administration, absorption is rapid with a high bioavailability of 60 – 80%, unaffected by food. The elimination half-life in healthy volunteers is between 11 and 15 hours with no gender differences, allowing for once daily dosing. At the clinical doses of 150 and 300mg daily, steady state is attained after 3 days and there is no significant accumulation. Higher plasma concentrations of irbesartan are observed in hypertensive females, but this does not affect half-life or accumulation, nor does renal or hepatic insufficiency (Powell *et al.*, 1998).

From trial data in 2600 patients, irbesartan also appears to be well tolerated with a frequency of adverse reactions similar to placebo. The incidence of first dose hypotension is also equivalent to placebo (Powell *et al.*, 1998).

Before starting this study there had only been a handful of papers published on irbesartan in hypertensive rat model. Initial research showed that a single oral dose of irbesartan could abolish the pressor response of angiotensin II in normotensive rats, and a dose of 30mg/Kg almost totally abolished the rise in blood pressure (Cazaubon *et al.*, 1993). In another dosing study by the same group, oral and intravenous administration of irbesartan was examined in a wide range of hypertensive models including renal artery-ligated rats, 2-kidney 1-clip Goldblatt rats, and DOCA treated rats. In the SHR, acute oral administration with 10mg/Kg significantly reduced mean arterial pressure (MAP) within 1½ hours and peaked at 3 to 5 hours with a reduction of 16mmHg. This effect lasted 8 hours, and at 24 hours the treated animals were still 10mmHg lower, although this was not statistically significant. After 2 weeks treatment at the same dose, a small but consistent reduction in MAP of 17mmHg was observed (Lacour *et al.*,

1994). These studies showed the potential for once daily dosing, but that doses of 30mg/Kg would be required for significant lowering of blood pressure in the rat.

The response to irbesartan clearly depends on the underlying aetiology of the model. In rats with pressure-overload due to aortic banding a dose of 50mg/Kg could only reduce systolic blood pressure by 8mmHg over a 15-week period. In addition, there was no effect of treatment on cardiac hypertrophy with left and right ventricular weights remaining elevated, as did myocyte cross-sectional area. It is not surprising that there was no improvement in survival despite a small decrease in LVEDP and normalisation of LV ACE mRNA levels (Weinberg *et al.*, 1995). The bottom line is that aortic banding does not produce a high renin dependent model, and so is less susceptible to modulation by AngII antagonists.

In male Wistar rats made hypertensive by administration of 50mg/Kg/day L-NAME, irbesartan (10mg/Kg/day) reduced but did not normalise blood pressure. Despite the low dose, irbesartan had a more profound effect on cardiac hypertrophy and in controlling inflammatory changes. It prevented the increase in heart to body weight ratio, and cardiac fibrosis and cell infiltration. It also prevented the inflammatory response in aortic smooth muscle, preventing the rise in protein and gene expression of iNOS, ICAM-1 and VCAM-1 (Luvvara *et al.*, 1998).

In a prevention study similar to the one reported here, SHR_s were treated orally with 60mg/Kg/day from 4 to 20 weeks of age. Animals treated with irbesartan had a consistently lower systolic blood pressure by around 40mmHg. Diastolic pressure was also lowered at all time points. Post-mortem cardiac morphology showed a decrease in heart weight, LV cross-sectional area and collagen content in the treated group, consistent with a reduction in cardiac hypertrophy. From 14 weeks of treatment onwards the aorta of treated rats exhibited a reduced media thickness and collagen content, while nuclear density was increased. These effects persisted for 8 weeks after cessation of irbesartan (Vacher *et al.*, 1995)

The aims of the present study were to examine in more detail the ability of irbesartan to prevent hypertension and its associated cardiac and vascular complications. The specific research questions were as follows,

- Is irbesartan effective in preventing blood pressure rise in the SHRSP?
- Will irbesartan prevent cardiac hypertrophy in the SHRSP? Can this be measured by serial echocardiography? What is the temporal relationship between rise in blood pressure and development of cardiac hypertrophy?
- Does irbesartan alter other markers of cardiac hypertrophy such as gene expression of ANP and BNP?
- Is irbesartan able to prevent vascular hypertrophy of resistance arteries associated with prolonged hypertension?

To what extent are these effects reliant on blockade of angiotensin II receptors compared to maintaining low blood pressure *per se*? This will be achieved by comparing results with a non-angiotensin II mechanism using hydralazine + hydrochlorothiazide.

4.2 Methods

Protocol

A total of 24 SHRSP rats were used in this study with 8 (4 males and 4 females) in each of the three treatment groups, control, irbesartan and hydralazine + hydrochlorothiazide (H+H). Drug treatment began shortly after weaning at between 6 and 7 weeks of age and continued daily at the same time each day for the entire 8 weeks of the study. Blood pressure was measured twice weekly by tail-cuff plethysmography from one week before entry until euthanasia. Echocardiographic examination was performed at baseline and then at study week 4 and 8. After 8 weeks of drug treatment animals were euthanased by an overdose of halothane anaesthetic, blood removed by cardiac puncture and the left ventricle weighed. At this time a small portion of the left ventricle was frozen in liquid nitrogen for subsequent isolation of RNA and Northern blot analysis for ANP and BNP. A section of jejunum with mesenteric arteries attached was placed in cold physiological salt solution and later fixed for study of mesenteric resistance arteries by laser scanning confocal microscopy.

Drug dosing

The normal method for delivering drugs in the rat is by dissolution in the drinking water. However, several properties of irbesartan make it less than ideal for this. Firstly it is only poorly water-soluble. To prepare a solution of appropriate strength and pH the manufacturers suggest dissolving the powder in a highly alkaline solution such as tribasic sodium phosphate. This requires the preparation of two buffer solutions and sonification may be necessary. This would not be a problem if large quantities could be prepared in advance. However, the stability of a 7mg/ml stock solution of irbesartan prepared in this way is very poor, with only 93% of the initial drug concentration remaining after 3 days at room temperature. There is also a high possibility of drug precipitation during storage as the solution is supersaturated. This would require solutions to be prepared and used on a 24-hour basis (Personal communication, Bristol-Myers Squibb).

For this reason, another system was required for delivering the drug. It was decided to create a simple suspension of drug in a small quantity of chocolate mousse. Animals were weighed weekly and the quantity of drug to provide 16mg/Kg/day of irbesartan or

4mg/Kg/day each of hydralazine and hydrochlorothiazide was calculated. Daily doses of the drug were weighed out several days in advance and stored in the dark until required. Immediately prior to administration, the dose was mixed with 1ml of chocolate mousse to form a suspension of drug. Control animals received 1ml mousse containing no treatment. The flavouring of the mousse was chosen to be most palatable to the rats, while disguising the taste of the drug. The drug-mousse mixture was almost always eaten immediately on introduction to the cage. The mousse was a commercial brand of chocolate pudding marketed for infants (H.J. Heinz Co. Ltd., Uxbridge, UK). The ingredients were as follows: skimmed milk (76%), water, cornflour, sugar, vegetable oil, fat reduced cocoa powder (1%) and natural flavouring. It contained no added preservative, artificial flavours, artificial colours, and no added salt. The nutritional status of the mousse is provided below, with the relative quantities provided for a 1ml daily intake.

<u>Nutrition Information</u>	<u>Per 100g</u>	<u>Per 1ml daily dose</u>
Energy	77kcal	0.8kcal
Protein	2.9g	32mg
Carbohydrate	13.2g	145mg
(of which sugars)	(8.7g)	96mg
Fat	1.4g	15mg
(of which saturates)	0.2g	2.2mg
Fibre	0.3g	3.3mg
Sodium	0.1g	1.1mg

The dose of irbesartan was chosen at 60mg/Kg/day, as this dose has been shown to prevent hypertension in the SHR (Vacher *et al.*, 1995). The dose of H+H has been used previously in this lab, and was effective at normalising blood pressure in the SHRSP (Devlin *et al.*, 1995).

Tail-cuff plethysmography

Measurements of systolic blood pressure and heart rate were performed twice weekly (48 hours apart) by tail-cuff plethysmography. The mean of these two independent readings was used to represent systolic blood pressure for that week for each individual animal. Method was as described in chapter 2.

Echocardiography

Method is as described in Chapter 3, using the Medison Sonoace SA8800 ultrasound machine interfaced to a 7.5MHz transducer. Light sedation was with 0.04 – 0.1ml of intraperitoneal hypnorm.

Northern analysis & Laser scanning confocal microscopy

Both as detailed in Methods chapter.

Statistics

Comparisons between groups were performed using one-way ANOVA corrected for multiple comparisons using the Newman-Keuls test, adopting a significance level of $P < 0.05$.

Spearman correlation was used where sample size was eight animals, since this is a non-parametric test and so does not assume a Gaussian distribution. For this sample size, a correlation co-efficient of $r > 0.71$ is considered significant ($P < 0.05$).

4.3 Results

Blood pressure

There were no differences between treatment groups as regards age, sex ratio or body weight at the start of this study (Table 4.1). All data are presented as the mean value for both males and females. Systolic blood pressures for the duration of the study are shown in Figure 4.1.

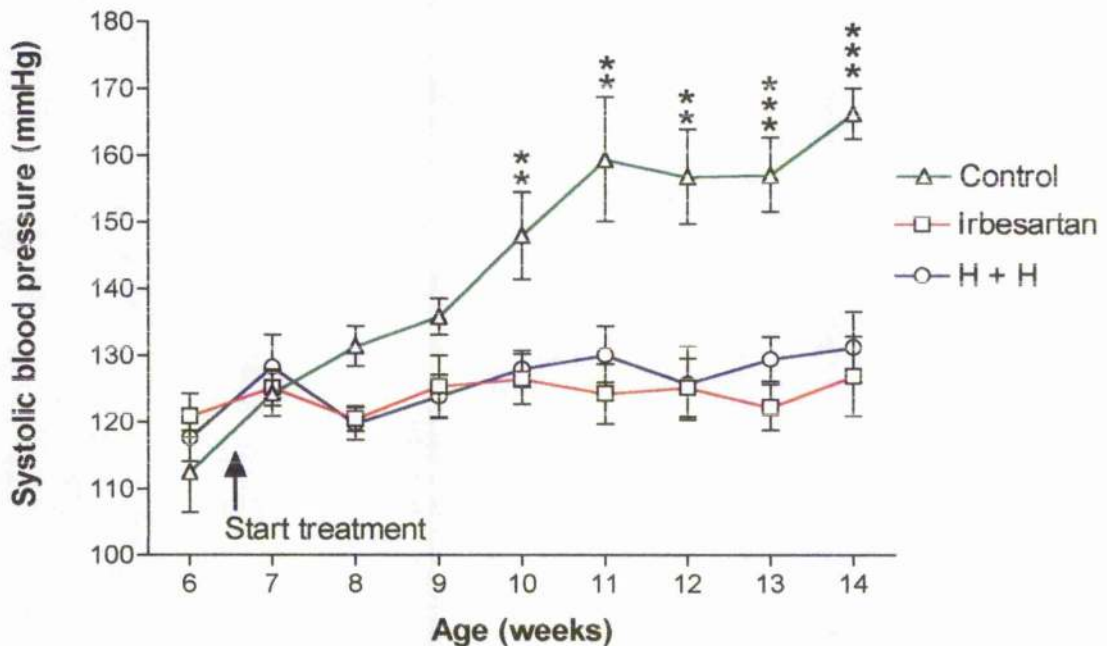


Figure 4.1 Systolic blood pressure measured by tail-cuff plethysmography in control and treated SHRSP. Week 6 refers to baseline measurements before treatment, with data shown until euthanasia at week 14. All data points are the mean \pm sem for 8 rats, each with two independent measurements performed 48 hours apart. Comparison between means using one-way ANOVA with Newman-Keuls correction for multiple comparisons, *** Denotes $P < 0.001$ and ** denotes $P < 0.01$ for both control vs. irbesartan and control vs. H+H.

Before treatment, there was no significant difference in systolic blood pressure (BP) between groups: 113, 121, 118 mmHg for control, irbesartan and H+H respectively. By four weeks into the study, BP in the untreated control group had risen significantly ($P < 0.01$) compared to both treatment arms, and continued to rise until a maximum of 166 mmHg at 8 weeks compared to 127 mmHg in irbesartan and 131 mmHg in H+H

animals. There were no differences in BP between irbesartan and H+H treated groups throughout the duration of this study.

Cardiac hypertrophy

Echocardiograms were taken at baseline, 4 and 8 weeks of treatment, when LV mass was confirmed by post-mortem examination. Figure 4.2 shows the LV mass to body weight ratio for all three groups throughout the study. The full range of results including LV dimensions and function is shown in Table 4.1 for baseline data, Table 4.2 for 4 week data, and in Table 4.3 for data obtained at 8 weeks immediately prior to sacrifice. In all tables, data are presented as absolute values since the groups are closely matched as regards age, body weight and sex ratio throughout the study. Similar results are obtained if normalised to body weight (data not shown), with the exception of LV mass when a difference between irbesartan and H+H groups is unmasked. For this reason Figure 4.2 shows data for LV mass normalised for body weight.

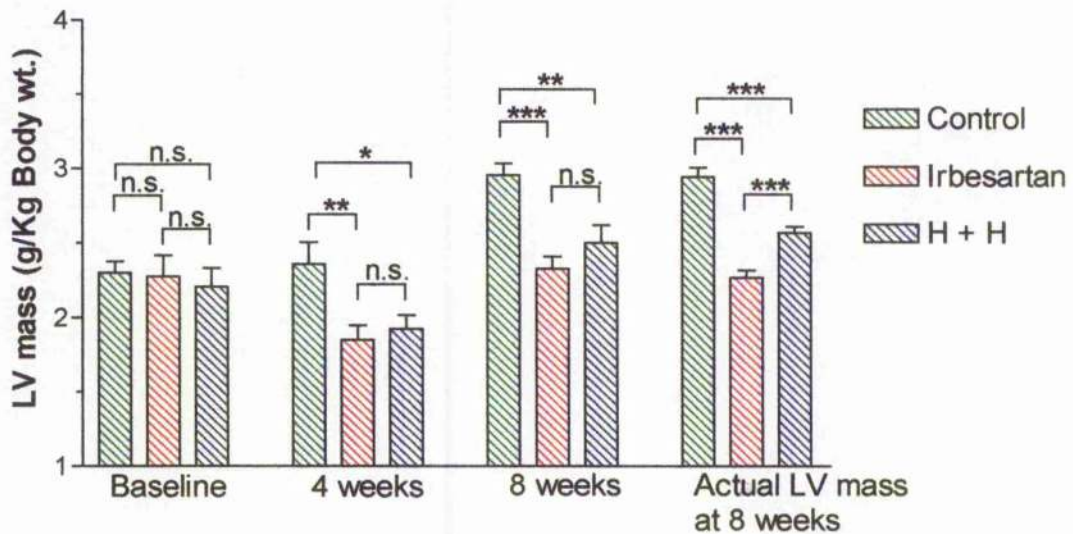


Figure 4.2 Left ventricular mass measured by echocardiography and normalised to body weight at baseline (before treatment), 4 weeks and 8 weeks of treatment. LV mass measured at post-mortem at 8 weeks is presented in the final column for comparison. All data are mean \pm sem, comparison by ANOVA with Newman-Keuls correction for multiple comparisons. *** Denotes $P < 0.001$; ** $P < 0.01$; * $P < 0.05$; n.s., difference not significant.

There were no significant differences between groups for any of the measured parameters at entry to the study (Table 4.1). However, by 4 weeks, control animals had a significantly increased LV mass when compared to either treatment ($P < 0.05$). As shown in Table 4.2, this difference was not just significant for LV mass, but was also highly significant for posterior wall thickness ($F=10.7$, $P=0.0006$) and myocardial cross-sectional area ($F=12.6$, $P=0.0003$). The trend was also observed in anterior wall thickness but just failed to reach significance ($F=3.15$, $P=0.06$). In all these measurements, control hearts had the largest dimensions, followed by H+H then irbesartan animals, which consistently had the smallest measurements for LV dimensions. In none of the parameters was the difference between irbesartan and H+H groups shown to be significant. Despite the greater wall thickness in control animals, no differences were observed in LV cavity dimensions (EDD & ESD), or in cardiac function as measured by fractional shortening.

Table 4.1 Echo-derived LV measurements obtained at baseline.

Baseline	Control	Irbesartan	H+H	P value
Age (days)	51 ± 6	49 ± 3	51 ± 3	n.s.
Body weight (g)	100 ± 14	98 ± 20	110 ± 18	n.s.
EDD (mm)	3.6 ± 0.6	3.5 ± 0.7	3.9 ± 0.1	n.s.
ESD (mm)	1.3 ± 0.5	1.3 ± 0.4	1.4 ± 0.1	n.s.
PWT (mm)	1.5 ± 0.1	1.6 ± 0.2	1.4 ± 0.1	n.s.
AWT (mm)	1.3 ± 0.2	1.3 ± 0.2	1.2 ± 0.1	n.s.
Myocardial CSA (mm ²)	22.2 ± 1.3	22.0 ± 3.6	21.7 ± 1.6	n.s.
LV mass (mg)	228 ± 31	225 ± 50	233 ± 22	n.s.
Fractional shortening (%)	65 ± 7	64 ± 8	66 ± 6	n.s.

All values are mean ± standard deviation. EDD represents end-diastolic dimension; ESD, end-systolic dimension; PWT, posterior wall thickness; AWT, anterior wall thickness; CSA, cross-sectional area and n.s., not significant.

Table 4.2 Echo-derived LV measurements obtained at 4 weeks of treatment.

4 weeks	Control	Irbesartan	H+H	P value
Age (days)	80 ± 6	79 ± 2	78 ± 1	n.s.
Body weight (g)	185 ± 28	175 ± 35	183 ± 31	n.s.
EDD (mm)	4.0 ± 0.3	4.0 ± 0.6	4.1 ± 0.5	n.s.
ESD (mm)	1.3 ± 0.2	1.4 ± 0.4	1.4 ± 0.2	n.s.
PWT (mm)	2.14 ± 0.14	1.75 ± 0.26***	1.80 ± 0.13**	0.0006
AWT (mm)	1.65 ± 0.13	1.42 ± 0.27	1.46 ± 0.15	0.06
Myo CSA (mm ²)	35.2 ± 2.8	27.1 ± 4.4***	29.4 ± 2.3**	0.0003
LV mass (mg)	428 ± 53	322 ± 69**	347 ± 42**	0.0024
FS (%)	68 ± 4	66 ± 8	66 ± 4	n.s.

All values are mean ± standard deviation. EDD represents end-diastolic dimension; ESD, end-systolic dimension; PWT, posterior wall thickness; AWT, anterior wall thickness; Myo CSA, myocardial cross-sectional area; FS, fractional shortening. *** denotes P<0.001 versus control group, ** P<0.01 versus control group and n.s., not significant.

The differences observed at 4 weeks were still present at 8 weeks and LV mass was confirmed by autopsy (Table 4.3). Both drug regimes significantly prevented cardiac hypertrophy when compared to control animals, however they were not equipotent in this respect. Irbesartan treated animals also had a significantly lower LV/body weight ratio when compared to H+H, indicating an additional effect over and above the ability to lower blood pressure. This was observed in the autopsy data, but was not significant in the echo-derived data, probably due to the variability of this method. As with data collected at 4 weeks, significantly smaller LV dimensions were observed with both drug treatments e.g. posterior wall thickness (F=20.3, P<0.0001), myocardial CSA (F=8.31, P=0.002) and this time anterior wall thickness (F=8.22, P=0.002). The rank order for LV dimensions was control>>>H+H>irbesartan. Again, there were no significant differences in LV cavity dimensions or function, which was confirmed by measurement of ejection fraction from two-dimensional echocardiograms. Representative M-mode

echocardiograms are shown in Figure 4.3 indicating the thicker left ventricular walls observed in untreated control animals.

Table 4.3 Echo-derived LV measurements obtained at 8 weeks of treatment and LV and RV mass at autopsy.

8 weeks	Control	Irbesartan	H+H	P value
Age (days)	106 ± 5	105 ± 3	107 ± 3	n.s.
Body weight (g)	217 ± 37	204 ± 49	214 ± 37	n.s.
EDD (mm)	4.4 ± 0.4	4.5 ± 0.3	4.7 ± 0.4	n.s.
ESD (mm)	1.3 ± 0.1	1.4 ± 0.1	1.5 ± 0.2	n.s.
PWT (mm)	2.41 ± 0.15	1.93 ± 0.17***	2.00 ± 0.17***	<0.0001
AWT (mm)	2.06 ± 0.13	1.70 ± 0.22**	1.81 ± 0.19*	0.0023
Myo CSA (mm ²)	46.8 ± 5.7	36.3 ± 5.6**	39.3 ± 4.5*	0.002
LV mass (mg)	645 ± 121	474 ± 98**	530 ± 83*	0.0096
FS (%)	70 ± 2	68 ± 2	68 ± 2	n.s.
EF (%)	74 ± 4	72 ± 4	71 ± 5	n.s.
LV mass actual	636 ± 103	461 ± 104**	548 ± 78	0.0058
LV mass (g/Kg)	2.95 ± 0.17	2.27 ± 0.13***	2.57 ± 0.12***#	<0.0001
RV mass	151 ± 25	145 ± 34	144 ± 29	n.s.

All values are mean ± standard deviation. EDD represents end-diastolic dimension; ESD, end-systolic dimension; PWT, posterior wall thickness; AWT, anterior wall thickness; Myo CSA, myocardial cross-sectional area; FS, fractional shortening; EF, ejection fraction. *** denotes P<0.001 versus control group, ** P<0.01 versus control group, * P<0.05 versus control group, # P<0.001 H+H versus irbesartan and n.s., not significant.

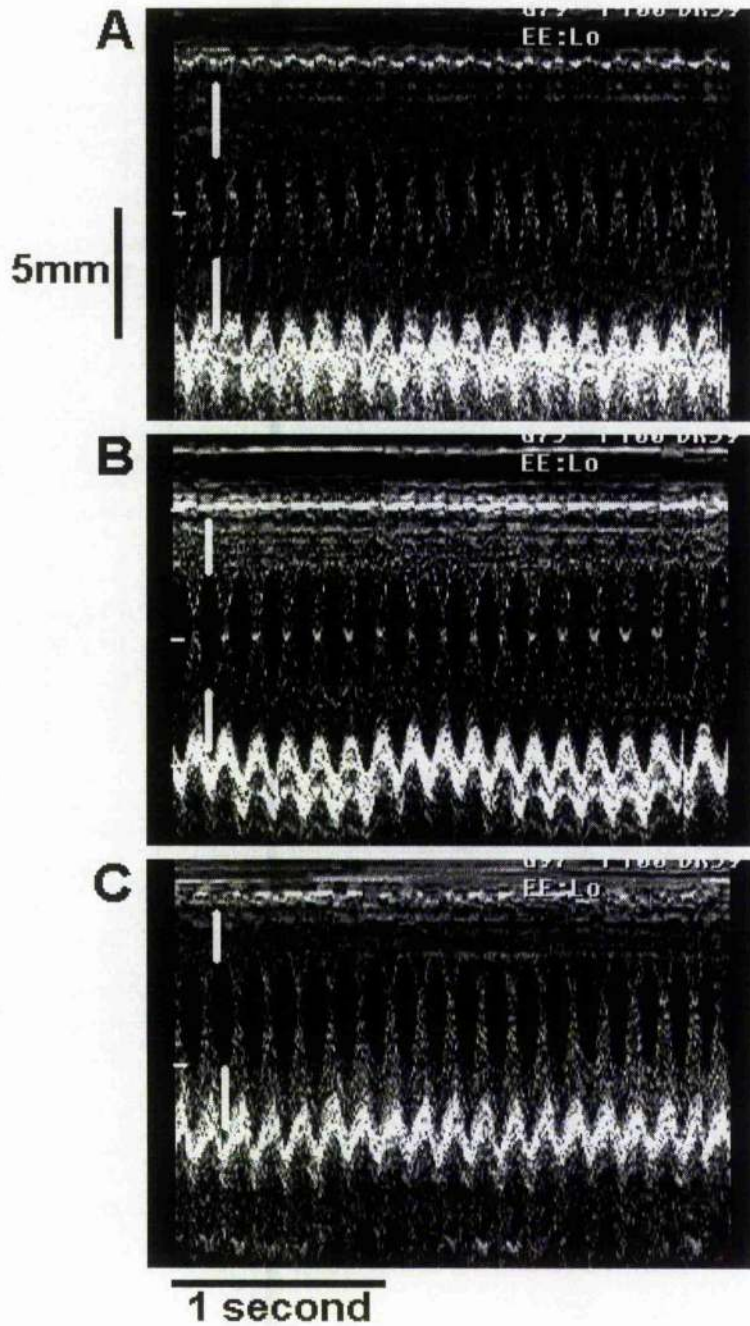


Figure 4.3 Sample M-mode echocardiograms of the left ventricle from control (A), irbesartan (B) and hydralazine/hydrochlorothiazide (C) treated rats obtained immediately before sacrifice at 8 weeks. The anterior wall is uppermost in these images, with the posterior wall below. Wall measurements are superimposed in white. Note the significantly thicker walls in the untreated control animal (A).

There was no relationship between LV mass/body wt. and systolic blood pressure in any of the groups (Figure 4.4, panel a). This was true irrespective of how blood pressure was expressed, for example, as mean blood pressure over whole 8 weeks, blood pressure readings at 4 or 8 weeks, or maximum attained blood pressure (data not shown). Although still poor, the best correlation was obtained by plotting change in LV mass with change in systolic blood pressure (Spearman correlation, $r = 0.38$) i.e. the difference between 8 week and baseline values (Figure 4.4, panel b). There was also no relationship between LV mass/body wt. and systolic blood pressure at entry to the study for all the animals combined (Figure 4.4, panel c), or for males and females only.

Gene expression of ANP and BNP

Cardiac mRNA expression of atrial & brain natriuretic peptides were compared as independent markers of cardiac hypertrophy. The Northern blot and mean data for ANP are shown in Figure 4.5. The size of the labelled mRNA was checked against molecular weight markers and atrial RNA was used as a positive control. Atrial tissue is known to have a very high concentration of ANP mRNA (Ogawa *et al.*, 1991), and as can be seen in panel A this is confirmed in this analysis. Untreated control animals had significantly greater gene expression than either treatment group ($F=15.4$, $P<0.0001$) and there was a non-significant trend for H+H to have a higher expression than irbesartan animals. This pattern is identical to that observed with the LV mass results from echocardiography. However, when the correlation was drawn between ANP gene expression and LV mass for control animals the correlation co-efficient was not significant (Figure 4.7, panel a). A much better relationship was observed between ANP and blood pressure ($r = 0.90$, Figure 4.7, panel b), which was significant at $P=0.005$. Due to the small sample size, non-parametric Spearman correlation was utilised. A correlation co-efficient >0.71 was considered significant.

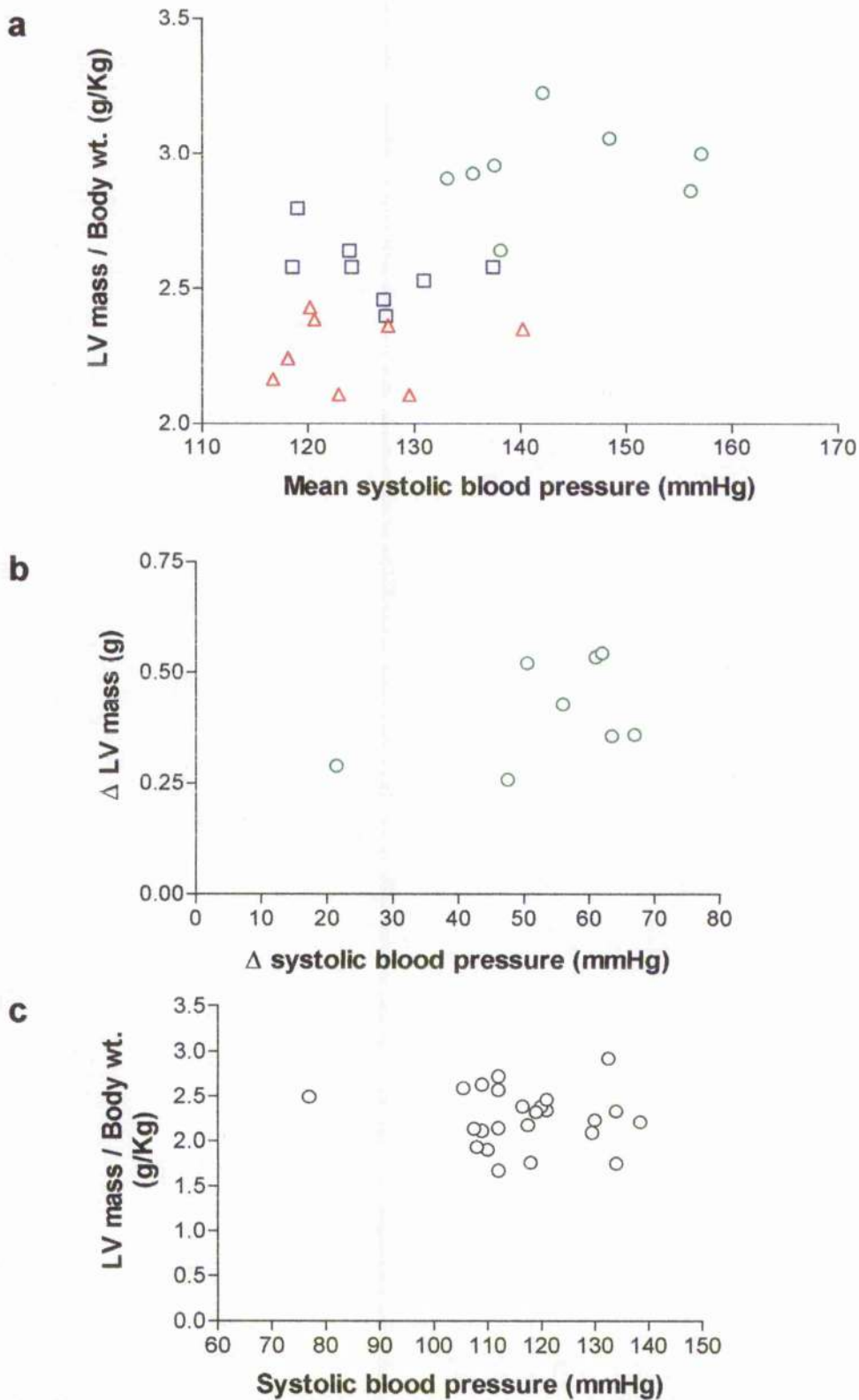


Figure 4.4 Correlation between LV mass and systolic blood pressure. Panel (a) indicates no positive correlation in control and treated animals at 8 weeks. Panel (b) shows the poor correlation between change in LV mass with change in systolic blood pressure between baseline to 8 weeks in control animals. Panel (c) indicates a lack of correlation for all animals at entry to this study (6-7 weeks of age).

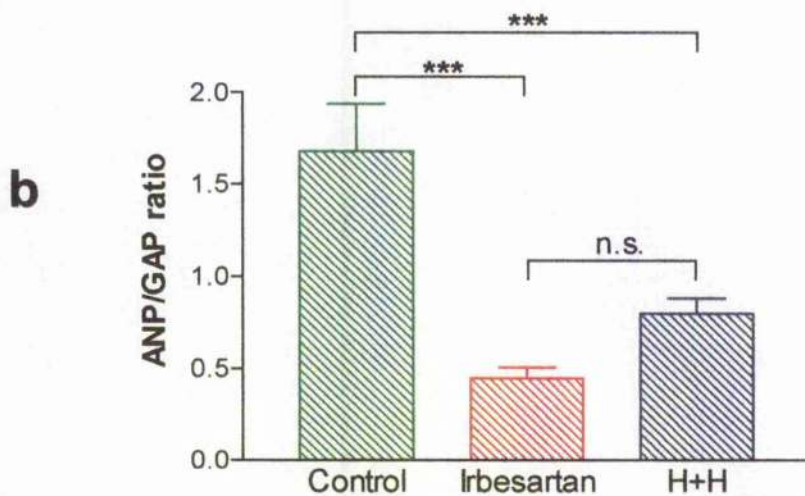
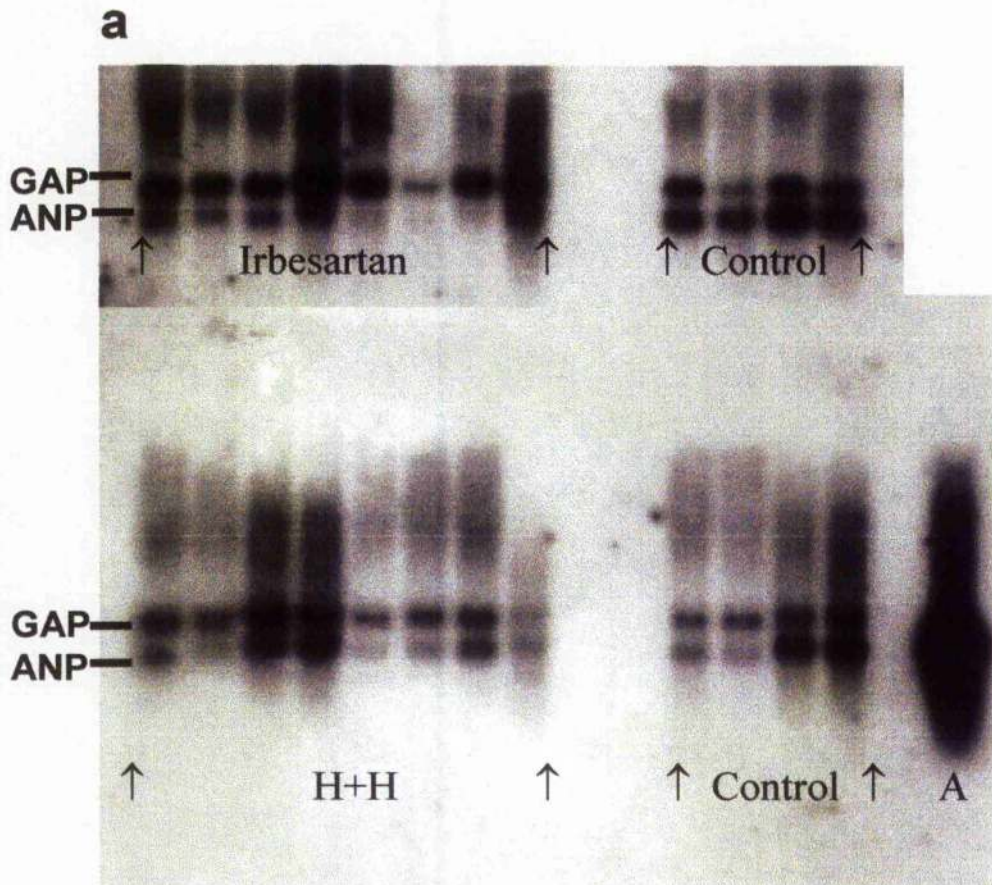
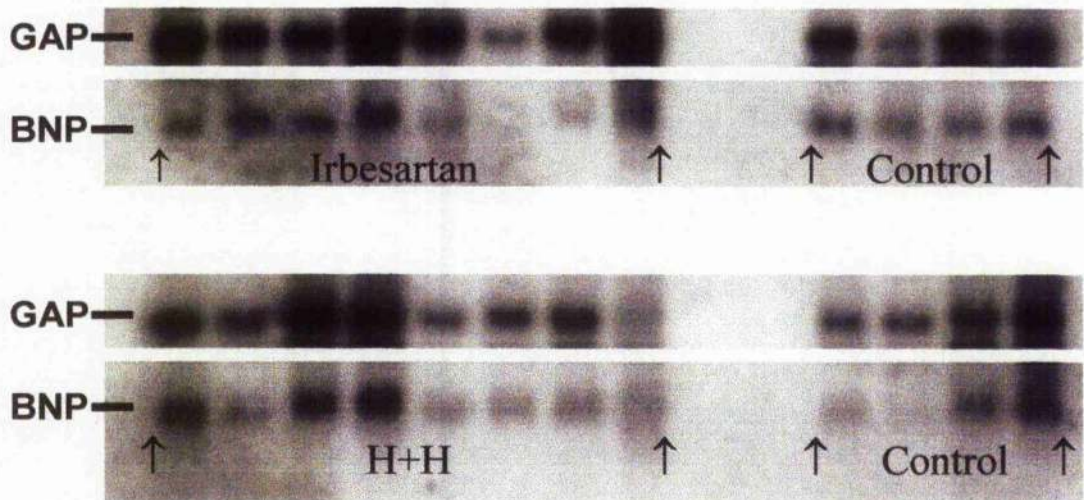


Figure 4.5 Panel (a) Northern blot indicating relative gene expression of GAP (1.8kb) and ANP (0.9kb) in the left ventricle of the SHRSP after 8 weeks of drug treatment. The first four lanes in each group are males, the latter four females. Lane A is atria from a control animal. Panel (b) shows the same data after quantification by densitometry. ANP expression has been normalised to GAP to correct for differences in loading of total RNA between lanes. Data are mean \pm sem, *** denotes $P < 0.001$ when analysed by one-way ANOVA with Newman-Keul's correction for multiple comparisons.

a



b

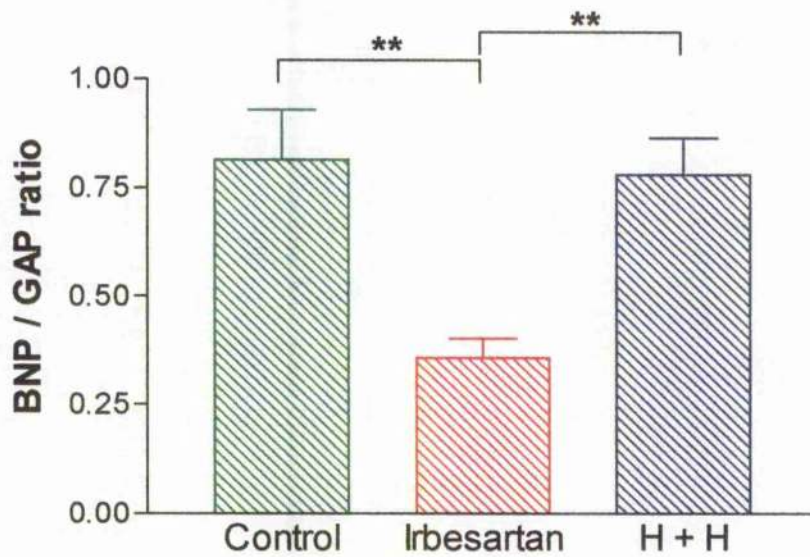


Figure 4.6 Panel (a) Northern blot indicating relative gene expression of GAP (1.8kb) and BNP (0.9kb) in the left ventricle of the SHRSP after 8 weeks of drug treatment. The first four lanes in each group are males, the latter four females. Panel (b) shows the same data after quantification by densitometry. BNP expression has been normalised to GAP to correct for differences in loading of total RNA between lanes. Data are mean \pm sem, ** denotes $P < 0.01$ when analysed by one-way ANOVA with Newman-Keul's correction for multiple comparisons. There is no significant difference between expression in control and H+H groups.

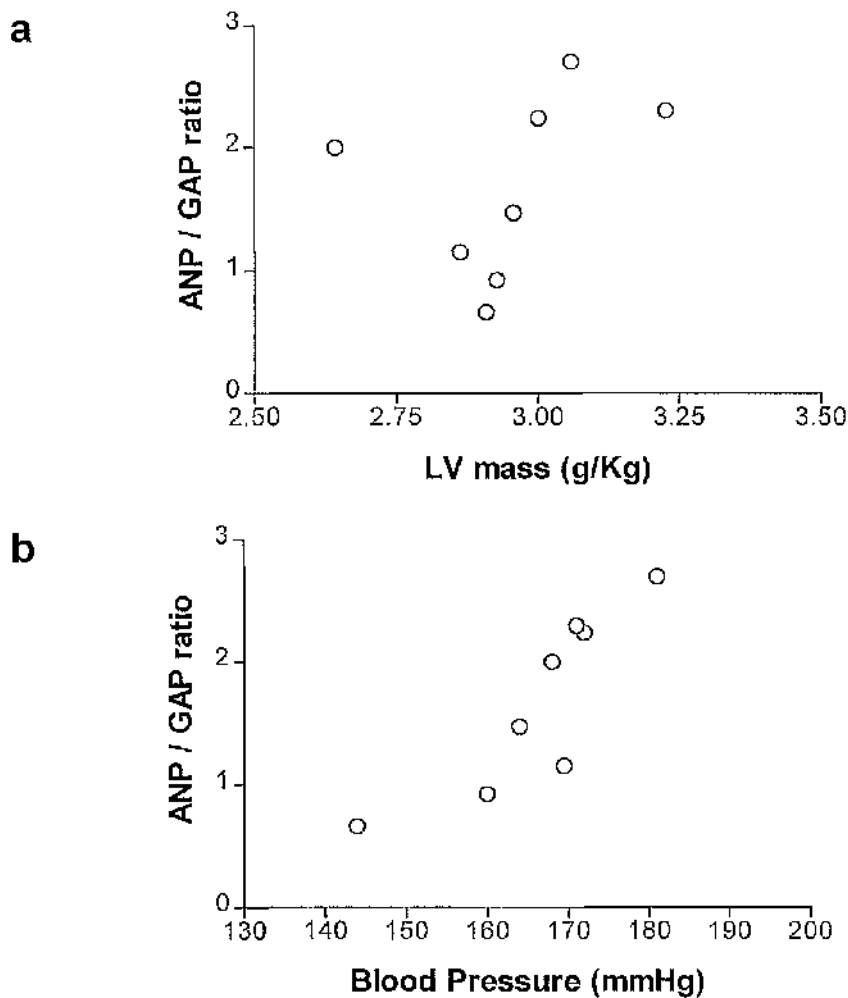


Figure 4.7 Correlation between mRNA expression of ANP in the left ventricle with (a) left ventricular mass (Spearman correlation, $r = 0.67$, $P = \text{n.s.}$) and (b) blood pressure ($r = 0.90$, $P = 0.005$) in control animals measured at 8 weeks.

Left ventricular gene expression of BNP is indicated in Figure 4.6. There was no significant difference in expression of BNP mRNA between control and H+H treated animals, however both these groups had significantly higher BNP expression than the irbesartan group ($F = 8.8$, $P = 0.002$). Lowering of blood pressure by H+H had almost no impact on the gene expression of BNP in the left ventricle. It is therefore not surprising that BNP expression does not correlate well with systolic blood pressure (Figure 4.8, panel b). However, unlike ANP, there is a strong positive relationship between BNP gene expression and LV mass (panel a, $r = 0.98$).

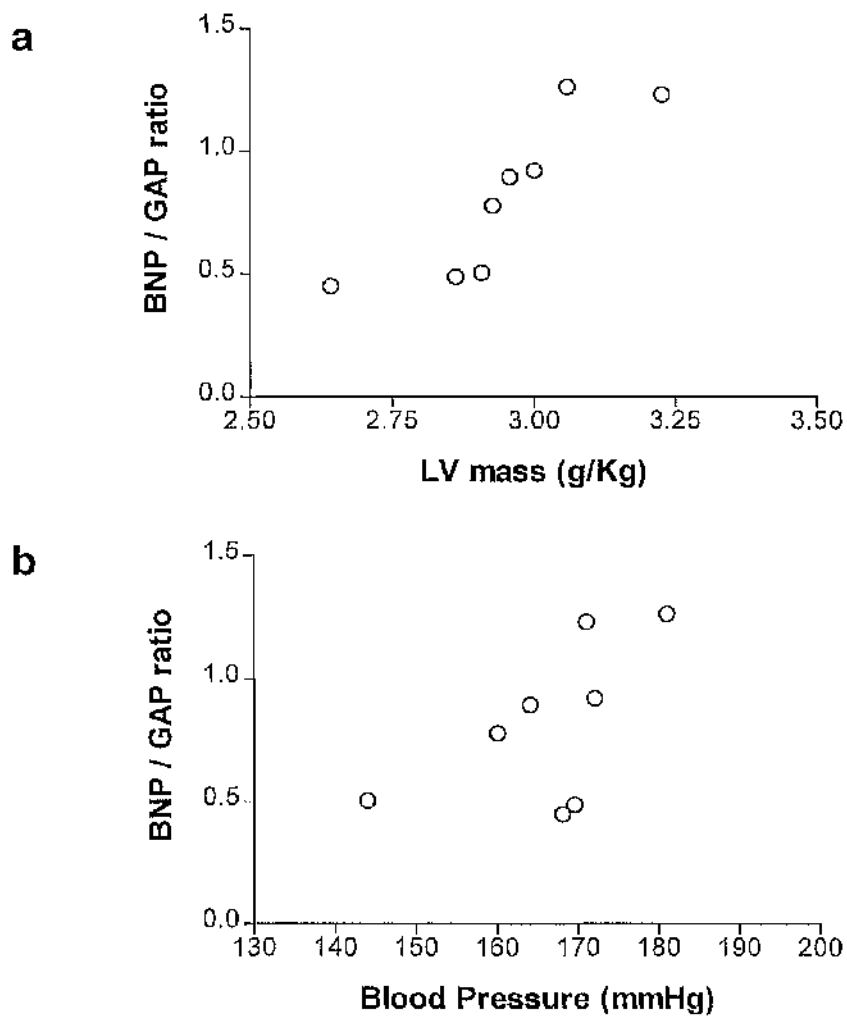


Figure 4.8 Correlation between mRNA expression of BNP in the left ventricle with (a) left ventricular mass (Spearman correlation, $r = 0.98$, $P=0.0004$) and (b) systolic blood pressure ($r = 0.62$, $P = \text{n.s.}$) in control animals measured at 8 weeks.

Caution should be used in interpreting the correlation results due to the small sample size. However, obvious trends are apparent.

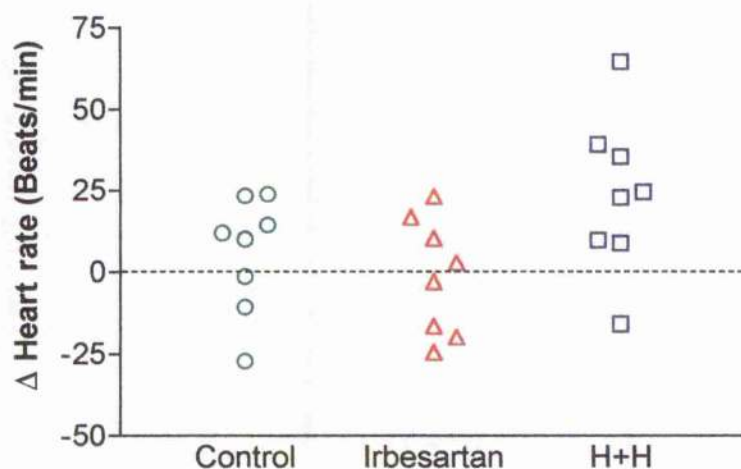


Figure 4.9 Change in heart rate during treatment from baseline values. Baseline was the mean of 2 measurements per animal, while treatment was the mean of 15 – 16 measurements per animal (n = 8 per group). There is no significant difference between groups by ANOVA (P = 0.06).

Heart rate

Heart rate was measured during tail-cuff plethysmography twice weekly for the duration of the study. Baseline data are the mean of two measurements per animal. The “during treatment” data represents mean heart rate for the entire period of treatment i.e. an average of 15 – 16 measurements. The rationale for this is that individual heart rate readings are highly variable and we want to detect long-term changes in heart rate in order to determine the effect on long-term responses such as LV mass and cardiac gene expression.

During treatment, H+H animals at 487 ± 19 beats/min had a higher heart rate than either irbesartan or control groups, which were almost identical at 451 ± 28 and 448 ± 19 respectively. However, before starting the study, H+H animals were already slightly higher. To account for this, the change in heart rate from baseline was calculated, and is shown in Figure 4.9. There is a trend for treatment with H+H to result in an increase in heart rate, although this just failed to reach significance (P=0.06).

To determine if the higher heart rate in H+H treated animals was significantly affecting LV mass or gene expression of natriuretic peptides, correlations between heart rate and

LV mass and ANP & BNP mRNA levels were calculated. A significant positive Spearman correlation was not obtained for any of these parameters (LV mass, $r = 0.61$; ANP, $r = -0.60$; BNP, $r = 0.30$). However, this does not rule out a more subtle effect of raised heart rate on these factors.

Plasma Renin & Aldosterone

Plasma concentrations of renin and aldosterone were measured from blood samples taken at sacrifice and are shown in Table 4.4. Adequate samples were not available from all animals, and so sample size is given in parenthesis. There was no significant difference between groups for either parameter; however, there was a trend for irbesartan animals to have elevated plasma renin concentrations. Although mean aldosterone concentration was higher in H+H rats, this could be entirely explained by one outlier with very high values. The remaining animals in this group had concentrations comparable to control and irbesartan animals.

Table 4.4 Plasma concentrations of renin and aldosterone at sacrifice.

	Renin	Aldosterone
Control	3.4 ± 1.2 (n=7)	32.0 ± 6.4 (n=6)
Irbesartan	8.6 ± 2.0 (n=8)	29.4 ± 8.1 (n=8)
H+H	5.7 ± 0.8 (n=7)	46.0 ± 13.7 (n=7)

Data are mean ± sem

Vascular hypertrophy

The presence of vascular hypertrophy was determined in 3rd order mesenteric resistance arteries using LSCM. Arteries from all twenty-four animals were measured, with the exception of the irbesartan group, where one was discarded after being identified as a vein under the confocal microscope. Arteries from control animals had significantly thicker vessel walls than either drug treatment ($P=0.02$). When this was broken down into the vessel component parts, there were no significant differences in adventitial or intimal thicknesses, but a significantly thicker media layer in the untreated controls ($P<0.01$, Figure 4.10). The relationship of these dimensions when applied to a cross-section of the artery are indicated in Table 4.5, with a significantly higher medial cross-sectional area (CSA) in control animals. There were no significant differences in cell

number in either adventitial, medial or intimal layers between any of the groups. However when expressed as smooth muscle cell (SMC) number normalised to medial volume, both treatment groups have a higher SMC density due to the same number of cells being arranged within a smaller volume. Lumen diameters were comparable, although tended to be lower in H+H animals. For this reason, wall/lumen and media/lumen ratios in the H+H group were closer to that of untreated controls. Representative cross-sections of the vessel wall are shown in Figure 4.11 to illustrate the greater thickness observed in untreated control animals.

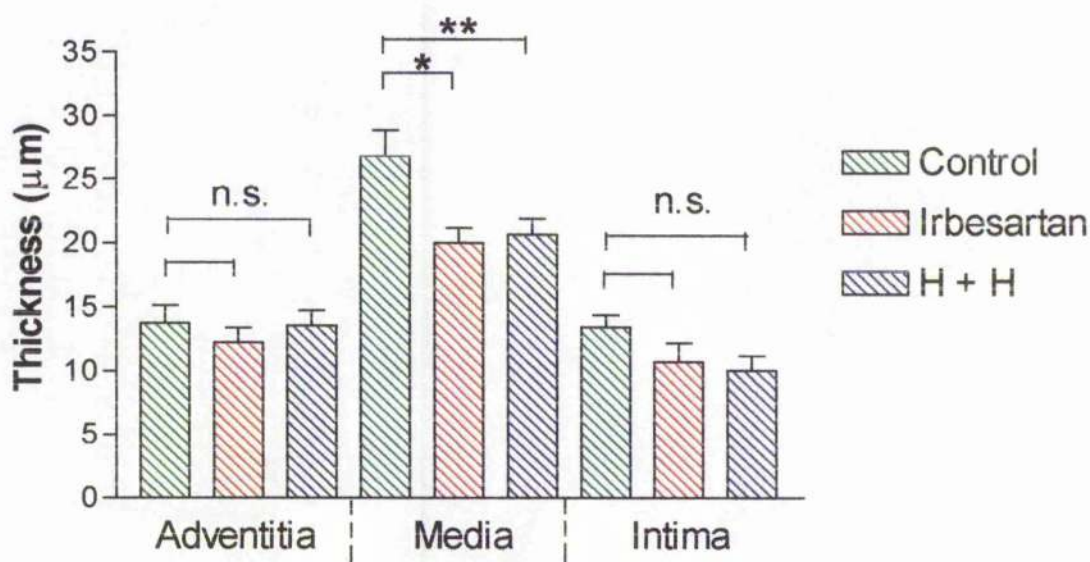


Figure 4.10 Relative thickness of the component parts of the arterial wall as measured by LSCM. All data are mean \pm sem, $n=8$ except irbesartan where $n=7$. * denotes $P<0.05$ for control versus irbesartan treated; ** $P<0.01$ for control versus H+H. There were no significant differences between treatment groups, and no significant differences between any groups for adventitia and intimal thickness.

Table 4.5 Measurements of 3rd order mesenteric resistance artery dimensions and cell numbers using LSCM.

		Control	Irbesartan	H+H	P value
		n=8	n=7	n=8	
Wall thickness	μm	53 ± 7	43 ± 8	44 ± 7	0.02 *#
A. thickness	μm	14 ± 4	12 ± 3	14 ± 3	n.s.
M. thickness	μm	27 ± 6	20 ± 3	21 ± 4	<0.01 *###
I. thickness	μm	13 ± 3	11 ± 4	10 ± 3	n.s.
Wall CSA	μm ²	39146 ± 7453	30444 ± 6075	28729 ± 8551	0.03 *#
A. CSA	μm ²	11194 ± 3331	9753 ± 2813	9887 ± 2115	n.s.
M. CSA	μm ²	19518 ± 3539	14162 ± 2388	13185 ± 4459	0.005 *###
I. CSA	μm ²	8433 ± 2858	6529 ± 2232	5656 ± 3071	n.s.
Lumen dia.	μm	181 ± 38	185 ± 28	160 ± 43	n.s.
Wall/lumen	%	31 ± 10	24 ± 6	29 ± 8	n.s.
Media/Lumen	%	16 ± 8	11 ± 3	14 ± 4	n.s.
External dia.	μm	288 ± 37	270 ± 26	249 ± 47	n.s.
A. cell number		19.5 ± 4.3	17.6 ± 4.4	15.4 ± 2.5	n.s.
SMC number		49.1 ± 8.0	44.5 ± 5.9	49.5 ± 4.9	n.s.
EC number/mm ²		1583 ± 591	1718 ± 572	1493 ± 333	n.s.
nA cells/A volume		126560±30059	135109±66356	98416±30727	n.s.
nSMC/M. volume		179858±40561	218632±49465	238921±39122	0.04 #

All data are derived from one vessel per animal and is presented as mean ± SD. A., adventitial; M., medial; I., intimal; CSA, cross-sectional area; dia., diameter; SMC, smooth muscle cell; EC, endothelial cell. Using one-way ANOVA with Newman-Keuls test to correct for multiple comparisons, * and ** denote P<0.05 and P<0.01 respectively for control versus irbesartan; # and ##, P<0.05 and P<0.01 respectively for control versus H+H group; n.s., not significant. There were no significant differences between irbesartan and H+H groups.

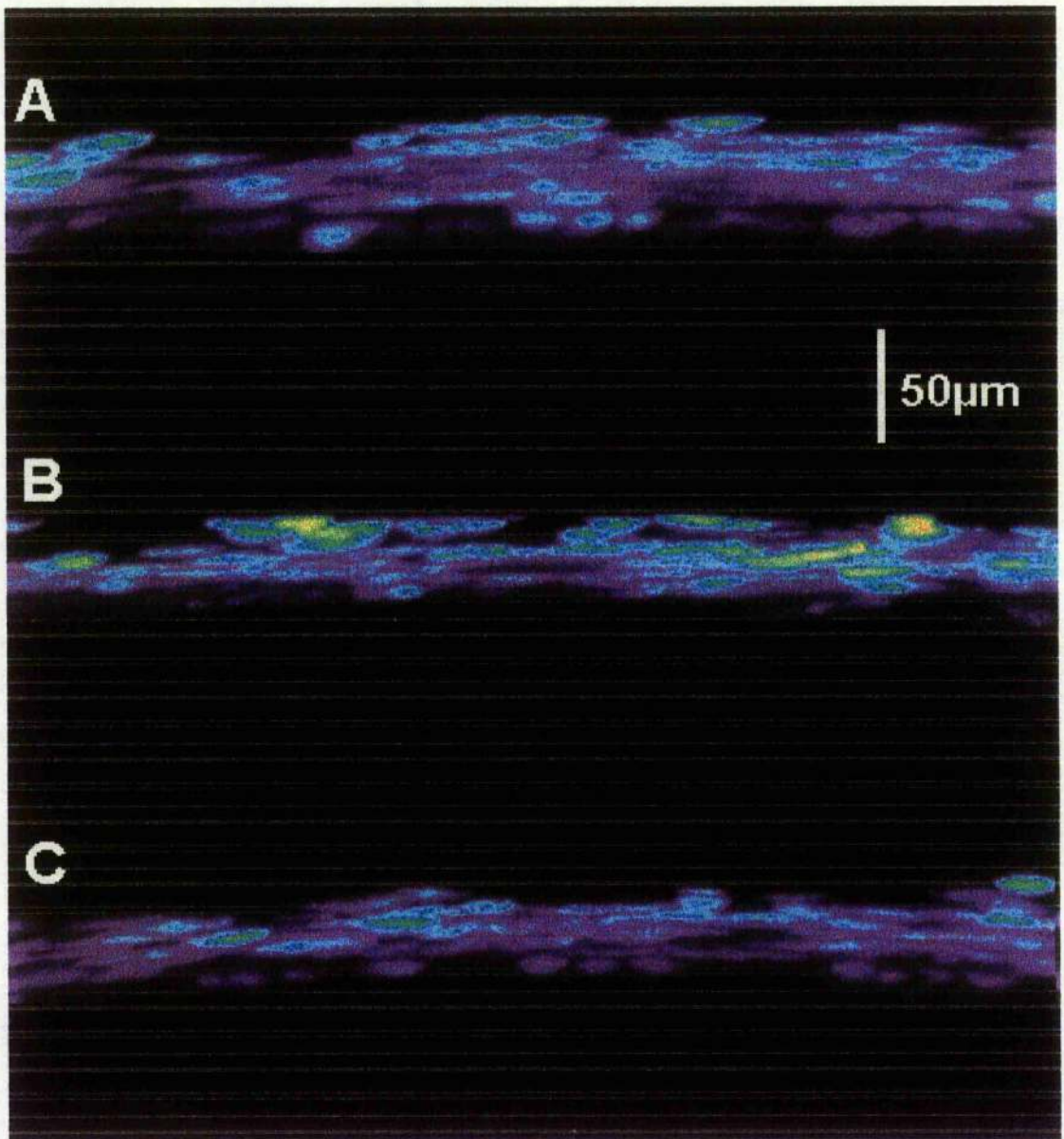


Figure 4.11 Representative cross-sections through the 3rd order mesenteric resistance artery wall from control (A), irbesartan (B) and hydralazine /hydrochlorothiazide (C) treated rats at 8 weeks. Images are 3-dimensional reconstructions of the vessel wall in cross-section. Vessels were fixed at half-systolic blood pressure by laser scanning confocal microscopy. Note the increased thickness of the vessel wall in untreated control animals (A).

There was no relationship between media thickness and systolic blood pressure in control SHRSP (Figure 4.12). This was true when looking at mean blood pressure throughout treatment or blood pressure at week 8.

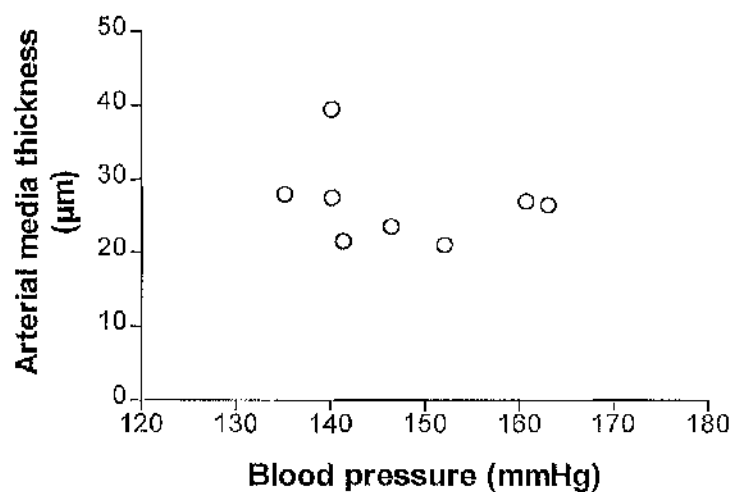


Figure 4.12 Lack of relationship between media thickness in mesenteric resistance arteries and mean systolic blood pressure in untreated control SHRSP.

4.4 Discussion

The addition to standard rat chow of 1ml chocolate mousse containing only trace amounts of fat and sodium does not represent a significant departure from the normal diet. In fact, the extra sodium intake of 1.1mg per day is less than half the 2.3mg extra sodium per day that would have been ingested if the irbesartan was forced into solution according to the manufacturers instructions. This is based on calculations for a 150g rat drinking 20ml daily, receiving 60mg/Kg/day irbesartan in drinking water that had been buffered using sodium phosphate. To put it in perspective, most commercial rat chow contains around 1% NaCl, and a minimum of 0.13% is required for normal growth (Rapp, 1987). The mousse contains only 0.1% sodium.

The use of chocolate mousse had a number of advantages over dissolution in drinking water. For example, in the ease of preparation: aliquots of dry powder could be weighed several days in advance without risk of degradation, such that admixture with the mousse could be performed by animal house staff minutes before administration. The mousse was highly palatable, even with large concentrations of drug. Although often cautious in the first few days of treatment, rats soon learnt to eagerly await their next dose, which was usually devoured within seconds. This gave the added advantage of allowing quick visual inspection that the full dose had been ingested, rather than calculating daily water intake. It also circumvents problems of variability in water intake that could occur on initiating treatment with irbesartan, as AngII is thought to regulate thirst via a central action (Morton *et al.*, 1982). That sufficient quantities of the drug were bioavailable in this formulation is evidenced by the convincing blood pressure effect. It could be concluded that creating a suspension in small quantities of infant mousse is a simple and effective way of delivering poorly soluble drugs in the rat.

Systolic blood pressure

By 4 weeks into the study, both treatment arms had significantly and consistently lower BP compared to the control group, and the 35 - 40mmHg difference by week 8 was almost identical to that observed in an irbesartan prevention study in the SHR (Vacher *et al.*, 1995). The blood pressure of the treatment groups remained within the 125 - 130mmHg range observed in the adult WKY (Figure 3.9, Chapter 3), and this was

firmly within the normotensive range. At these doses irbesartan and H+H appear to be equipotent at preventing the rise in systolic BP associated with genetic hypertension. Drug treatments were given as once daily doses in the afternoon, while blood pressure was measured in the morning. Thus, both irbesartan and H+H effectively lowered blood pressure for *at least* 20 hours of every day.

LV function

Ejection fraction and fractional shortening were within normal values for all rats at all time points, indicating that systolic function was not compromised by left ventricular hypertrophy. This suggests well compensated hypertrophy in agreement with that observed in aortic-banded rats 4-5 weeks after surgery (Pawlush *et al.*, 1993) and in the 6 month old SHR (Pfeffer *et al.*, 1979).

Cardiac hypertrophy

A similar picture was observed in the prevention of cardiac hypertrophy, with both drug groups preventing the increase in LV mass observed in untreated controls. Significant differences between treated and control groups were apparent at 4 weeks corresponding with the rise in blood pressure, which also became significant at 4 weeks. The hypertrophic response occurred fairly rapidly after the increase in blood pressure, which is consistent with the dynamic response to exogenous AngII (Kim *et al.*, 1995) or after myocardial infarction (Reiss *et al.*, 1993). The question remains whether the LV mass differences at 4 weeks are real, and not due to variability in echo measurements. However, the observed differences at 27% and 22% for irbesartan and H+H respectively, were greater than could have been explained by variability of the method alone. The differences are also observed when looking at the raw data, or other measures of hypertrophy with lower co-efficient of repeatability, such as posterior wall thickness or myocardial CSA. Between baseline and 4 weeks the LV/Body weight ratio actually got smaller in all 3 groups (Figure 4.2). However, on examining raw LV mass data, LV mass actually increased by 73%, 43% and 53% in control, irbesartan and H+H respectively over those 4 weeks. It appears that over this time, body mass increased to a greater extent.

At week 8 (Table 4.3), differences in LV dimensions remained pronounced, and anterior wall thickness was also significantly smaller in both treatment groups. For all measurements of anterior and posterior wall thickness, myocardial CSA and LV mass

made at 4 and at 8 weeks, II+H treated animals were consistently, but not significantly, greater than those treated with irbesartan. The only time that this difference became significant was for autopsy LV mass normalised to body weight.

According to the defined limits in Chapter 3, cardiac hypertrophy is present in this population of rats when LV/body weight ratio exceeds 2.86g/Kg. Thus, none of the rats had actual cardiac hypertrophy at 4 weeks, but by week 8 all but one control animal exhibited hypertrophy by this criterion. In contrast, none of the rats from either treatment group had a ratio above 2.86g/Kg.

There was no relationship between LV mass/body wt and systolic blood pressure in control animals or treatment groups (Figure 4.4, panel a). Normalisation to body weight was used as in Chapter 3, as this was shown to correct for sex differences. As discussed in the introduction, this is a common finding in animals (Pfeffer *et al.*, 1979) and humans with established hypertension (Devereux *et al.*, 1987), and indicates the importance of other trophic factors over and above blood pressure. In older animals, this lack of correlation is not surprising, considering that LV mass continues to rise for many months after maximum blood pressure has been attained (Pfeffer *et al.*, 1979). This suggests that blood pressure is not a major determinant of LV mass maintenance, yet it may still be important in the development of LVH. In the present study, there was a close temporal relationship between the rise in blood pressure and LV mass. By using serial echocardiography to determine LV mass, this allowed the determination of change in LV mass in relation to blood pressure change. Although this did provide a better correlation, the correlation co-efficient was still poor (Figure 4.4, panel b). Finally, baseline LV mass/body wt. was compared to blood pressure to determine if there was any relationship prior to the study at 6-7 weeks of age. SHRSP and SHR are reported to have a higher LV mass compared to WKY as young as 30 days (Yamori *et al.*, 1979). Again, any early differences are not heavily dependent on blood pressure (Figure 4.4, panel c).

However, as this study did not include normotensive controls, the presence of LVH on entry to the study was not determined. Therefore, the improved ability of irbesartan compared to H+H in preventing the increase in LV mass may be due not only to prevention of hypertrophy, but also to an increased ability to regress any LVH that was

already present. In regression studies of established hypertension, losartan has been shown to regress LVMI in the SHRSP (Kim *et al.*, 1996), while hydralazine alone has no effect in the SHR (Yamori *et al.*, 1979). In a regression study from this laboratory, 5 month old SHRSP treated with H+H or the ACE inhibitor perindopril provided a similar result to the present study with both drugs reducing LV mass compared to controls, but perindopril treatment being significantly more efficacious (Devlin *et al.*, 1995). This suggests that similar mechanisms are governing development and maintenance of cardiac hypertrophy.

In summary, untreated control animals exhibited significantly larger LV wall thickness and mass at 4 and 8 weeks when compared to either irbesartan or H+H treated animals. Treatment with either drug regimen prevents cardiac hypertrophy in the SHRSP, and produces a LV mass/body weight ratio normally observed in WKY rats. Despite preventing the rise in blood pressure to a similar extent, treatment with irbesartan tends to be better at preventing cardiac hypertrophy.

Gene expression of ANP & BNP

ANP gene expression in the left ventricle was significantly higher in untreated controls when compared to either treatment group. As with LV mass, the rank order was control>>>H+H>irbesartan, although the difference between treated groups failed to reach significance. Several groups cite ANP gene expression as a marker for cardiac hypertrophy (Kim *et al.*, 1996; Harada *et al.*, 1998), however, there is only a poor correlation with LV mass in these animals (Figure 4.7, panel a) in contrast with renal hypertensive rats (Kawakami *et al.*, 1996). However, a good positive correlation between ANP gene expression and systolic blood pressure was observed ($r = 0.90$; Figure 4.7, panel b), and this is consistent with ANP release occurring in response to atrial and left ventricular stretch due to pressure overload (Sadoshima *et al.*, 1993). Good correlates between plasma ANP concentration and blood pressure are also observed in renal hypertensive rats (Garcia *et al.*, 1987).

As with LV mass, there was a trend for ANP gene expression to be lower in irbesartan-treated animals compared to H+H rats, despite both treatments lowering blood pressure to an identical degree. This disparity cannot be explained by differences in blood volume status between treated groups. Hydrochlorothiazide will result in fluid depletion due to its diuretic effects, and ANP release is known to be sensitive to blood

volume (Levin *et al.*, 1998). However, reduced volume would result in lower expression of ANP, not more. Another possibility is that ANP gene expression may also depend on AngII, as there was an additional benefit associated with blocking AT₁ receptors. The implication is that AngII may be involved in regulating the hypertrophic response and perhaps the expression of ANP. This is in agreement with *in vitro* systems where AngII can increase ANP gene expression independent of blood pressure (Molkentin *et al.*, 1998).

A slightly different picture was observed for left ventricular BNP gene expression where irbesartan treated animals had a much lower mRNA expression than either control or H+H groups. The rank order was control=H+H>>>irbesartan. Despite the fact that treatment with H+H decreased cardiac hypertrophy and normalised blood pressure, it had absolutely no effect to alter levels of BNP gene expression.

The relationship between BNP and systolic blood pressure in control animals was not significant, and yet there is an excellent positive correlation with LV mass (Figure 4.8). Since expression of BNP mRNA is known to be elevated in the hypertrophied heart of the SHRSP (Ogawa *et al.*, 1991), and H+H treatment prevented LV hypertrophy, we would expect it also to affect BNP expression, and yet it does not. As with ANP gene expression, it would be expected that diuretic treatment would reduce blood volume and thereby reduce stretch, and decrease BNP levels in the heart. The fact that it does not, may suggest an AT₁ dependent mechanism for control of BNP gene expression in the left ventricle of the SHRSP, since H+H had absolutely no effect on BNP gene expression despite lowering blood pressure and LV mass, while irbesartan was highly effective. This is consistent with studies in cultured cardiomyocytes where the BNP promoter is activated in response to the transcription factor NF-AT, a known intracellular mediator of AngII-induced hypertrophy (Molkentin *et al.*, 1998). However, other pathways must also control BNP gene expression as BNP mRNA is up regulated in the left ventricle of mice after aortic banding, despite lacking AT₁ receptors (Harada *et al.*, 1998). Another possible mechanism is that AT₂-receptors are mediating some of the beneficial effects of irbesartan. Blockade of AT₁-receptors results in elevated AngII levels that could have an unopposed effect on the AT₂-receptor. In rats with heart failure, AT₁-antagonists can reduce LVH and myocyte CSA, and this can be prevented by co-administration of an AT₂-receptor antagonist (Liu *et al.*, 1997).

However, an AT₁-, but not an AT₂- antagonist, can prevent the increase in ANP gene expression associated with pressure-overload hypertrophy (Sadoshima *et al.*, 1993). What is evident, is that ANP and BNP gene expression in the left ventricle are differentially regulated, and that both involve factors in addition to hypertrophy or blood pressure.

Another explanation of why irbesartan was more effective would be if H+H treatment had trophic effects on the myocardium, independent of blood pressure lowering. We know from echo data (Table 4.3) that there is no difference in systolic function that could explain differences in LV mass and gene expression. Reflex activation of the sympathetic nervous system could account for these differences and increased exposure to noradrenaline causes myocyte hypertrophy *in vitro* (Bishopric *et al.*, 1987). Heart rate was used as a marker for sympathetic activation, and there was a non-significant trend for elevated heart rate during treatment in the H+H rats (Figure 4.9). Could this be the cause of the higher LV mass and gene expression of natriuretic peptides? Probably not, correlations of LV mass, ANP or BNP with heart rate in H+H animals failed to show any significant relationship. Thus, the modest elevation in heart rate observed during treatment with H+H probably does not explain differences in LV mass and cardiac gene expression. However, treatment with this dose of H+H (4mg/Kg/day of each) has been shown to increase plasma AngII levels in the SHRSP (Devlin *et al.*, 1995), and elevated AngII is capable of inducing hypertrophy in myocytes independent of blood pressure (Sadoshima *et al.*, 1993). The slightly higher LV mass and natriuretic peptide expressions may be due to a direct hypertrophic effect of AngII. In the present study, AngII was not measured directly, but plasma renin and aldosterone concentrations were not significantly elevated in the H+H group (Table 4.4). Also arguing against this is that both drug treatments were equally effective at preventing medial hypertrophy in resistance arteries, which would also be sensitive to an increase in circulating AngII. However, changes in local tissue RAS can not be excluded. The LV is known to have a local tissue RAS that is up-regulated in hypertensive animals, and myocardial AngII levels correlate with extent of hypertrophy (Yamazaki & Yazaki, 1997; Johnston, 1994).

Regardless of whether the differences observed between irbesartan and H+H are due to activation of the RAS by H+H, both drugs lowered blood pressure to comparable levels.

Thus, the difference in LV mass and gene expressions between treatments are consistent with AngII having a role in regulating LV mass independent of its pressor effects. This is in agreement with other pharmacological studies that have shown an additional benefit on LV hypertrophy of blocking the RAS, greater than can be expected due to lowering blood pressure alone (Baker *et al.*, 1990; Kim *et al.*, 1996). This also appears to be true in human essential hypertension, where in a recent meta-analysis, ACE inhibition was found to be more effective at regressing LV hypertrophy than Ca²⁺ channel blockers, diuretics or β -blockers (Schneider *et al.*, 1996).

Vascular hypertrophy

The LSCM technique used for studying resistance artery morphology and cell number was developed in this laboratory, and was fully validated in a study by Arribas *et al.* (1997). In that study, the effect of fixation on measured parameters was quantified by examining vessels before and after fixation with 10% formal-saline. Fixation resulted in a 13% reduction in lumen diameter, but had absolutely no effect on wall thickness measurements in any of the component parts, adventitia, media or intima. It has the advantage over histological methods of providing objective measurements in intact arteries.

The confocal microscopy results clearly indicate that the vessel wall of mesenteric resistance arteries is thicker in untreated hypertensive animals (Table 4.5). This difference resides within the medial layer, which has approximately 28% greater thickness than either treatment group. As there are no differences in cell number, this suggests a role for hypertrophy rather than hyperplasia. Either there is more connective tissue in the media of these animals, or the smooth muscle cells are larger. Confocal microscopy does not answer this question as propidium iodide is a nuclear dye, and so differences in cell size were not apparent.

Having one less animal in the irbesartan group is unlikely to have affected the results other than to slightly reduce the power of the study to detect significant differences. This is probably the reason that SMC density achieved significance in the H+H, but not in the irbesartan group. The missing animal was a female, which may have biased the results in favour of a male phenotype. However, sex differences were not observed in

any of the groups, and there appeared to be no relationship between sex and wall thickness, external or internal dimensions (data not shown). This is further supported by the lack of correlation between vessel thickness and systolic blood pressure, which does exhibit sex differences (Figure 4.12).

Both drug regimes appeared to be equally effective in preventing vascular hypertrophy in the SHRSP. This suggests the balance of variables mediating LV mass and medial hypertrophy of resistance arteries are not the same, as there was no additional benefit observed with blockade of AT₁ receptors. However, the greater wall/lumen ratio observed in H+H animals when compared to irbesartan allows for a second interpretation. It could be argued that the smaller lumen diameter indicates that hypertrophy of the vessel wall has encroached into the luminal space i.e. inward remodelling. This seems unlikely as the wall dimensions are not thickened when compared to irbesartan animals, and there is no correlation between increased wall thickness and a smaller lumen diameter in this group. It is the author's experience that lumen diameter is highly variable even between two branches of the same artery within the same animal. It is therefore likely that the small difference in lumen diameters is due to natural variation and not differences in remodelling. However, since this study represents a snapshot of the artery at 8 weeks, with no baseline data to determine the type of remodelling that has occurred, such differences cannot be ruled out.

Differences in morphology between 3rd order mesenteric resistance arteries in WKY and SHRSP have previously been quantified in this laboratory using identical methodology (Arribas *et al.*, 1997). The only difference was in the age of the animals, which were 8-10 months old in the Arribas study, and 14-15 weeks old in the present study. Compared to WKY, SHRSP animals had a decreased lumen diameter, increased wall thickness due to hypertrophy in the medial layer, with no increase in cell number in the media i.e. inward hypertrophic remodelling. This is in agreement with untreated SHRSP in the present study, with the treated animals being similar to the WKY results. However, several other differences were noted such as an increase in adventitial cell numbers (almost double) in the SHRSP, and a large decrease in the number of endothelial cells in the intima. These factors, along with lumen diameter, were not altered by either treatment in the present study. If they are also present in the 14 week old SHRSP, then the inability of antihypertensive treatment to modify lumen diameter

or numbers of adventitial and endothelial cells may represent treatment failure. It is possible that such subtle changes may develop regardless of treatment, or are already in place in the young SHRSP before 6 weeks of age.

If a reduction in endothelial cell number remained with antihypertensive treatment it is easy to speculate how this might significantly affect function. The endothelial layer is responsible for flow-mediated vasodilatation via the release of nitric oxide (Joannides *et al.*, 1995), and by responding to circulating vasoactive agents, controls lumen diameter. Indeed, fewer endothelial cells could explain why treatment failed to improve lumen diameter in this study. The endothelium may also have a direct role in hypertrophic growth as nitric oxide has anti-proliferative effects in vascular smooth muscle cells (Garg *et al.*, 1989) and is open to modulation by circulating trophic factors. An increase in adventitial cell number may also have an important role in remodelling or vascular function. Little is known about the influence of adventitia on function, but in rat aorta stimulated with lipopolysaccharide, vessels with intact adventitia produced 3.5 times more nitrite and nitrate than those with adventitia removed, with a resultant hyporeactivity to noradrenaline (Kleschyov *et al.*, 1998). This suggests the ability of the adventitia to produce bioactive nitric oxide at least in certain pathological conditions. Further characterisation of these changes in young and treated animals deserves further study.

The pattern of medial hypertrophy observed in the study of Arribas *et al.* (1997) is common to other models of hypertension. Third order mesenteric resistance arteries from renal hypertensive WKY (1 kidney, 1 clip) have increased smooth muscle cell volume but not cell number (Korsgaard & Mulvany, 1988), and increased medial hypertrophy is also observed in subcutaneous resistance arteries from patients with essential hypertension (Falloon & Heagerty, 1994). In contrast several studies in the SHR (reviewed in Heagerty *et al.*, 1993) have indicated a relative increase in smooth muscle cell number, with a minor role for hypertrophy. The reason for this disparity is not obvious, but may include methodological reasons, as cell number is seldom counted directly as in the present study and that of Arribas *et al.* (1997).

Further up the vascular tree, studies in conduit arteries have also emphasised the importance of hypertrophy over hyperplasia. Owens & Schwartz (1982) showed that the thoracic aorta of 5-month-old SHR had increases in smooth muscle cell volume

density, medial cross-sectional area and nuclear volume density compared to age-matched WKY. The percentage of polyploid cells was greater than WKY from 3 months onwards and increased with age and blood pressure. The number of DNA copies (ploidy) was directly related to the mass of the cell. The authors concluded that the increase in aortic smooth muscle cell mass in the SHR could be fully accounted for by cellular hypertrophy without hyperplasia.

As with the relationship for blood pressure versus LV mass, smooth muscle cell hypertrophy is probably controlled by other trophic factors such as AngII. For example, in a further study by Owens using the same technique, treatment with captopril decreased polyploidy more than would be expected for blood pressure lowering effect alone, while propranolol had no effect on polyploidy despite lowering blood pressure (Owens, 1987). Similarly, in SHRSP with established hypertension, perindopril treatment reduced smooth muscle cell polyploidy in the aorta to WKY levels. An equihypotensive dose of H+H was ineffective in this regard (Devlin *et al.*, 1995). Likewise, resistance artery hypertrophy can be regressed by ACE inhibitors, but not hydralazine (Stryker-Boudier *et al.*, 1990), and infusion of AngII results in hypertrophy of mesenteric resistance arteries (Daemen *et al.*, 1995). In addition, a direct trophic effect of AngII has been demonstrated in smooth muscle cell cultures (Owens, 1989). Further, there is evidence for a local RAS in conduit and resistance arteries, which can alter local and downstream function, and presumably therefore structure (Henrion *et al.*, 1997). Given the strong evidence for AngII involvement in vascular hypertrophy, it is an important finding of the present study that irbesartan and H+H were equally effective in preventing medial hypertrophy. This suggests that in the mesenteric resistance arteries of the SHRSP, AngII does not play an important role in the hypertrophy of the vascular wall.

4.5 Conclusions

This study examined the ability of irbesartan (60mg/Kg/day) and hydrochlorothiazide + hydralazine (4mg/Kg/day of each) compared to a control group (all delivered in mousse) in preventing cardiac and vascular remodelling in the SHRSP. The main findings are:

- A suspension of drug in infant mousse is a convenient and effective method of delivering poorly soluble drugs by the oral route in the rat.
- By 14-15 weeks of age the SHRSP develops concentric LVH that is well compensated with no change in systolic function.
- There is no correlation between systolic blood pressure and LV mass even when expressed as unit change of these values.
- Irbesartan is as effective as H+H at preventing the elevation of blood pressure observed in the young SHRSP.
- Irbesartan prevents the subsequent increase in LV mass and associated left ventricular gene expression of ANP and BNP with greater efficacy than H+H despite identical blood pressure lowering effect. This indicates an additional benefit of blocking AT₁ receptors, which may represent a role for angiotensin II in the hypertrophic response.
- ANP and BNP mRNA expression in the left ventricle are differentially regulated. ANP correlates with blood pressure, while BNP correlates with LV mass. In addition, H+H treatment had no effect on BNP gene expression suggesting a role for the AT₁ receptor pathway for mediating BNP mRNA.
- Irbesartan and H+H were equally effective in preventing medial hypertrophy in 3rd order mesenteric resistance arteries, with no change in smooth muscle cell number or in adventitial or intimal cells. This argues against a local trophic effect of AngII in mediating hypertrophy in these vessels.

5. Cardiac and vascular remodelling after coronary artery ligation in the rat.

5.1 Introduction

The alterations that occur in the heart and blood vessels after myocardial infarction (MI) determine the onset and severity of heart failure, and therefore outcome, in man and animal models. To study this process, rat models have commonly been used where the left descending coronary artery is permanently occluded. The haemodynamic and neurohormonal consequences of this have been discussed fully in Chapter one. Such a model of coronary artery ligation (CAL) is described in this chapter for the WKY rat, and comparisons are made with sham-operated controls.

Confirmation of heart failure

Due to the variability in infarct size in CAL rats, it is necessary to attempt to quantify LV dysfunction and recognise congestive heart failure on an individual animal basis. Even in rats with large infarcts, clinical signs such as peripheral oedema, respiratory distress or poor grooming are seldom apparent (Pfeffer *et al.*, 1979). Although it has been claimed that a conscious respiratory rate greater than 100 breaths per minute is indicative of "clinical" heart failure in the rat (Latini *et al.*, 1998), in practice, it is difficult to make these observations without the presence of an observer influencing respiration. Objective measurements are therefore essential.

A number of studies have indicated that infarct size is in itself a good indicator of myocardial function (Pfeffer *et al.*, 1979; Pfeffer *et al.*, 1984). However, histological measurements may only be made post-mortem, and do not provide direct evidence of dysfunction. Many groups have made use of LV catheterisation to gain detailed information on haemodynamics and function. There is a typical haemodynamic profile after CAL in the rat which mirrors that observed in human heart failure (see Figure 1.5, Chapter 1). However, this is an invasive procedure and is often a terminal end-point. Echocardiography is being increasingly used to study cardiac function in rodent models of heart failure. The obvious advantage is its non-invasive nature, which in theory allows serial measurements, but which has seldom been employed in practice.

Echocardiography after myocardial infarction

The changes that occur in LV geometry post-myocardial infarction such as ventricular dilatation pose a problem for echo methods that assume a uniform geometric shape, such as the cubed formula for LV mass, or even 2-D estimation of ejection fraction. Such assumptions of LV shape appear to be valid in healthy animals and even hypertensive animals, but the asymmetry of infarcted ventricles can lead to serious errors. The only simple way to describe LV structure and function post-MI in the rat is via one-dimensional regional analysis. To say anything about systolic function as a whole it would be necessary to either:

1. Use Simpson's rule. This requires the ability to obtain reliable long-axis views and short-axis views at multiple levels. In rats after MI, Litwin *et al.* (1994) concluded that the long-axis view was unreliable and inconsistent. Therefore they could not make use of Simpson's rule for calculating volume in asymmetric chambers.
2. Use free-hand 3-D echo facilities. However, this technique does not yet have the spatial resolution for rat work.
3. Use echo doppler for cardiac output and ejection fraction estimations. Again, technically difficult in the rat, with imaging of the aortic root often unobtainable (Pawlush *et al.*, 1993).

In this study, serial echocardiography was used to follow the temporal evolution of LV structural and functional changes. However, echocardiographic results for this chapter will only discuss data that does not require assumptions concerning LV geometry such as wall thickness, and from 2-D images, end-diastolic cross-sectional area and ejection fraction.

Further characterisation of the extent of insult will be obtained by measuring relative abundance of ANP & BNP mRNA in the LV of sham and ligated rats. While increased ANP mRNA expression has been well characterised in this model (Passier *et al.*, 1996), there is a relative paucity of data on the role of BNP in post-infarction rats, despite the known importance of plasma BNP as a prognostic marker in human heart failure (Mukoyama *et al.*, 1991).

The aims of this study were as follows:

- 1) To introduce the rat CAL model into our laboratories for the first time.
- 2) To demonstrate the utility of serial echocardiography to chart changes in LV structure and function over time in heart failure rats.
- 3) To determine the changes in ANP & BNP gene expression in the surviving myocardium.
- 4) To confirm whether endothelial dysfunction is present in the thoracic aorta of rats after coronary artery ligation.
- 5) To determine if there are alterations in small artery structure at a cellular level, using laser scanning confocal microscopy (LSCM) for the first time in this model.

5.2 Methods

Protocol

Male Wistar-Kyoto (WKY) rats weighing 300-400g were used from the colony of Professor Dominiczak at the University of Glasgow. Prior to surgery, a baseline echocardiogram was performed to measure ejection fraction, LV cavity cross-sectional area (CSA) and posterior wall thickness (described in Chapter 3). They were then subjected to thoracotomy and either ligation of the left anterior descending coronary artery or sham operation (described below). Further echocardiograms were taken at 2-, 4-, 6- and 8-weeks post-surgery.

At 8-weeks after surgery, animals were euthanased by overdose of halothane anaesthetic and the tissue utilised as follows:

1. Blood was removed by cardiac puncture and plasma extracted. Plasma concentrations of renin, ANP and BNP were quantified (see Methods chapter).
2. Heart chambers were weighed and blotted, also lung, liver and kidney were dissected free of connective tissue, blotted and weighed (see Methods chapter).
3. A portion of the non-infarcted posterior left ventricular wall was removed and snap frozen in liquid nitrogen. This was used for subsequent Northern blot analysis as described in Methods chapter.
4. The remaining LV was placed in formaldehyde for histological measurement of infarct size (described below).

5. The descending thoracic aorta was placed in physiological salt solution (PSS) at 4°C for subsequent organ bath studies of endothelial function (described below).
6. The mesenteric arcade was dissected out and stored in PSS at 4°C, from which 3rd order mesenteric resistance arteries were later dissected. Measurement of vessel structure was performed by laser scanning confocal microscopy (LSCM) as described in Methods chapter.

Coronary artery ligation in the rat

Twenty-four hours before surgery, animals were given an intramuscular (IM) injection of 0.2ml anhydrous ampicillin 100mg/ml (Amfipen® LA, Intervet UK Ltd.) as prophylaxis against infection. The next day anaesthesia was induced by an intraperitoneal (IP) injection Hypnorm (fentanyl + fluanisone) and Hypnovel (midazolam). The left side of the chest was shaved and the animal intubated. Mechanical ventilation was provided at a rate of 72 breaths per minute and a stroke volume of 2.5ml, using a Harvard Apparatus rodent ventilator (model 683). Halothane 0.25-2% in O₂ was used to maintain adequate anaesthesia. Positive end expiratory pressure was applied by exhausting the exhaled gases into 0.5cm of water.

A thoracotomy was performed between the 4th and 5th intercostal space, the left lung collapsed, and the pericardium opened. The heart was then exteriorised and an apical tie placed to aid manipulation. A 4/0 Ethibond Excel (Ethicon W6935) suture was placed around the left anterior descending coronary artery a few millimetres from its origin, and tied tight. The infarcted area was immediately apparent due to blanching of the affected myocardium. The target infarct size was around 30-40% of the left ventricular free wall, and in animals with smaller infarcts, further sutures were placed closer to the artery origin until this figure was achieved. In sham operated animals neither apical tie nor ligation suture were placed in the heart.

The heart was replaced into the pericardium and the chest wall closed using an interrupted chromic 3/0 suture (Ethicon W437). Hyperinflation of the lungs during closure ensured expulsion of air, and prevention of a pneumothorax. The muscle layer was closed with an interrupted Ethibond 4/0 suture, and the skin using a continuous Dexon II 2/0 (Sherwood Davis & Geek 6160-87B) subcutaneous suture.

To reverse the effects of the fentanyl and provide adequate post-operative pain relief, 0.2ml buprenorphine (Vetergesic) was administered IM. A further pain relieving dose

was given the next day after an assessment of pain in the individual. In some of the animals this dose was not necessary. Further post-operative care included 3-5ml subcutaneous normal saline, depending on extent of blood loss, supplemental oxygen, and a heating blanket until such times as the righting reflex had been regained.

A more detailed description of the surgical technique is provided in appendix II, along with suppliers for all drugs.

Histological measurement of infarct size

The methodology for estimating infarct size is identical to that used by the groups of Jos Smits and Jo de Mey in Maastricht (Stassen *et al.*, 1997, with further modifications from Dr. Gregorio Fazzi in a personal communication).

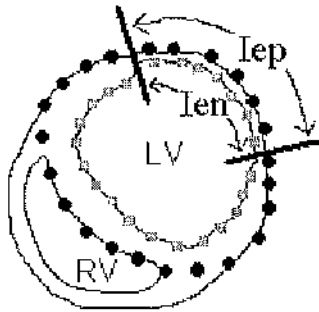
Preparation

The excised heart was immediately placed in neutral buffered formalin (NBF) and stored at room temperature until processed. The first stage was a 70% ethanol wash for at least an hour. A set of razor blades 2mm apart was used to cut sections of the heart. The first blade was set level with the apex and four slices were made. These slices were stored in 70% alcohol until processed further. The slices are dehydrated by alcohol and xylene followed by embedding in paraffin wax overnight. Only the third slice was used to determine infarct size. Experience in Maastricht has shown that it is the most representative of the whole myocardium, and yields comparable results to averaging many slices at varying levels of the heart.

The paraffin wax embedded slice was cooled and 4 μ m sections cut using a microtome and placed on glass slides. The slides were then washed in xylene and ethanol to remove the paraffin wax, as detailed in the wax removing protocol in appendix I. Staining was with Azan dyes according to the staining protocol, also detailed in appendix I. Using this protocol, the infarcted area stained bright blue, and the viable myocardium as red.

Measurement of infarct size

Only one section is required for the measurement of infarct size which calculates the percentage involvement of the left ventricular circumference as follows:-



- Iep** (length of infarcted epicardial circumference)
- Ien** (length of infarcted endocardial circumference)
- **Tep** (total epicardial circumference)
- ▣ **Ten** (total endocardial circumference)

$$\left[\frac{Iep}{Tep} + \frac{Ien}{Ten} \right] / 2 * 100\% = \text{Infarct size}$$

Organ bath studies

Aortas were cleaned of connective tissue under a dissecting microscope and cut into 4x4mm ring segments. These were suspended in 10ml organ baths by fine wire hoops, taking care not to damage the endothelium. The upper wire was attached by thread to a Grass FTO3c transducer, interfaced to a Linseis L2006 chart recorder for display of isometric tension. The lower wire was connected to a glass tissue holder. The mounted rings were immersed in PPS and continuously bubbled with 95% O₂ : 5% CO₂ at 37°C. They were placed under an initial tension of 3g and re-tensioned to that level after 20 minutes. A minimum of 40 minutes was then given for equilibration before starting the experimental protocol. Indomethacin (1μM) was present throughout to block endothelium-derived prostanoids. After equilibration, vessels were exposed to a sighting dose of noradrenaline (NA) 1μM, followed by acetylcholine (ACh) 1μM to test for the presence of a functioning endothelium, then washed for 20 minutes. Concentration response curves for NA and ACh were constructed in the range 10⁻¹⁰ to 10⁻⁵M in half log increments, with 30 minutes wash-out between curves. Vessels were then incubated for 30 minutes with L-NAME 100μM, before constructing new concentration response curves for NA and ACh. At least one bath in each experiment was used as a time control, whereby L-NAME was not added. After a final 30-minute wash, a concentration response curve was constructed to sodium nitroprusside (SNP) 10⁻¹⁰ to 10⁻⁵M. At the end of the experiment, aortic rings were blotted and weighed. Contractile responses were expressed as generated tension per milligram tissue weight. Relaxant responses were expressed as percentage relaxation of NA contractile response.

5.3 Results

Survival

A total of 26 WKY males were subjected to either sham or CAL surgery, of these, 19 remained alive for the 8-week duration of the study giving a survival rate of 73%. Unusually, survival was poorer in the sham-operated animals at 69% (9/13) compared to 77% in ligated (10/13). No clear explanation was found for the death of the sham-operated animals, all of which died suddenly a few days after the procedure. As a precaution antibiotic cover was introduced for all subsequent procedures after the first two fatalities, however, there was no evidence of infection when the pathology results were returned from a full post-mortem. The three fatalities in the ligated group all occurred between 1 and 14 days after surgery, with the most likely cause being acute congestive heart failure. All these animals exhibited either laboured breathing immediately prior to death, or had very large infarcts coupled with severe congestion of the lungs and liver on post-mortem. There were no fatalities during surgery in either group.

Infarct Size

Azan staining was performed with the help of Dr. Ian Montgomery, for visualisation of the infarct region. Representative heart slices are shown in Figure 5.1. Panel A shows a cross-section of the left ventricle in a sham-operated animal at the level of the papillary muscles, which are clearly visible as round discs “floating” in the cavity space. There are a few artifactual tears in the myocardium, but otherwise the heart tissue is healthy, staining bright pink to indicate viable myocardium. The right ventricle was removed for weighing at post-mortem and so is no longer visible. However, it is possible to see where it was attached at the top left aspect of the image.

Panel B shows the same view in a heart 8 weeks after coronary artery ligation. The infarcted area is clearly visible as an extremely thin blue staining region. This is the connective tissue laid down during scar formation, which still contains a few pockets of viable myocytes staining pink. This is typical of the type of infarct observed in these animals, all of which were full-thickness affecting the anterior aspect. The cross-sectional area of the LV cavity is grossly oversized in this example indicating

significant dilatation. This infarct is large affecting approximately 48% of the left ventricular free wall.

It was originally planned to estimate infarct size from these histological sections using computerised planimetry, however, in many of the animals sections had been cut too high in the heart for this purpose. This has been remedied for future experiments when infarct size will be available. For this study, emphasis has been placed on changes in function using echocardiography as a measure of infarct severity.

Organ weights

There was no significant difference in body weight between groups before entering the study or on completion 8 weeks after surgery (Table 5.1). Whole heart weight and heart weight minus the right ventricle were both significantly elevated in the ligated group indicating a degree of compensatory hypertrophy. Right ventricular weight was also significantly increased. The spread of data is indicated in Figure 5.2.

Table 5.1 Body and organ weights 8 weeks after sham or CAL surgery.

	Sham n=9	Ligated n=10	P value
Body weight at baseline (g)	361 ± 59	370 ± 54	0.71
Body weight at 8 weeks (g)	409 ± 47	407 ± 29	0.87
Heart weight (g/Kg)	3.37 ± 0.16	3.73 ± 0.28	0.007 **
Right ventricle (g/Kg)	0.56 ± 0.10	0.67 ± 0.06	0.012 *
Heart – RV (g/Kg)	2.81 ± 0.14	3.06 ± 0.26	0.03 *
Long-axis (mm)	14.6 ± 0.9	14.7 ± 1.0	0.96
Lung (g/Kg)	3.99 ± 0.62	4.61 ± 1.04	0.14
Liver (g/Kg)	33.27 ± 2.82	35.31 ± 2.83	0.14
Kidney (g/Kg)	5.48 ± 0.27	5.30 ± 0.48	0.35

All data are mean ± SD. * and ** denote P<0.05 and P<0.01 respectively for sham versus ligated by unpaired Student's t test.

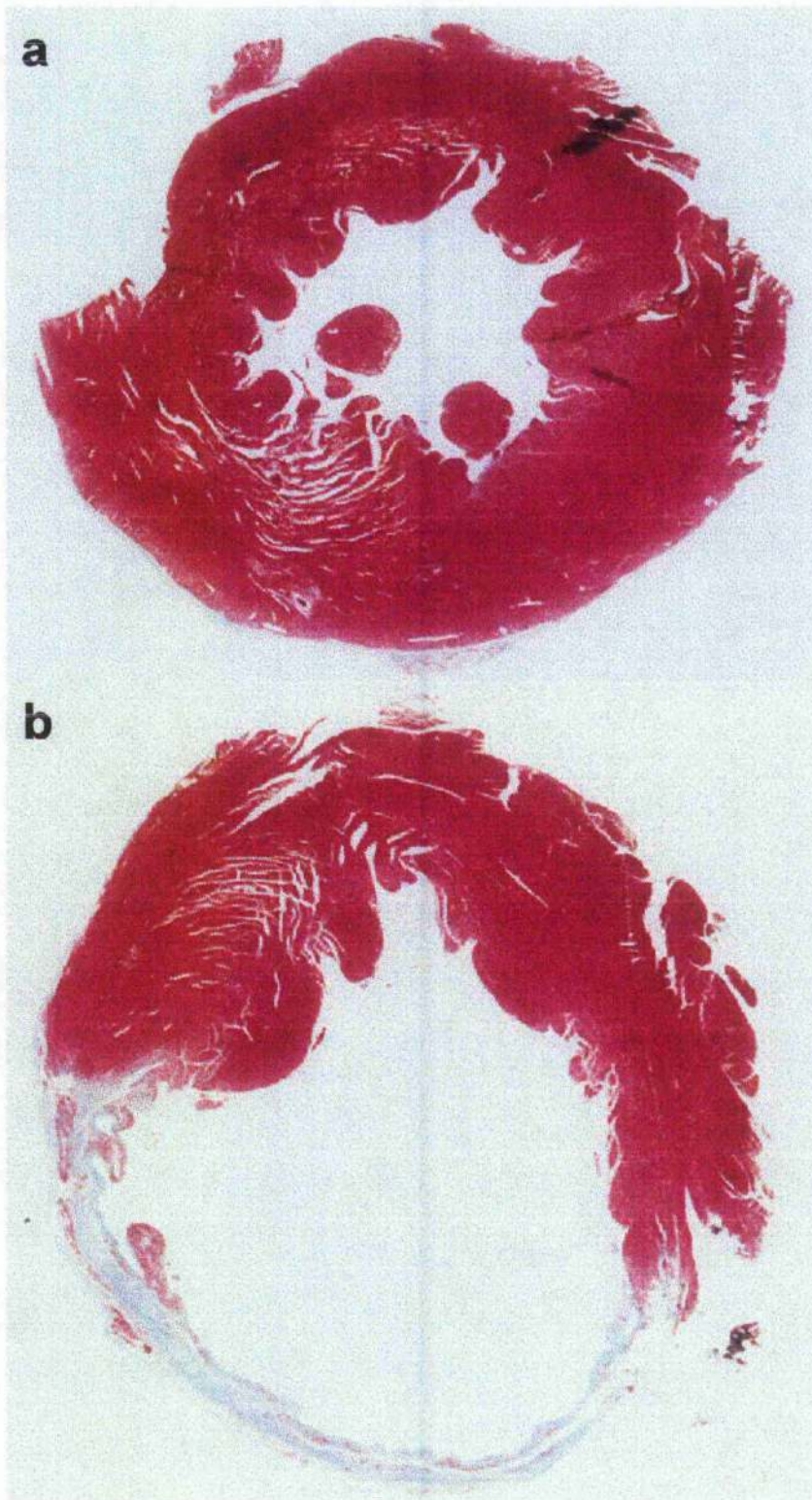


Figure 5.1 Examples of infarct size histology using the Azan dye technique. Panel A shows the heart of a sham-operated animal, panel B the heart from an animal 8 weeks after coronary artery ligation. In both cases the heart has been cut in cross-section through the centre of the left ventricle. The right ventricle is not visible as this was removed for weighing at post-mortem. Healthy myocardium is dyed pink, blue staining represents connective tissue.

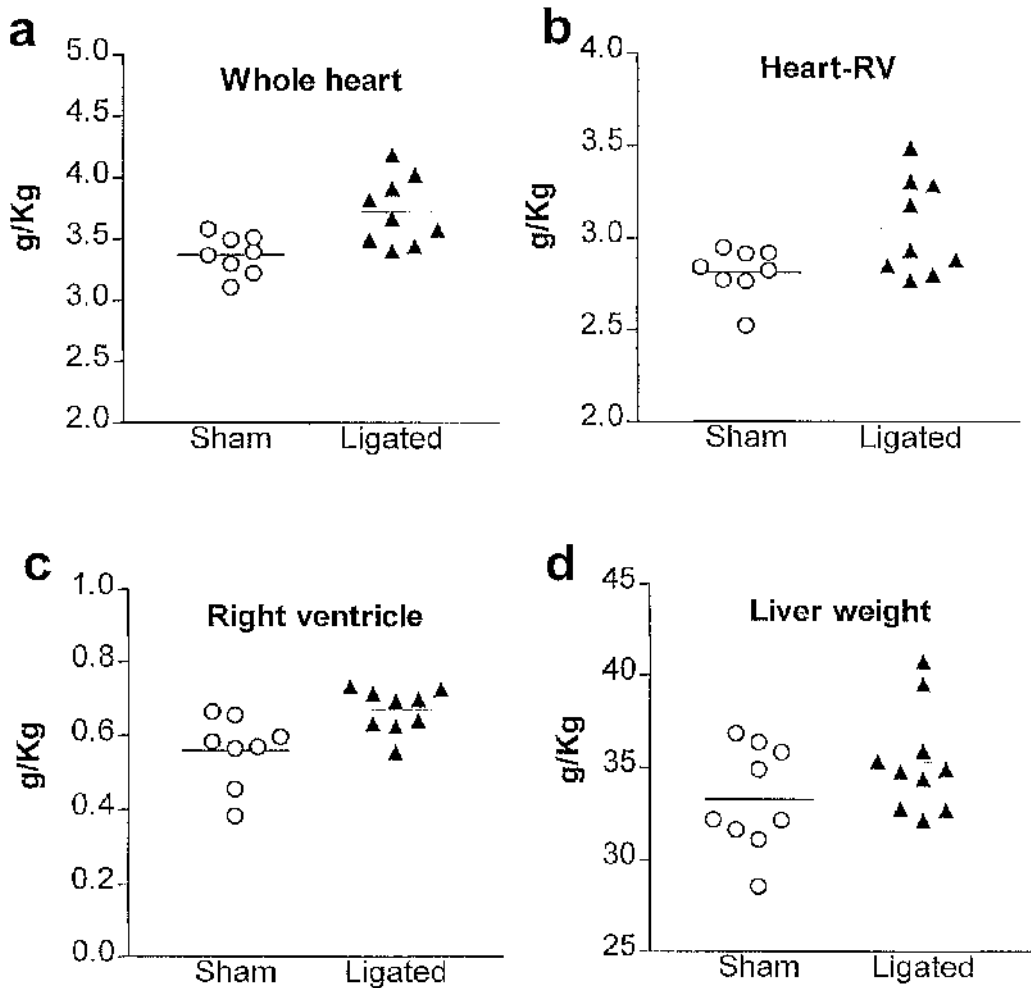


Figure 5.2 Organ weights normalised to body weight in sham and ligated animals 8-weeks after surgery. Panel A is whole heart weight, panel B heart weight minus RV, panel C right ventricular weight, panel D liver weight. Horizontal bars represent mean values.

Lung and liver weights tended to be heavier in ligated animals, although this failed to reach significance. More detailed analysis in Figure 5.2 (panel D) indicates that for liver weights most animals remained normal, while two animals in the ligated group had a much higher liver/body weight ratio. It is interesting to note that these two also had the lowest ejection fraction, and their livers had a mottled, nutmeg appearance at post-mortem. This suggests that congestion was present in these animals.

Echocardiography

Ejection fraction was measured by echocardiography at baseline and at 2-week intervals for the duration of the study. The mean values are shown in Figure 5.3. Immediately prior to surgery, ejection fraction in sham and ligated groups was almost identical, 77.8 ± 2.4 and $76.1 \pm 1.4\%$ respectively. By 8-weeks after surgery ejection fraction was 76.5 ± 5.0 in shams and 45.9 ± 6.6 in ligated rats. At all time points following surgery, animals with a coronary artery ligation exhibited a significantly lower ejection fraction ($P < 0.0001$) commensurate with impaired left ventricular function.

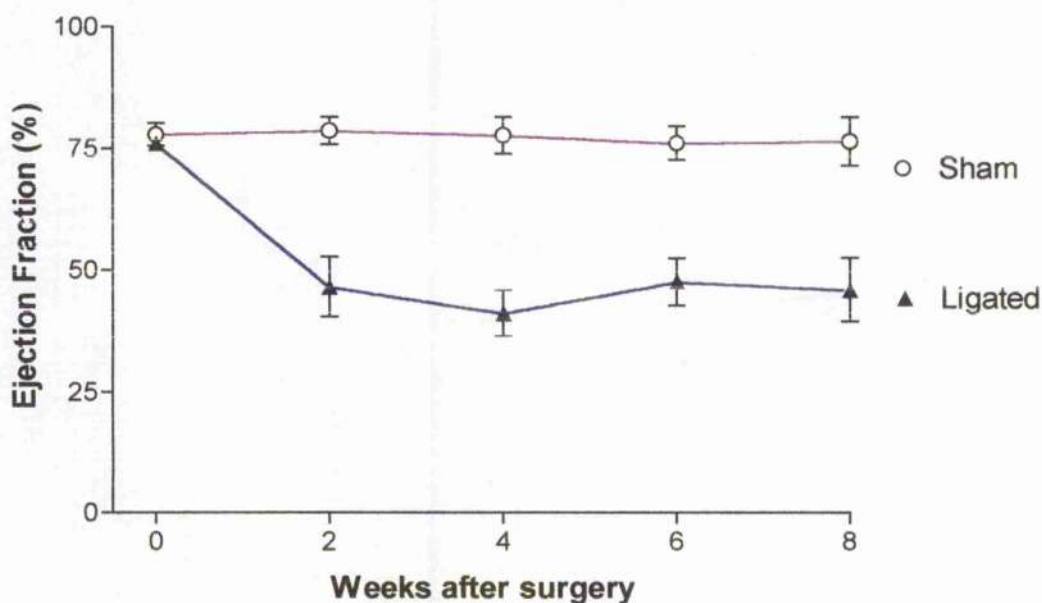


Figure 5.3 Ejection fraction measured by echocardiography in rats before and after sham or CAL surgery. All data points are mean \pm sem. There was no significant difference between groups at baseline, but at all subsequent time points difference in mean are highly significant ($P < 0.0001$, unpaired Student's *t* test, significance level $P < 0.01$ to correct for multiple comparisons).

Two-dimensional images were used to calculate cross-sectional area of the left ventricular cavity during diastole. Before surgery, there was no significant difference between groups. After CAL there was a progressive enlargement of the LV cross-

sectional area representing increasing ventricular dilatation. This was significantly larger than sham-operated animals at 4, 6 and 8 weeks post surgery (Figure 5.4). Representative echocardiograms are shown in Figure 5.

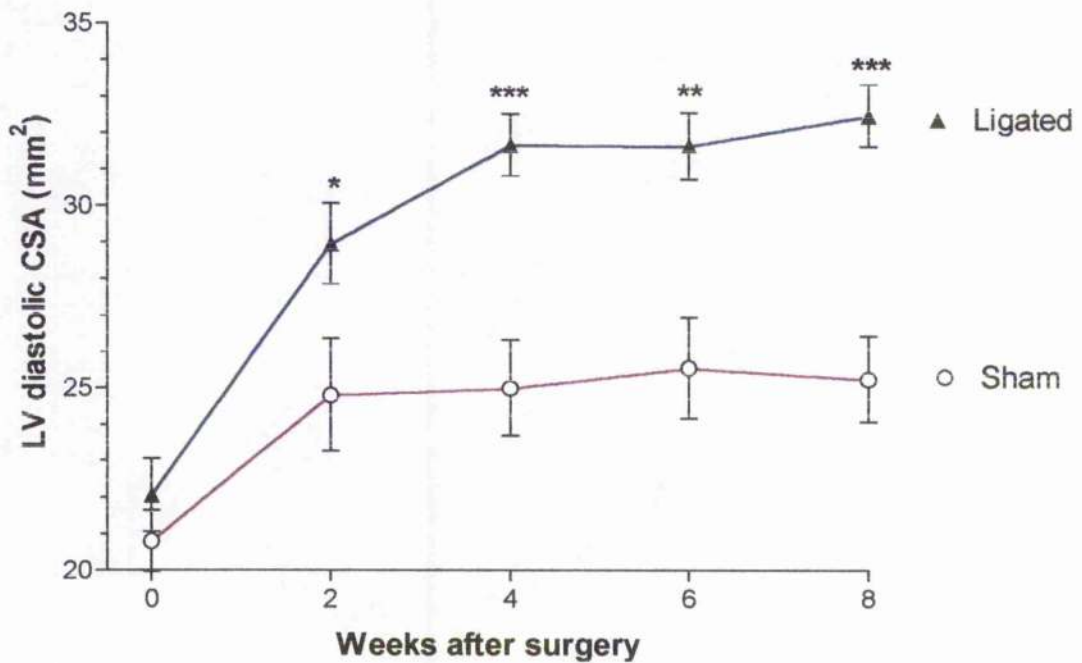


Figure 5.4 Cross-sectional area (CSA) of the left ventricular cavity measured at diastole by echocardiography in rats before and after sham or CAL surgery. Data points are mean \pm sem. *, ** and *** denotes $P < 0.05$, $P < 0.01$ and $P < 0.001$ respectively for sham versus ligated animals by unpaired Student's t test. Significance level is $P < 0.01$ to correct for multiple comparisons.

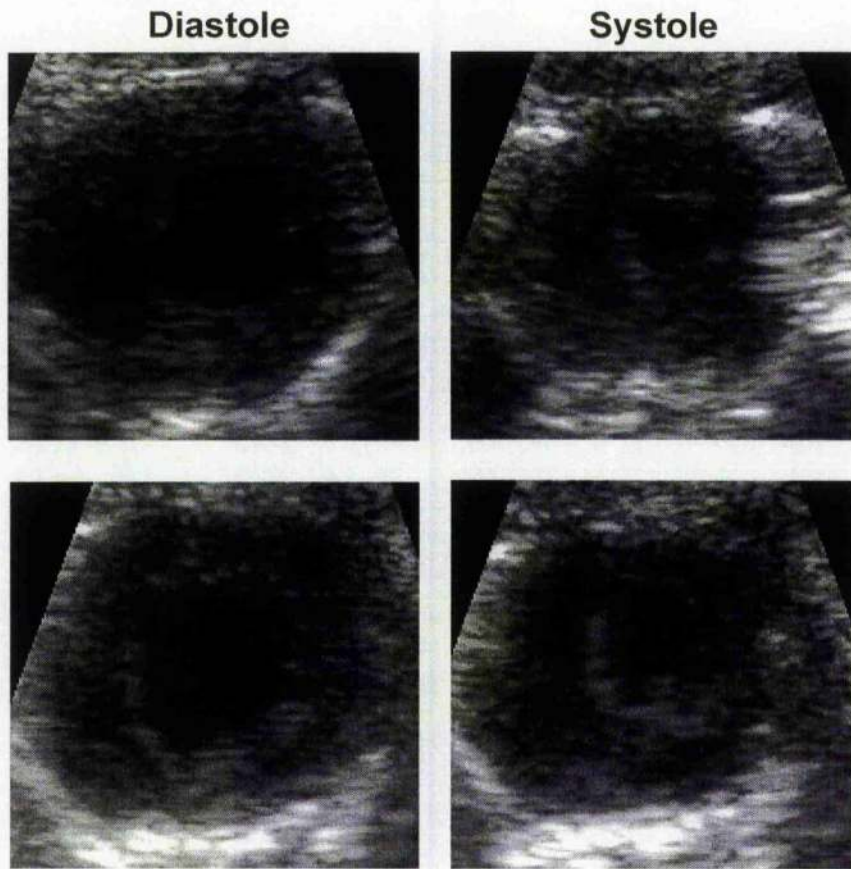


Figure 5.5 Representative 2-D echocardiograms from the parasternal short-axis view. Top panels are from a WKY rat before surgery at end diastole and systole; lower panels are from the same rat six weeks after coronary artery ligation. Note the enlarged cavity area at diastole and anterior infarct resulting in systolic dysfunction.

M-mode images were used to measure non-infarcted posterior wall thickness. CAL resulted in a progressive compensatory hypertrophy of the LV wall, which was significant from week 4 onwards and continued to rise in a linear fashion (Figure 5.6). Representative echocardiograms are shown in Figure 5.7.

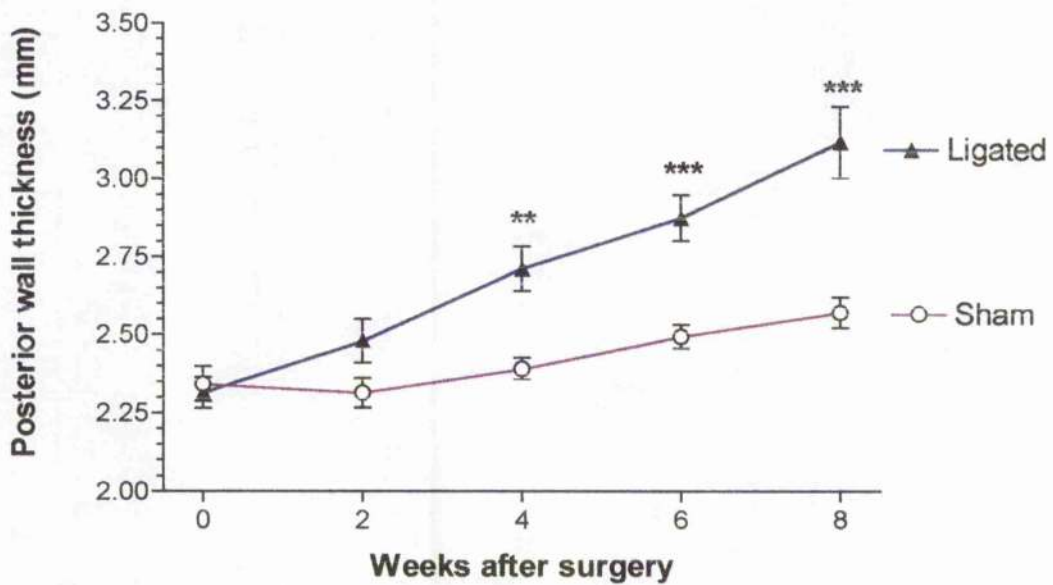


Figure 5.6 Thickness of the non-infarcted posterior LV wall measured at diastole by echocardiography in rats before and after sham or CAL surgery. Data points are mean \pm sem. ** and *** denote $P < 0.01$ and $P < 0.001$ respectively for sham versus ligated animals by unpaired Student's t test. Significance level is $P < 0.01$ to correct for multiple comparisons

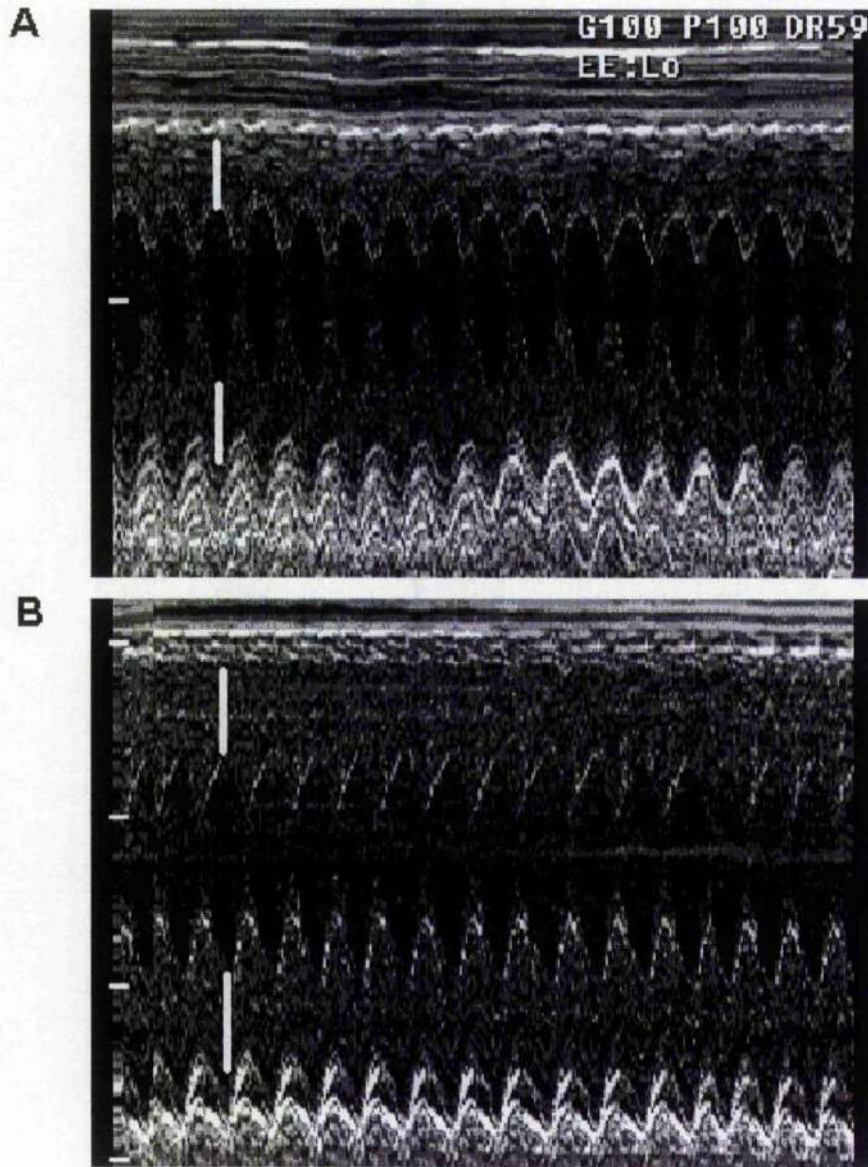


Figure 5.7 Sample M-mode echocardiograms of the left ventricle in a WKY rat before (A) and eight weeks after (B) coronary artery ligation in the same animal. The anterior wall is uppermost in these images, with the posterior wall below. Wall measurements are superimposed in white. Note increased wall thickness and end-diastolic dimension.

Natriuretic peptides

Qualitative measurement of ANP and BNP mRNA expression were obtained in the atria and surviving left ventricle of rats eight weeks after surgery. ANP gene expression was high in the atria of sham rats and was unaltered by coronary artery ligation (Figure 5.8). Atrial levels of BNP mRNA were also unchanged (Figure 5.9). However, levels of ANP mRNA in the left ventricle were more than doubled in ligated animals, and this was statistically significant ($P < 0.05$, Figure 5.10). BNP gene expression in the left ventricle tended to increase after ligation, but despite being an average 34% higher, this failed to reach significance (Figure 5.11). The densitometry analysis of mRNA expression is summarised in Table 5.2.

Table 5.2 Densitometric analysis of ANP & BNP mRNA expression in the heart.

	Atria		Left ventricle	
	Sham (n=5)	Ligated (n=7)	Sham (n=6)	Ligated (n=8)
ANP	2.45 ± 0.39	2.61 ± 0.30	1.14 ± 0.27	2.54 ± 0.50 *
BNP	1.43 ± 0.10	1.64 ± 0.25	0.65 ± 0.06	0.87 ± 0.10

Values are mean ± standard error of the mean for arbitrary densitometry units. * denotes $P < 0.05$ by Student's *t*-test.

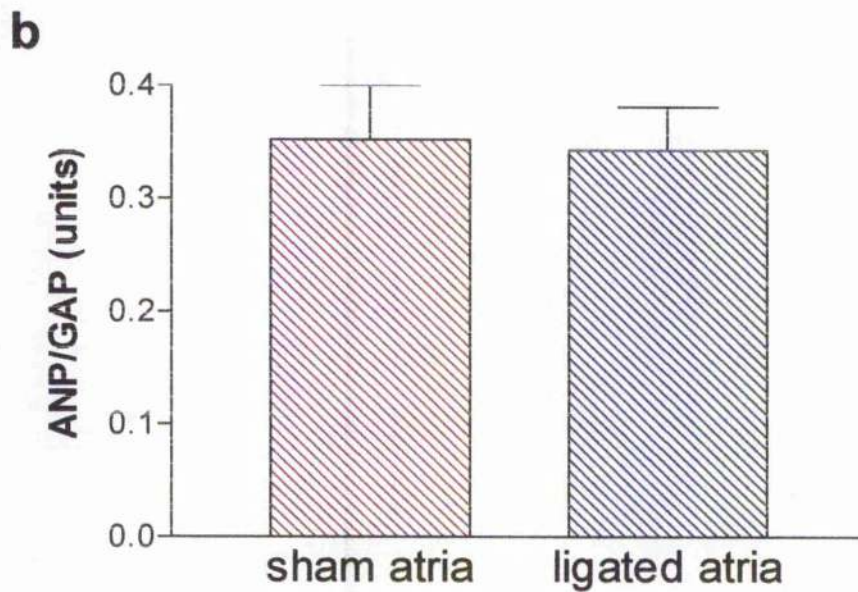
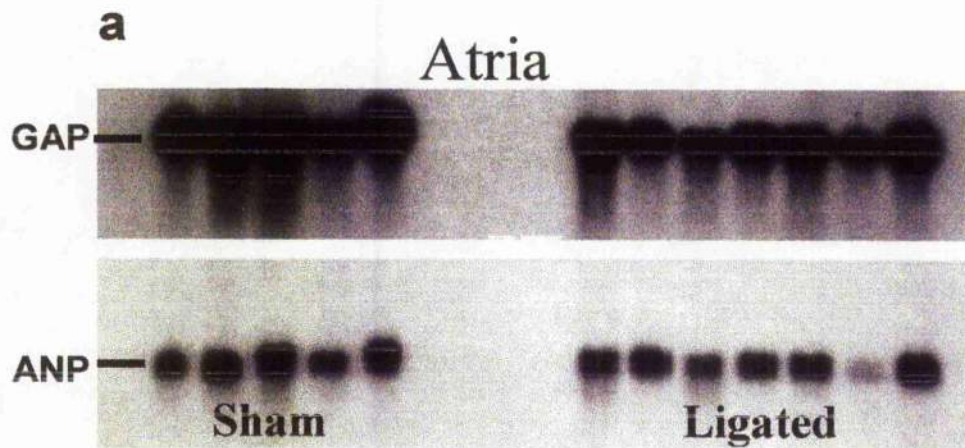


Figure 5.8 Northern blot analysis of ANP gene expression in the atria of sham (n=5) and ligated (n=7) WKY rats. There was no significant difference in mRNA expression.

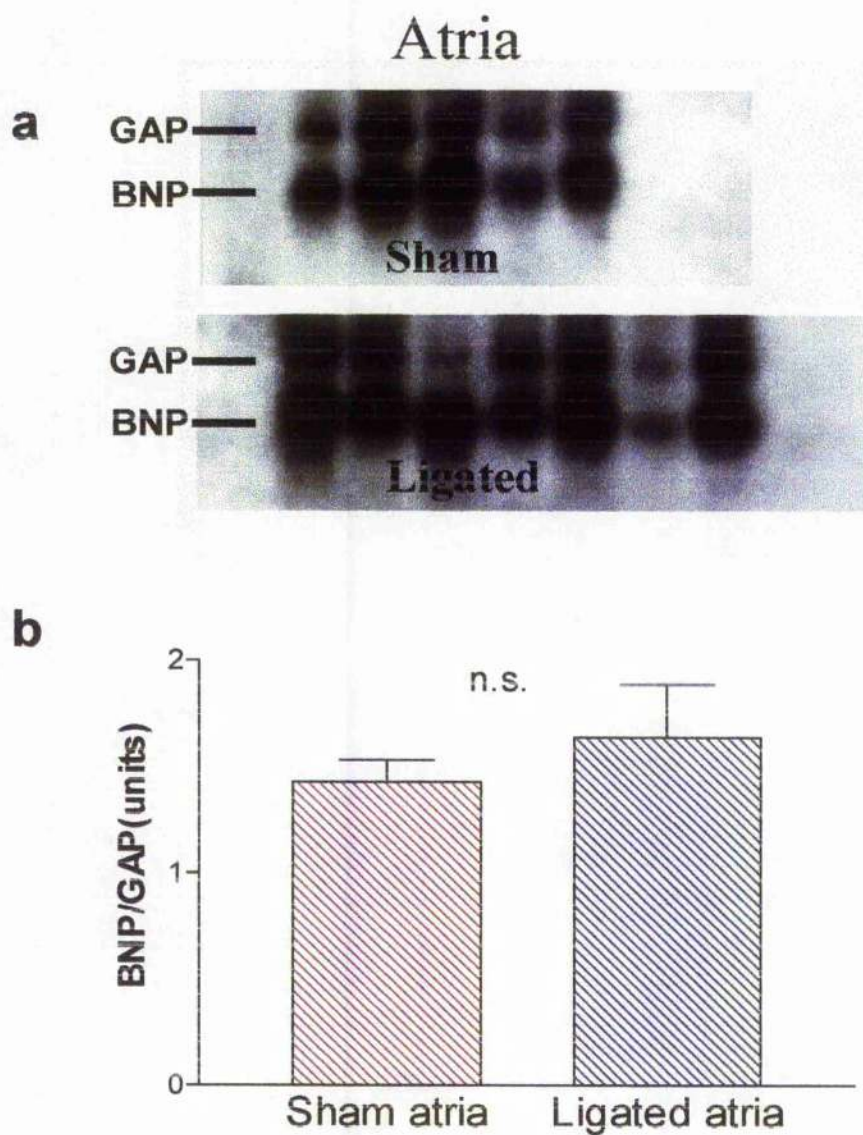


Figure 5.9 Northern blot analysis of BNP gene expression in the atria of sham (n=5) and ligated (n=7) WKY rats. There was no significant difference in mRNA expression.

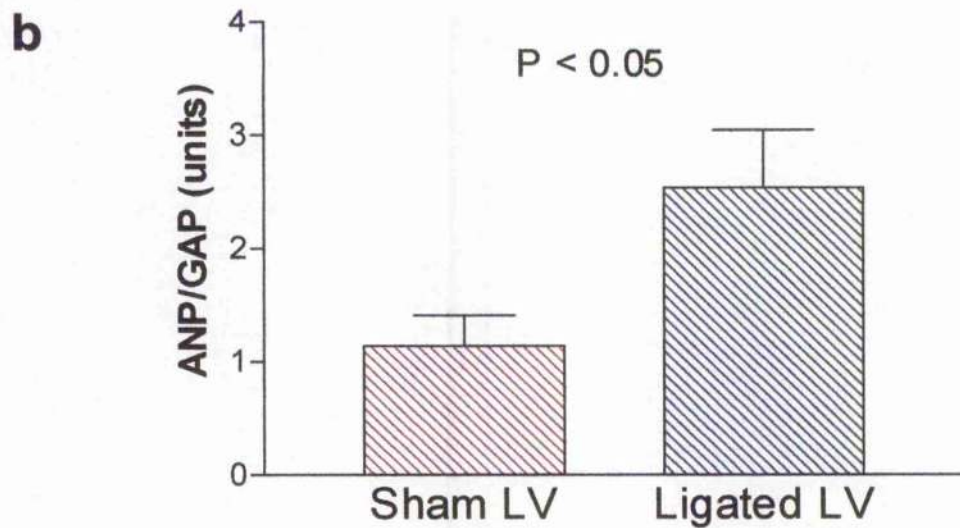
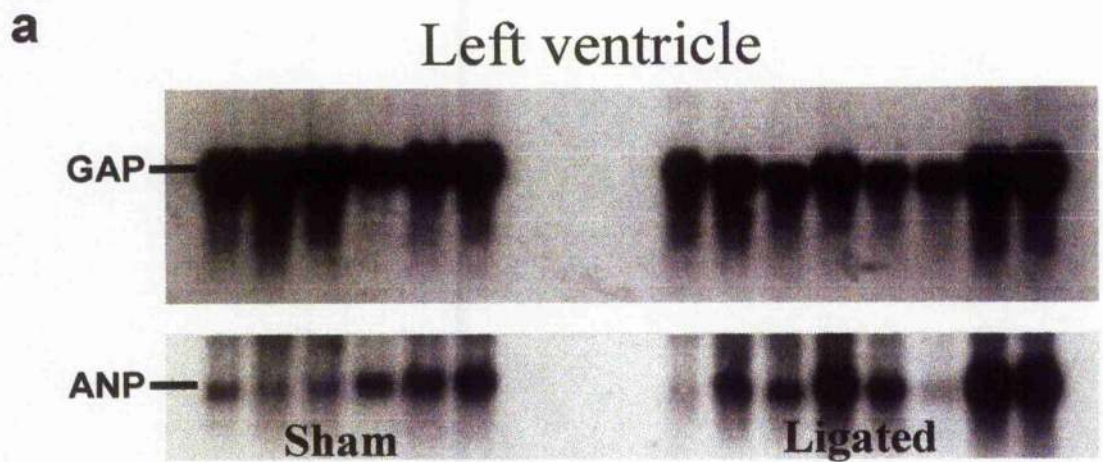


Figure 5.10 Northern blot analysis of ANP gene expression in the left ventricle of sham ($n=6$) and ligated ($n=8$) WKY rats. Data are mean \pm sem, compared by Student's *t*-test.

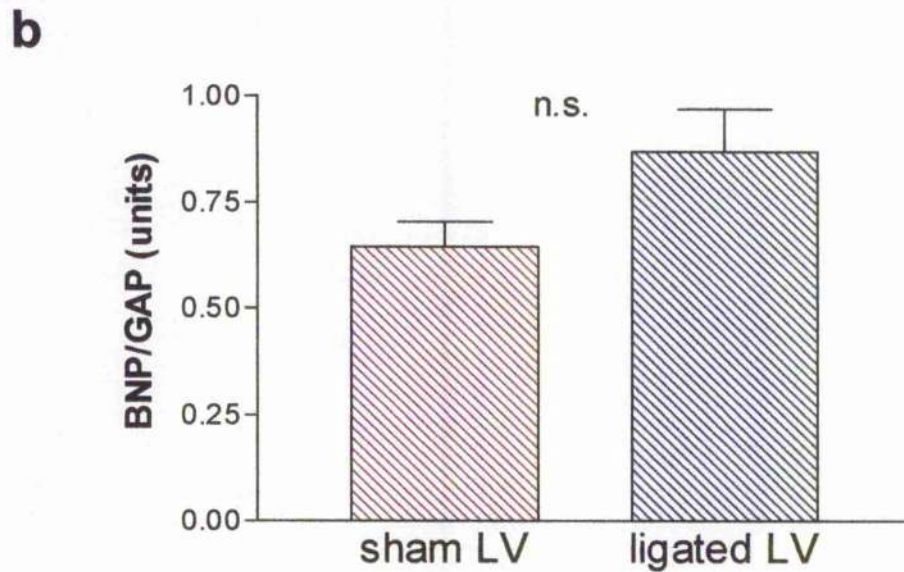
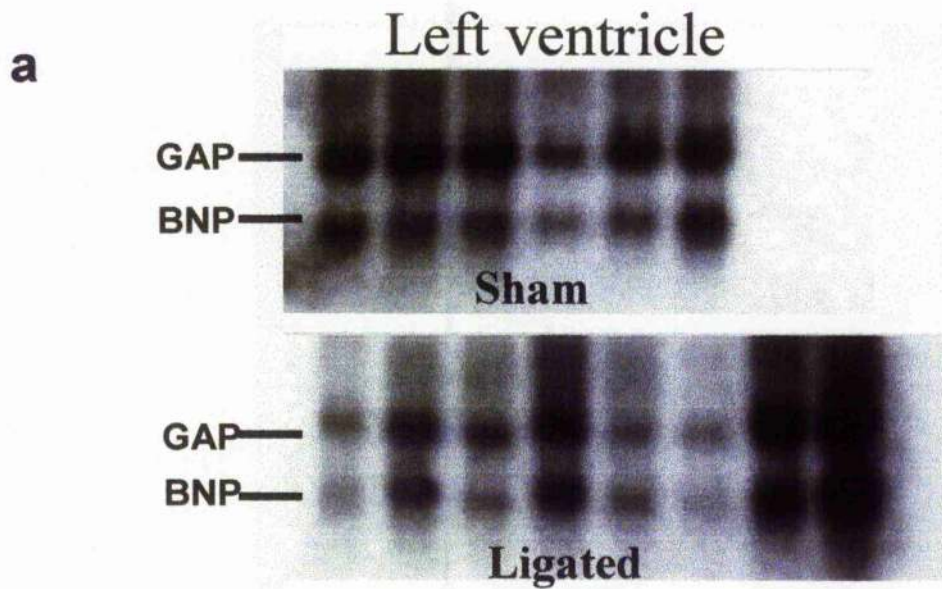


Figure 5.11 Northern blot analysis of BNP gene expression in the left ventricle of sham (n=6) and ligated (n=8) WKY rats. Data are mean \pm sem, compared by Student's *t*-test.

Endocrine

Plasma concentrations of Renin, ANP and BNP were measured 8 weeks after surgery (summarised in Table 5.3). There was no significant difference in renin levels, and a non-significant increase in plasma BNP. However, plasma ANP concentration was 80% higher in ligated animals. In two sham animals there was insufficient plasma to obtain ANP and BNP measurements, therefore n=7 in these groups.

Table 5.3 Plasma concentrations of renin, ANP & BNP eight weeks post-infarct.

	Sham n=7- 9	Ligated n=10	P value
Renin uU/ml	10.9 ± 1.4	12.1 ± 1.6	0.59
ANP pg/ml	123 ± 9	222 ± 32	0.01
BNP pg/ml	90 ± 13	113 ± 9	0.15

All values are mean ± standard error of the mean. Comparison by Student's *t*-test.

Vascular function

Aortic rings were mounted in an organ bath for study of endothelial function. Contractile responses to noradrenaline were identical for both sensitivity and maximum tension between sham and ligated animals (Figure 5.12).

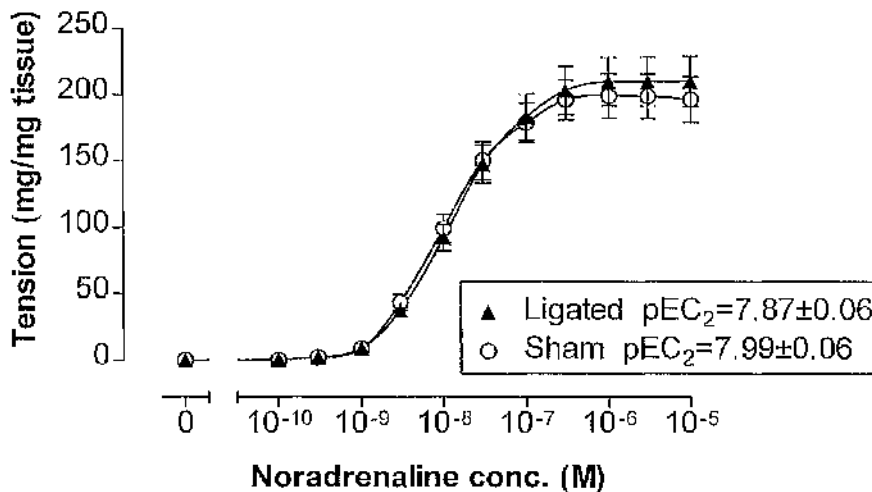


Figure 5.12 Noradrenaline concentration response curves in isolated aortic rings from sham (n=5) and coronary artery ligated (n=8) rats. Values are mean ± standard error of the mean.

There was no difference in relaxant response to acetylcholine. Aortas pre-contracted with noradrenaline exhibited 73% relaxation in ligated and 72% in sham animals, with almost identical sensitivity (Figure 5.13).

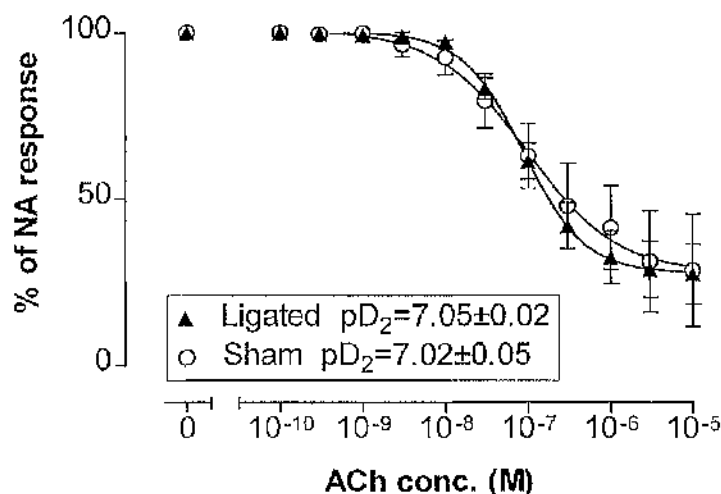


Figure 5.13 Acetylcholine concentration response curves in isolated aortic rings pre-contracted with noradrenaline, from sham (n=5) and coronary artery ligated (n=8) rats. Values are mean \pm standard error of the mean.

Basal release of NO was also similar. Blockade of NOS in unstimulated vessels by incubation with L-NAME (100 μ M) for 30 minutes resulted in an average increase in resting tension of 103 \pm 12 mg/mg tissue in sham animals compared to 96 \pm 23 mg/mg tissue in the ligated group. This resulted in an identical inhibition of acetylcholine-induced relaxations in both groups, at only 3% relaxation. This was not due to a time-dependent loss of endothelial function as control vessels not receiving L-NAME continued to relax in response to ACh.

Very powerful relaxations to sodium nitroprusside (SNP) were obtained in both groups. All vessels relaxed to below baseline tone and neither maximal response nor sensitivity were different between sham and ligated animals (Figure 5.14).

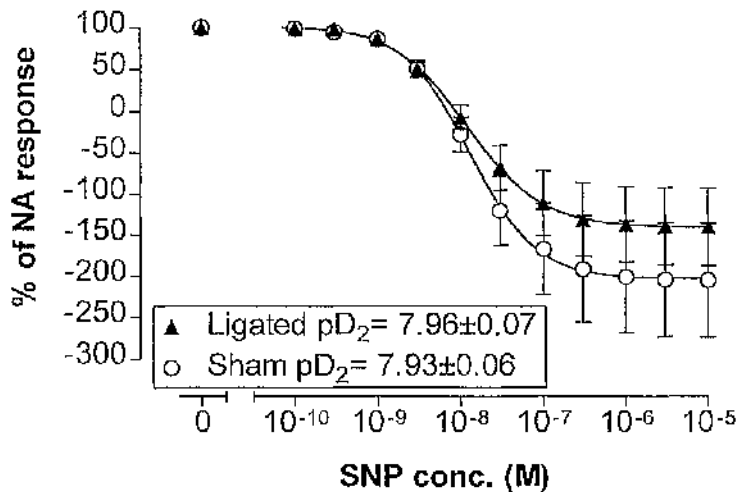


Figure 5.14 Sodium nitroprusside (SNP) concentration response curves in isolated aortic rings pre-contracted with noradrenaline, from sham (n=5) and coronary artery ligated (n=8) rats. Values are mean \pm standard error of the mean.

Resistance artery structure

Laser scanning confocal microscopy (LSCM) was used to determine vascular structure at a cellular level in 3rd order mesenteric resistance arteries. Vessels from seven sham animals and nine ligated were available for measurements. The thickness of the vessel wall was greater in arteries from ligated rats, although this just failed to reach significance (P=0.07). The relative proportions of the component parts are indicated in Figure 5.15. This shows that while adventitia and media thickness were similar, most of the increased wall thickness can be explained by a thicker intimal layer (again not quite significant, P=0.06).

External diameter was almost identical, while lumen diameter was smaller in ligated rats, but not significantly so (Figure 5.16, Table 5.4). Thus, there appears to be a thickening of the intimal layer that encroaches into the luminal space. This could not be explained by changes in endothelial cell number, which were comparable between sham and ligated groups (Table 5.4).

There were fewer smooth muscle cells in the media of ligated animals. Since medial cross-sectional area was almost identical between groups, this resulted in a significantly lower smooth muscle cell density, whereby ligated animals had 24% fewer cells per unit volume of media (figure 5.17 and 5.18).

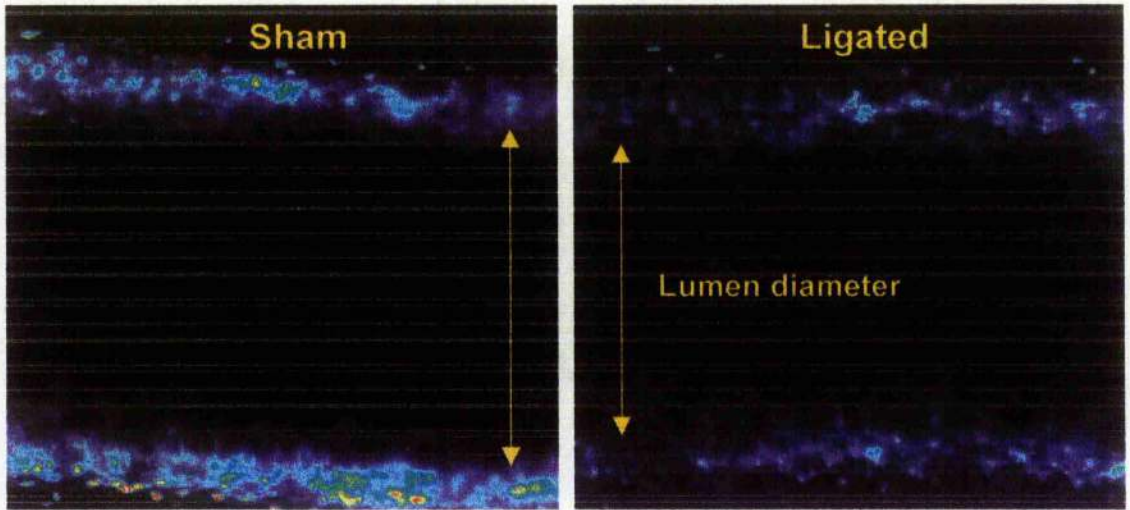


Figure 5.16 Measurement of lumen diameter in mesenteric resistance arteries of sham and ligated rats by LSCM. Yellow lines are approximately 200 μ m and 180 μ m for sham and ligated images respectively.

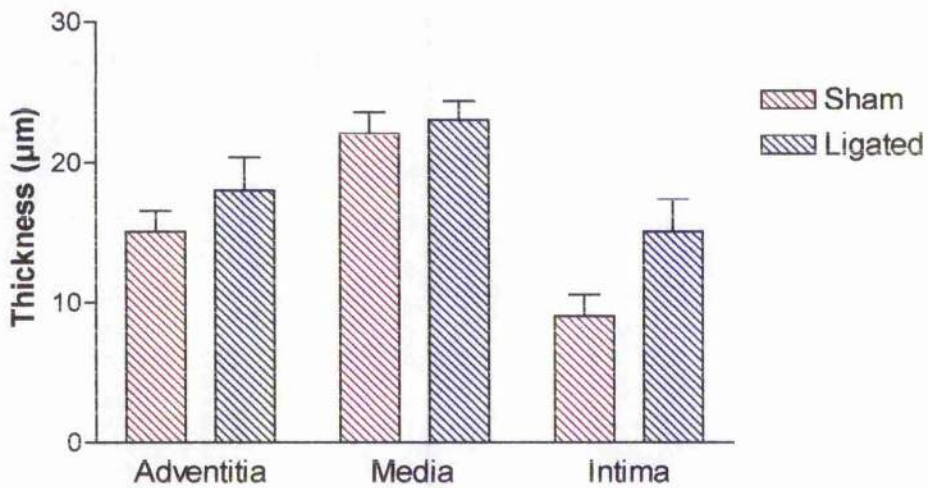


Figure 5.15 Relative thickness of the component parts of the arterial wall as measured by LSCM. All data is mean \pm sem, sham n=7, ligated n=9.

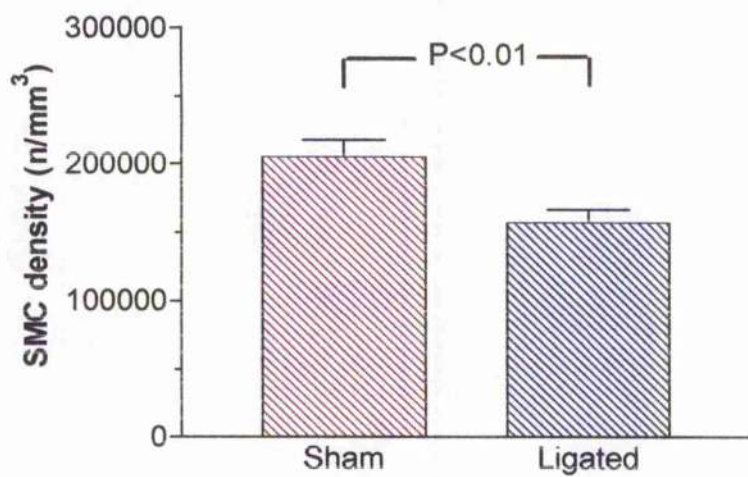


Figure 5.17 Smooth muscle cell density (number of cells per mm³ of media) from mesenteric resistance arteries of sham and ligated rats. Mean \pm sem.

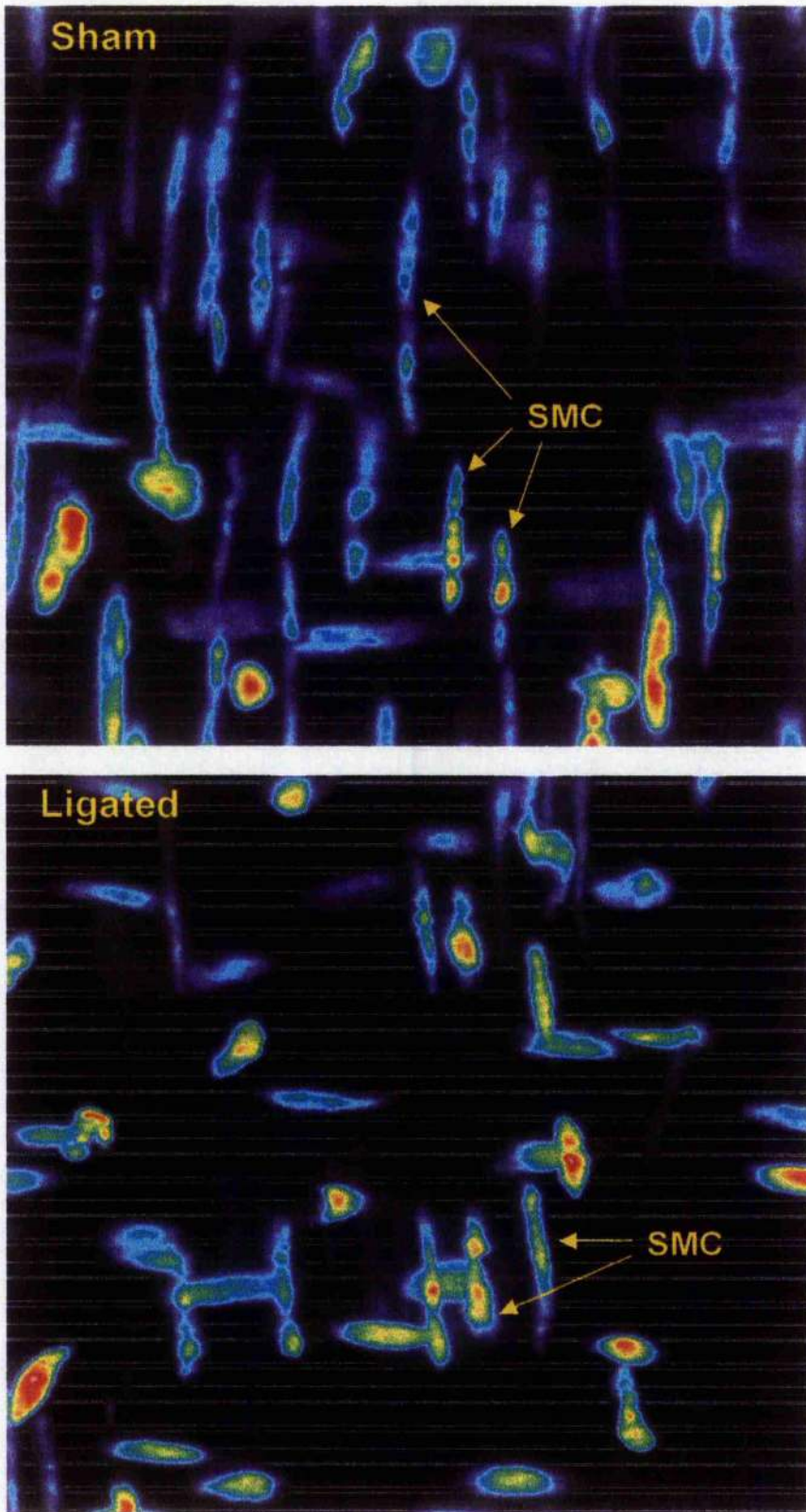


Figure 5.18 Representative 3-D reconstructions through the arterial wall of mesenteric resistance arteries. Smooth muscle cells (SMC) are oriented in the vertical plane, while endothelial cells lie perpendicular to this. Adventitial cells are more rounded with stronger signals. Note that the ligated animal has fewer SMCs.

Table 5.4 Measurements of 3rd order mesenteric resistance artery dimensions and cell numbers using LSCM.

		Sham	Ligated	P value
		n=7	n=9	
Wall thickness	μm	46 ± 9	55 ± 9	0.07
Adventitia thickness	μm	15 ± 4	18 ± 7	n.s.
Media thickness	μm	22 ± 4	23 ± 4	n.s.
Intima thickness	μm	9 ± 4	15 ± 7	0.06
Wall CSA	μm ²	34779 ± 7846	40364 ± 9450	n.s.
Adventita CSA	μm ²	13001 ± 3495	15043 ± 6687	n.s.
Media CSA	μm ²	16357 ± 4390	16328 ± 3962	n.s.
Intima CSA	μm ²	5421 ± 1574	8993 ± 4949	0.09
Lumen diameter	μm	200 ± 60	177 ± 30	n.s.
Wall/lumen ratio	%	25 ± 10	32 ± 9	n.s.
Media/lumen ratio	%	12 ± 4	13 ± 3	n.s.
External diameter	μm	292 ± 52	287 ± 32	n.s.
Adventita cell number		21.0 ± 8.6	18.4 ± 5.7	n.s.
SMC number		45.4 ± 9.0	37.1 ± 10.2	0.11
EC number/mm ²		1274 ± 323	1083 ± 502	n.s.
nA cells/A volume		131038 ± 87894	106447 ± 81767	n.s.
nSMC/media volume		205357 ± 32148	157057 ± 26840	0.006 **

All data are derived from one vessel per animal and is presented as mean ± standard deviation. CSA, cross-sectional area; SMC, smooth muscle cells; A, adventitia; EC, endothelial cell; n.s., not significant. Comparison by Student's *t*-test, significance level $P < 0.05$.

5.4 Discussion

Survival was good in the ligated animals at 77%, especially as this includes the learning curve for this procedure. There was no difference between survival when the procedure was performed by an experienced animal surgeon (M.Hicks) or by the author. The level of sham fatalities is puzzling, and was not resolved despite veterinary advice. Why similar types of death were not observed in the ligated group is unknown.

There were no early arrhythmic deaths, which may be a benefit of the anaesthetic regime used. In a direct comparative study, rats anaesthetised with halothane had fewer arrhythmias and lower mortality after CAL than those animals receiving pentobarbitone (Au *et al.*, 1983).

Infarct size

Ligation of the left coronary artery of the rat results in transmural anterior infarction (Figure 5.1). Within the scar tissue, which is much thinner than the surviving myocardium, there is a central core of connective tissue strongly staining blue. This area is surrounded by macrophages (ghost cells) which stain lightly red with large nuclei. Sometimes there is a thin layer of healthy myocardium near the lumen, which may have been able to obtain enough nutrients from intra-luminal blood to survive. Small arteries and veins may also be visualised within the scar tissue.

Organ weights

Cachexia may be present in severe heart failure in humans (Levine *et al.*, 1990), but was not observed in these rats, whose body weight remained close to sham values (Table 5.1). Indeed, in all but two ligated animals, body weight increased over the duration of the study. The two that lost weighed had the poorest cardiac function as measured by ejection fraction, but weight loss was not great at only 3 – 4 %. However, true weight loss could be masked in the presence of peripheral oedema.

Ligated animals had a higher heart weight and heart – RV weight i.e. left ventricle + atria + great vessels (Table 5.1). This represents the balance between the lost myocardial mass of the infarct scar, and hypertrophy of the surviving myocardium. This suggests that even in those animals with a heart weight similar to sham, that hypertrophy was considerable to compensate for the loss of tissue. Right ventricular

weight was higher in almost all of the ligated animals (Figure 5.2) and is indicative of an increased pulmonary pressure, probably due to mild congestion.

Congestion of the liver was present in two out of 10 ligated animals (Figure 5.2). Why these two exhibited congestion while the others did not, was probably due to their lower ejection fraction suggesting more severe dysfunction. However, the difference in ejection fraction between these and the non-congested animals was not great, which suggests that the level of insult inflicted in this study is on the borderline between LV dysfunction and congestive heart failure.

Measurement of long-axis length from the mitral annulus to the apex was not possible by echocardiography, and so was measured at autopsy using digital callipers. Villarreal *et al.* (1999) reported shortening of the long-axis after myocardial infarction in the rat. However in the present study, long-axis geometry was almost identical between groups, with no evidence for spheration.

Echocardiography

In man, changes in cardiac position after surgical procedures can have a dramatic influence to reduce the number of acceptable echocardiograms (Wallerson & Devereux, 1987). The same effect was apparent in rats after coronary artery ligation. In particular, image quality was often poor in the first echocardiogram after surgery, which was thought to relate to inflammation in the thoracotomy scar, and the fact that two adjacent ribs are splinted together when closing the chest wall. In most animals, image quality improved thereafter, presumably as the scar healed. In most animals where image quality remained poor, focal adhesions of the heart to the chest wall were noted at post-mortem.

Left ventricular function was clearly compromised after CAL in these rats, with ejection fraction consistently lower than either baseline or sham values (Figure 5.3). Values for ligated animals ranged from 35 to 57% which does not sound particularly severe when compared to human heart failure. However, these figures are not directly comparable as rats have a higher normal ejection fraction, and this study did not attempt to measure absolute values, but to demonstrate a change from baseline. The extent of dysfunction was fairly similar between all the ligated animals as can be seen from the small error bars in Figure 5.3. This uniform response may be due to using an inbred population. Infarcts in Lewis inbred rats are also highly reproducible (Liu *et al.*, 1997).

Measuring ejection fraction after myocardial infarction by this method may introduce some additional errors. It assumes contractility to be constant at all levels of the heart, which will not be true at the infarct zone. In order to maintain reproducibility, all short-axis views were taken at the level of the papillary muscles. In the majority of animals this was above the infarct zone, as no evidence of papillary muscle involvement was observed. However, it must be acknowledged that serious miss-calculations may have occurred in the following instances; 1) where the function of the mitral valve was compromised such that a significant level of mitral regurgitation was present. In these circumstances, there will be an over estimate of ejection fraction using this method, as no account is made of a regurgitated volume. 2) Where the imaging plane overlaps the infarct zone. In this case, ejection fraction may be under-estimated especially when the infarct scar is akinetic, as ejection fraction is likely to be higher at areas of non-infarcted myocardium. By the same reasoning, in the present study which contained only a few rats with infarct zones in the imaging plane, the actual ejection fraction is probably lower than the calculated values.

It is important to remember that no attempt was made to validate the ejection fraction measurements by comparison with a gold standard, such as the thermodilution technique (de Simone *et al.*, 1990). However, due to the longitudinal nature of this study, values of absolute ejection fraction were not of interest here, rather the change in ejection fraction relative to the baseline value. The issue therefore becomes one of reproducibility of day-to-day measurements, which was shown to be acceptable using this method (Chapter 3). Indeed, the very low week-to-week variability in sham animals suggests that reproducibility may have improved on that observed in Chapter 3, probably due to the increased experience of the sonographer.

Ejection fraction in the ligated animals did not significantly improve or worsen with time, indicating fairly stable pump performance. However, a slight dip in ejection fraction was observed at 4 weeks from 46% to 41% with recovery to 47% by week 6. Although this was not significant, it is interesting because the week 4 measurement represented the nadir for every one of the ligated animals studied. This suggests that the dip may be real and not simply due to random variation. Although there is little or no evidence from this study to explain this phenomenon, it is tempting to suggest an explanation. Studies on infarct healing after myocardial infarction have shown scar maturation to be taking place within this time frame (Sun & Weber, 1996).

Alterations in left ventricular geometry may be connected to these phenomenon. A major increase in LV dilatation also occurred between weeks 2 and 4, which then steadied off, rising only slightly after that (Figure 5.4). It is of interest to note that LV cross-sectional area increased in both sham and ligated groups after surgery, although there was no subsequent increase in the sham animals. Why this slight dilatation should consistently occur after sham operations is not clear, but is probably a consequence of handling the heart and removing the pericardium. This demonstrates the importance of using sham animals as opposed to stock controls.

LVH was significant and progressive (Figure 5.6) and looks to be increasing beyond the end-point of this study. There was a small, non-significant increase in wall thickness in sham animals, probably associated with ageing. The strong hypertrophic response in ligated animals indicates that they are compensating well for loss of function.

The results from this study are in agreement with other groups that have used echocardiography in post-infarction rats. Burrell *et al.* (1996) used short-axis images to examine regional changes in rats four weeks after CAL. They were able to show significant differences in LV cavity dilation, hypertrophy of surviving myocardium, and impaired systolic function, as did Litwin *et al.* (1994). However, this is the first study to use serial echocardiographic measurements to determine temporal changes in structure and function. It is interesting to note that ejection fraction did not deteriorate with time after infarct, despite a progressive LV dilatation. This is in accordance with the view that LV dilatation (in the short-term) is a positive adaptation to maintain stroke volume in the face of a reduced ejection fraction (Pfeffer *et al.*, 1984). Indeed, ejection fraction would be very low if LV dilatation did not occur in these animals. The ligated animals are obviously compensating well for the LV dysfunction, and it would be interesting to see if the continuing LV dilatation and hypertrophy will eventually result in decompensation to overt failure. Serial echocardiography in the rat may therefore represent a useful tool for future studies on the transition from compensated dysfunction to failure.

Most of the ligated hearts exhibited wall motion abnormalities in the short-axis view, which may have contributed to systolic dysfunction. This type of dysfunction is difficult to quantify or describe, but is obvious to the observer from the moving images. Hunziker *et al.* (1999) have recently devised a holographic method to portray these

defects on the two-dimensional printed page. They describe a technique for printing holograms where the motion of the heart can be viewed through a complete cardiac cycle by tilting the image up and down. The printing technology is still at the prototype stage, but if it becomes available in the future, will aid communication of wall motion or valvular abnormalities.

Echocardiography may also be used to measure the degree and rate of left ventricular systolic contraction, and rate of diastolic relaxation. It would have been useful to be able to measure LV wall stress, as increased wall stress is thought to represent an increased risk of myocardial ischaemia (Liebson *et al.*, 1987). It may also be involved in regulating the gene expression of ANP (Wijbenga *et al.*, 1999). In order to calculate wall stress it is necessary to have simultaneous measurement of blood pressure. The original plan when designing this study was to implant radiotelemetry probes in these animals for continuous blood pressure monitoring, which would have allowed for calculation of wall stress. There were fears that strong reflections from the implanted probe may have swamped out the returning echo, but preliminary studies showed this not to be a problem. However, concurrent use of radiotelemetry was not adopted as the extra surgical procedure is likely to have increased mortality. It remains an option for the future if mortality from the coronary artery ligation procedure remains low.

Natriuretic peptides

ANP levels may be increased by stretch of either atria (Garcia *et al.*, 1987), left ventricle (Kinnunen *et al.*, 1992), or associated with LV hypertrophy and elevated AngII concentrations (Molkentin *et al.*, 1998).

Anaesthetic choice may affect natriuretic peptide levels. Administration of pentobarbital sodium in the rat increases plasma ANP in a dose-dependent manner for up to one week. ANP mRNA expression increases to peak at two-weeks after a single dose, and only returns to normal by week 6. The mechanism for this was not elucidated, but the effect was further exacerbated under conditions of surgical stress (Seul *et al.*, 1993). Whether other anaesthetics have similar effects on the natriuretic peptide system has not been established, however, significant effects after 8 weeks seem unlikely. Long-lasting effects caused by anaesthetics or due to surgery emphasises the importance of having sham-operated controls.

The Northern analysis for RNA was not quantified, but where data was obtained from the same autoradiograph, it is possible to comment on relative abundance. The expression of ANP mRNA was exceptionally high in the atria. Exposure time for autoradiography was only 30 minutes for atrial samples, whereas LV samples on the same blot were optimally visualised at eight hours exposure. This indicates that expression in the LV was around 6% of that in the atria, which was confirmed in an intermediary timed blot when all bands were visible. This is in good agreement with the 7% LV/atria level observed in the WKY by Ogawa *et al.*, (1991), and is similar to normotensive human subjects (Mukoyama *et al.*, 1991; Saito *et al.*, 1989). CAL did not change ANP gene expression in the atria, but levels doubled in the surviving left ventricle. This is a common observation in the rat where it is a measure of LV dysfunction (Passier *et al.*, 1996; Oie *et al.*, 1998; Gidh-Jain *et al.*, 1998) and is probably triggered by a combination of myocyte hypertrophy and increased filling pressures (Wijbenga *et al.*, 1999). The increase in ANP mRNA expression results in an increased secretion of active protein, as there is a near doubling in plasma ANP concentration (Table 5.3). Thus, gene expression in the LV appears to be a reliable indicator of plasma concentration.

BNP mRNA expression was higher in the atria, with the level of expression in the LV around 45% of atrial levels. This confirms the work of Ogawa *et al.* (1991), who observed a 40% relative abundance in the LV versus atria in normal WKY. When adjusted for tissue weight, they found the LV to be the major source of BNP in the rat. After CAL, atrial levels barely changed, while LV expression increased by 34%. Again, the increase in mRNA expression in the LV was mirrored by an increase (26%) in plasma BNP. Although just failing to reach statistical significance for either, this increase is likely to be real, as it was observed by independent measurements at both the mRNA and protein level. BNP is the best marker of prognosis in human heart failure, correlating with NYHA functional class (Mukoyama *et al.*, 1991). As with ANP, gene expression of BNP is switched-on by myocyte cellular hypertrophy (Molkentin *et al.*, 1998), but is also thought to reflect wall stress, as levels have been found to correlate with LV dilatation (Nagaya *et al.*, 1999), low ejection fraction, and high LVEDP (Yamamoto *et al.*, 1996).

Activation of the BNP system is undoubtedly weak in this study and probably reflects the fact that these animals have left ventricular dysfunction and not overt failure. By

comparison, in the LV of the SHRSP, gene expression doubles compared to WKY (Ogawa *et al.*, 1991), and in human heart failure the BNP plasma concentration is higher than ANP, which is not the case here (Mukoyama *et al.*, 1991). Clear differences may have been obscured by mild activation of the BNP system in sham animals. Sham rats exhibited slight LV dilatation in the first two weeks (Figure 5.4), which may have increased BNP expression.

Vascular function

In rings of thoracic aorta, neither contractile response to noradrenaline (NA) nor endothelium-dependent relaxation to acetylcholine were altered in ligated animals when compared to their sham-operated controls (Figures 5.12 & 5.13). Thus, stimulated release of EDRF was normal in these vessels. When L-NAME was added to block nitric oxide synthase activity, the increase in baseline tension was similar between groups, indicating that in unstimulated vessels, basal release of nitric oxide is also normal.

That L-NAME resulted in total block of ACh-induced relaxation suggests that endothelium-derived nitric oxide is responsible for all of the relaxant response to ACh in the aorta of both sham and ligated animals i.e. other EDRFs are not involved.

Finally, no differences were observed in non-endothelium dependent relaxation to sodium nitroprusside i.e. the sensitivity and maximum response is not altered at the level of the smooth muscle (Figure 5.14). Therefore, endothelial-dysfunction was not observed at any level in the aorta of these CAL rats. This is in contrast to a number of other studies that have demonstrated impaired endothelium-dependent relaxation in the thoracic aorta of rats post-MI e.g. Ontkcan *et al.* (1991), Lindsay *et al.* (1992), Toyoshima *et al.* (1998). The obvious explanation is that infarct sizes were not large enough in this study for altered vascular function to become evident. In humans, the extent of vascular dysfunction correlates with the severity of heart failure (Carville *et al.*, 1998). However, recent evidence suggests that endothelium dependent relaxation is actually enhanced in rats with small (<20%) infarcts, and is impaired in animals with larger infarcts (Gschwend *et al.*, 1999). Therefore, one could speculate that since in the present study there was no stratification for infarct size, the response to ACh may represent an average of large and small infarcts, the result being no net difference in relaxation.

Another explanation is that relaxation to ACh is thought to be due to a combination of endothelium derived relaxing factors (EDRF), hyperpolarising factors (EDHF) and contracting factors (EDCF). In a study by Nasa *et al.* (1996), impaired relaxation to ACh was partially restored by inhibiting EDCF production using a cyclooxygenase inhibitor. In this study, indomethacin was present throughout and may have hidden any dysfunction caused by increased release of EDCF's.

In the aorta of rats with large infarcts, impaired endothelium dependent relaxation may be a result of reduced EDHF's (Gschwend *et al.*, 1999). However, EDHF does not appear to have a significant role in relaxation in the present study as only 3% of the relaxation persisted in the presence of L-NAME and indomethacin.

In the ligated rats, vascular function may yet have been impaired in more distal portions of the vascular tree. In the few animals that underwent tail-cuff plethysmography, it was substantially more difficult to dilate the tail artery for blood pressure measurements, providing circumstantial evidence for impaired peripheral vasodilatation.

Resistance artery structure

Remodelling of mesenteric resistance arteries in the CAL rats was mild, with only minor changes in vessel dimensions at eight weeks after surgery. Lumen diameter was slightly reduced, mainly due to a thicker intimal layer. As there was no difference in endothelial cell number, this suggests an increase in connective tissue. However, the one study that has addressed this issue found no difference in collagen or elastin density in rat mesenteric resistance arteries at a variety of time points up to one year (Mulder *et al.*, 1996). Intimal thickening has not been previously described in any heart failure model, and the reason for this type of remodelling remains obscure.

The most striking difference observed in this study was a reduced number of smooth muscle cells in the media of ligated animals, despite an identical media cross-sectional area (Figure 5.17). Therefore, despite there being no net change in the volume of material, there was a substantial restructuring of the medial layer i.e. eutrophic remodelling. The loss of smooth muscle cells must have been counterbalanced by an increase in connective tissue, or hypertrophy of the remaining cells to maintain the same volume. This is the first time that such remodelling has been described in heart failure.

Only a handful of studies have examined resistance artery structure in heart failure and they are all in broad agreement, that changes in vessel dimensions are minor or not apparent. In rats after CAL, Mulder *et al.*, (1996) found no differences in either femoral or mesenteric resistance artery structure at 0, 30 or 365 day's post-MI. Likewise, at 5 weeks there was no difference in media CSA, lumen diameter, or wall-to-lumen ratio in mesenteric small arteries in a study by Stassen *et al.* (1997a). Resistance arteries in the surviving myocardium are also unaffected at 3- and 8-weeks, with no change in media-to-lumen ratio (Kalkman *et al.*, 1996). In human gluteal subcutaneous resistance arteries the picture is the same, no change in vessel dimensions or media-to-lumen ratio (Stephens *et al.*, 1998). The results from the present study fall into this pattern, with no significant differences in media-to-lumen ratio, lumen diameter or wall thickness.

Only two studies have reported small artery remodelling, both in 3rd order mesenteric resistance arteries after CAL in the rat. Buus *et al.* (1999) describe remodelling of existing material around a slightly enlarged lumen i.e. outward eutrophic remodelling, while Heeneman *et al.* (1995) show outward hypertrophic remodelling. In both, lumen diameter tended to increase, resulting in a reduced media-to-lumen ratio. However, in the study by Buus *et al.* (1999) media CSA remained normal, while there was a tendency for medial CSA to increase in the report by Heeneman *et al.* (1995). The reason for this discrepancy is likely to be changes in regional blood flow. In the former study, blood flow to the small intestines was unchanged, but in the latter, flow was significantly increased. Thus, the increase in material in the media observed by Heeneman and colleagues was probably due to flow-induced hypertrophy. Why there was a difference in small intestine blood flow between these studies is not apparent. However, it is probably not related to severity of heart failure as both studies employed Wistar rats with identical average infarct size, examined at comparable time points, when heart failure was well compensated.

In all the studies described above, structure was determined by either wire or perfusion myography or by standard histology in perfusion fixed vessels. Therefore, no information was available at a cellular level, making the reduction in SMC density observed in this study unique. Loss of smooth muscle cells may have a functional significance. Stassen *et al.* (1997a) describe a generalised hyporeactivity to all major vasoconstrictors in mesenteric resistance arteries from rats 5-weeks post-MI. They also determine vascular structure, but noted no change in media thickness, CSA, lumen

diameter or wall-to-lumen ratio. They conclude that the decrease in contractility cannot be explained by a reduction in media mass. However, although in a further study they attempt to explain this in terms of impaired agonist-induced calcium influx (Stassen *et al.*, 1997b), an alternative explanation would be a reduced number of smooth muscle cells as observed in the same vessels in the present study.

The loss of SMC could be due to decreased blood pressure or reduced flow as a direct effect of myocardial infarction. However, Buus *et al.* (1999) measured blood flow to the small intestine in heart failure rats and found no difference between sham and ligated animals. The drop in blood pressure is typically around 15-20mmHg after coronary artery ligation in the rat (Mulder *et al.*, 1996). Whether this small difference is still apparent at the level of the resistance arteries has not been established. Although elevated blood pressure is a known stimulus for vascular hypertrophic remodelling, little is known about the effect of hypotension on vascular remodelling.

It is surprising that small artery structure is not radically altered in heart failure given the number of vasoactive substances that become elevated, many of which can modulate vascular growth. Angiotensin II promotes growth and SMC hypertrophy (Heeneman *et al.*, 1997), as do noradrenaline and endothelin (Wu *et al.*, 1997). All have been reported as increased after myocardial infarction. Counterbalancing these effects are NO, TNF- α and ANP which have growth inhibitory effects, and may induce SMC apoptosis (Stassen *et al.*, 1997a; Wu *et al.*, 1997; Pinsky *et al.*, 1999). It is tempting to speculate that the loss of smooth muscle cells in the ligated animals was due to programmed cell death. Apoptotic cell death has been documented in myocytes in the failing myocardium (Ruffalo *et al.*, 1998), and in cultured SMCs obtained from the hypertensive rats (Hamet *et al.*, 1995). However, to the best of our knowledge, has yet to be described in the vasculature of rats with heart failure. It is interesting to note that plasma ANP remains strongly activated in the ligated animals, while plasma renin is normal (Table 5.3). Other groups have noted that plasma noradrenaline and angiotensin II have returned to normal five-weeks after infarction in the rat, while ANP remains elevated (Stassen *et al.*, 1997a). This could represent a pro-apoptotic or growth inhibitory mechanism, whereby persistently raised ANP is the prevailing influence on SMC growth in the longer term. However, this remains speculative and merits further study.

Summary

This study examined cardiac and vascular function and structure in WKY rats eight weeks after occlusion of the left anterior descending (LAD) coronary artery, and compared them with sham operated controls. The main findings were:

- The rat model of coronary artery ligation was successfully introduced to this laboratory with an acceptable level of mortality.
- Occlusion of the LAD coronary artery resulted in anterior transmural infarcts.
- Echocardiography two-weeks post-surgery demonstrated that ligated hearts had a significantly reduced ejection fraction with LV dilatation hypertrophy.
- LV dilatation increased progressively for the duration of the study, while there was no further change in ejection fraction.
- Compensatory hypertrophy of the surviving posterior wall was apparent from week 4 onwards and increased in a linear fashion.
- In the surviving myocardium, ANP mRNA expression is significantly elevated, which corresponds with a similar increase in plasma ANP concentration.
- BNP mRNA was only weakly induced with a corresponding non-significant increase in plasma BNP.
- In isolated aortic rings, endothelial function was normal in ligated animals.
- Gross structural alterations in mesenteric resistance arteries were not significant. However, using LSCM, extensive eutrophic remodelling of the medial layer was apparent, with ligated animals having 24% fewer smooth muscle cells.

5.5 Conclusions

The rats in this study exhibit left ventricular dysfunction resulting in moderate impairment of ejection fraction. Over the time period observed, the responses of LV hypertrophy and dilatation are adequately compensating for the loss of functioning myocardium. However, both these parameters were still increasing at the study endpoint, and serial echocardiography may be a useful tool to determine when cardiac remodelling becomes detrimental. The absence of strong BNP activation and aortic endothelial dysfunction probably confirms that heart failure is mild in these animals. Despite this, a novel type of remodelling was observed in the mesenteric resistance arteries, which could have implications for small artery function.

6. Coronary artery ligation in SHRSP: feasibility study

6.1 Introduction

Hypertensive patients are at greater risk of developing ischaemic heart failure and when they do, prognosis is particularly bleak. In the Framingham heart study, only 24% of men and 31% of women with hypertension and myocardial infarction survived five years (Levy *et al.*, 1996). To mimic this situation in the clinic, some groups have used CAL in hypertensive animal models to determine the factors in hypertension that contribute to poor prognosis. Fletcher *et al.* (1982) compared haemodynamic parameters after MI in the SHR and WKY rat strains. Animals were stratified according to infarct size and measurements taken at 26 days. Compensatory LV hypertrophy was not yet detectable in normotensive animals. Despite the presence of LV hypertrophy in the SHR rats, absolute values for peak LV developed pressure, peak stroke volume and stroke work were comparable to normotensive rats, although the initial values prior to ligation were higher in the SHR. Therefore, the percentage decrease was greater in the SHR, such that the increased pressure developing capacity of the hypertrophied myocardium was lost. The greater effect on SHR hearts could not be explained by alterations in LV dilatation, which were similar between strains.

The reduction in blood pressure post-MI was doubled in the SHR, bringing them within the normotensive range, but was still higher than WKY. Thus, afterload remained elevated, which may have accounted for the relatively reduced cardiac function (Fletcher *et al.*, 1982).

There is evidence for an increased infarct size in the hypertensive heart, which would contribute to poor prognosis, as many of the haemodynamic indicators of LV dysfunction correlate with infarct size (Fletcher *et al.*, 1982). When the SHR is subjected to CAL, mortality is significantly greater than in WKY animals for the same insult. This is due to increased infarct size and sudden death, mainly in the first 30 minutes (Morita *et al.*, 1996).

In dogs with renal hypertension, CAL resulted in a 50% increase in infarct size over normotensive animals, and a 3-fold increase in sudden death due to ventricular fibrillation (Inou *et al.*, 1987). Infarct size and mortality were almost normalised by

infusion of sodium nitroprusside for 7 ½ hours, starting 30 minutes after occlusion. This effectively lowered blood pressure without affecting LV hypertrophy, suggesting that high blood pressure is more important than LVH in the increased susceptibility to infarct expansion and sudden death. Likewise, infusion of pressure-agents after MI in pigs also increases infarct size, while pacing induced tachycardia had no effect (Garcia-Dorado *et al.*, 1988). Presumably, increased afterload is placing more stress on the failing heart.

Later studies in the dog model indicated that the rate of infarct expansion (i.e. the rate of spread of myocyte necrosis) was increased in hypertensive animals, and could be modulated by blood pressure control (Dellsperger *et al.*, 1991). Sudden death could be normalised by immediate treatment with a β -blocker but not ACE inhibitor, despite both drugs reducing infarct size and blood pressure. This suggests that the risk of sudden arrhythmic death is not related to blood pressure or infarct size, but is due to other factors such as sympathetic activation or presence of LV hypertrophy.

In contrast to Fletcher *et al.* (1982), LV dilatation was increased in SHRs after infarction in a study by Nishikimi *et al.* (1995), indicating a more rapid deterioration in LV geometry. The reason for these conflicting results is not clear, as both studies took measurements at around three weeks with similar sized infarcts.

All these studies dealt with immediate or early (< 3 weeks) effects. Very little information is available on the natural progression to heart failure in the longer-term. From the limited data, progression appears to be accelerated. In the absence of a control group Itter *et al.* (1998) describe ligated SHRs as exhibiting severe heart failure at five weeks, with peripheral and lung oedema, ascites, enlarged left and right ventricles and impaired ejection fraction. Mean survival was only 15 weeks. The influence of neurohormonal or vascular alterations due to hypertension on the progression to heart failure has never been studied.

6.2 Results & discussion

A total of eleven SHRSP were subject to coronary artery ligation. The surgical procedure was identical to that in WKY animals, with no additional precautions. Mortality was high with only three animals surviving the full eight weeks. This is similar to the 24% survival reported at one week in the SHR by (Morita *et al.*,1996). Outcome for individual animals is given in Table 6.1.

Table 6.1 Outcome in SHRSP after coronary artery ligation.

Animal numbers	Outcome
C2113	Confirmed stroke at day 14 post-ligation.
C2273	Sudden death day 13.
C2392	Sudden death day 12.
C2313	Survived but infarct very small
C2359	
C2360	
C2312	Died 5 minutes after surgery – confirmed arrhythmias
C2391	
C2311	Blood loss during surgery, died next day
C2383	Sudden death day 3 after good recovery from surgery.
C2384	

Due to the exceptionally high blood pressure in these animals, blood loss during surgery tended to be greater than in WKY rats. The act of placing the suture was frequently accompanied by spurts of blood from the left ventricle that required rapid application of pressure to bring under control. Despite this, only one animal died as a direct result of blood loss from the surgical procedure. Two animals died immediately post-surgery of confirmed arrhythmic death, and this corresponds with the known period of increased ventricular fibrillation and tachycardia that occurs in the first 30 minutes after ligation in the rat (Opitz *et al.*, 1995). A further two animals recovered well after surgery, but were found dead on day 3, while three more animals died suddenly at around 2 weeks after being otherwise well. In one of these animals, the cause of death was due to

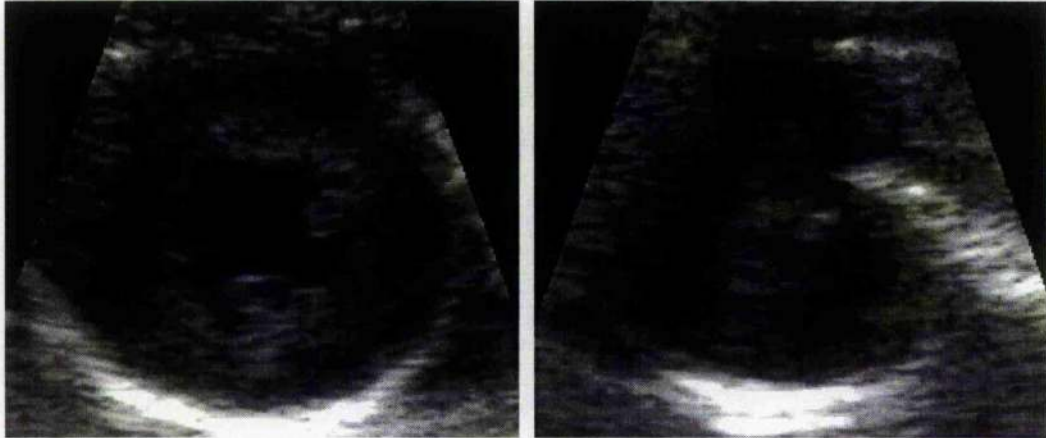
stroke, and a large haemorrhage was observed on post-mortem. This is unsurprising as this animal was old by SHRSP standards at 10-months of age, well within the time frame that strokes are common in these animals (Okamoto *et al.*, 1974). In the remainder, cause of death was not established, although acute heart failure was unlikely, as lung pathology was normal and at 4-5 months old, stroke is less common. Deaths were probably due to myocardial infarction or fatal arrhythmias, although stroke was not excluded. Unfortunately, all of the three animals that survived the eight-week follow-up period had no evidence of LV dysfunction by echocardiography, and were found to have very small or no infarcts on post-mortem. Since none of the WKY rats in the previous chapter had such small infarcts and the ligation was placed in the same position, this may represent a divergence in coronary artery anatomy between SHR and WKY rats which merits further investigation. However, in these rats with no apparent infarct at 8-weeks, blanching of the myocardium was still observed on tying the suture, indicating that ischaemia was present in these animals, at least initially. This apparent recovery of the infarcted myocardium may be due to the hypertrophied myocytes representing a physical barrier to protect the artery from total occlusion. Another explanation could be that; because hypertrophy was well established in these animals, they might have developed a more extensive collateral circulation to compensate i.e. new capillaries to feed the enlarged myocardium.

It is not possible to say from this preliminary work whether it is feasible to produce SHRSPs with moderate to large infarcts within acceptable mortality limits. Obviously there is a learning curve for ligation in the SHRSP and more animals are required. Cardiovascular pathology is already well advanced in these morbidly hypertensive animals and it is perhaps optimistic to use eight weeks as the study period. We would expect progression to heart failure to be more rapid in hypertensive compared to normotensive rats. Indeed, if the study time had been reduced to 10-12 days, then survival would have doubled in this study. An echocardiogram was obtained in one of the animals that died at two-weeks which clearly shows an anterior infarct, resulting in impaired systolic function (Figure 6.1). The ejection fraction in this animal reduced from 82% to 45% after infarction.

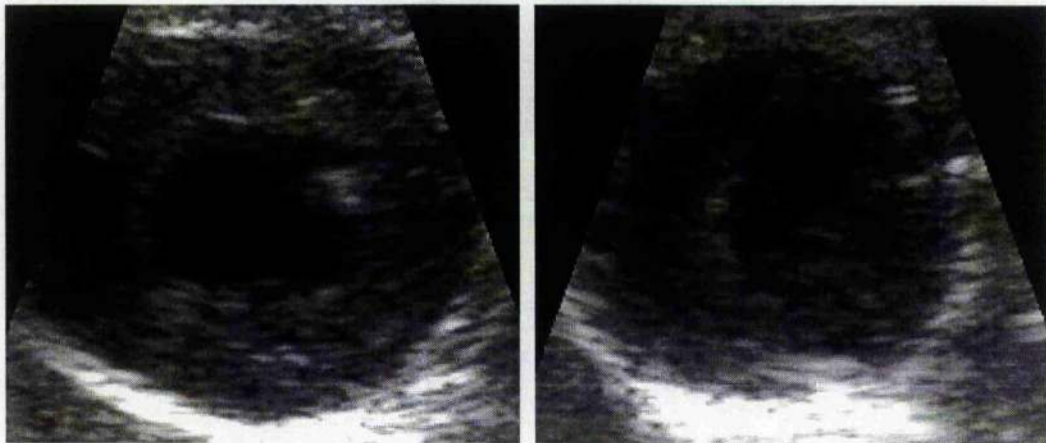
Other approaches may yet be tried to bring mortality within acceptable limits. These could include administration of anti-arrhythmic drugs, using females as a moderately

less severe hypertensive model, or lowering blood pressure during and immediately after surgery to minimise infarct expansion.

Before surgery



After CAL



Diastole

Systole

Figure 6.1 Parasternal short-axis view of the left ventricle in a SHRSP rat before and two weeks after surgical ligation of a coronary artery. Infarcted area is clearly visible during systole resulting in a larger end systolic volume.

7. Venous function in the rabbit after coronary artery ligation

7.1 Introduction

A rabbit model of coronary artery ligation was developed in Glasgow as part of the Medical Research Council's Clinical Research Initiative in Heart Failure. The model was produced centrally, and tissue distributed to several research groups studying cardiac and vascular function. This section will describe work undertaken by the author on venous function in this model.

There is a dearth of information on the venous circulation in general, and no published analysis of venous function during heart failure. Despite this, there are good reasons to suspect that heart failure may be associated with altered venous function. In rat models of coronary artery ligation, central venous pressure is elevated (Mulder *et al.*, 1996; Mulder *et al.*, 1997), thereby contributing to increased pre-load on the heart. In the same model, increased peripheral resistance may be explained, in part, by impaired endothelium-dependent relaxation in large conduit arteries such as the aorta (Lindsay *et al.*, 1992; Toyoshima *et al.*, 1998) and in the resistance arteries (Drexler & Wenyuan, 1992). It is conceivable that similar dysfunction may occur in the venous circulation. The venous circulation is highly innervated by sympathetic nerves at all levels in the vascular tree, and due to the relatively thin smooth muscle layer, when compared to arteries, neurogenic constriction is more pronounced in veins (Nilsson *et al.*, 1986). Since heart failure is associated with a strong activation of the sympathetic nervous system in man (Meredith *et al.*, 1993) and animal models (Deck *et al.*, 1992), studies on neurogenic vasoconstriction are a logical starting point for examining venous function during heart failure.

This provides the rationale for the following study, which examined endothelium-dependent relaxation to acetylcholine, and vasoconstriction in response to electrical field stimulation in isolated rings of saphenous vein from stock and CAI rabbits. Since vascular alterations may be a long-term consequence of LV dysfunction, animals were studied at two time points, 8-weeks and 32-weeks after surgery.

7.2 Methods

The rabbit model of coronary artery ligation (CAL) was provided by the University Department of Medical Cardiology using New Zealand white rabbits obtained from stocks kept at Glasgow Royal Infirmary. Methods for this surgery and echocardiography are published in (Pye *et al.*, 1996). This study includes full validation of echocardiographic estimation of ejection fraction in the rabbit, by comparison with the thermodilution method. Two sets of experiments were conducted: in rabbits 8-weeks after surgery and 32-weeks after surgery.

Stock and ligated rabbits were killed by overdose of anaesthetic. Skin was cut away from the leg to expose the lateral saphenous vein which runs from the knee up towards the femoral, as far as the first visible bifurcation. A 2cm portion was taken from just above the knee and stored in cold physiological salt solution (PSS) until required. On some days an identical portion was taken from both legs to allow a second day of experiments on the same animal. There was no difference in responses when tissue was used immediately compared to the same experiment repeated after 24 hours refrigeration.

Saphenous vein was cleaned of connective tissue under a dissecting microscope and cut into 4x4mm ring segments. These were suspended in 30ml organ baths by fine wire hoops, taking care not to damage the endothelium. The upper wire was attached by thread to a Grass FT03c transducer, balanced by Flyde Electronics FE BBS bridge conditioners, to a Linseis L2006 chart recorder for display of isometric tension. The lower wire was connected to a glass tissue holder, which incorporated dual platinum plates parallel to the tissue for electrical field stimulation (EFS). A multi-channel stimulator from Applegarth Electronics produced square wave pulses.

The mounted rings were immersed in PSS and continuously bubbled with 95% O₂ : 5% CO₂ at 37°C. They were placed under an initial tension of 2g, which in this preparation gives the optimal contractile response, and re-tensioned to that level after 20 minutes. A minimum of 40 minutes was then given for equilibration before starting the experimental protocol.

Protocol

After equilibration, a sighting concentration of 1µM noradrenaline (NA) was added to each bath and the tissues allowed to contract to the plateau phase. The presence of a

functioning endothelium was then assessed by relaxation to 1 μ M acetylcholine (ACh). After a 30-minute wash out, this was repeated in 8-week animals or a full ACh concentration response curve (CRC) constructed in 32-week rabbits. After a further 30-minutes wash period, frequency response curves were constructed for the range 4, 8, 16, 32, and 64Hz. Each square wave pulse was delivered at 5-minute intervals, with a train duration of 1s, 0.1ms pulse width, at 35 volts. FRCs were repeated after 30 minutes incubation with 1 μ M cocaine and then 100 μ M L-NAME. Optimal blockade of nitric oxide synthase by L-NAME was confirmed by absence of relaxation to ACh.

Drugs

Composition of PSS was as follows (mM): NaCl, 118.4; KCl, 4.7; CaCl₂, 2.5; MgSO₄·7H₂O, 1.2; NaHCO₃, 24.9; KH₂PO₄, 1.2; and glucose, 11.1. Na₂ EDTA at 23 μ M was included to prevent oxidative degradation of NA.

The following drugs were used: noradrenaline bitartrate (Sigma), acetylcholine chloride (Sigma), N^o-nitro-L-arginine methyl ester (L-NAME) (Sigma), and cocaine HCl (Macarthis).

7.3 Results

Results with animals 8- and 32-weeks after coronary artery ligation were essentially identical and are presented side-by-side. The results are not directly comparable between 8- and 32-weeks as electrodes for electrical field stimulation were replaced between these two groups of animals. Therefore, results are not drawn on the same graphs. After washing, and a further 30-minutes

Ejection fraction measured by echocardiography for 32-week animals is shown in Figure 7.1. Systolic dysfunction was mild in the ligated animals, with a mean ejection fraction of 48.5%, but the difference was highly significant.

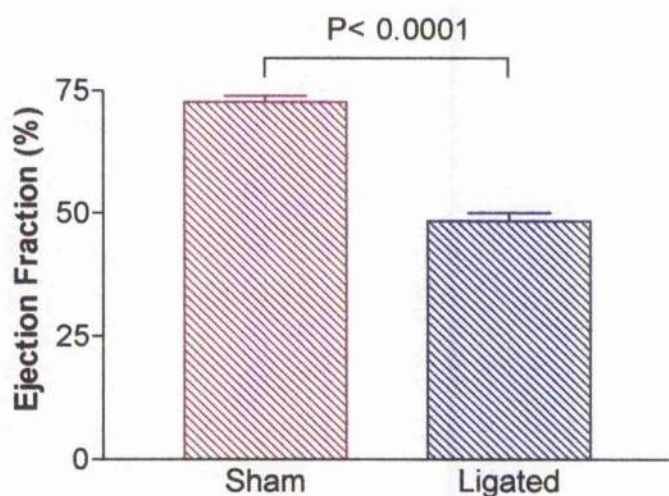


Figure 7.1 Left ventricular ejection fraction in rabbits 32-weeks after coronary artery ligation. Data are mean \pm sem, n=6 in each group.

The maximum relaxant response to acetylcholine (ACh) was tested in rings pre-contracted with noradrenaline (NA). In the 8-week animals, there was a trend for ligated animals to exhibit reduced relaxation, however, this difference was small and failed to reach significance (Figure 7.2). A full concentration response curve for ACh was constructed in the 32-week animals (Figure 7.3). Again there was a trend for a reduced maximal response and sensitivity to ACh that was not statistically significant.

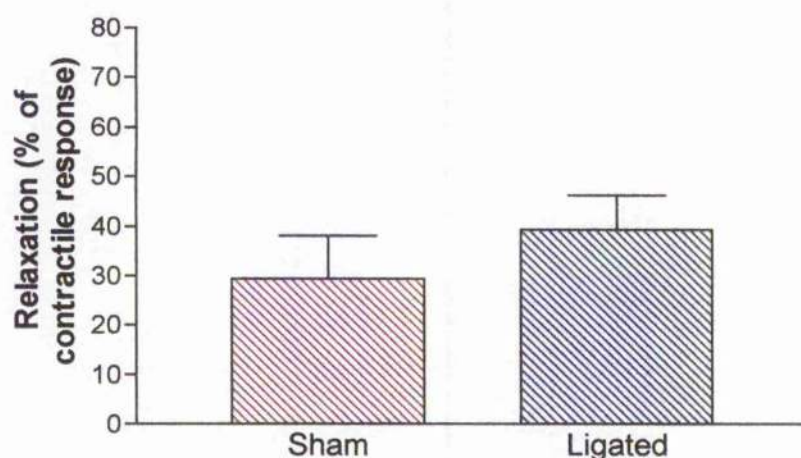


Figure 7.2 Relaxation responses to 1 μ M ACh in rabbit saphenous vein from sham and ligated animals. Rings were pre-contracted with 1 μ M NA. Data are mean \pm sem, there was no significant difference between groups (n=11 in each).

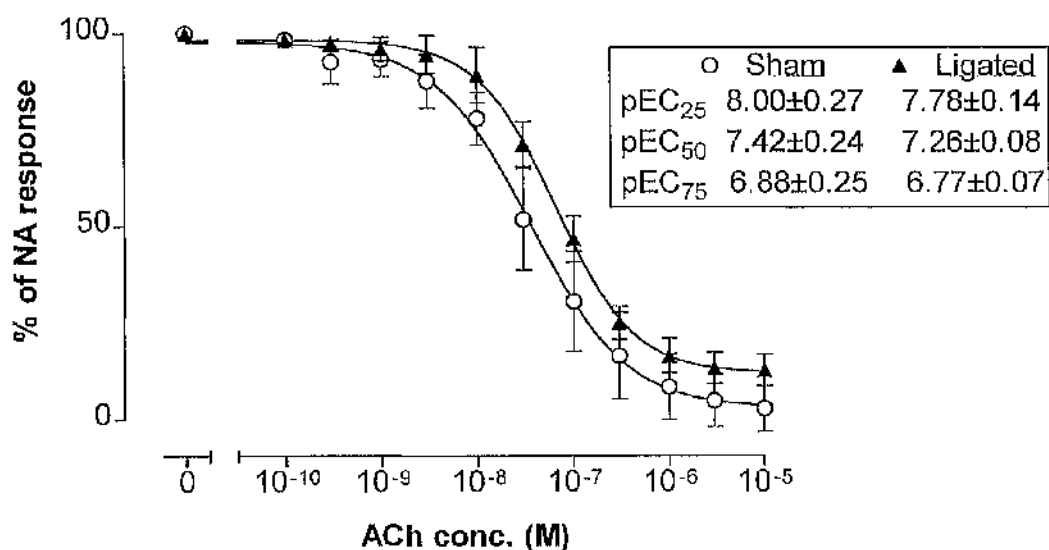


Figure 7.3 ACh concentration response curves in rabbit saphenous vein 32-weeks after CAL. There were no significant differences in either maximal responses or sensitivity between sham and ligated animals (mean \pm sem, n=6 in each).

Frequency response curves were constructed in the range of 4-64Hz in the presence and absence of cocaine (1 μ M) to block neuronal uptake of noradrenaline, and of L-NAME (10⁻⁴M) to inhibit nitric oxide synthase. Responses at 8- and 32-weeks show the same picture. There are no differences between sham and ligated animals in their response to electrical field stimulation (Figure 7.4), nor in the presence of cocaine (Figure 7.5) nor in the presence of L-NAME (Figure 7.6). All data are presented as raw developed tension in milligrams, however, the same results are obtained when responses are normalised to maximum contractile response.

Contractions are potentiated by cocaine by around 100%, and this increase is similar in both sham and ligated groups. Likewise, a further doubling of contractile response is observed on incubation with L-NAME, with again no difference between groups.

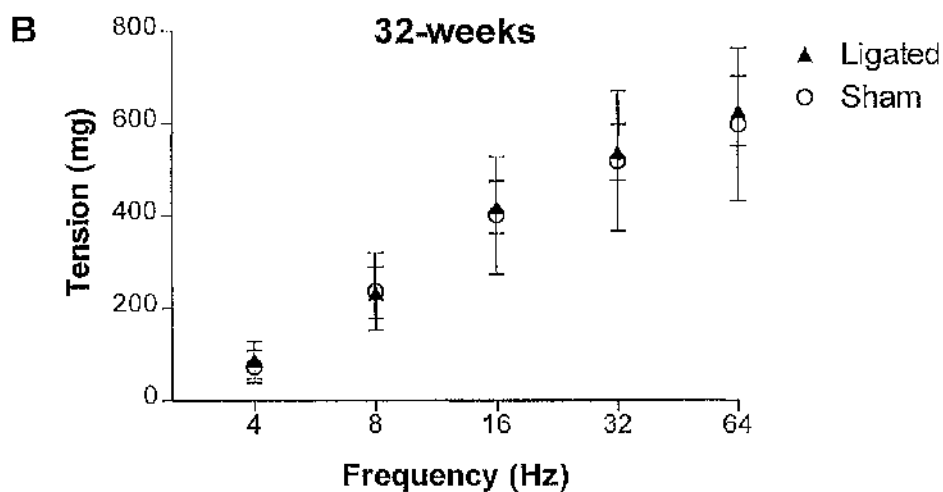
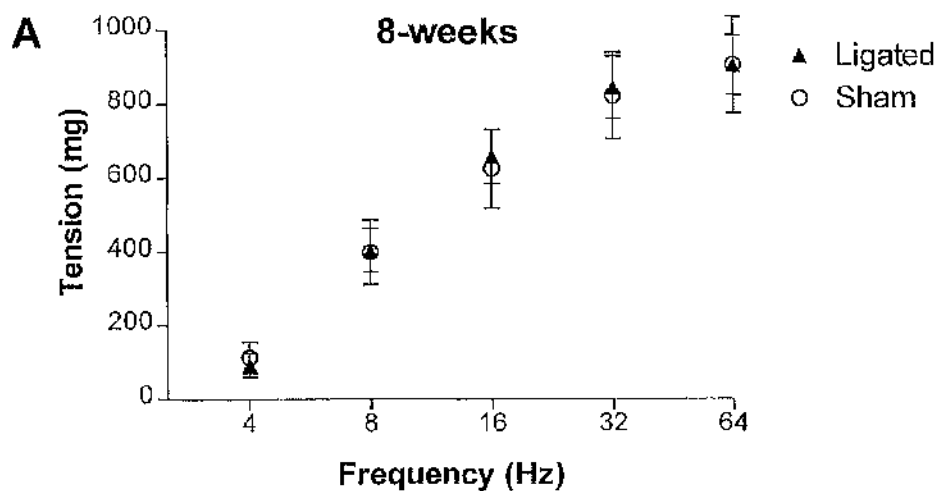


Figure 7.4 Frequency response curves in rabbit saphenous vein from sham and ligated animals. Data show developed tension at 8-weeks (A) and 32-weeks (B) after coronary artery ligation. Data are mean \pm scm, n=11 in each group at 8-weeks, and n=6 for each group at 32-weeks.

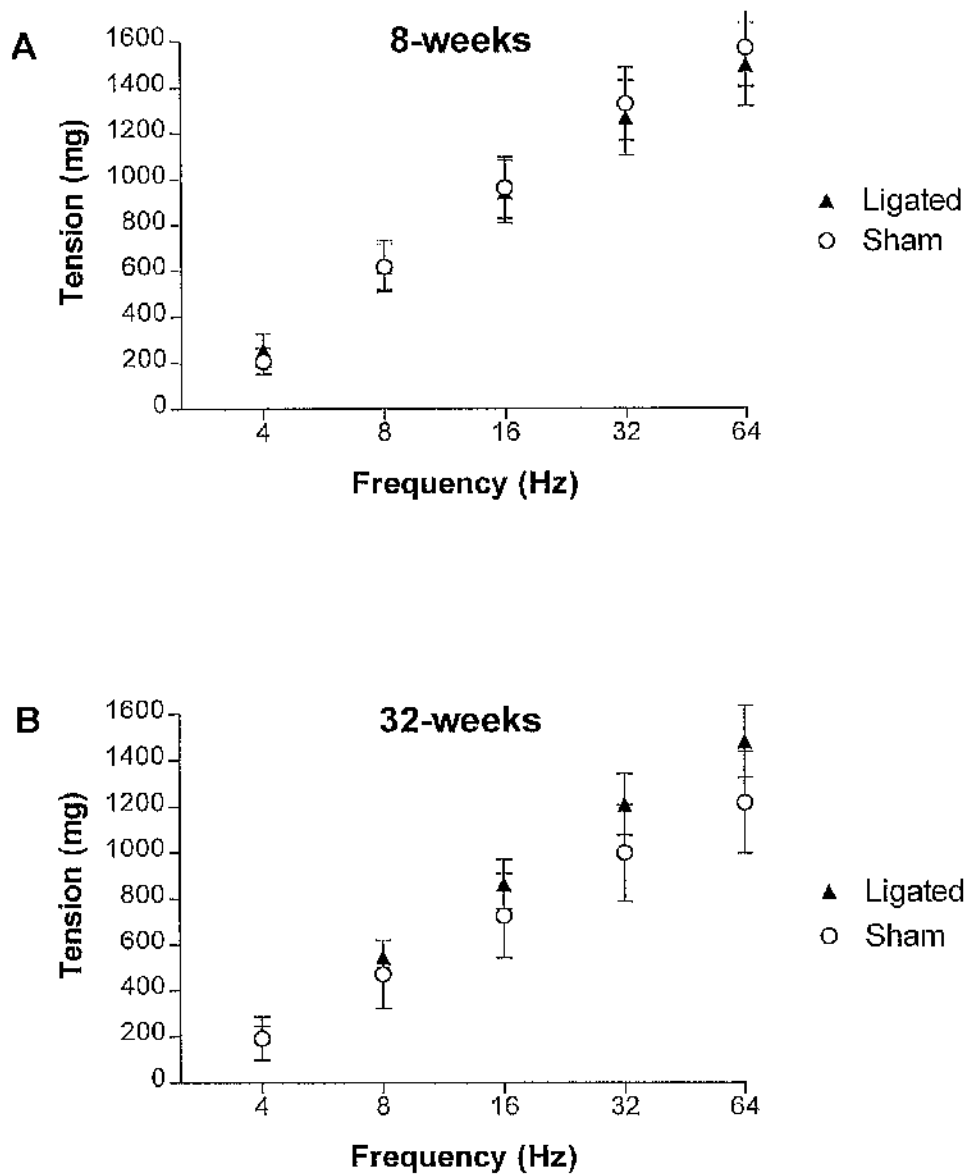


Figure 7.5 Frequency response curves in rabbit saphenous vein in the presence of cocaine ($10^{-6}M$) from sham and ligated animals. Data show developed tension at 8-weeks (A) and 32-weeks (B) after coronary artery ligation. Data are mean \pm sem, $n=11$ in each group at 8-weeks, and $n=6$ for each group at 32-weeks.

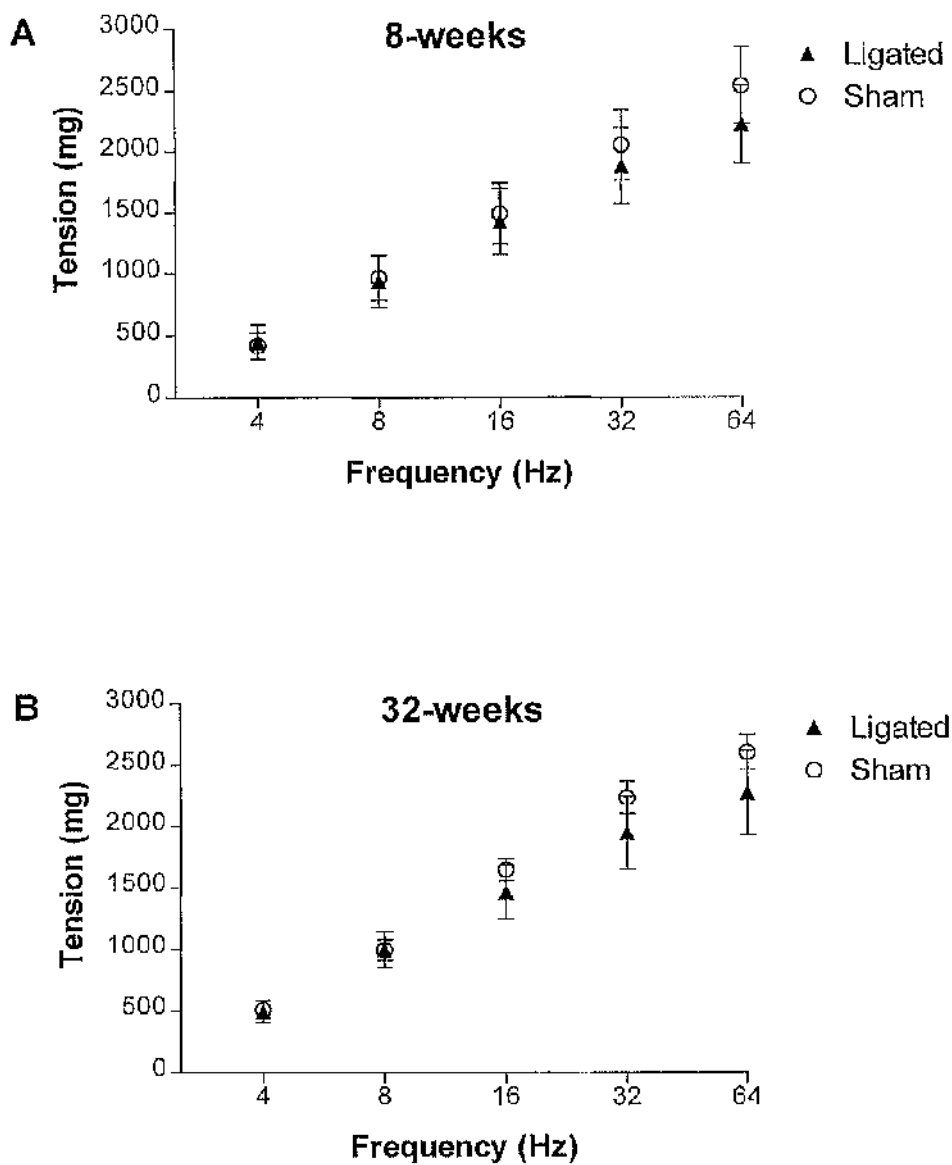


Figure 7.6 Frequency response curves in rabbit saphenous vein in the presence of L-NAME (10^{-4} M) from sham and ligated animals. Data show developed tension at 8-weeks (A) and 32-weeks (B) after coronary artery ligation. Data are mean \pm sem, $n=11$ in each group at 8-weeks, and $n=6$ for each group at 32-weeks.

7.4 Discussion

After coronary artery ligation in these rabbits, LV systolic function was compromised, as evidenced by a reduced ejection fraction (Figure 7.1). As dysfunction was only moderate, this diminishes the ability of this study to distinguish changes that may only be apparent in more severely affected animals.

Responses to ACh were similar in both sham and ligated groups, although responses in ligated animals tended to be less (Figures 7.2 & 7.3). The fact that this trend was observed in both groups suggests that this small difference may be real, but is unlikely to be physiologically important. Contractions of saphenous vein were not observed at high concentrations of ACh (Figure 7.3), therefore, endothelium-derived vasoconstricting prostanoids are not prominent in this tissue.

Electrical field stimulation was used to determine alterations at the neuromuscular junction. Sympathetic activity is elevated in heart failure and could result in altered sensitivity to neurotransmitters, or changes in sympathetic innervation, or alterations in NA clearance. A parallel exists for this in hypertension, where blockade of NA uptake with cocaine causes a leftward shift in the concentration response curve for NA, which is greater in small arteries from hypertensive subjects than in their normotensive counterparts, suggesting increased uptake of NA in hypertension (Mulvany, 1991). However, no such difference was observed in this heart failure model. Frequency response curves were normal between sham and ligated rabbits at both time-points (Figure 7.4), and were potentiated to a similar extent when neuronal amine uptake was blocked by cocaine (Figures 7.5).

Nitric oxide has been shown to modulate neurogenic vasoconstriction in the rabbit saphenous vein (Gordon *et al.*, 1992), and this was confirmed in the present study. Inhibition of nitric oxide production with L-NAME strongly increased the responses to electrical field stimulation. However, once again, there was no difference between sham and ligated groups in this regard (Figure 7.6). This is in contrast to the arterial circulation where impaired endothelium-dependent release of nitric oxide has been implicated in the vascular dysfunction observed in the aortas of rats after CAL (Ontkean *et al.*, 1991; de Vries *et al.*, 1997).

7.5 Conclusions

In the saphenous vein of rabbits after coronary artery ligation, there is no alteration in responses to endothelium-dependent relaxation, nor to electrical field stimulation. In particular, neuronal uptake of NA is normal, as is the modulation of neurogenic vasoconstriction by nitric oxide. These observations were true, whether compared early at 8-weeks or late at 32-weeks after coronary artery ligation.

These results do not exclude a role for venous dysfunction in animals with more severe left ventricular dysfunction.

8. General Discussion

Several techniques used in this thesis were common to more than one chapter. This section will discuss the overlap between these chapters and make suggestions for further work where appropriate.

Echocardiography in the rat was used extensively in this thesis. In Chapter 3, the estimation of LV mass by echocardiography was validated against actual LV mass measured at autopsy, and a good positive correlation was obtained. Measures of repeatability were also calculated for serial measurements, and these were utilised in Chapters 4&5. Altogether, experience was gained of over 300 echocardiographic examinations in the rat. The optimum conditions were the use of light sedation with Hypnorm, with the rats in the left lateral position, the chest fur closely shaved, and using copious amounts of gel. In this way, parasternal short-axis views at the level of the papillary muscles were readily obtained.

The results in Chapter 3 were collated during the learning curve for this procedure, and the measures of repeatability reflect this. It is fair to say that echocardiographic measurements were probably more accurate in the subsequent chapters. For example, serial assessment of ejection fraction in sham operated rats exhibited very little variation in Chapter 5 (Figure 5.3), as did LV luminal cross-sectional area (Figure 5.4). Chapter 5 also indicated that useful data could be obtained using echocardiography in the infarcted heart without the need to make assumptions concerning LV geometry. For example wall thickness measurements of the surviving myocardium (Figure 5.6).

Further work in this area could include validation of ejection fraction measurements against ejection fraction calculated using the thermodilution method (Pye *et al.*, 1996). This would allow determination of an absolute value for ejection fraction in these rats. This would be particularly useful to validate in rats after coronary artery ligation, since the assumptions made in calculating ejection fraction in these animals are even greater than in normal rats. Doppler flow measurements would also be an attractive proposition in these animals, in order to more accurately assess LV global function. However, this would require the acquisition of a higher frequency transducer (10MHz), as the present set-up did not have the resolution to image the LV outflow diameter.

Another attractive proposition would be to combine radiotelemetry with echocardiography. A telemetry probe implanted with a catheter to the abdominal aorta, would be capable of accurate measurements of systolic and diastolic blood pressure and heart rate. Combined with simultaneous echocardiographic measurements this would allow calculation of such parameters as wall stress, which is thought to be an important factor in myocardial thickening and dilatation after myocardial infarction (Hsu *et al.*, 1998a). It would also allow the measurement of blood pressure before, during and after coronary artery ligation in order to study the interaction between elevated blood pressure and infarct size. There is extensive experience of radiotelemetry in this laboratory, and it remains an option for future work if mortality after coronary artery ligation can be kept low.

Northern blot analysis for measurement of natriuretic peptide gene expression was utilised in both hypertensive (Chapter 4) and heart failure rats (Chapter 5). The relative abundance in atrial and left ventricular tissues reported in Chapter 4 mirrored the published values for the SHRSP (Ogawa *et al.*, 1991). Given that BNP concentration is a good prognostic indicator in heart failure in man (Nagaya *et al.*, 1999), it was surprising that activation of mRNA in the left ventricle failed to reach statistical significance after coronary artery ligation in the rat. This was the first such measurement in the rat, and may simply represent a species difference, or the moderate infarct size in this model. Another possibility is that BNP gene expression is elevated in the LV by sham operation, such that any difference is masked. It would be interesting to compare levels of BNP mRNA between sham, ligated and age-matched stock animals to clarify this point.

The two most interesting observations in this thesis arise from the laser scanning confocal microscope work. In Chapter 4, treatment with either irbesartan or H+H was found to be equally effective in preventing the vascular hypertrophy observed in control SHRSP. This was surprising given the wealth of evidence implicating Ang II in this type of structural remodelling (discussed fully in Chapter 4). As this technique used a nuclear dye it was not possible to determine whether the greater medial thickness in untreated hypertensive animals was due to hypertrophy of smooth muscle cells or deposition of extra-cellular matrix. Work is ongoing in this laboratory to answer this problem by the use of extracellular dyes.

In Chapter 5, confocal microscopy allowed the description of a novel type of structural adaptation not previously described in vessels from heart failure animals. Namely, a 24% reduction in the density of smooth muscle cells in the medial layer. This could have obvious implications to impair vascular function. Given more time, it would have been interesting to assess function in these vessels using wire or perfusion myography. From the structural data, you would hypothesise a generalised hyporeactivity to vasoconstrictors, particularly in response to KCl.

It is also tempting to speculate that apoptosis may be involved in the loss of smooth muscle cells. Nuclear condensation and fragmentation should be observable using propidium iodide in the confocal studies. This would be an interesting experiment for the future, but was not performed due to the time consuming nature of this type of search. It may also be necessary to examine rats at different time points after ligation to determine if apoptosis is more prevalent at a particular stage.

The use of the above techniques in both hypertensive and coronary artery ligated rats has provided valuable data that begs the question of what would happen if both conditions were superimposed, as is commonly observed in man. For example, can the already severely hypertrophied SHRSP heart exhibit further hypertrophy in response to CAL? What effect will this have on progression to heart failure? Likewise, will loss of smooth muscle cells from the media of the resistance arteries also occur in vessels with medial hypertrophy? Is there a functional consequence of this? This was the rationale for attempting to ligate the coronary arteries of SHRSP in Chapter 6, and this model will be further developed in this laboratory.

Appendix I Drugs & solutions

Tris-Acetate (TAE) Buffer

Stock solution made at 50x strength

Tris base	242g
Glacial Acetic Acid	57.1ml
0.5M EDTA (pH8.0) to	100ml

Stock solution was diluted with H₂O for 1 x TAE buffer.

Agarose Blue Loading Dye

For a 6x solution

Ficoll	1.5g
Bromophenol Blue	25mg
Xylene Cyanol	25mg
H ₂ O to	10ml

20x SSC

NaCl	175.3g
Na ₃ Citrate	88.2g
Distilled H ₂ O	800ml

Adjusted to pH 7.0 with 1M HCl, made up to 1000ml with H₂O and autoclaved.

TE

1M Tris pH 8.0	200μl
0.5M EDTA pH 8.0	40μl
Distilled H ₂ O to	20ml

20x SSPE

NaCl	175.3g
NaH ₂ PO ₄	27.6g
Na ₂ EDTA.2H ₂ O	7.4g
Distilled H ₂ O	900ml

Adjusted to pH 7.4 with 1M NaOH, made up to 1000ml with H₂O and autoclaved.

Sodium Dodecyl Sulphate (SDS 10% w/v)

Electrophoresis grade SDS	50g
Distilled water	450ml

Solution was heated to 68°C to aid dissolution, pH adjusted to 7.2 with 1M HCl and made up to 500ml with distilled water.

Northern blot – wash protocol & solutions

1. 2x rinse at room temperature with 20ml wash solution 1.
2. 2x 15 minute at 42°C with 20ml wash solution 1.
3. 2x 10minute at 42°C with 20ml wash solution 2.
4. 2x 30 minutes at 42°C with 20ml wash solution 2.

Wash solution 1 :	20x SSPE	20ml
	10% (w/v) SDS	2ml
	Distilled H ₂ O	178ml

Wash solution 2 :	20x SSPE	10ml
	10% (w/v) SDS	2ml
	Distilled H ₂ O	188ml

Physiological salt solution (PSS or Krebs)

Composed of (mM) NaCl 118.4, KCl 4.7, CaCl₂ 2.5, MgSO₄.7H₂O 1.2, NaHCO₃ 24.9, KH₂PO₄ 1.2 and glucose 11.1 made up in distilled water at pH7.4

Na₂EDTA was added at 23µM to prevent oxidation of noradrenaline.

Infarct Histology – wax removing protocol

xylene 5mins

xylene 5mins

100% ethanol quick wash

100% ethanol “ “

96% ethanol “ “

96% ethanol “ “

70% ethanol “ “

deionised water “ “

Infarct Histology – Staining protocol

1. Azan I at 37°C for 30mins
2. Wash in deionised water
3. 5% phosphotungstic acid at room temperature for 45mins
4. Wash in water
5. Azan II 1:3 in deionised water at room temp. for 10 mins
6. Wash in 96% alcohol
7. Dehydrate: wash in 70% alcohol, 96%, 96%, 100%, 100%, xylene, xylene
8. Fix coverslip.

Azan I

Azocarmine G 0.5g (Sigma)

Deionised water 100ml

Conc. acetic acid 1ml

Dissolve by heating, cool down and filter.

Azan II

Aniline blue, water soluble 0.5g (Clin-tech; colour index 42755))

Orange G 2g (Sigma)

Conc. acetic acid 8ml

Deionised water 100ml

Dissolve by heating, cool down and filter.

Suppliers

10x denaturing gel buffer	Ambion
Northern sample loading dye	Ambion
Pre-hybridisation / hybridisation solution	Ambion
Ready to Go DNA labelling beads	Pharmacia Biotech
Agarose electrophoresis grade	Ambion
Nick Columns	Pharmacia Biotech

Appendix II

Detailed notes on Thoracotomy & Coronary Artery Ligation in the rat.

Pre-operatively.

1. Administer 0.2ml of ampicillin I.M. 24-hours prior to procedure.
2. Switch on heating pad at least 30 minutes before procedure. Temperature under a 500g weight should be $\sim 35^{\circ}\text{C}$.
3. Rats should weigh a minimum of 270g, preferably 300g, to achieve the lowest mortality rates.
4. Make Hypnorm + Hypnovel mixture: Draw 1ml of Hypnovel (midazolam) into syringe and make to 10ml with normal saline. Take 0.2ml of this mixture and add 0.2ml of Hypnorm (fentanyl + fluanisone). Administer the full 0.4ml mixture I/P. This dose will suit a 300-400g rat and can be adjusted accordingly outside this range.
5. Once the animal has lost consciousness shave entire left chest from sternum to half-way across back. Give supplemental oxygen until ready for intubation.

Intubation

6. To intubate: lie animal on its back. It is important to keep the animal straight with the head raised. The mouth is kept open by an elastic band looped round the incisors and pulled downward. A better view can be obtained by using forceps to push apart the animal's cheek pouches. Shine one light source into the mouth and the other directly onto its throat. The head is pulled back and the tongue lifted out of the way. The intubation spatula is advanced to the back of the pharynx and used to push the tongue upwards. A cotton bud wetted with normal saline may be used to moisten the entrance to the trachea, which can be visualised by the appearance of a small spot of light appearing with each inhalation. The cannula is directed towards this and a few moments of gentle pressure gains entrance into the trachea and advancement of the cannula approximately x cm. Intubation is with a white cannula (or red cannula for large rats) the tip of which has been cut diagonally and the edges

blunted. When placing the tube, the long end of the tip must be orientated upwards. Marking the tip black will aid visibility while intubating. The cannula is in the trachea if you can still see the light when you look down the tube. If it is pink then the tubing has entered the oesophagus.

7. Lie the animal on its right side and start ventilating. Ensure cannula is in the lungs by listening for breath sounds with a stethoscope. A whooshing sound should be heard entering the lungs in time with the ventilator. If this sound can be heard in the stomach, then the lungs are not being ventilated, the tube should be removed and intubation re-started. If the animal looks blue then give it oxygen for a few minutes before trying again. The whooshing sound should be at the same volume on both sides of the chest. If it is not then adjust the depth of cannula until it is. It is of fundamental importance to ventilate both lungs, as during the procedure, the left lung is collapsed.
8. When ventilation is satisfactory, tape the tube in place. Immobilise the head relative to the tube by taping the animal's paw over its head on to the table. Place a gauze swab over its eye and tape the head to the cannula. The object being to prevent the possibility of the cannula advancing further or being pulled out during surgery.

Monitoring

9. The assistant applies light pressure to the throat in order to obtain a good seal. This can be assessed by the waste gases, which are vented to a glass beaker filled with ~1cm of water. To apply positive end expiratory pressure, the exit tube should be 0.5cm below the water surface. If there is a good seal then the bubbles leaving the tube will be of a regular size and speed. A squeaking sound in the throat means air is escaping around the vocal chords and the seal should be readjusted.
10. The assistant should also monitor heart rate throughout the procedure by feeling for the femoral pulse. Any change in strength or rate should be noted. If the pulse is lost then the heart should be felt for through the chest. The finger should be rested periodically to prevent desensitisation. If the pulse slows or weakens this may be a sign that too much halothane has been given, as this is a cardiac depressant. Action should be rapid to reduce or switch off the halothane. A level of 0.25 - 0.5% in oxygen (flow rate 0.4L/min.) is usually sufficient for the procedure. However, the

minimum should be used depending on the individual reaction of the rat, and some may not even need any. N.B. If nitrous oxide is available then this should be used at a continuous flow rate of 200ml/min, and will greatly reduce the amount of halothane required (nitrous oxide is less cardiac depressant). Another cause of a depressed or irregular heart rate is mechanical stimulation of the carotid body possibly interfering with the baroreceptor reflex. This is due to the position of the assistant's hand on the throat, and often simply repositioning this will solve the problem.

11. Throughout the procedure it is a good practice to keep an eye on the colour of extremities such as feet and ears as an indicator of how well the animal is being perfused.

Thoracotomy

12. Spray the surgical area with chlorhexidine skin disinfectant. Take the paper surgical towel and cut a 2 inch² hole to form a hernia towel.
13. The incision should be made between the 4th and 5th intercostal space. As the ribs are difficult to count accurately in the rat, you should feel for the first ribs that attach to the sternum (as opposed to loosely attached to the xiphisternum). The rib space one up from this is where to make the incision with the scalpel blade. The incision should be around 3cm long, running parallel with the ribs, and just breaking the skin. Open the top connective tissue layer by blunt dissection using the small curved scissors. Any bleeding from superficial arteries may be stopped or prevented using electrocautery. If this is not available then use the gauze swabs to exert pressure on the bleeding area for a few minutes. Also, if arteries are cut cleanly in one motion, perpendicular to their flow, then they should not bleed. Use blunt dissection to loosen the skin all around the incision.
14. The muscle layer should be prised apart and cut in a similar fashion, this seldom bleeds in the rat.
15. Great care should be taken when the intercostal muscles are reached. One hand is used to steady the animal while a pair of fine blunt forceps are used to slide underneath the muscle layer. This can then be held up out of the way of the lungs to

- allow cutting with scissors (remember to always keep the points upwards away from the lungs). Continue in this way until the sternum is reached, and the lungs exposed.
16. The obvious danger is that the lungs may be damaged or punctured during this procedure. If you suspect that the lung has been punctured confirm this by drawing a few millilitres of saline into a syringe barrel and dribbling over the lungs looking for air bubbles. A very small hole may heal spontaneously if covered with a Q-tip for a few minutes, but most punctures will necessitate the removal of that lung. To do this, collapse the lung with a piece of gauze and use a length of mersilk 0 to tie off the entire lung at the level of the bronchi. Then cut off the lung close to this tie. Care must also be taken to avoid the internal thoracic artery, which runs alongside the sternum.
 17. Collapse the left lung by folding a small square of gauze and using it to envelope the lung which can then be gently pushed downward and away from the heart using a Q-tip. If at this stage the animal starts breathing against the pump, this is indicative that the right lung is not being ventilated, if this is the case, the heart will fall down, away from the incision as the right lung no longer supports it. (N.B. do not give more anaesthetic, the gasping is a strong chemoreceptor reflex due to the lack of oxygen, not because the animal is too light.) Action must be immediate, to re-gain the seal, re-position intubation tube or re-inflate left lung as soon as possible.
 18. The pericardium may now be removed by pinching with a pair of bent blunt forceps and tearing a hole by counter pressure with a Q-tip. This is best done close to the level of the atria, as near the apex there is the risk of also rupturing the pleura of the right lung. With the Q-tip, brush the pericardium down and behind the heart, such that the heart is fully exteriorised. Slight pressure with the hand to the outer chest wall will lift the heart up and out of the cavity which may be useful for ligation, however, cardiac function is compromised due to incomplete filling of the ventricles, and so this position should not be maintained for long.

Ligation

19. To ligate the coronary artery an apical tie is first placed in the apex. This consists of a simple suture pulled through the myocardium but not tied. The ends of this can be pulled to exteriorise the heart and hold it steady, and after the ligation is complete

the suture is pulled out again. Ethibond 4/0 can be used for this and also for the coronary artery ligation (remember the right ventricle extends down to the apex and care should be taken not to put suture through this). Locate the coronary artery by looking for the coronary vein, the artery is embedded in the myocardium just to the right of this. To ligate, use the curve of the needle to take a small bite the full thickness of the myocardium a few mm from the origin of the artery. When tying, take care not to lift the heart upwards to avoid tearing the myocardium. The infarcted area will appear blanched within minutes and an estimate of infarct size can be made at this point. If this is less than 30-40% then a further ligation can be made closer to the origin of the artery, or taking out another branch.

20. After ligation, replace the heart back in the chest and wait with the incision open for 15 minutes. This represents the most likely time period for cardiac arrhythmia's after myocardial infarction in the rat i.e. at 7 and 14 minutes. If the heart stops during this time it is possible to manipulate it manually to re-start rhythm. After 15 mins the chest may be closed as outlined for sham animals

Closing up.

21. The heart is then coaxed back into the pericardium using a Q-tip and the gauze removed from around the lung, which will slowly begin to inflate. In this time the ribs are closed using chromic catgut as an interrupted suture. The ribs should be held using toothed forceps, and extreme care taken not to puncture the lungs. If necessary the assistant can take pressure off the throat to decrease ventilation and allow the lung to fall back out of the way. The first suture is most important in getting the wound to line up evenly and ensure adequate healing. The ribs form a natural elbow, and the first suture should be placed here, splinting both ribs together. When pulled together, the whole wound should approximate to a perfect fit. A further two sutures are placed equidistant along the wound, then the first is tied. Pull the suture up to expand the thorax, and hyper-inflate if necessary to expel any air from the lung cavity, thereby preventing a pneumothorax. Tie the remaining two sutures.
22. Close the muscle layer using the Ethibond sutures and an interrupted stitch. Ragged pieces of muscle should be cut off at this stage as these will become necrotic

if left. Finally, use the Dexon to close the skin layer with a continuous subcutaneous stitch. When finishing the stitch, pull the knot back into the wound and exteriorise about 1cm away, and cut short. Gaseous anaesthetics may be stopped at this stage. Three large holding stitches are then placed equidistant to one another along the wound. These serve as extra support, but also as something for the animal to nibble rather than attack the more important sutures.

23. Give 0.2ml buprenorphine S.C. to reverse the actions of the Fentanyl. Then remove the tape restraints and unplug the intubation tube from the ventilator. The animal should start spontaneous respiration within ~30 seconds. If it does not, then continue ventilation testing periodically. If the animal's respiration is good and even, then remove the tube and place it on its front.

Post-operative care.

24. Give ~3ml of normal saline S.C. Place in a recovery cage with some vet bed and a heat lamp if cold. Keep an eye on the animal until it regains a righting reflex when gently pushed over. At this stage it can return to the animal facility. Keep the vet bed for the first 24 hours.
25. First thing next morning the animal should be checked and given a second 0.175ml S.C. dose of buprenorphine as pain relief. Pain should be assessed on an individual basis, and particularly with sham animals, it may be appropriate to reduce or forgo this dose. A further 3-4ml of S.C. saline should be given daily until the animal's weight begins to rise. Try and tempt the animal to eat by making mash out of water and chow and placing on the floor of the cage, add sweetened condensed milk if the animal is still not eating. If weight loss >20% then inform the vet. The animal may require to be euthanased.
26. Post-operatively look at regularity of breathing, listen for breath sounds. Is the animal moving freely? Is there fresh faeces and urine in the cage? Are there signs that the animal has been eating? A red discharge from the eyes, which may colour surrounding fur pink, is a common sign of stress in the rat. This should only last a few days post-operatively. Pilo-erection is a sign of pain, as is a lack of interest in the surroundings and absence of grooming, resulting in loss of sheen from the coat.

Check the wound daily for signs of infection. Remaining sutures should be removed 7-10 days post-op.

Equipment suppliers.

Adams Healthcare – there are no laryngoscopes small enough for the rat, and finding the right shaped tool can be difficult. We have used a Macdonald dissector 19cm (51-5299)

Fine Science Tools – selection of surgical instruments

Harvard Apparatus – small animal ventilator

Ethicon – Ethibond Excel 4/0 (W6935) polyester braided non-absorbable suture

Chromic 3/0 (W437) catgut absorbable suture

Mersilk 0 (W224) silk braided non-absorbable suture

Sherwood Davis & Geek – Dexon II 2/0 (6160-87B) braided polyglycolic acid with polycaprolate coating.

Drugs

Anhydrous ampicillin Ph. Eur. 100mg/ml (Amfipen® LA) Intervet UK Ltd, Cambridge.

Midazolam HCl B.P. 10mg/2ml (Hypnovel®) Roche, Welwyn Garden City, UK.

Buprenorphine HCl 0.3mg/ml (Vetergesic®) Reckitt & Colman Products Ltd., York.

Fentanyl citrate 0.315mg/ml + fluanisone 10mg/ml (Hypnorm®) Janssen Animal Health, High Wycombe, UK.

Halothane Ph. Eur. 100% w/w (Fluothane®) Zeneca, Macclesfield, UK.

Pentobarbitone Sodium B.P. 200mg/ml (Euthatal®) Rhône Mérieux, Harlow, UK.

Sodium Chloride 0.9% for injection, Baxter Healthcare, UK.

References

- Aalkjaer, C., A. M. Heagerty, and M. J. Mulvany. In vitro characteristics of vessels from patients with essential hypertension. *Journal of Clinical Hypertension* 3: 317-322, 1987.
- Akiyama, K., H. Suzuki, P. Grant, and R. J. Bing. Oxidation products of nitric oxide, NO₂ and NO₃, in plasma after experimental myocardial infarction. *J Mol Cell Cardiol* 29: 1-9, 1997.
- Alderman, M. H., H. Cohen, and S. Madhavan. Epidemiology of risk in hypertensives. Experience in treated patients. *Am J Hypertens* 11: 874-876, 1998.
- Ambrose, J., D. G. Pribnow, G. D. Giraud, K. D. Perkins, L. Muldoon, and B. H. Greenberg. Angiotensin type 1 receptor antagonism with irbesartan inhibits ventricular hypertrophy and improves diastolic function in the remodelling post-myocardial infarction ventricle. *J Cardiovas Pharmacol* 33: 433-439, 1999.
- Anand, I. S., D. Liu, S. S. Chugh, A. J. C. Prahash, S. Gupta, R. John, F. Popescu, and Y. Chandrashekhar. Isolated myocyte contractile function is normal in postinfarct remodeled rat heart with systolic dysfunction. *Circulation* 96: 3974-3984, 1997.
- Andersson, O. K., T. Almgren, B. Persson, O. Samuelsson, and T. Hedner. Survival in treated hypertension: follow up study after two decades. *BMJ* 317: 167-171, 1998.
- Angus, J. A., C. P. Ferrier, K. Sudhir, D. M. Kaye, and G. L. Jennings. Impaired contraction and relaxation in skin resistance arteries from patients with congestive heart failure. *Cardiovasc Res* 27: 204-210, 1993.
- Antonios, T. F. T., D. R. J. Singer, N. D. Markandu, and P. S. Mortimer. Structural skin capillary rarefaction in essential hypertension. *Hypertension* 33: 998-1001, 1999.
- Anversa, P., A. V. Loud, V. Levicky, and G. Guideri. Left ventricular failure induced by myocardial infarction. I. Myocyte hypertrophy. *Am J Physiol* 248: H876-H882, 1985a.
- Anversa, P., A. V. Loud, V. Levicky, and G. Guideri. Left ventricular failure induced by myocardial infarction. II. Tissue morphometry. *Am J Physiol* 248: H883-H889, 1985b.

- Arribas, S. M., C. J. Daly, J. F. Gordon, and J. C. McGrath. Confocal myography: applications for the study of resistance arteries. In Halpern, W., ed. *The resistance arteries: integration of the regulatory pathways*. New Jersey, USA, Humana Press. 1996, 259-264.
- Arribas, S. M., C. Hillier, C. Gonzalez, S. McGrory, A. F. Dominiczak, and J. C. McGrath. Cellular aspects of vascular remodelling in hypertension revealed by confocal microscopy. *Hypertension* 30: 1455-1464, 1997.
- Au, T. L. S., G. A. Collins, B. A. Macleod, and M. J. A. Walker. Effects of prostaglandin E₂, propranolol and nitroglycerine with halothane, pethidine or pentobarbitone anaesthesia on arrhythmias and other responses to ligation of a coronary artery in rats. *Br J Pharmacol* 79: 929-937, 1983.
- Baggia, S., K. Perkins, and B. Greenberg. Endothelium-dependent relaxation is not uniformly impaired in chronic heart failure. *J Cardiovas Pharmacol* 29: 389-396, 1997.
- Baker, K. M., M. I. Chernin, S. K. Wixson, and J. F. Aceto. Renin-angiotensin system involvement in pressure-overload cardiac hypertrophy in rats. *Am J Physiol* 259: H324-H332, 1990.
- Balke, C. W. and S. R. Shorofsky. Alterations in calcium handling in cardiac hypertrophy and failure. *Cardiovasc Res* 37: 290-299, 1998.
- Balligand, J.-C., D. Ungureanu-Langrois, and T. W. Smith. Role of a cytokine-inducible nitric oxide synthase in the control of myocardial contractile state. *Heart Failure Reviews* 1: 193-201, 1996.
- Ben-Ishay, D., J. Mekler, and R. Saliternick-Vardi. Sabra hypertension-prone and hypertension-resistant rats. *Hypertension* 9 (Suppl. 1): I-24-I-26, 1987.
- Bergman, M. R., R. H. Kao, S. A. McCunc, and B. J. Holyeross. Myocardial tumor necrosis factor- α secretion in hypertensive and heart failure-prone rats. *Am J Physiol* 277: H543-H550, 1999.

- Biron, P., J.-G. Mongeau, and D. Bertrand. Familial aggregation of blood pressure in 558 adopted children. *Canadian Medical Association Journal* 115: 253-259, 1976.
- Bishopric, N. H., P. C. Simpson, and C. P. Ordahl. Induction of the skeletal α -actin gene in α_1 -adrenoceptor-mediated hypertrophy of rat cardiac myocytes. *J Clin Invest* 80: 1194-1199, 1987.
- Bland, J. M. and D. G. Altman. Statistical methods for assessing agreement between two methods of clinical measurement. *Lancet* 1: 307-310, 1986.
- Boluyt, M. O., J. A. Opiteck, K. A. Esser, and T. P. White. Cardiac adaptations to aortic constriction in adult and aged rats. *Am J Physiol* 257: H643-H648, 1989.
- Botting, J. H., K. M. Johnston, B. A. Macleod, and M. J. A. Walker. The effect of modification of sympathetic activity on responses to ligation of a coronary artery in the conscious rat. *Br J Pharmacol* 79: 265-271, 1983.
- Bozkurt, B., S. B. Kribbs, F. J. Clubb, L. H. Michael, V. V. Didenko, P. J. Hornsby, Y. Seta, H. Oral, F. G. Spinale, and D. L. Mann. Pathophysiological relevant concentrations of tumor necrosis factor- α promote progressive left ventricular dysfunction and remodeling in rats. *Circulation* 97: 1382-1391, 1998.
- Brock, J. A., D. F. Vanhelden, P. Dosen, and R. A. Rush. Prevention of high blood-pressure by reducing sympathetic innervation in the spontaneously hypertensive rat. *Journal of the Autonomic Nervous System* 61: 97-102, 1996.
- Brosnan, M. J., A. M. Devlin, J. S. Clark, J. J. Mullins, and A. F. Dominiczak. Different effects of antihypertensive agents on cardiac and vascular hypertrophy in the transgenic rat line TGR(mRen2)27. *Am J Hypertens* 12: 724-731, 1999a.
- Brosnan, M. J., J. S. Clark, B. Jeffs, C. D. Negrin, P. Van Vooren, S. M. Arribas, H. Carswell, T. J. Aitman, C. Szpirer, I. M. Macrae, and A. F. Dominiczak. Genes encoding atrial and brain natriuretic peptides as candidates for sensitivity to brain ischaemia in stroke-prone hypertensive rats. *Hypertension* 33: 290-297, 1999b.

- Bryant, D., L. Becker, J. Richardson, J. Shelton, F. Franco, R. Peshock, M. Thompson, and B. Giroir. Cardiac failure in transgenic mice with myocardial expression of tumor necrosis factor- α . *Circulation* 97: 1375-1381, 1998.
- Bund, S. J. Influence of mode of contraction on the mechanism of acetylcholine-mediated relaxation of coronary arteries from normotensive and spontaneously hypertensive rats. *Clin Sci* 94: 231-238, 1998.
- Burke, W. and A. G. Motulsky. Molecular genetics of hypertension. In Lusis, A. J., J. I. Rotter, and R. S. Sparkes, eds. Molecular genetics of coronary artery disease. Candidate genes and processes in atherosclerosis. Basel, Karger. 1992, 228-236.
- Burrell, L. M., R. Chan, P. A. Phillips, P. Calafiore, A. M. Tonkin, and C. I. Johnston. Validation of an echocardiographic assessment of cardiac function following moderate size myocardial infarction in the rat. *Clinical and Experimental Pharmacology and Physiology* 1997.
- Buus, N. H., O. Kahr, and M. J. Mulvany. Effect of short- and long-term failure on small artery morphology and endothelial function in the rat. *J Cardiovas Pharmacol* 34: 34-40, 1999.
- Campbell, D. J., A.-M. Duncan, A. Kladis, and S. B. Harrap. Angiotensin peptides in spontaneously hypertensive and normotensive Donryu rats. *Hypertension* 25: 928-934, 1995.
- Carville, C., S. Adnot, S. Sediame, S. Benacerraf, A. Castaigne, F. Calvo, P. de Cremou, and J.-L. Dubois-Rande. Relation between impairment in nitric oxide pathway and clinical status with congestive heart failure. *J Cardiovas Pharmacol* 32: 562-570, 1998.
- Casolo, G., E. Balli, T. Taddei, J. Amulasi, and C. Gori. Decreased spontaneous heart rate variability in congestive heart failure. *Am J Cardiol* 64: 1162-1167, 1989.
- Cazaubon, C., J. Gougat, F. Bousquet, P. Guiraudou, R. Gayraud, C. Lacour, A. Roccon, G. Galindo, G. Barthelemy, B. Gautret, C. Bernhart, P. Perreault, J.-C. Breliere, G. Le Fur, and

- D. Nisato. Pharmacological characterisation of SR 47436, a new nonpeptide AT₁ subtype angiotensin II receptor antagonist. *J Pharm Exp Ther* 265: 826-834, 1993.
- Ceiler, D. L., H. J. M. G. Nelissen-Vrancken, J. G. R. de Mey, and J. F. M. Smits. Effect of chronic blockade of angiotensin II-receptor subtypes on aortic compliance in rats with myocardial infarction. *J Cardiovas Pharmacol* 31: 630-637, 1998.
- Charchar, F. J., M. K. Kapuscinski, and S. B. Harrap. Persistent reduction in renal nerve growth factor mRNA after perindopril treatment of young spontaneously hypertensive rats. *Hypertension* 31: 678-683, 1998.
- Chiba, K., S. Moriyama, Y. Ishigai, A. Fukuzawa, K. Irie, and T. Shibano. Lack of correlation of hypotensive effects with prevention of cardiac hypertrophy by perindopril after ligation of rat coronary artery. *Br J Pharmacol* 112: 837-842, 1994.
- Clark, J. S., B. Jeffs, A. O. Davidson, Wai Kwong Lee, N. H. Anderson, M.-T. Bihoreau, M. J. Brosnan, A. M. Devlin, A. W. Kelman, K. Lindpainter, and A. F. Dominiczak. Quantitative trait loci in genetically hypertensive rats: Possible sex specificity. *Hypertension* 28: 898-906, 1996.
- Clark, R. D., K. Korcusk, and K. Cohn. Serial echocardiographic evaluation of left ventricular function in valvular disease, including reproducibility guidelines for serial studies. *Circulation* 62: 564-575, 1980.
- Coats, A. J. S. The "muscle hypothesis" of chronic heart failure. *J Mol Cell Cardiol* 28: 2255-2262, 1996.
- Comini, L., T. Bachetti, G. Gaia, E. Pasini, L. Agnoletti, P. Pepi, C. Ceconi, S. Curello, and R. Ferrari. Aorta and skeletal muscle NO synthase expression in experimental heart failure. *J Mol Cell Cardiol* 28: 2241-2248, 1996.
- Cowie, M. R., A. Mosterd, D. A. Wood, J. W. Deckers, P. A. Poole-Wilson, G. E. Sutton, and D. E. Grobbee. The epidemiology of heart failure. *Eur Heart J* 18: 208-225, 1997.

Cowie, M. R. Annotated references in epidemiology. *European Journal of Heart Failure* 1: 101-107, 1999.

Crabos, M., P. Coste, M. Paccalin, L. Tariosse, D. Daret, P. Besse, and S. Bonoron-Adele. Reduced basal NO-mediated dilation and decreased endothelial NO-synthase expression in coronary vessels of spontaneously hypertensive rats. *J Mol Cell Cardiol* 29: 55-65, 1997.

Cutilletta, A. F., L. Erinoff, A. Heller, J. Low, and S. Oparil. Development of left ventricular hypertrophy in young spontaneously hypertensive rats after peripheral sympathectomy. *Circ Res* 40: 428-434, 1977.

Daemen, M. J. A. P. and J. G. R. de Mey. Regional heterogeneity of arterial structural changes. *Hypertension* 25: 464-473, 1995.

Daly, L. E., G. J. Bourke, and J. McGilvray. Interpretation and uses of medical statistics. Oxford, Blackwell Scientific Publications. 1991, 1-441.

Dargie, H. J., J. J. V. McMurray, and T. A. McDonagh. Heart failure - implications of the true size of the problem. *J Int Med* 239: 309-315, 1996.

Davidson, A. O., N. Schork, B. C. Jaques, A. W. Kelman, R. G. Sutcliffe, J. L. Reid, and A. F. Dominiczak. Blood pressure in genetically hypertensive rats: Influence of the Y chromosome. *Hypertension* 26: 452-459, 1995.

Davies, M. J. Apoptosis in cardiovascular disease. *Heart* 77: 498-501, 1997.

de Simone, G., D. C. Wallerson, M. Volpe, and R. B. Devereux. Echocardiographic measurement of left ventricular mass and volume in normotensive and hypertensive rats. Necropsy validation. *Am J Hypertens* 3: 688-696, 1990.

de Simone, G., R. B. Devereux, and D. C. Wallerson. Echocardiographic assessment of left ventricular hypertrophy in rats using a simplified approach. *Am J Hypertens* 7: 555-558, 1994.

- de Tombe, P. P. Altered contractile function in heart failure. *Cardiovasc Res* 37: 367-380, 1998.
- de Vries, R. J. M., R. Anthonio, D. J. van Veldhuisen, E. Scholtens, H. Buikema, and W. H. van Gilst. Effects of amlodipine on endothelial function in rats with chronic heart failure after experimental myocardial infarction. *J Cardiovas Pharmacol* 30: 683-689, 1997.
- Deck, C. C., T. E. Raya, M. A. Gaballa, and S. Goldman. baroreflex control of heart rate in rats with heart failure after myocardial infarction: Effects of captopril. *J Pharm Exp Ther* 263: 1424-1431, 1992.
- Dellsperger, K. C., J. L. Clothier, S. Koyanagi, T. Inou, and M. L. Marcus. Effects of coronary artery occlusion in animals with hypertension and left ventricular hypertrophy. *J Cardiovas Pharmacol* 17(Suppl. 2): S40-S45, 1991.
- Devereux, R. B. and N. Reichek. Echocardiographic determination of left ventricular mass in man. Anatomic validation of the method. *Circulation* 55: 613-618, 1977.
- Devereux, R. B., D. R. Alonso, E. M. Lutas, G. J. Gottlieb, E. Campo, I. Sachs, and N. Reichek. Echocardiographic assessment of left ventricular hypertrophy: comparison to necropsy findings. *Am J Cardiol* 57: 450-458, 1986.
- Devereux, R. B., P. R. Liebson, and M. J. Horan. Recommendations concerning use of echocardiography in hypertension and general population research. *Hypertension* 9 (Suppl. II): II-97-II-104, 1987.
- Devereux, R. B. Detection of left ventricular hypertrophy by M-mode echocardiography. Anatomic validation, standardisation, and comparison to other methods. *Hypertension* 9 (Suppl. II): II-19-II-26, 1987.
- Devereux, R. B., G. de Simone, A. Ganau, M. J. Roman, and D. C. Wallerson. Left ventricular mass as an indicator of hemodynamic load in hypertension. *J Cardiovas Pharmacol* 17 (Suppl. 2): S33-S33, 1991.

Devlin, A. M., J. F. Gordon, A. O. Davidson, J. S. Clark, C. A. Hamilton, J. J. Morton, A. M. Campbell, J. L. Reid, and A. F. Dominiczak. The effects of perindopril on vascular smooth muscle polyploidy in stroke-prone spontaneously hypertensive rats. *J Hypertens* 13: 211-218, 1995.

Devlin, A. M., M. J. Brosnan, D. Graham, J. J. Morton, A. R. McPhaden, M. McIntyre, C. A. Hamilton, J. L. Reid, and A. F. Dominiczak. Vascular smooth muscle cell polyploidy and cardiomyocyte hypertrophy due to chronic NOS inhibition in vivo. *Am J Physiol* 274: H52-H59, 1998.

Didion, S. P., P. K. Carmines, H. Ikenaga, and W. G. Mayhan. Enhanced constrictor responses of skeletal muscle arterioles during chronic myocardial infarction. *Am J Physiol* 273: H1502-H1508, 1997.

Doggrell, S. A. and L. Brown. Rat models of hypertension, cardiac hypertrophy and failure. *Cardiovasc Res* 39: 89-105, 1998.

Dominiczak, A. F., A. M. Devlin, W. K. Lee, N. H. Anderson, D. F. Bohr, and J. L. Reid. Vascular smooth muscle polyploidy and cardiac hypertrophy in genetic hypertension. *Hypertension* 27: 752-759, 1996.

Dominiczak, A. F., A. M. Devlin, M. J. Brosnan, N. H. Anderson, D. Graham, J. S. Clark, A. McPhaden, C. A. Hamilton, and J. L. Reid. Left ventricular hypertrophy and arterial blood pressure in experimental models of hypertension. In Zanchetti, ed. Hypertension and the heart. New York, Plenum Press. 1997, 23-33.

Dominiczak, A. F., J. S. Clark, B. Jeffs, N. H. Anderson, C. D. Negrin, W. K. Lee, and M. J. Brosnan. Genetics of experimental hypertension. *J Hypertens* 16: 1859-1869, 1998.

Dovak, H. C., Nul, D. R., Grancelli, H. O., Varini, S. D., Soifer, S., Corrado, G., Dubner, S., Scapin, O., and Perrone, S. V. Nonsustained ventricular tachycardia in severe heart failure: independent marker of increased mortality due to sudden death. *Circulation* 94, 3198-3203. 1996.

- Drexler, H. and L. Wenyan. Endothelial dysfunction of hindquarter resistance vessels in experimental heart failure. *Am J Physiol* 262: H1640-H1645, 1992.
- Du, X.-J., H. S. Cox, A. M. Dart, and M. D. Esler. Depression of efferent parasympathetic control of heart rate in rats with myocardial infarction: Effect of losartan. *J Cardiovas Pharmacol* 31: 937-944, 1998.
- Eaton, L. W., J. L. Weiss, B. H. Bulkley, J. B. Garrison, and M. L. Weisfeldt. Regional cardiac dilatation after acute myocardial infarction. *N Eng J Med* 300: 57-62, 1979.
- Eckberg, D. L., M. Drabinsky, and E. Braunwald. Defective cardiac parasympathetic control in patients with heart disease. *N Eng J Med* 285: 877-883, 1971.
- Eriksson, H. Heart failure: a growing public health problem. *J. Internal Med.* 237: 135-141, 1995.
- Fabris, B., B. Jackson, M. Kohzucki, R. Perich, and C. I. Johnston. Increased cardiac angiotensin-converting enzyme in rats with chronic heart failure. *Clinical and Experimental Pharmacology and Physiology* 17: 309-314, 1990.
- Falloon, B. J. and A. M. Heagerty. In vitro perfusion studies of human resistance artery function in essential hypertension. *Hypertension* 24: 16-23, 1994.
- Fan, X. M., E. D. Hendley, and C. J. Forehand. Enhanced vascular neuropeptide Y-immunoreactive innervation in two hypertensive rat strains. *Hypertension* 26: 758-763, 1995.
- Feinlieb, M., R. J. Garrison, R. Fatsitz, J. C. Christian, Z. Hrubec, N. O. Borhani, W. B. Kannel, R. Rosenman, J. T. Schwartz, and J. O. Wagner. The NHLBI twin study of cardiovascular risk factors: Methodology and summary of results. *American Journal of Epidemiology* 106: 284-295, 1977.
- Feng, Q.-P., A. Bergdahl, X.-R. Lu, X.-Y. Sun, L. Edvinsson, and T. Hedner. Vascular alpha-2 adrenoceptor function is decreased in rats with congestive heart failure. *Cardiovasc Res* 31: 577-584, 1996.

- Flecknell, P. A. Laboratory animal anaesthesia. London, Academic Press. 1996, 1-274.
- Fletcher, P. J., J. M. Pfeffer, M. A. Pfeffer, and E. Braunwald. Effects of hypertension on cardiac performance in rats with myocardial infarction. *Am J Cardiol* 50: 488-496, 1982.
- Folkow, B. Commentary. *J Hypertens* 5: 335-337, 1997.
- Fortuno, M. A., S. Ravassa, J. C. Etayo, and J. Diez. Overexpression of Bax protein and enhanced apoptosis in the left ventricle of spontaneously hypertensive rats. Effects of AT₁ blockade with losartan. *Hypertension* 32: 280-286, 1998.
- Fouad-Tarazi, F. M. and P. R. Liebson. Echocardiographic studies of regression of left ventricular hypertrophy in hypertension. *Hypertension* 9 (Suppl. II): II-65-II-68, 1987.
- Fraccarollo, D., K. Hu, P. Galuppo, P. Gaudron, and G. Ertl. Chronic endothelin receptor blockade attenuates progressive ventricular dilation and improves cardiac function in rats with myocardial infarction. *Circulation* 96: 3963-3973, 1997.
- Franco, F., G. D. Thomas, B. Giroir, D. Bryant, M. C. Bullock, M. C. Chwiealkowski, R. G. Victor, and R. M. Peshock. Magnetic resonance imaging and invasive evaluation of development of heart failure in transgenic mice with myocardial expression of tumor necrosis factor- α . *Circulation* 99: 448-454, 1999.
- Frohlich, E. D. Is the spontaneously hypertensive rat a model for human hypertension? *J Hypertens* 4 (Suppl. 3): S15-S19, 1986.
- Fukuchi, M., S. N. A. Hussain, and A. Giaid. Heterogeneous expression and activity of endothelial and inducible nitric oxide synthases in end-stage human heart failure: Their relation to lesion site and β -adrenoceptor therapy. *Circulation* 98: 132-139, 1998.
- Ganten, D. Role of animal models in hypertension research. *Hypertension* 9 (Suppl I): I2-I4, 1987.

- Garcia-Dorado, D., P. Theroux, J. Elizaga, F. F. Aviles, J. Alonso, and J. Solares. Influence of tachycardia and arterial hypertension on infarct size in the pig. *Cardiovasc Res* 22: 620-626, 1988.
- Garcia, R., M. Cantin, J. Gutkowska, and G. Thibault. Atrial natriuretic factor during development and reversal of one-kidney, one clip hypertension. *Hypertension* 9: 144-149, 1987.
- Garcia, S. R. and S. J. Bund. Nitric oxide modulation of coronary artery myogenic tone in spontaneously hypertensive and Wistar-Kyoto rats. *Clin Sci* 94: 225-229, 1998.
- Gardin, K. M., D. D. Savage, J. H. Ware, and W. L. Henry. Effect of age, sex, and body surface area on echocardiographic left ventricular wall mass in normal subjects. *Hypertension* 9 (Suppl. II): II-36-II-39, 1987.
- Garg, U. C. and A. Hassid. Nitric oxide-generating vasodilators and 8-bromo-cyclic guanosine monophosphate inhibit mitogenesis and proliferation of cultured rat vascular smooth muscle cells. *J Clin Invest* 83: 1774-1777, 1989.
- Gaudron, P., K. Hu, R. Schamberger, M. Budin, B. Walter, and G. Frtl. Effect of endurance training early or late after coronary artery occlusion in left-ventricular remodeling, hemodynamics, and survival in rats with chronic transmural myocardial infarction. *Circulation* 89: 402-412, 1994.
- Gidh-Jain, M., B. Huang, P. Jain, G. Gick, and N. El-Sherif. Alterations in cardiac gene expression during ventricular remodeling following experimental myocardial infarction. *J Mol Cell Cardiol* 30: 627-637, 1998.
- Gomez, A. M., H. H. Valdivia, H. Cheng, M. R. Lederer, L. F. Santana, M. B. Cannel, S. A. McCune, R. A. Altschuld, and W. J. Lederer. Defective excitation-contraction coupling in experimental cardiac hypertrophy and heart failure. *Science* 276: 800-806, 1997.
- Gopal, A. S., M. J. Schnellbaecher, Z. Shen, O. O. Akinboboye, P. M. Sapin, and D. L. King. Frechand three-dimensional echocardiography for measurement of left ventricular

mass: In vivo anatomic validation using explanted human hearts. *J Am Coll Cardiol* 30: 802-810, 1997.

Gordon, J. F., M. Baird, C. J. Daly, and J. C. McGrath. Endogenous nitric oxide modulates sympathetic neuroeffector transmission in the isolated rabbit lateral saphenous vein. *J Cardiovas Pharmacol* 20(Suppl. 12): S68-S71, 1992.

Grunfeld, S., C. A. Hamilton, S. Mesaros, S. W. McClain, A. F. Dominiczak, D. F. Bohr, and T. Malinski. Role of superoxide in the depressed nitric oxide production by the endothelium of genetically hypertensive rats. *Hypertension* 26: 854-857, 1995.

Gschwend, S., Buikema, H., Pinto, Y. M., Paul, M., de Zeeuw, D., and van Gilst, W. H. Impairment of EDHF rather than NO system may be responsible for the attenuated endothelium dependent relaxation in an experimntal rat model of chronic heart failure. *Hypertension* . 1999.

Ref Type: In Press

Gu, X. H., A. R. Kompa, and R. J. Summers. Regulation of β -adrenocceptors in a rat model of cardiac failure: effect of perindopril. *J Cardiovas Pharmacol* 32: 66-74, 1998.

Hallback-Nordlander, M., E. Noresson, and P. Thoren. Hemodynamic consequences of left ventricular hypertrophy in spontaneously hypertensive rats. *Am J Cardiol* 44: 986-993, 1979.

Hamet, P., L. Richard, T.-V. Dam, E. Teiger, S. N. Orlov, L. Gaboury, F. Gossard, and J. Tremblay. Apoptosis in target organs of hypertension. *Hypertension* 26: 642-648, 1995.

Harada, K., I. Komuro, I. Shiojima, D. Hayashi, S. Kudoh, T. Mizuno, K. Kijima, H. Matsubara, Y. Sugaya, K. Murakami, and Y. Yazaki. Pressure overload induces cardiac hypertrophy in angiotension II type 1A receptor knockout mice. *Circulation* 97: 1952-1959, 1998.

Harrington, D. and A. J. S. Coats. Skeletal muscle abnormalities and evidence for their role in symptom generation in chronic heart failure. *Eur Heart J* 18: 1865-1872, 1997.

Harrison, D. G., M. L. Marcus, K. C. Dellsperger, K. G. Lamping, and R. J. Tomanek. Pathophysiology of myocardial perfusion in hypertension. *Circulation* 83 (Suppl. III): III-14-III-18, 1991.

Hasenfuss, G. Animal models of human cardiovascular disease, heart failure and hypertrophy. *Cardiovasc Res* 39: 60-76, 1998.

Haywood, G. A., P. S. Tsao, H. E. von der Leyen, M. J. Mann, P. J. Keeling, P. T. Trindale, N. P. Lewis, C. D. Byrne, P. R. Rickenbacher, N. H. Bishopric, J. P. Cooke, W. J. McKenna, and M. B. Fowler. Expression of inducible nitric oxide synthase in human heart failure. *Circulation* 93: 1087-1094, 1996.

Heagerty, A. M., C. Aalkjaer, S. J. Bund, N. Korsgaard, and M. J. Mulvany. Small artery structure in hypertension: dual processes of remodelling and growth. *Hypertension* 21: 391-397, 1993.

Hedner, T. Treating hypertension - effect of treatment and cost-effectiveness in respect to later cardiovascular diseases. *Scand Cardiovasc J* 32: 31-35, 1998.

Heeneman, S., P. J. A. Leenders, P. J. J. W. Aarts, J. F. M. Smits, J. W. Arends, and M. J. A. P. Daemen. Peripheral vascular alterations during experimental heart failure in the rat: Do they exist? *Arterioscler Thromb Vasc Biol* 15: 1503-1511, 1995.

Heeneman, S., Smits, J. F. M., and Daemen, M. J. A. P. Opposing effects of nitric oxide and angiotensin receptors in the regulation of blood pressure and vascular structure during experimental heart failure. *Hypertension* 30, 999-999. 1997.

Ref Type: Abstract

Henrion, D., J. Benessiano, and B. I. Levy. In vitro modulation of a resistance artery diameter by the tissue renin-angiotensin system of a large donor artery. *Circ Res* 80: 189-195, 1997.

Hirooka, Y., T. Imaizumi, S. Harada, H. Masaki, M. Momohara, T. Tagawa, and A. Takeshita. Endothelium-dependent forearm vasodilation to acetylcholine but not substance

- P is impaired in patients with heart failure. *J Cardiovas Pharmacol* 20(Suppl. 12): S221-S225, 1992.
- Hirsch, A. T., C. E. Talsness, H. Schunkert, M. Paul, and V. J. Dzau. Tissue-specific activation of cardiac angiotensin converting enzyme in experimental heart failure. *Circ Res* 69: 475-482, 1991.
- Hodsman, G. P., M. Kohzuki, L. G. Howes, E. Sumithran, K. Tsunoda, and C. I. Johnston. Neurohumoral responses to chronic myocardial infarction in rats. *Circulation* 78: 376-381, 1988.
- Hoiike, G. and H. J. Jacob. Hypertension. In Jameson, J. L., ed. Principles of molecular medicine. Totowa, Humana Press Inc. 1998, 145-155.
- Holycross, B. J., M. J. Peach, and G. K. Owens. Angiotensin II stimulates increased protein synthesis, not increased DNA synthesis, in intact rat aortic segments, in vitro. *J Vasc Res* 30: 80-86, 1993.
- Horie, R., M. Kihara, W. Lovenberg, D. Ben-Ishay, G. Bianchi, J. Iwai, A. Nagaoka, J. P. Rapp, J. Sassard, F. O. Simpson, and Y. Yamori. Comparison of various genetic hypertensive rat strains. *J Hypertens* 4 (Suppl. 3): S11-S14, 1986.
- Hornig, B., N. Arakawa, and H. Drexler. Effect of ACE inhibition on endothelial dysfunction in patients with chronic heart failure. *Eur Heart J* 19 (Suppl. G): G48-G53, 1998a.
- Hornig, B., N. Arakawa, C. Kohler, and H. Drexler. Vitamin C improves endothelial function of conduit arteries in patients with chronic heart failure. *Circulation* 97: 363-368, 1998b.
- Horstick, G., O. Berg, A. Heimann, H. Darius, H. A. Lehr, S. Bhakdi, O. Kempfski, and J. Meyer. Surgical procedure affects physiological parameters in rat myocardial ischemia: need for mechanical ventilation. *Am J Physiol* 276: H472-H479, 1999.

- Hu, K., P. Gaudron, H.-J. Anders, F. Weideman, O. Turschner, M. Nahrendorf, and G. Ertl. Chronic effects of early started angiotensin converting enzyme inhibition and angiotensin AT₁-receptor subtype blockade in rats with myocardial infarction: role of bradykinin. *Cardiovasc Res* 39: 401-412, 1998a.
- Hu, K., P. Gaudron, T. J. Schmidt, K. D. Hoffman, and G. Ertl. Aggravation of left ventricular remodeling by a novel specific endothelin ET_A antagonist EMD94246 in rats with experimental myocardial infarction. *J Cardiovas Pharmacol* 32: 505-508, 1998b.
- Hunziker, P. R., S. Smith, M. Scherrer-Crosbie, N. Liel-Cohen, R. A. Levine, R. Nesbitt, S. A. Benton, and M. H. Picard. Dynamic holographic imaging of the beating human heart. *Circulation* 99[Suppl. I]: I-698, 1999.
- Iannini, J. P. and F. G. Spinale. The identification of contributory mechanisms for the development and progression of congestive heart failure in animal models. *J Heart Lung Transplant* 15: 1138-1150, 1996.
- Ikeda, U., Y. Murakami, T. Kanbe, and K. Shimada. α -Adrenergic stimulation enhances inducible nitric oxide synthase expression in rat cardiac myocytes. *J Mol Cell Cardiol* 28: 1539-1545, 1996.
- Inou, T., W. C. Lamberth, S. Koyanagi, D. G. Harrison, C. L. Eastham, and M. L. Marcus. Relative importance of hypertension after coronary occlusion in chronic hypertensive dogs with LVH. *Am J Physiol* 253: H1148-H1158, 1987.
- Isgaard, J., V. Kujacic, E. Jennische, A. Holmang, X. Y. Sun, T. Hedner, and A. Hjalmarson. Growth hormone improves cardiac function in rats with experimental myocardial infarction. *European Journal of Clinical Investigation* 27: 517-525, 1997.
- Ishigai, Y., T. Mori, T. Ikeda, A. Fukuzawa, and T. Shibano. Role of bradykinin - NO pathway in prevention of cardiac hypertrophy by ACE inhibitor in rat cardiomyocytes. *Am J Physiol* 273: H2659-H2663, 1997.

- Itter, G., W. Linz, W. Jung, P. Juretschke, G. Wiemer, and B. A. Schölkens. Severe symptomatic heart failure in spontaneously hypertensive rats. *Hypertension* 34: 807-807, 1998.
- Iwai, J. Dahl salt-sensitive and salt-resistant rats. *Hypertension* 9 (Suppl. 1): I-18-I-20, 1987.
- Izumo, S. and H. Aoki. Calcineurin - the missing link in cardiac hypertrophy. *Nature Medicine* 4: 661-662, 1998.
- Jaber, M., W. J. Koch, H. Rockman, B. Smith, R. A. Bond, K. K. Sulik, J. Ross, R. J. Lefkowitz, M. G. Caron, and B. Girois. Essential role of β -adrenergic receptor kinase 1 in cardiac development and function. *Proc Natl Acad Sci USA* 93: 12974-12979, 1996.
- Jacobs, M. Mechanism of action of hydralazine on vascular smooth muscle. *Biochem Pharmacol* 33: 2915-2919, 1984.
- Jefferson, S., R. Rush, C. Zettler, D. B. Frewin, and R. J. Head. The influence of the renin-angiotensin system on abnormal expression of nerve growth-factor in the spontaneously hypertensive rat. *Clinical and Experimental Pharmacology and Physiology* 22: 478-480, 1995.
- Jensen, K. T., H. Eiskjaer, J. Carstens, and E. B. Pedersen. Renal effects of brain natriuretic peptide in patients with congestive heart failure. *Clin Sci* 96: 5-15, 1999.
- Jespersen, L. T., N. C. B. Nyborg, O. Lederballe Pederson, E. O. Mikkelsen, and M. J. Mulvany. Cardiac mass and peripheral vascular structure in hydralazine-treated spontaneously hypertensive rats. *Hypertension* 7: 734-741, 1985.
- Joannides, R., W. E. Haefeli, L. Linder, V. Richard, E. H. Bakkali, C. Thuillez, and T. F. Luscher. Nitric oxide is responsible for flow-dependent dilatation of human peripheral conduit arteries in vivo. *Circulation* 91: 1314-1319, 1995.
- Joe, E. K., A. E. Schussheim, D. Longrois, T. Maki, R. A. Kelly, T. W. Smith, and J.-L. Balligand. Regulation of cardiac myocyte contractile function by inducible nitric oxide

synthase (iNOS): mechanisms of contractile depression by nitric oxide. *J Mol Cell Cardiol* 30: 303-315, 1998.

Johnston, C. I. Tissue angiotensin converting enzyme in cardiac and vascular hypertrophy, repair, and remodeling. *Hypertension* 23: 258-268, 1994.

Jones, E. F., S. B. Harrap, P. Calafiore, and A. M. Tonkin. Development and validation of echocardiographic methods for estimating left ventricular mass in rats. *Clinical and Experimental Pharmacology and Physiology* 19: 361-364, 1992.

Jones, J. K., L. Gorkin, J. A. Staffa, and A. P. Fletcher. Discontinuation of and changes in treatment after start of new courses of antihypertensive drugs: a study of a United Kingdom population. *BMJ* 311: 293-295, 1995.

Kajstura, J., A. Leri, N. Finato, C. Di Loretto, C. A. Beltrami, and P. Anversa. Myocyte proliferation in end-stage cardiac failure in humans. *Proc Natl Acad Sci USA* 95: 8801-8805, 1998.

Kalkman, E. A. J., Y. M. Bilgin, P. van Haren, R.-J. van Suylen, P. R. Saxena, and R. G. Schoemaker. Determinants of coronary reserve in rats subjected to coronary artery ligation or aortic banding. *Cardiovasc Res* 32: 1088-1095, 1996.

Kalkman, E. A. J., P. van Haren, P. R. Saxena, and R. G. Schoemaker. Regionally different vascular response to vasoactive substances in the remodelled infarcted rat heart; aberrant vasculature in the infarct scar. *J Mol Cell Cardiol* 29: 1487-1497, 1997.

Kannel, W. B. Blood pressure as a cardiovascular risk factor. *JAMA* 275: 1571-1576, 1996.

Katz, A. M. Heart Failure. In Fozzard, H. A., E. Haber, R. B. Jennings, A. M. Katz, and H. E. Morgan, eds. *The heart and cardiovascular system*. New York, Raven Press Ltd. 1992, 333-353.

Katz, S. D., M. Schwarz, J. Yuen, and T. H. LeJemtel. Impaired acetylcholine-mediated vasodilation in patients with congestive heart failure: Role of endothelium-derived vasodilating and vasoconstricting factors. *Circulation* 88: 55-61, 1993.

Kawakami, H., H. Okayama, M. Hamada, and K. Hiwada. Alteration of atrial peptide and brain natriuretic peptide gene expression associated with progression and regression of cardiac hypertrophy in renovascular hypertensive rats. *Clin Sci* 90: 197-204, 1996.

Kaye, D. M. and M. D. Esler. Abnormalities of the autonomic nervous system in heart failure: Assessment, potential mechanisms, and implications. *Cardiol Rev* 3: 184-195, 1995.

Kelley, S. T., R. Malekan, J. H. Gorman, B. M. Jackson, R. C. Gorman, Y. Suzuki, T. Plappert, D. K. Bogen, M. G. St. John Sutton, and L. H. Edmunds. Restraining infarct expansion preserves left ventricular geometry and function after acute anteroapical infarction. *Circulation* 99: 135-142, 1999.

Kerr, S., M. J. Brosnan, M. McIntyre, J. L. Reid, A. F. Dominiczak, and C. A. Hamilton. Superoxide anion production is increased in a model of genetic hypertension: role of the endothelium. *Hypertension* 33: 1353-1358, 1999.

Kim, S., K. Ohta, A. Hamaguchi, T. Yukimura, K. Miura, and H. Iwao. Angiotensin II induces cardiac phenotypic modulation and remodeling in vivo in rats. *Hypertension* 25: 1252-1259, 1995.

Kim, S., K. Ohta, A. Hamaguchi, T. Yukimura, K. Miura, and H. Iwao. Effects of an AT₁ receptor antagonist, an ACE inhibitor and a calcium channel antagonist on cardiac gene expressions in hypertensive rats. *Br J Pharmacol* 118: 549-556, 1996.

Kinnunen, P., O. Vuolteenaho, P. Uusimaa, and H. Ruskoaho. Passive mechanical stretch releases atrial natriuretic peptide from rat ventricular myocardium. *Circ Res* 70: 1244-1253, 1992.

Kiowski, W., G. Sutsch, C. Schalcher, H. R. Brunner, and E. Oechslin. Endothelial control of vascular tone in chronic heart failure. *J Cardiovas Pharmacol* 32(Suppl. 3): S67-S73, 1998.

- Kleschyov, A. L., B. Muller, C. Schott, and J.-C. Stoclet. Role of adventitial nitric oxide in vascular hyporeactivity induced by lipopolysaccharide in rat aorta. *Br J Pharmacol* 124: 623-626, 1998.
- Kohzuki, M., G. P. Hodsman, R. W. Harrison, P. S. Western, and C. I. Johnston. Atrial natriuretic peptide infusion in chronic heart failure in the rat. *J Cardiovas Pharmacol* 13 (Suppl. 6): S43-S46, 1989.
- Kondo, M., T. Miyazaki, T. Fujiwara, A. Yano, and R. Tabei. Increased density of fluorescent adrenergic fibers around the middle cerebral arteries of stroke-prone spontaneously hypertensive rats. *Virchows Archiv B Cell Pathol* 61: 117-122, 1991.
- Korner, P. I. and J. A. Angus. Vascular remodeling. *Hypertension* 29: 1065-1066, 1997.
- Korsgaard, N. and M. J. Mulvany. Cellular hypertrophy in mesenteric resistance vessels from renal hypertensive rats. *Hypertension* 12: 162-167, 1988.
- Krum, H. β -adrenoceptor blockers in chronic heart failure - a review. *Br J Clin Pharmacol* 44: 111-118, 1997.
- Kubo, S. H., T. S. Rector, A. J. Bank, R. E. Williams, and S. M. Heifetz. Endothelium-dependent vasodilation is attenuated in patients with heart failure. *Circulation* 84: 1589-1596, 1991.
- Kuecherer, H. F., L. L. Lee, G. Modin, M. D. Cheitlin, and N. B. Schiller. Echocardiography in serial evaluation of left ventricular systolic and diastolic function: importance of image acquisition, quantitation, physiologic variability in clinical and investigational applications. *J Am Soc Echo* 4: 203-214, 1991.
- Kuecherer, H. F. and W. W. Kuebler. Diagnosis of left ventricular hypertrophy by echocardiography. *J Cardiovas Pharmacol* 19 (Suppl. 5): S81-S86, 1992.
- Kuijpers, M. H. M., B. F. M. van Zutphen, and W. de Jong. The Fawn-Hooded rat. *Hypertension* 9 (Suppl. 1): I-34-I-36, 1987.

Kupari, M., M. Lindroos, A. M. Iivanainen, J. Heikkila, and R. Tilvis. Congestive heart failure in old age: prevalence, mechanisms and 4-year prognosis in the Helsinki ageing study. *J Int Med* 241: 387-394, 1997.

Lacour, C., F. Canals, G. Galindo, C. Cazaubon, D. Segondy, and D. Nisato. Efficacy of SR 47436 (BMS-186295), a non-peptide angiotensin AT₁ receptor antagonist in hypertensive rat models. *European Journal of Pharmacology* 264: 307-316, 1994.

Latini, R., S. Masson, G. Jeremic, G. Luvara, F. Fiordaliso, L. Calvillo, R. Bernasconi, M. Torri, I. Rondelli, R. Razzetti, and S. Bongrani. Comparative efficacy of a DA₂/α₂ agonist and a β-blocker in reducing adrenergic drive and cardiac fibrosis in an experimental model of left ventricular dysfunction after coronary artery occlusion. *J Cardiovas Pharmacol* 31: 601-608, 1998.

Lee, M. E., W. L. Miller, B. S. Edwards, and J. C. Burnett. Role of endogenous atrial natriuretic factor in acute congestive heart failure. *J Clin Invest* 84: 1962-1966, 1989.

Lee, R. M. K. W., K. R. Borkowski, F. H. H. Leenen, J. Tsoporis, and M. Coughlin. Combined effect of neonatal sympathectomy and adrenal demedullation on blood-pressure and vascular changes in spontaneously hypertensive rats. *Circ Res* 69: 714-721, 1991.

Leenen, F. H. H., V. Skarda, B. Yuan, and R. White. Changes in cardiac ANG II postmyocardial infarction in rats: effects of nephrectomy and ACE inhibitors. *Am J Physiol* 276: H317-H325, 1999.

Levin, E. R., D. G. Gardner, and W. K. Samson. Natriuretic peptides. *N Eng J Med* 339: 321-328, 1998.

Levine, B., J. Kalman, L. Mayer, H. M. Fillit, and M. Packer. Elevated circulating levels of tumor necrosis factor in severe chronic heart failure. *N Eng J Med* 323: 236-241, 1990.

- Levy, D., R. J. Garrison, D. D. Savage, W. B. Kannel, and W. P. Castelli. Prognostic implications of echocardiographically determined left ventricular mass in the Framingham heart study. *N Eng J Med* 322: 1561-1566, 1990.
- Levy, D. Clinical significance of left ventricular hypertrophy: Insights from the Framingham Study. *J Cardiovas Pharmacol* 17 (Suppl. 2): S1-S6, 1991.
- Levy, D., M. G. Larson, R. S. Vasan, W. B. Kannel, and K. K. L. Ho. The progression from hypertension to congestive heart failure. *JAMA* 275: 1557-1562, 1996.
- Li, Y. Y., A. M. Feldman, Y. Sun, and C. F. McTiernan. Differential expression of tissue inhibitors of metalloproteinases in the failing human heart. *Circulation* 98: 1728-1734, 1998.
- Li, Z., O. H. L. Bing, X. Long, K. G. Robinson, and E. G. Lakatta. Increased cardiomyocyte apoptosis during the transition to heart failure in the spontaneously hypertensive rat. *Am J Physiol* 272: H2313-H2319, 1997.
- Liebson, P. R., R. B. Devereux, and M. J. Horan. Hypertension research: Echocardiography in the measurement of left ventricular wall mass. *Hypertension* 9 (Suppl. II): II-2-II-5, 1987.
- Lindsay, D. C., C. Jiang, F. Brunotte, S. Adamopoulos, A. J. S. Coats, B. Rajagopalan, P. A. Poole-Wilson, and P. Collins. Impairment of endothelium dependent responses in a rat model of chronic heart failure: effects of an exercise training protocol. *Cardiovasc Res* 26: 694-697, 1992.
- Linz, W. and B. A. Schölkens. A specific B₂-bradykinin receptor antagonist HOE 140 abolishes the antihypertrophic effect of ramipril. *Br J Pharmacol* 105: 771-772, 1992.
- Litwin, S. E., S. E. Katz, J. P. Morgan, and P. S. Douglas. Serial echocardiographic assessment of left ventricular geometry and function after large myocardial infarction in the rat. *Circulation* 89: 345-354, 1994.

- Liu, Y.-H., X.-P. Yang, V. G. Sharov, O. Nass, H. N. Sabbah, E. Peterson, and O. A. Carretero. Effects of angiotensin-converting enzyme inhibitors and angiotensin II type I receptor antagonists in rats with heart failure. *J Clin Invest* 99: 1926-1935, 1997.
- Liu, Y.-H., X.-P. Yang, O. Nass, H. N. Sabbah, E. Peterson, and O. A. Carretero. Chronic heart failure induced by coronary artery ligation in Lewis inbred rats. *Am J Physiol* 272: H722-H727, 1997.
- Love, M. P. and J. J. V. McMurray. Endothelin in chronic heart failure: current position and future prospects. *Cardiovasc Res* 31: 665-674, 1996.
- Luchner, A., T. L. Stevens, D. D. Borgeson, M. Redfield, C.-M. Wei, J. G. Porter, and J. C. Burnett. Differential atrial and ventricular expression of myocardial BNP during evolution of heart failure. *Am J Physiol* 274: H1684-H1689, 1998.
- Luvara, G., M. E. Pueyo, M. Phillippe, C. Mandet, F. Savoie, D. Henrion, and J.-B. Michel. Chronic blockade of NO synthase activity induces a proinflammatory phenotype in the arterial wall: Prevention by angiotensin II antagonism. *Arterioscler Thromb Vasc Biol* 18: 1408-1416, 1998.
- Mann, D. L. and F. G. Spinale. Activation of matrix metalloproteinases in the failing human heart. Breaking the tie that binds. *Circulation* 98: 1699-1702, 1998.
- Marshall, R. A. L., R. A. Levine, and A. E. Weyman. Echocardiography in cardiac research. In Fozzard, H. A., E. Haber, R. B. Jennings, A. M. Katz, and H. E. Morgan, eds. *The heart and cardiovascular system*. New York, Raven Press Ltd. 1992, 745-837.
- Matsuoka, H., M. Nakata, K. Kohno, Y. Koga, G. Nomura, H. Toshima, and T. Imaizumi. Chronic L-arginine administration attenuates cardiac hypertrophy in spontaneously hypertensive rats. *Hypertension* 27: 14-18, 1996.
- McGrath, J. C., S. M. Arribas, C. J. Daly, and J. F. Gordon. Confocal microscopy for structure and real-time pharmacology in blood vessels. *J Human Hypertension* 9: 645-647, 1995.

- McIntyre, M., C. A. Hamilton, D. D. Rees, J. L. Reid, and A. F. Dominiczak. Sex differences in the abundance of endothelial nitric oxide in a model of genetic hypertension. *Hypertension* 30: 1517-1524, 1997.
- McLenachan, J. M., E. Henderson, K. I. Morris, and H. J. Dargie. Ventricular arrhythmias in patients with hypertensive left ventricular hypertrophy. *N Eng J Med* 317: 787-792, 1987.
- Meldrum, D. R. Tumor necrosis factor in the heart. *Am J Physiol* 274: R577-R595, 1998.
- Mento, P. F., M. E. Pica, J. Hilepo, J. Chang, L. Hirsch, and B. M. Wilkes. Increased expression of glomerular AT₁ receptors in rats with myocardial infarction. *Am J Physiol* 275: H1247-H1253, 1998.
- Meredith, I. T., G. Eisenhofer, G. W. Lambert, E. M. Dewar, G. L. Jennings, and M. D. Esler. Cardiac sympathetic nervous activity in congestive heart failure. Evidence for increased neuronal norepinephrine release and preserved neuronal uptake. *Circulation* 88: 136-145, 1993.
- Michel, M. C. and W. Rascher. Neuropeptide Y: a possible role in hypertension? *J Hypertens* 13: 385-395, 1995.
- Min, A. L., M. P. P. Bohm, and D. Ganten. Tissue renin-angiotensin systems: Their role in cardiovascular disease. *Circulation* 87(Suppl.IV): IV7-IV13, 1993.
- Missouris, C. G., E. Grouzmann, M. G. Buckley, J. Barron, G. A. MacGregor, and D. R. J. Singer. How does treatment influence endocrine mechanisms in acute heart failure? Effects on cardiac natriuretic peptides, the renin system, neuropeptide Y and catecholamines. *Clin Sci* 94: 591-599, 1998.
- Molkentin, J. D., J.-R. Lu, C. L. Antos, B. Markham, J. Richardson, J. Robbins, S. R. Grant, and E. N. Olson. A calcineurin-dependent transcriptional pathway for cardiac hypertrophy. *Cell* 93: 215-228, 1998.

- Monaghan, M. J. Practical echocardiography and doppler. Chichester, John Wiley & Sons. 1990, 1-142.
- Mongcau, J.-G., P. Biron, and C. F. Sing. The influence of genetics and household environment upon the variability of blood pressure: The Montreal Adoption Study. *Clinical and Experimental Hypertension (A)* 8: 653-660, 1986.
- Morita, M., S. Kawashima, K. Ikeoka, and T. Iwasaki. Effects of chronic hypertension and left ventricular hypertrophy on the extent of infarct expansion in rats. *Am J Hypertens* 9: 753-759, 1996.
- Morton, J. J. and E. C. H. Wallace. The importance of the renin angiotensin system in the development and maintenance of hypertension in the two kidney one clip hypertensive rat. *Clin Sci* 64: 359-370, 1983.
- Motz, W., M. Vogt, S. Scheler, B. Schwartzkopff, and B. E. Strauer. Coronary circulation in arterial hypertension. *J Cardiovas Pharmacol* 17 (Suppl. 2): S35-S39, 1991.
- Mukoyama, M., K. Nakao, K. Hosoda, S. Suga, Y. Saito, Y. Ogawa, G. Shirakami, M. Jougasaki, K. Obata, H. Yasue, Y. Kambayashi, K. Inouye, and H. Imura. Brain natriuretic peptide as a novel cardiac hormone in humans. *J Clin Invest* 87: 1402-1412, 1991.
- Mulder, P., L. Elfertak, V. Richard, P. Compagnon, B. Devaux, J.-P. Henry, E. Scalbert, P. Desche, B. Mace, and C. Thuillez. Peripheral artery structure and endothelial function in heart failure: effect of ACE inhibition. *Am J Physiol* 271: H469-H477, 1996.
- Mulder, P., B. Devaux, V. Richard, J.-P. Henry, M.-C. Wimar, E. Thibout, B. Mace, and C. Thuillez. Early versus delayed angiotensin-converting enzyme inhibition in experimental heart failure. *Circulation* 95: 1314-1319, 1997.
- Mulvany, M. J. Are vascular abnormalities a primary cause or secondary consequence of hypertension? *Hypertension* 18 (Suppl. 1): I-52-I-57, 1991.
- Mulvany, M. J., G. L. Baumbach, C. Aalkjaer, A. M. Heagerty, N. Korsgaard, E. L. Schiffrin, and D. D. Heistad. Vascular remodelling. *Hypertension* 28: 505-506, 1996.

- Mulvany, M. J. Vascular remodelling of resistance vessels: can we define this? *Cardiovasc Res* 41: 9-13, 1999.
- Musch, T. I. and J. A. Terrell. Skeletal muscle blood flow abnormalities in rats with a chronic myocardial infarction: rest and exercise. *Am J Physiol* 262: H411-H419, 1992.
- Nagaya, N., Y. Goto, T. Nishikimi, M. Uematsu, Y. Miyao, Y. Kobayashi, S. Miyazaki, S. Hamada, S. Kuribayashi, M. Takamiya, H. Matsuo, K. Kangawa, and H. Nonogi. Sustained elevation of plasma brain natriuretic peptide levels associated with progressive ventricular remodelling after acute myocardial infarction. *Clin Sci* 96: 129-136, 1999.
- Nakamura, M., N. Arakawa, H. Yoshida, S. Makita, H. Niinuma, and K. Hiramori. Vasodilatory effects of B-type natriuretic peptide are impaired in patients with chronic heart failure. *Am Heart J* 135: 414-420, 1998.
- Nakamura, T., K. Shimoo, T. Kuribayashi, K. Matsubara, M. Shima, A. Matsumuro, A. Azuma, H. Katsume, and M. Nakagawa. Visualisation of the heart and determination of left ventricular mass in rats by echocardiography. *Jpn Heart J* 32: 481-491, 1991.
- Nakamura, T., A. Matsumuro, T. Kuribayashi, K. Matsubara, M. Shima, K. Shimoo, H. Katsume, and M. Nakagawa. Echocardiographic determination of stroke volume during rapid atrial pacing and volume loading in normal rats. *Cardiovasc Res* 26: 765-769, 1992.
- Nakayama, K., M. Yoshiyama, K. Takeuchi, S. Kim, Y. Ikuno, T. Omura, H. Iwao, and J. Yoshikawa. Doppler-echocardiographic assessment and cardiac gene expression analysis of the left ventricle in myocardial infarcted rats. *Not yet in print* 1: 1-1, 1997.
- Narula, J., S. Kharbanda, and B.-A. Khaw. Apoptosis and the heart. *Chest* 112: 1358-1362, 1997.
- Nasa, Y., H. Toyoshima, H. Ohaku, Y. Hashizume, A. Sanbe, and S. Takeo. Impairment of cGMP- and cAMP-mediated vasorelaxations in rats with chronic heart failure. *Am J Physiol* 271: H2228-H2237, 1996.

Nava, E., G. Noll, and T. F. Luscher. Increased activity of constitutive nitric oxide synthase in cardiac endothelium in spontaneous hypertension. *Circulation* 91: 2310-2313, 1995.

Nekooeian, A. A. and C. C. Y. Pang. Estrogen restores role of basal nitric oxide in control of vascular tone in rats with chronic heart failure. *Am J Physiol* 274: H2094-H2099, 1998.

Newton, G. E. and Parker, J. D. Cardiac sympathetic responses to acute vasodilation: normal ventricular function versus congestive heart failure. *Circulation* 94, 3161-3167. 1996.

Nguyen, T., F. El Salibi, and J. L. Rouleau. Postinfarction survival and inducibility of ventricular arrhythmias in the spontaneously hypertensive rat. Effects of ramipril and hydralazine. *Circulation* 98: 2074-2080, 1998.

Nilsson, H., M. Goldstein, and O. Nilsson. Adrenergic innervation and neurogenic responses in large and small arteries and veins from the rat. *Acta Physiol Scand* 126: 121-133, 1986.

Nishikimi, T., H. Yamagishi, K. Takeuchi, and T. Takeda. An angiotensin II receptor antagonist attenuates left ventricular dilatation after myocardial infarction in the hypertensive rat. *Cardiovasc Res* 29: 856-861, 1995.

Ogawa, Y., K. Nakao, M. Mukoyama, K. Hosoda, G. Shirakami, H. Arai, M. Saito, S. Suga, M. Jougasaki, and H. Imura. Natriuretic peptides as cardiac hormones in normotensive and spontaneously hypertensive rats. The ventricle is a major site of synthesis and secretion of brain natriuretic peptide. *Circ Res* 69: 491-500, 1991.

Oie, E., R. Bjonerheim, H. K. Groggaard, H. Kongshaug, O. A. Smiseth, and H. Attramadal. ET-receptor antagonism, myocardial gene expression, and ventricular remodeling during CHF in rats. *Am J Physiol* 275: H868-H877, 1998.

Okamoto, K., Y. Yamori, and A. Nagaoka. Establishment of the stroke-prone spontaneously hypertensive rat (SHR). *Circ Res* 34-35 (Suppl. 1): I-143-I-153, 1974.

- Ono, K., A. Matsumori, T. Shioi, Y. Furukawa, and S. Sasayama. Cytokine gene expression after myocardial infarction in rat hearts: possible implication in left ventricular remodeling. *Circulation* 98: 149-156, 1998.
- Ontkcan, M., R. Gay, and B. Greenberg. Diminished endothelium-derived relaxing factor in an experimental model of chronic heart failure. *Circ Res* 69: 1088-1096, 1991.
- Opitz, C. F., G. F. Mitchell, M. A. Pfeffer, and J. M. Pfeffer. Arrhythmias and death after coronary artery occlusion in the rat. *Circulation* 92: 253-261, 1995.
- Orenstein, T. L., T. G. Parker, J. W. Butany, J. M. Goodman, F. Dawood, W.-H. Wen, L. Wee, T. Martino, P. R. McLaughlin, and P. P. Liu. Favourable left ventricular remodelling following large myocardial infarction by exercise training. *J Clin Invest* 96: 858-866, 1995.
- Osterziel, K. J., D. Hänlein, and R. Dietz. Interactions between the renin-angiotensin system and the parasympathetic nervous system in heart failure. *J Cardiovas Pharmacol* 24 (Suppl. 2): S70-S74, 1994.
- Owens, G. K. and S. M. Schwartz. Alterations in vascular smooth muscle mass in the spontaneously hypertensive rat: role of cellular hypertrophy, hyperploidy, and hyperplasia. *Circ Res* 51: 280-289, 1982.
- Owens, G. K. Influence of blood pressure on development of aortic medial smooth muscle hypertrophy in spontaneously hypertensive rats. *Hypertension* 9: 178-187, 1987.
- Owens, G. K. Control of hypertrophic versus hyperplastic growth of vascular smooth muscle cells. *Am J Physiol* 257: H1755-H1765, 1989.
- Pai, R. G. and P. M. Shah. Echocardiographic and other noninvasive measurements of cardiac hemodynamics and ventricular function. *Curr Probl Cardiol* 20: 721-770, 1995.
- Passier, R. C. J. J., J. F. M. Smits, M. J. A. Verluyten, R. Studer, H. Drexler, and M. J. A. P. Daemen. Activation of angiotensin-converting enzyme expression in infarct zone following myocardial infarction. *Am J Physiol* 269: H1268-H1276, 1995.

- Passier, R. C. J. J., J. F. M. Smits, M. J. A. Verluyten, and M. J. A. P. Daemen. Expression and localisation of renin and angiotensinogen in rat heart after myocardial infarction. *Am J Physiol* 271: H1040-H1048, 1996.
- Pawlush, D. G., R. L. Moore, T. I. Musch, and W. R. Davidson. Echocardiographic evaluation of size, function, and mass of normal and hypertrophied rat ventricles. *J Appl Physiol* 74: 2598-2605, 1993.
- Pfeffer, J. M., M. A. Pfeffer, P. J. Fletcher, and E. Braunwald. Alterations of cardiac performance in rats with established spontaneous hypertension. *Am J Cardiol* 44: 994-998, 1979a.
- Pfeffer, J. M., M. A. Pfeffer, P. J. Fletcher, and E. Braunwald. Ventricular performance in rats with myocardial infarction and failure. *American Journal of Medicine* 76: 99-103, 1984.
- Pfeffer, J. M., M. A. Pfeffer, P. J. Fletcher, and E. Braunwald. Progressive ventricular remodeling in rat with myocardial infarction. *Am J Physiol* 260: H1406-H1414, 1991.
- Pfeffer, M. A., J. M. Pfeffer, M. C. Fishbein, P. J. Fletcher, J. Spadaro, R. A. Kloner, and E. Braunwald. Myocardial infarct size and ventricular function in rats. *Circ Res* 44: 503-512, 1979b.
- Pinsky, D. J., W. Aji, M. Szaboles, E. S. Athan, Y. Liu, Y. M. Yang, R. P. Kline, K. E. Olsen, and P. J. Cannon. Nitric oxide triggers programmed cell death (apoptosis) of adult rat ventricular myocytes in culture. *Am J Physiol* 277: H1189-H1199, 1999.
- Pinto, Y. M., M. Paul, and D. Ganten. Lessons from rat models of hypertension: from Goldblatt to genetic engineering. *Cardiovasc Res* 39: 77-88, 1998.
- Pitt, B., F. Zannad, W. J. Remme, R. Cody, A. Castaigne, A. Perez, J. Palensky, J. Wittes, and The randomised aldactone evaluation study investigators. The effect of spironolactone on morbidity and mortality in patients with severe heart failure. *N Eng J Med* 341: 709-717, 1999.

- Ponicko, K., M. Vogelsang, M. Heinroth, K. Becker, O. Zolk, M. Bohm, H.-R. Zerkowski, and O.-E. Brodde. Endothelin receptors in the failing and nonfailing human heart. *Circulation* 97: 744-751, 1998.
- Poulos, J. E., W. R. Gower, J. T. Sullebarger, H. L. Fontanet, and D. L. Vesely. Congestive heart failure: Increased cardiac and extracardiac atrial natriuretic peptide gene expression. *Cardiovasc Res* 32: 909-919, 1996.
- Pousset, F., R. Isnard, P. Lechat, H. Kalotka, A. Carayon, G. Maistre, S. Escolano, D. Thomas, and M. Komajda. Prognostic value of plasma endothelin-1 in patients with chronic heart failure. *Eur Heart J* 18: 254-258, 1997.
- Powell, J. R., R. A. Reeves, M. R. Marino, C. Cazaubon, and D. Nisato. A review of the new angiotensin II-receptor antagonist irbesartan. *Cardiovascular Drug Reviews* 16: 169-194, 1998.
- Pye, M. P., M. Black, and S. M. Cobbe. Comparison of in vivo and in vitro haemodynamic function in experimental heart failure: use of echocardiography. *Cardiovasc Res* 31: 873-881, 1996.
- Qiu, H. Y., J. Benessiano, C. Heymes, B. Tournier, and B. I. Levy. Decreased flow-induced dilation and increased production of cGMP in spontaneously hypertensive rats. *Hypertension* 32: 1098-1103, 1998.
- Ramesh, G., J. S. Varma, N. K. Ganguly, V. Dhawan, H. K. Bali, and M. Singh. Increased plasma nitrite level in cardiac failure. *J Mol Cell Cardiol* 31: 1495-1500, 1999.
- Rapp, J. P. Development of inbred Dahl salt-sensitive and inbred Dahl salt-resistant rats. *Hypertension* 9 (Suppl. I): I-21-I-23, 1987.
- Reichek, N. Standardisation in the measurement of left ventricular wall mass: M-mode echocardiography. *Hypertension* 9 (Suppl. II): II-27-II-29, 1987a.
- Reichek, N. Standardisation in the measurement of left ventricular wall mass: two-dimensional echocardiography. *Hypertension* 9 (Suppl. II): II-30-II-32, 1987b.

- Reiss, K., J. M. Capasso, H.-R. Huang, L. G. Meggs, P. Li, and P. Anversa. ANG II receptors, *c-myc*, and *c-jun* in myocytes after myocardial infarction and ventricular failure. *Am J Physiol* 264: H760-H769, 1993.
- Richards, M. A., G. Tonolo, G. D. McIntyre, B. J. Leckie, and J. I. S. Robertson. Radioimmunoassay for plasma human atrial natriuretic peptide: a comparison of direct and pre-extracted methods. *J Hypertens* 5: 227-236, 1987.
- Richer, C., P. Mulder, P. Fornes, V. Domergue, D. Heudes, and J.-F. Giudicelli. Long-term treatment with trandolapril opposes cardiac remodelling and prolongs survival after myocardial infarction in rats. *J Cardiovas Pharmacol* 20: 147-156, 1992.
- Rooke, G. A. and J. Y. Su. Left-ventricular hypertrophy in rabbits does not exaggerate the effects of halothane on the intracellular components of cardiac contraction. *Anesthesiology* 77: 513-521, 1992.
- Rubanyi, G. M. and M. A. Polokoff. Endothelins: Molecular biology, biochemistry, pharmacology, physiology, and pathophysiology. *Pharmacological Reviews* 46: 325-415, 1994.
- Ruffalo, R. R. and G. Z. Feuerstein. Neurohormonal activation, oxygen free radicals, and apoptosis in the pathogenesis of congestive heart failure. *J Cardiovas Pharmacol* 32 (Suppl. 1): S22-S30, 1998.
- Sadoshima, J., Y. Xu, H. S. Slayter, and S. Izumo. Autocrine release of angiotensin II mediates stretch-induced hypertrophy of cardiac myocytes in vitro. *Cell* 75: 977-984, 1993.
- Safar, M. E., B. I. Levy, and G. M. London. Arterial structure in hypertension and the effects of angiotensin converting enzyme inhibition. *J Hypertens* 10 (Suppl. 5): S51-S57, 1992.
- Sahn, D. J., A. DeMaria, J. Kisslo, and A. Weyman. Recommendations regarding quantitation in M-mode echocardiography: results of a survey of echocardiographic measurements. *Circulation* 58: 1072-1083, 1978.

Saito, Y., K. Nakao, H. Arai, K. Nishimura, G. Takemura, H. Fujiwara, A. Sugawara, T. Yamada, H. Itoh, M. Makoyama, K. Hosoda, G. Shirakami, C. Kawai, T. Ban, and H. Imura. Relationship between ventricular expression of atrial natriuretic polypeptide gene and hemodynamic parameter in old myocardial infarction. *J Cardiovas Pharmacol* 13 (Suppl. 6): S1-S4, 1989.

Sakai, S., T. Miyauchi, M. Kobayashi, I. Yamaguchi, K. Goto, and Y. Sugishita. Inhibition of myocardial endothelin pathway improves long-term survival in heart failure. *Nature* 384: 353-355, 1996.

Samani, N. J., J. D. Swales, A. J. Jeffreys, D. B. Morton, A. J. Naffilan, K. Lindpainter, D. Ganten, and W. J. Brammer. DNA fingerprinting of spontaneously hypertensive and Wistar-Kyoto rats: implications for hypertension research. *J Hypertens* 7: 809-816, 1989.

Sambrook, J., E. F. Fritsch, and T. Maniatis. Molecular cloning: a laboratory manual. Cold Spring Harbor, Cold Spring Harbor Laboratory Press, 1989.

Savage, D. D., J. B. Garrison, W. B. Kannel, S. J. Anderson, M. Feinleib, and W. P. Castelli. Considerations in the use of echocardiography in epidemiology: the Framingham study. *Hypertension* 9 (Suppl. II): II-40-II-44, 1987.

Schiller, N. B. Considerations in the standardisation of measurement of left ventricular myocardial mass by two-dimensional echocardiography. *Hypertension* 9 (Suppl. II): II-33-II-35, 1987.

Schmid-Schönbcin, G. W., B. W. Zweifach, F. A. DeLano, and P. C. Y. Chen. Microvascular tone in a skeletal muscle of spontaneously hypertensive rats. *Hypertension* 9: 164-171, 1987.

Schmieder, R. E., P. Martus, and A. Klingbeil. Reversal of left ventricular hypertrophy in essential hypertension. A meta-analysis of randomized double-blind studies. *JAMA* 275: 1507-1513, 1996.

Schotten, U., B. Koenigs, M. Rueppel, F. Schoendube, P. Boknik, W. Schmitz, and P. Hanrath. Reduced myocardial sarcoplasmic reticulum Ca^{2+} -ATPase protein expression in

- compensated primary and secondary human cardiac hypertrophy. *J Mol Cell Cardiol* 31: 1483-1494, 1999.
- Schrier, R. W. and W. T. Abraham. Hormones and hemodynamics in heart failure. *N Eng J Med* 341: 577-585, 1999.
- Schulz, R., E. Nava, and S. Moncada. Induction and potential biological relevance of a Ca^{2+} -independent nitric oxide synthase in the myocardium. *Br J Pharmacol* 105: 575-580, 1992.
- Selye, H., E. Bajusz, S. Grasso, and P. Mendell. Simple techniques for the surgical occlusion of coronary vessels in rats. *Angiology* 11: 398-407, 1960.
- Semigran, M. J., C. N. Aroncy, H. C. Herrmann, G. W. Dee, C. A. Boucher, and M. A. Fifer. Effects of atrial natriuretic peptide on left ventricular function in hypertension. *Hypertension* 24: 271-279, 1994.
- Seul, K. H., K. W. Cho, S. H. Kim, Y. H. Hwang, C. U. Park, and G. Y. Koh. Single injection of pentobarbital induces long-lasting effects on ANP synthesis and gene-expression in the rat aorta. *Life Sciences* 16: 1351-1359, 1993.
- Shimamura, K., S. Osugi, K. Moriyama, and S. Sunano. Impairment and protection of endothelium-dependent relaxation in aortae of various strains of spontaneously hypertensive rats. *J Cardiovas Pharmacol* 17 (Suppl. 3): S133-S136, 1991.
- Simpson, P. B. and R. A. J. Challiss. Neuronal Ca^{2+} stores: activation and function. *Trends Neurosci* 18: 299-306, 1995.
- Sirvio, M.-L., K. Helin, P. Stewen, I. Tikkanen, and F. Fyhrquist. Endothelin-1 in heart and pulmonary tissue in experimental heart failure. *Blood Pressure* 6: 250-255, 1997.
- Smith, C. J., D. Sun, C. Hoegler, B. S. Roth, X. Zhang, G. Zhao, X.-B. Xu, Y. Kobari, K. Pritchard, W. C. Sessa, and T. H. Hintze. Reduced gene expression of vascular endothelial NO synthase and cyclooxygenase-1 in heart failure. *Circ Res* 78: 58-64, 1996.

- Smits, J. F. M., C. van Krimpen, R. G. Schoemaker, J. P. M. Cleutjens, and M. J. A. P. Daemen. Angiotensin II receptor blockade after myocardial infarction in rats: Effects on haemodynamics, myocardial DNA synthesis, and interstitial collagen content. *J Cardiovas Pharmacol* 20: 772-778, 1992.
- Stassen, F. R. M., M. J. J. M. F. Willemsen, G. M. J. Janssen, G. E. Fazzi, P. M. H. Schiffers, J. F. M. Smits, and J. G. R. de Mey. Reduced responsiveness of rat mesenteric resistance artery smooth muscle to phenylephrine and calcium following myocardial infarction. *Br J Pharmacol* 120: 1505-1512, 1997a.
- Stassen, F. R. M., G. E. Fazzi, P. J. A. Lccnders, J. F. M. Smits, and J. G. R. de Mey. Coronary arterial hyperreactivity and mesenteric arterial hyporeactivity after myocardial infarction in the rat. *J Cardiovas Pharmacol* 29: 780-788, 1997b.
- Stephens, N., M. J. Drinkhill, A. S. Hall, S. G. Ball, and A. M. Heagerty. Structure and in vitro function of human subcutaneous small arteries in mild heart failure. *Am J Physiol* 274: C1298-C1305, 1998.
- Stier, C. T., G. T. Sim, and S. Levine. Dietary arginine fails to protect against cerebrovascular damage in stroke-prone hypertensive rats. *Brain Research* 549: 354-356, 1991.
- Strachan, F. E., J. C. Spratt, I. B. Wilkinson, N. R. Johnston, G. A. Gray, and D. J. Webb. Systemic blockade of the endothelin-B receptor increases peripheral vascular resistance in healthy men. *Hypertension* 33: 581-585, 1999.
- Struyker Boudier, H. A. J., L. M. A. B. van Bortel, and J. G. R. de Mey. Remodeling of the vascular tree in hypertension: drug effects. *TIPS* 11: 240-245, 1990.
- Sun, Y. and K. T. Weber. Angiotensin converting enzyme and myofibroblasts during tissue repair in the rat heart. *J Mol Cell Cardiol* 28: 851-858, 1996.
- Sumano, S., H. Watanabe, S. Tanaka, F. Sekiguchi, and K. Shimamura. Endothelium-derived relaxing, contracting and hyperpolarising factors of mesenteric arteries of hypertensive and normotensive rats. *Br J Pharmacol* 126: 709-716, 1999.

Sutsch, G., W. Kiowski, X.-W. Yan, P. Hunziker, S. Christen, W. Strobel, J.-H. Kim, P. Rickenbacher, and O. Bertel. Short-term oral endothelin-receptor antagonist therapy in conventionally treated patients with symptomatic severe chronic heart failure. *Circulation* 98: 2262-2268, 1998.

Sutton, M. St. J., M. A. Pfeffer, L. Moye, T. Plappert, J. L. Rouleau, G. Lamas, J. Rouleau, J. O. Parker, M. O. Arnold, B. Sussex, and E. Braunwald. Cardiovascular death and left ventricular remodeling two years after myocardial infarction - Baseline predictors and impact of long-term use of captopril: Information from the survival and ventricular enlargement (SAVE) trial. *Circulation* 96: 3294-3299, 1997.

Taddei, S., A. Virdis, L. Ghiadoni, and A. Salvetti. Endothelial dysfunction in hypertension: fact or fancy? *J Cardiovas Pharmacol* 32 (Suppl. 3): S41-S47, 1998.

Tagawa, H., N. Wang, T. Narishige, D. E. Ingber, M. R. Zile, and G. Cooper. Cytoskeletal mechanics in pressure-overload cardiac hypertrophy. *Circ Res* 80: 281-289, 1997.

Tanase, H., Y. Yamori, C. T. Hansen, and W. Lovenberg. Heart size in inbred strains of rats. Part 1. Genetic determination of the development of cardiovascular enlargement in rats. *Hypertension* 4: 864-872, 1982a.

Tanase, H., Y. Yamori, C. T. Hansen, and W. Lovenberg. Heart size in inbred strains of rats. Part 2. cardiovascular DNA and RNA contents during the development of cardiac enlargement in rats. *Hypertension* 4: 872-880, 1982b.

Taylor, K., R. D. Patten, J. J. Smith, M. J. Aronovitz, J. Wight, R. N. Salomon, and M. A. Konstam. Divergent effects of angiotensin-converting enzyme inhibition and angiotensin II-receptor antagonism on myocardial cellular proliferation and collagen deposition after myocardial infarction in rats. *J Cardiovas Pharmacol* 31: 654-660, 1998.

Teerlink, J. R. and J. P. Clozel. Hemodynamic variability and circadian rhythm in rats with heart failure: role of locomotor activity. *Am J Physiol* 264: H2111-H2118, 1993.

- Teerlink, J. R., G. A. Gray, M. Clozel, and J. P. Clozel. Increased vascular responsiveness to norepinephrine in rats with heart failure is endothelium dependent: Dissociation of basal and stimulated nitric oxide release. *Circulation* 89: 393-401, 1994.
- Testaert, E., J. R. Cusson, D. C. Phaneuf, R. Essiambre, F. Lemire, P. Hamet, G. Thibault, and P. Larochelle. Echocardiographic measurements and plasma levels of atrial natriuretic factor. *J Cardiovas Pharmacol* 13 (Suppl. 6): S47-S50, 1989.
- Thai, H. M., H. T. Van, M. A. Gaballa, S. Goldman, and T. E. Raya. Effects of AT₁ receptor blockade after myocardial infarct on myocardial fibrosis, stiffness, and contractility. *Am J Physiol* 276: H873-H880, 1999.
- Thomas, C. J., G. A. Head, and R. L. Woods. ANP and bradycardic reflexes in hypertensive rats. Influence of cardiac hypertrophy. *Hypertension* 32: 548-555, 1998.
- Thomas, D. P., O. Hudlicka, M. D. Brown, and D. Devect. Alterations in small arterioles precede changes in limb skeletal muscle after myocardial infarction. *Am J Physiol* 275: H1032-H1039, 1998.
- Toyoshima, H., Y. Nasa, Y. Kohsaka, Y. Isayama, F. Yamaguchi, A. Sanbe, and S. Takeo. The effect of chronic treatment withtrandolapril on cyclic AMP- and cyclic GMP-dependent relaxations in aortic segments of rats with chronic heart failure. *Br J Pharmacol* 123: 344-352, 1998.
- Trippodo, N. C. and E. D. Frohlich. Similarities of genetic (spontaneous) hypertension. *Circ Res* 48: 309-319, 1981.
- Troy, B. L., J. Pombo, and C. E. Rackley. Measurement of left ventricular wall thickness and mass by echocardiography. *Circulation* 45: 602-611, 1972.
- Tschudi, M. R., S. Mesaros, T. F. Luscher, and T. Malinski. Direct in situ measurement of nitric oxide in mesenteric resistance arteries. Increased decompensation by superoxide in hypertension. *Hypertension* 27: 32-35, 1996.

- Tsutamoto, T., A. Wada, K. Maeda, T. Hisanaga, Y. Maeda, D. Fukai, M. Ohmishi, Y. Sugimoto, and M. Kinoshita. Attenuation of compensation of endogenous cardiac natriuretic peptide system in chronic heart failure. *Circulation* 96: 509-516, 1997.
- Tuiniga, Y. S., D. J. van Veldhuisen, J. Brouwer, J. Haaksma, H. J. G. M. Crijns, A. J. Man in't Veld, and K. I. Lie. Heart rate variability in left ventricular dysfunction and heart failure: effects and implications of drug treatment. *Br Heart J* 72: 509-513, 1994.
- Ueyama, T., M. Hamada, T. Hano, I. Nishio, Y. Masuyama, and S. Furukawa. Increased nerve growth-factor levels in spontaneously hypertensive rats. *J Hypertens* 3: 215-219, 1992.
- Urata, H., B. Healy, R. W. Stewart, F. M. Bumpus, and A. Husain. Angiotensin II-forming pathways in normal and failing human hearts. *Circ Res* 66: 883-890, 1990.
- Vacher, E., P. Fornes, C. Richer, P. Bruneval, D. Nisato, and J.-F. Giudicelli. Early and late haemodynamic and morphological effects of angiotensin II subtype 1 receptor blockade during genetic hypertension development. *J Hypertens* 13: 675-682, 1995.
- van de Borne, P., M. Abramowicz, S. Degre, and J.-P. Degaute. Effects of chronic congestive heart failure on 24-hour blood pressure and heart rate patterns: a haemodynamic approach. *Am Heart J* 123: 998-1004, 1992.
- Vanhoutte, P. M. Endothelial dysfunction in hypertension. *J Hypertens* 14 (Suppl. 5): S83-S93, 1996.
- Vaziri, N. D., Z. Ni, and F. Oveysi. Upregulation of renal and vascular nitric oxide synthase in young spontaneously hypertensive rats. *Hypertension* 31: 1248-1254, 1998.
- Verdouw, P. D., M. A. van den Doel, S. de Zeeuw, and D. J. Duncker. Animal models in the study of myocardial ischaemia and ischaemic syndromes. *Cardiovasc Res* 39: 121-135, 1998.
- Vicaut, E. Hypertension and the microcirculation: a brief overview of experimental studies. *J Hypertens* 10 (Suppl. 5): S59-S68, 1992.

- Villarreal, F. J., D. Hong, and J. Omens. Nicotine-modified postinfarction left ventricular remodeling. *Am J Physiol* 276: H1103-H1106, 1999.
- Vincent, M. and J. Sassard. The Lyon model of genetic hypertension in the rat. *Hypertension* 9 (Suppl. I): I-27-I-29, 1987.
- Wallerson, D. C. and R. B. Devereux. Reproducibility of echocardiographic left ventricular measurements. *Hypertension* 9 (Suppl. II): II-6-II-18, 1987.
- Walsh, R. A. Microtubules and pressure-overload hypertrophy. *Circ Res* 80: 295-296, 1997.
- Weinberg, E. O., M. A. Lee, M. Weigner, K. Lindpainter, S. P. Bishop, C. R. Benedict, K. K. L. Ho, P. S. Douglas, E. Chafizadeh, and B. H. Lorell. Angiotensin AT sub 1 receptor inhibition: Effects on hypertrophic remodeling and ACE expression in rats with pressure-overload hypertrophy due to ascending aortic stenosis. *Circulation* 95: 1592-1600, 1995.
- Wijbenga, A. A. M., A. H. M. M. Balk, F. A. M. Jonkman, F. Boomsma, M. L. Simoons, and A. J. Man in 't Veld. Relation of atrial natriuretic peptides to left ventricular systolic and diastolic function in heart failure. *European Journal of Heart Failure* 1: 51-58, 1999.
- Wildhirt, S. M., R. R. Dudek, H. Suzuki, V. Pinto, K. S. Narayan, and R. J. Bing. Immunohistochemistry in the identification of nitric oxide synthase isoenzymes in myocardial infarction. *Cardiovasc Res* 29: 526-531, 1995.
- Winlaw, D. S., G. A. Smythe, A. M. Keogh, C. G. Schyvens, P. M. Spratt, and P. S. Macdonald. Increased nitric oxide production in heart failure. *Lancet* 344: 373-374, 1994.
- Winlaw, D. S., G. A. Smythe, A. M. Keogh, C. G. Schyvens, P. M. Spratt, and P. S. Macdonald. Nitric oxide production in heart failure. *Lancet* 345: 390-391, 1995.
- Wodey, E., P. Pladys, C. Copin, M. M. Lucas, A. Chaumont, P. Carre, B. Lelong, O. Azzis, and C. Ecoffey. Comparative hemodynamic depression of sevoflurane versus halothane in infants - an echocardiography study. *Anesthesiology* 87: 795-800, 1997.

- Wolny, A., J. P. Clozel, J. Rein, P. Mory, P. Vogt, M. Turino, W. Kiowski, and W. Fischli. Functional and biochemical analysis of angiotenin II-forming pathways in the human heart. *Circ Res* 80: 219-227, 1997.
- Wu, C.-F., N. H. Bishopric, and R. E. Pratt. Atrial natriuretic peptide induces apoptosis in neonatal rat cardiac myocytes. *J Biol Chem* 272: 14860-14866, 1997.
- Wyatt, H. T., M. K. Heng, S. Meerbaum, J. D. Hestenes, J. M. Cobo, R. M. Davidson, and E. Corday. Cross-sectional echocardiography. 1. Analysis of mathematic models for quantifying mass of the left ventricle in dogs. *Circulation* 60: 1104-1113, 1979.
- Xu, D.-L., P.-Y. Martin, M. Ohara, J. St.John, T. Pattison, X. Meng, K. Morris, J. K. Kim, and R. W. Schrier. Upregulation of aquaporin-2 water channel expression in chronic heart failure rat. *J Clin Invest* 99: 1500-1505, 1997.
- Yamaguchi, F., A. Sanbe, and S. Takeo. Effects of long-term treatment with trandolapril on sarcoplasmic reticulum function of cardiac muscle in rats with chronic heart failure following myocardial infarction. *Br J Pharmacol* 123: 326-334, 1998.
- Yamamoto, K., J. C. Burnett, M. Jougasaki, R. A. Nishimura, K. R. Bailey, Y. Saito, K. Nakao, and M. M. Redfield. Superiority of brain natriuretic peptide as a hormonal marker of ventricular systolic and diastolic dysfunction and ventricular hypertrophy. *Hypertension* 28: 988-994, 1996.
- Yamazaki, T. and Y. Yazaki. Is there major involvement of the renin-angiotensin system in cardiac hypertrophy? *Circ Res* 81: 639-642, 1997.
- Yamori, Y., C. Mori, T. Nishio, A. Ooshima, R. Horie, M. Ohtaka, T. Soeda, M. Saito, K. Abe, Y. Nara, Y. Nakao, and M. Kihara. Cardiac hypertrophy in early hypertension. *Am J Cardiol* 44: 964-969, 1979.
- Yamori, Y. and W. Lovenberg. Spontaneously hypertensive rats. *Hypertension* 9 (Suppl. 1): I-13-I-14, 1987.

- Yang, X.-P., Y.-H. Liu, E. G. Shesely, M. Bulagannawar, F. Liu, and O. A. Carretero. Endothelial nitric oxide gene knockout mice. Cardiac phenotypes and the effect of angiotension-converting enzyme inhibitor on myocardial ischaemia/reperfusion injury. *Hypertension* 34: 24-30, 1999.
- Yoshida, K., M. Kohzuki, D. J. Casley, and C. I. Johnston. Angiotensin-converting enzyme inhibition and salt in experimental myocardial infarction. *J Cardiovas Pharmacol* 32: 357-365, 1998.
- Yoshiyama, M., K. Takeuchi, T. Omura, S. Kim, H. Yamagishi, I. Toda, M. Teragaki, K. Akioka, H. Iwao, and J. Yoshikawa. Effects of candesartan and clizapril on rats with myocardial infarction assessed by echocardiography. *Hypertension* 33: 961-968, 1999.
- Yoshizumi, M., M. A. Perrella, J. C. Burnett, and M.-E. Lee. Tumor necrosis factor downregulates an endothelial nitric oxide synthase mRNA by shortening its half-life. *Circ Res* 73: 205-209, 1993.
- Young, M. S., Magid, N. M., Wallerson, D. C., Goldweit, R. S., Carter, J. N., Devereux, R. B., and Borer, J. S. Echocardiographic left ventricular mass measurement in small animals: anatomic validation in normal and aortic regurgitant rabbits. *Clin Res* 34, A865-A865. 1986.
- Yu, C. M. and J. E. Sanderson. Plasma brain natriuretic peptide - an independent predictor of cardiovascular mortality in acute heart failure. *European Journal of Heart Failure* 1: 59-65, 1999.
- Zimmerman, R., J. Kastens, W. Linz, G. Wiemer, B. A. Schölkens, and J. Schaper. Effect of long-term ACE inhibition on myocardial tissue in hypertensive stroke-prone rats. *J Mol Cell Cardiol* 31: 1447-1456, 1999.
- Zisman, L. S., K. Asano, D. L. Dutcher, A. Ferdensi, A. D. Robertson, M. Jenkin, E. W. Bush, T. Bohlmeier, B. Perryman, and M. R. Bristow. Differential regulation of cardiac angiotensin converting enzyme binding sites and AT₁ receptor density in the failing human heart. *Circulation* 98: 1735-1741, 1998.

